IMPROVEMENTS IN THE PERFORMANCE AND UNDERSTANDING OF SWITCHABLE-HYDROPHILICITY SOLVENTS

by

Jesse R. Vanderveen

A thesis submitted to the Department of Chemistry

In conformity with the requirements for

the degree of Doctor of Philosophy

Queen's University

Kingston, Ontario, Canada

April, 2018

Copyright © Jesse R. Vanderveen, 2018

Abstract

Switchable-hydrophilicity solvents (SHSs) are amine and amidine solvents that can be reversibly switched between two forms: one that forms a biphasic mixture with water and another that forms a monophasic mixture with water. The addition or removal of CO_2 from SHS-based systems acts as the trigger to switch between these two forms. SHSs have attracted attention as alternative solvents for a variety of applications because their switchable behaviour allows them to be used in energy- or material- efficient ways. One such application is distillation-free solvent-solute separations. The present research builds an understanding of the properties of amines that determine whether they are SHSs or not. It also applies this understanding to the development of new SHSs with fewer health and environmental hazards, such as decreased acute toxicity and decreased volatility, as well as improved performance with respect to solvent-solute separations.

The relationship between the pK_{aH} and log K_{ow} of an amine and the ability of the amine to act as a SHS is established. A mathematical model is described that can be used to predict whether an amine acts as a SHS based on these two properties. Furthermore, the influence of CO_2 partial pressure and the water/amine volume ratio on these pK_{aH} and log K_{ow} requirements are investigated. The model acts as a guide when identifying new SHSs.

Many new SHSs are identified with a variety of beneficial properties. SHSs that have oxygen-containing functional groups have decreased environmental, health, and safety risks than trialkylamine SHSs. Secondary amine SHSs are shown to switch to their hydrophilic state more rapidly than tertiary amine SHSs. Diamine SHSs can be more completely separated from solutes than monoamines, resulting in a more pure isolated solute after a SHS-based separation. A virtual screening approach to the design of SHSs is presented that can be used to rapidly screen thousands of compounds to identify those that are estimated to be SHSs with few environmental, health, and safety risks. The identification of new SHSs increases the options when selecting a solvent for a SHS-based process and provides data to improve the understanding of SHSs.

Acknowledgements

My graduate studies at Queen's has been a wonderful experience. The people I've come to know during my studies have been a major part of this experience and the parts they played in the creation of this thesis must be acknowledged.

First, I thank my supervisor Philip Jessop for his support, guidance, and advice over the course of my studies. His input was invaluable to my research. His passion for green chemistry and the responsible use of chemical technologies was and remains an inspiration to me.

I also thank the members of the Jessop group, past and present, for creating a positive work environment. Everyone has been open for fruitful scientific discussions and the sharing of ideas with me since the day I joined. I have enjoyed discussing the problems being faced for various projects and enjoyed more the solutions we came up with, whether they were successful, elegant, impractical, or even bizarre. I hope this practice continues long into the future. I thank Jeremy Durelle specifically for sharing the SHS project with me for two years. It was a pleasure working with him and many of my successes stem from his work.

I thank all of my collaborators for assisting me with their expertise in fields of study which I am less familiar with.

I thank Switchable Solutions, Inc. for its financial support throughout my studies and Lowy Gunnewieck for his inputs to my work and his enthusiasm for my results. I am also grateful for financial support from the government of Ontario and the Natural Sciences and Engineering Research Council of Canada.

Finally, I thank my family. I would not be who I am today without you. Your constant love and support is a true blessing.

Statement of Originality

I hereby certify that all of the work described within this thesis is the original work of the author. Any published (or unpublished) ideas and/or techniques from the work of others are fully acknowledged in accordance with the standard referencing practices. The contributions from collaborators are clearly noted below. All of the work was performed under the supervision of Dr. Philip Jessop.

In Chapter 2, Jeremy Durelle contributed some data regarding the behaviour of some of the tertiary amines. The X-ray crystallography data was collected and interpreted by Dr. Jai-sheng Lu.

In Chapter 3, Jeremy Durelle developed the models describing the two-component and three-component system with my input and assistance. Courtney B. Chalifoux and Julia E. Kostin helped with the optimization of these models. The data used to develop the models was collected by Jeremy Durelle, Yi Quan, and myself. I derived the equations used to calculate the fraction of protonation presented in section 3.4.

In Chapter 4, the software used to screen the structures was developed by Dr. Luc Patiny. Courtney B. Chalifoux and Michael J. Jessop helped in the literature search for amines with experimentally determined properties relevant to the article.

In Chapter 5, Roberto I. Canales determined the values for the non-random two-liquid model presented in the chapter under the supervision of Dr. Mark A. Stadtherr and Dr. Joan F. Brennecke using experimental data I collected with the assistance of Yi Quan and Courtney B. Chalifoux.

In Chapter 6, Jialing Geng and Susanna Zhang tested compounds for switchable hydrophilicity under my supervision. Chemical syntheses were also performed by Jialing Geng and Susanna Zhang when required.

Portions of this thesis have been published previously:

Chapter 2: J. R. Vanderveen, J. Durelle, and P. G. Jessop, *Green Chem.*, 2014, **16**, 1187-1197. Reproduced with the permission of the Royal Society of Chemistry.

Chapter 3: i) J. Durelle, J. R. Vanderveen, and P. G. Jessop, *Phys. Chem. Chem. Phys.*, 2014, **16**, 5270-5275. Reproduced with the permission of the Royal Society of Chemistry.

ii) J. Durelle, J. R. Vanderveen, Y. Quan, C. B. Chalifoux, J. E. Kostin, and P. G. Jessop, *Phys. Chem. Chem. Phys.*, 2015, **17**, 5308-5313. Reproduced with the permission of the Royal Society of Chemistry.

iii) A. K. Alshamrani, J. R. Vanderveen, and P. G. Jessop, *Phys. Chem. Chem. Phys.*, 2016, **18**, 19276-19288. Reproduced with the permission of the Royal Society of Chemistry.

Chapter 4: J. R. Vanderveen, L. Patiny, C. B. Chalifoux, M. J. Jessop, and P. G. Jessop, *Green Chem.*, 2015, **17**, 5182-5188. Reproduced with the permission of the Royal Society of Chemistry.

Chapter 5: J. R. Vanderveen, Roberto I. Canales, Y. Quan, C. B. Chalifoux, M. A. Stadtherr, J. F. Brennecke, P. G. Jessop, *Fluid Ph. Equilibria*, 2016, **409**, 150-156. Reproduced with the permission of the Elsevier.

Jesse R. Vanderveen

February, 2018

Table of Contents

List of Figures

List of Tables

List of Symbols and Abbreviations

A_x	Acceptability value for property x
ATR	Attenuated total reflectance
BAF	Bioaccumulation factor
bp	Boiling point
D	Distribution coefficient
DECA	*N*,*N*-Diethylcyclohexylamine
DIPEA	*N*,*N*-Diisopropylethylamine
DLLME	Dispersive liquid-liquid microextraction
DMAP	1-Dimethylamino-2-pentyne
DMBA	*N*,*N*-Dimethylbenzylamine
DMBIPA	Di-(4-methoxybutyl)isopropylamine
DMCA	*N*,*N*-Dimethycylcohexylamine
DMCAH	*N*,*N*-Dimethylcyclohexylammonium
EHS	Environment, health, and safety
EI	Electron impact
FID	Flame ionization detector
FT	Fourier-transform
GC	Gas Chromatography
g^E	Excess Gibb's energy
g_{ij}	Gibb's energy for the interaction of component i with component j
$g^{(j)}$	Residual Gibb's energy of component j
GHS	Globally Harmonized System
HLLE	Homogeneous liquid-liquid extraction
HRMS	High-resolution mass spectrometry

i.d.	Inner diameter
IR	Infrared
J	NMR coupling constant
K_1	Acid dissociation constant for CO_2
K_H	Henry's constant
K_w	Auto-dissociation constant of water
K_{ow}, K_{ow}', or K_{ow}''	Octanol-water partition coefficient
K_P or K_P'	Partition coefficient
LC_{50}	Lethal concentration that kills 50 percent of a test sample
LCA	Life-cycle assessment
LD_{50}	Lethal dose that kills 50 percent of a test sample
LLE	Liquid-liquid equilibrium
m_{ij}	Mass fraction of component i in phase j
MSDS	Material Safety Data Sheet
MW	Molecular weight
m/z	Mass-to-charge ratio
n_B	Moles of amine base
$n_{B,undiss}$ or $n'_{B,undiss}$	Moles of undissolved amine base
n_{ij}	Mole fraction of component i in phase j
NMR	Nuclear magnetic resonance
NRTL	Non-random two-liquid
P	Fraction of protonation
P_{CO2} or P_{CO2}'	Pressure of CO_2
pK_a	Acid dissociation constant
pK_{a1}	First acid dissociation constant

pK_{a2}	Second acid dissociation constant
pK_{aH}	pK_a of the conjugate acid of a base
pK_{aH1}	pK_a of a monoprotonated dibasic amine
pK_{aH2}	pK_a of a diprotonated dibasic amine
ppm	parts per million
QSAR	Quantitative structure-activity relationships
R	Ideal gas constant
RMSD	Root mean square deviation
S or S′	Solubility or miscibility of an amine in water
s	selectivity
SHS	Switchable-hydrophilicity solvent
SS LPME	Switchable solvent liquid phase microextraction
T	Temperature
TCD	Thermal conductivity detector
TEST	Toxicity Estimation Software Tool
TPA	Tripropylamine
V_B	Volume of amine base
V_w	Volume of water
V_{rat}	Ratio of V_B/V_w
w_{ij}	Normalized mass fraction of component i in phase j
x_i^{α} and x_i^{β}	Mole fraction of component i in phase α or β
Z	Mapping parameter to quantify switchable hydrophilicity in the two-component system
α_{ij}	Nonrandomness parameter for the interaction between component i and component j

δ	Chemical shift
ρ	Density
τ_{ij}	NRTL binary parameter for the interaction between component i and component j
ν_{max}	Wavenumber of absorbance maxima in IR spectrum
ν_N	Number of nitrogen atoms in a molecule
ν_P	Number of phosphorus atoms in a molecule
ν_{ThOD}	Theoretical oxygen demand
γ_i^{α} or γ_i^{β}	Activity coefficient of component i in phase α or β
Ω	Mapping parameter to quantify switchable hydrophilicity in the three-component system

Chapter 1

Introduction

1.1 Green Chemistry

Chemistry offers many benefits to the world – increased food production, better medicine, and durable materials, for example – but historically there have been drawbacks to these chemical inventions in the form of health, safety, and environmental risks. Many inventions are used despite having known drawbacks because the benefits outweigh the risks, while others are used without fully understanding the risks they pose. Examples of the latter case having major consequences make for popular case studies, such as dichlorodiphenyltrichloroethane (DDT) insecticide, chlorofluorocarbon refrigerants, and fossil fuel combustion. Each of these examples demonstrates valuable benefits to humanity (disease prevention, temperature control, and inexpensive energy, respectively) but also has negative effects on the environment (bird population decline, ozone depletion, and climate change, respectively).[1–3] Examples such as these emphasize the importance of understanding hazards associated with chemical technologies and eliminating them, ideally before they are used on large scales. New chemical technologies must not only provide benefits, but also consider drawbacks to avoid repeating the mistakes of the past.

Green chemistry is a sub-discipline of chemistry that seeks to benefit society while avoiding the drawbacks such as those described above. According to the United States Environmental Protection Agency, "green chemistry is the design of chemical products and processes that reduce or eliminate the use or generation of hazardous substances".[4] Green chemistry is guided by twelve principles that were proposed by Anastas and Warner in 1998 to help create sustainable chemical processes, listed in Table 1.1.[5] Related to the principles of green chemistry are the twelve principles of green engineering, proposed by Anastas and Zimmerman in 2003.[6] These principles are listed in Table 1.2. While most fields of chemistry focus solely on maximizing

Table 1.1 The 12 principles of green chemistry, as described by the American Chemical Society.[7]

1.	Prevention	It is better to prevent waste than to treat or clean up waste after it has been created.
2.	Atom economy	Synthetic methods should be designed to maximize the incorporation of all materials used in the process into the final product.
3.	Less hazardous chemical syntheses	Wherever practicable, synthetic methods should be designed to use and generate substances that possess little or no toxicity to human health and the environment.
4.	Designing safer chemical	Chemical products should be designed to affect their desired function while minimizing their toxicity.
5.	Safer solvents and auxiliaries	The use of auxiliary substances (e.g. solvents, separation agents, etc.) should be made unnecessary wherever possible and innocuous when used.
6.	Design for efficiency	Energy requirements of chemical processes should be recognized for their environmental and economic impacts and should be minimized. If possible, synthetic methods should be conducted at ambient temperature and pressure.
7.	Use of renewable feedstocks	A raw material or feedstock should be renewable rather than depleting whenever technically and economically practicable.
8.	Reduce derivatives	Unnecessary derivatization (use of blocking groups, protection/deprotection, temporary modification of physical/chemical processes) should be minimized or avoided if possible, because such steps require additional reagents and can generate waste.
9.	Catalysis	Catalytic reagents (as selective as possible) are superior to stoichiometric reagents.
10.	Design for degradation	Chemical products should be designed so that at the end of their function they break down into innocuous degradation products and do not persist in the environment.
11.	Real-time analysis for pollution prevention	Analytical methodologies need to be further developed to allow for real-time, in-process monitoring and control prior to the formation of hazardous substances.
12.	Inherently safer chemistry for accident prevention	Substances and the form of a substance used in a chemical process should be chosen to minimize the potential for chemical accidents, including releases, explosions, and fires.

Table 1.2 The 12 principles of green engineering, as described by the American Chemical Society.[8]

1. Inherent rather than circumstantial	Designers need to strive to ensure all materials and energy inputs and outputs are as inherently nonhazardous as possible.
2. Prevention instead of treatment	It is better to prevent waste than to treat or clean up waste after it is formed.
3. Design for separation	Separation and purification operations should be designed to minimize energy consumption and materials use.
4. Maximize efficiency	Products, processes, and systems should be designed to maximize mass, energy, space, and time efficiency.
5. Output-pulled versus input-pushed	Products, processes, and systems should be "output-pulled" rather than "input-pushed" through the use of energy and materials.
6. Conserve complexity	Embedded entropy and complexity must be viewed as an investment when making design choices on recycle, reuse, or beneficial disposition.
7. Durability rather than immortality	Targeted durability, not immortality, should be a design goal.
8. Meet need, minimize excess	Design for unnecessary capacity or capability (e.g. "one size fits all") solutions should be considered a design flaw.
9. Minimize material diversity	Material diversity in multicomponent products should be minimized to promote disassembly and value retention.
10. Integrate material and energy flows	Design of products, processes, and systems must include integration and interconnectivity with available energy and materials flows.
11. Design for commercial "afterlife"	Products, processes, and systems should be designed for performance in a commercial "afterlife".
12. Renewable rather than depleting	Material and energy inputs should be renewable rather than depleting.

the benefits of chemical technologies, green chemistry seeks to do the same while also minimizing the drawbacks by adhering to the twelve principles of green chemistry. Many researchers recognize the importance of green chemistry and incorporate elements of green chemistry in their studies of other areas of chemistry. Chemical processes that follow the guidelines of green chemistry and green engineering can bring benefits to our society while presenting little risk to humans and the environment.

In addition to the *qualitative* measures used in green chemistry outlined in the twelve principles in Table 1.1, several *quantitative* measures have been proposed. One quantitative measure, atom economy, is green chemistry principle #2.[9] The atom economy of a reaction can be calculated using Equation 1.1. Reactions with high atom economies create less byproduct waste than ones with low atom economies. However, atom economy only considers the materials used directly in a chemical reaction and excludes solvents, catalysts, and other additives. "E-factor" is a quantitative metric that accounts for all waste generated in a process.[10] It is defined as the ratio of waste mass per product mass (Equation 1.2). By considering all waste from a process, E-factors help to compare processes in terms of waste prevention (green chemistry principle #1). A drawback of E-factors is that they do not distinguish between wastes with different hazards. For example, 1 kg of waste water is considered equivalent to 1 kg of heavy metal waste by this measurement, which is a flawed assessment because heavy metals have a larger negative effect on the environment than an equivalent mass of water. A more complex method of quantification is necessary to describe the risks of a given process more completely and accurately. Life-cycle assessments (LCAs) attempt to characterize all of the environmental risks associated with a process.[11,12] LCAs include an inventory of every material used and every waste product created in a given process. The risks associated with each chemical in this inventory are assessed for a wide range of hazards (e.g. smog formation, aquatic toxicity, eutrophication) relative to reference

compounds. The risks are then adjusted based on how much is used/produced per unit of desired product (a process that uses twice as much reagent to obtain the same amount of product should be twice as hazardous, for example) and added together for each hazard to determine how much risk the overall process presents for a given hazard (e.g., accounting for every compound used and every waste product made, how much potential for smog formation does the process present?). The results of a LCA describe the risk a process presents with respect to many different hazards, with each hazard given a separate number. In effect, LCAs provide a list of the risks associated with different processes, each treated on an individual basis. By making use of atom economies, E-factors, and LCAs, and by interpreting these measures appropriately, quantitative measurements of sustainability can be obtained for individual processes.

$$Atom\ Economy = \frac{mass\ of\ desired\ products}{mass\ of\ reactants} \times 100\% \qquad \text{Eqn. 1.1}$$

$$E\ factor = \frac{mass\ of\ waste}{mass\ of\ product} \qquad \text{Eqn. 1.2}$$

1.2 Solvents

Solvents are some of the most widely used chemicals in the world. A solvent is, quite simply, a compound that can dissolve another compound (the solute) to form a solution (a homogeneous mixture of the two substances). While solids, gasses, and supercritical fluids can be solvents, liquids are the most common type of solvent and it follows that the terms “solvent” and “solution” typically refer to liquids. Using a solvent to create a solution changes the properties of the solute and can improve the outcome of many processes. For example, a solvent can be added to a solid to allow the solid to be pumped through a pipeline more easily than if the solvent were not present. Since they can improve the properties of mixtures in a given process, solvents are used for many applications, including separations, chemical reactions, purifications, and chemical analyses.

Every solvent has different properties, and these properties determine which solvents will be useful in different applications. Polarity is one of the most important properties, with solvents often being described as either polar or non-polar. Polar solvents, such as water, tend to dissolve polar molecules well (e.g. sucrose) but dissolve non-polar molecules, such as naphthalene, poorly. Non-polar solvents such as toluene have the opposite behaviour, dissolving non-polar molecules well, but dissolving polar molecules poorly. Several different values can be used to describe solvent polarity, such as the solvent's dielectric constant, its $E_T(30)$ value (transition energy between the ground and excited states of Reichardt's dye), and its Kamlet-Taft dipolarity/polarizability parameter (π^*).[13,14] Another important property of solvents is their ability to donate protons. Solvents with the ability to donate protons are called "protic" solvents, while solvents that do not have protons available to donate are called "aprotic" solvents. Beyond these classifications of polar/non-polar and protic/aprotic, other properties must also be considered when selecting a solvent. The melting point of the solvent must be sufficiently low and its boiling point sufficiently high to fit within the operating temperature of the process. Viscosity and density are other important properties to consider. Process designers generally choose a solvent that has the right properties for the process in order to gain the most benefit from the solvent.

Solutes are usually separated from solvents at the end of a process, and several techniques can be employed to bring about this separation. A common separation technique is distillation, in which the solution is heated to evaporate the solvent. The solute, now free of solvent, remains as a solid or liquid. Alternatively, if the solute is more volatile than the solvent, it can be evaporated and then condensed in a separate container. Another separation technique is precipitation followed by filtration. The solubility of a solid can be decreased by a variety of means, such as changing the temperature of the solution, adding salts to the mixture, or adding a second solvent. These changes cause the solute to precipitate from the solution. The mixture can then be filtered to separate the solid from the liquid. Other separation techniques involving transfer of a solute from one solvent

to another, such as liquid-liquid extractions, do not result in the compound being removed from solvents entirely. Rather, one solvent is simply replaced with another and this new solvent must also be removed from the compound at the end of the process by distillation or precipitation. Therefore, processes that require the solute to be removed from their solutions will typically end with a distillation. Processes that involve the addition of a second solvent to trigger precipitation or liquid-extraction will require distillation when the resulting solvent mixture is to be recycled.

Solvents are an important consideration in green chemistry. Because solvents usually make up the bulk of a solution, they are used on a much larger scale than other components in a process and therefore have a larger impact on the sustainability of the process than the other components. Processes can be considered unsustainable simply because the solvent used in the process has some negative effects on humans or the environment. Even when the solvent is not inherently hazardous, the separation steps used to remove the solvent (precipitation/filtration, distillation) are energy and/or material intensive, which violate green chemistry principles #5 and #6 as well as green engineering principles #3 and #4. The importance of the solvent choice is highlighted by green chemistry principle #5, in which solvents are named explicitly.

Because solvents have a large effect on the environmental impacts of chemical processes, there is much interest in identifying green solvents to use industrially. Several industrial groups have categorized common solvents in terms of their effects on safety, health, and the environment through solvent selection guides which can be used to select preferred solvents.[15–22] Prat *et al.* surveyed some of these selection guides and found good agreement between the different guides, with water, alcohols, ketones, and esters generally being recommended and most other solvents being problematic or hazardous based on health, safety, and environmental impacts.[23] Efforts have also been made to develop alternative solvents with beneficial properties that may be superior to traditional solvents in a variety of ways. Biomass-derived solvents are developed to perform similarly to traditional solvents with the added benefit of being renewably sourced.[24–26] Ionic liquids

are composed of liquid salts with negligible vapour pressures; therefore, they are not flammable and do not pose risks as airborne contaminants.[27–30] Solvents in the supercritical state have different properties than when in the liquid state, so safe solvents that are unsuitable for use in the liquid state may be useful in the supercritical state. Supercritical carbon dioxide is of particular interest because it is a common substance that has few associated risks and, importantly, enters the supercritical state at (relatively) mild pressures and temperatures.[31] The solvatochromic parameters of many of these alternative solvents have been reported to provide details about their behaviour to help promote their adoption into common use. Jessop *et al.* have compiled solvatochromic data for traditional solvents and alternative solvents in two reviews that highlight which alternative solvents could be used to replace which traditional solvents.[32,33] They also highlight traditional solvents that do not have similar properties to any reported alternative solvents and, therefore, do not have suitable replacements. Identifying replacements to these solvents indicates possible avenues for future research. These initiatives from industrial groups via solvent selection guides and academic researchers via studies into alternative solvents is a clear indication of the need and the desire to use safer solvents to create inherently safer chemical processes.

Identifying green solvents is not a straight-forward task and the alternative solvents discussed above are not always the best choices for making chemical processes safe for both humans and the environment. Water, despite having almost no risks associated with safety, is often not a good choice for a solvent. It requires large amounts of energy to distill and this energy often comes from the combustion of fossil fuels, resulting in large amounts of CO_2 emissions. Its use in chemical processes also competes with its use for consumption by humans, plants, and animals. The water used in chemical processes is rendered unsuitable for consumption and thereby limits the supply of available drinking water. Ionic liquids are often energy- and material-intensive to prepare and their preparation alone presents risks to humans and the environment.[34] Furthermore, they cannot be distilled, making solvent-solute separations difficult. A volatile organic solvent is

often used to facilitate these separations, removing the primary advantage of ionic liquids: avoiding the use of volatile organic compounds. Supercritical solvents require high pressures as well as vessels that can withstand high pressure conditions. The energy and materials costs for using high pressures as well as the dangers associated with pressurized systems are drawbacks of supercritical fluid solvents. The complications of using these alternative solvents can make their use less beneficial than the use of typical volatile organic solvents in many cases, causing what may appear to be green solvents at first glance to be undesirable upon closer examination. These alternative solvents must be carefully considered in order to determine whether they are actually provide more benefits than drawbacks when compared to typical organic solvents.

1.3 CO_2

Carbon dioxide is a common substance on Earth with well-understood properties. It is a colourless, odourless gas present in the atmosphere at concentrations of ~400 ppm. It is a linear molecule composed of a single carbon atom bound to two oxygen atoms. Each bond has a dipole moment and the dipoles cancel each other giving CO_2 a net-zero dipole moment, but a substantial quadrupole moment. The enthalpy of formation for CO_2 is -393.5 kJ/mol, so it is often considered to be inert.[35] However, it is weakly electrophilic and Lewis-acidic because the carbon atom is electron poor due to the higher electronegativity of the oxygen atoms. The carbon atom is also in a +4 oxidation state and can react with reducing agents, such as in the reaction of CO_2 with magnesium to form magnesium oxide and elemental carbon. The properties of CO_2 and its abundance make it an appealing choice for a variety of applications.

The acid/base behaviour of CO_2 in aqueous solutions is more complex than for many other acids. In aqueous solution, CO_2 reacts with water to form carbonic acid, a diprotic acid with a pK_{a1} value of 3.6 and a pK_{a2} value of 10.3. The first conjugate base of carbonic acid is bicarbonate (HCO_3^-) and the second conjugate base is carbonate (CO_3^{2-}). However, the formation of carbonic acid is unfavourable, having a hydration equilibrium constant of $K_h = [H_2CO_3]/[CO_2] = 1.7*10^{-3}$ in

water at 25 °C, so most of the CO_2 does not react with the water and is present in solution as dissolved CO_2.[36] Both carbonic acid and dissolved CO_2 act as Brønsted acids with bicarbonate as their conjugate base. Because the two acids are in equilibrium with each other, a mixture of the two species is often considered to be a single acidic species. The pK_{a1} of the mixture under standard conditions is 6.3, weaker than carbonic acid. The equilibrium of carbonic acid with dissolved CO_2 and the combined acidity of the two species make the acid/base properties of CO_2 more complicated than many other acids.

Although it is a gas under standard conditions, CO_2 can exist in other states under non-standard conditions. The phase diagram shown in Fig. 1.1 shows the state of CO_2 at different pressures and temperatures. Gaseous CO_2 is often used as a (relatively) inert gas in fire extinguishers, welding equipment, and aerosol cans. It is also used to create carbonated beverages. As a solid, CO_2 is commonly known as "dry ice" and is used for cooling materials. Liquid and supercritical CO_2 can be used as solvents for extractions and chemical transformations. Whether as a gas, solid, liquid, or supercritical fluid, CO_2 has proven to be a versatile compound for use in industry.

CO_2 also plays an important role in nature. It is the product of the biochemical cellular respiration process which converts chemical energy in sugars into a form of energy usable by organisms.[37] It is consumed by plants, algae, and other photosynthetic organisms and is converted to sugars by the process of photosynthesis.[37] In the ocean, CO_2 is converted to carbonate ions that are part of the structural materials of the shells of aquatic organisms.[38] CO_2 in the atmosphere plays a role in determining the temperature of Earth through its action as a greenhouse gas.[38] CO_2 therefore plays a major role in many crucial natural processes.

Although CO_2 occurs commonly in nature, high levels of CO_2 in the atmosphere can be detrimental to the environment. Since the start of the industrial revolution, the concentration of CO_2 in the atmosphere has risen from approx. 280 ppm to over 400 ppm.[39,40] Due to the role of CO_2 as

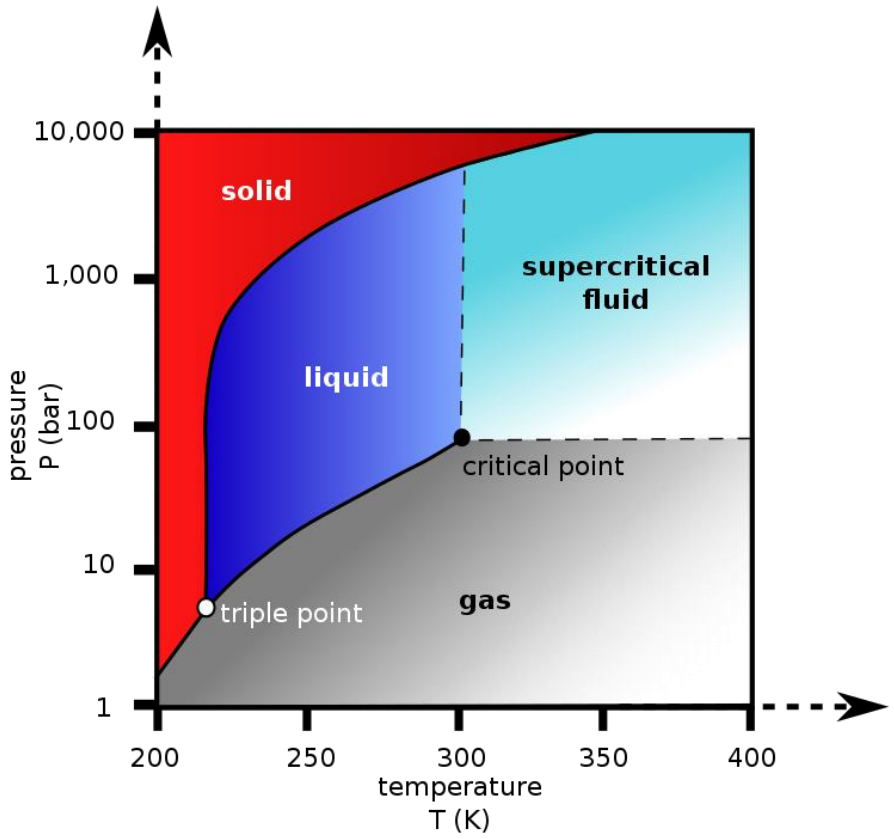

Fig. 1.1 The pressure-temperature phase diagram for CO_2. This image was reproduced under the Creative Commons CC0 1.0 license.[43]

---

a greenhouse gas, its increasing atmospheric concentration has contributed to an increase in global mean temperatures.[41] Higher concentrations of CO_2 in the atmosphere have also caused a decrease in ocean pH.[41] These changes caused by CO_2 have widespread consequences for the environment including coral bleaching, rising sea levels, deglaciation, and increasing frequency of extreme weather events.[42] As CO_2 continues to build up in the atmosphere, these effects of CO_2 on the environment are likely to become increasingly more pronounced and problematic.

While CO_2 generation can cause environmental problems, CO_2 can also be a solution to some of these problems if it can serve as a substitute for more harmful substances. For example, supercritical CO_2 can be used to decaffeinate coffee beans, replacing more harmful decaffeinating

solvents such as dichloromethane. CO_2 can be used as an alternative to common acids such as sulfuric and hydrochloric acid to control the pH of aqueous solutions or to perform acid catalysis.[44] When used in place of more dangerous substances, CO_2 can help to limit the impact of human activity on the environment.

1.4 Switchable hydrophilicity solvents

The field of research on CO_2-switchable materials has attracted increasing interest since the first report of switchable polarity solvents in 2005.[45] These switchable materials all contain a switchable functional group, typically an amine or amidine, which can react reversibly with CO_2 to form a different compound with different properties. The reaction with CO_2 is most commonly an acid-base reaction in the presence of water that converts the switchable material between a neutral compound and a bicarbonate salt (Equation 1.3). The reaction can be driven to one side by bubbling CO_2 into a solution containing the switchable material and can be driven to the other side by heating the system and/or adding an inert gas to displace the CO_2. Although this acid-base reaction is the most commonly used reaction to induce switching in CO_2-switchable materials, other reversible reactions are possible. Primary and secondary amines can react directly with CO_2 to form ammonium carbamate salts (Equation 1.4). The carbamate anions can be converted to bicarbonate ions by hydrolysis (Equation 1.5). Carbamate salt formation typically occurs faster than bicarbonate formation, but a larger energy input is required to reverse the reaction.[46] Primary amines can also react with CO_2 to form ureas (Equation 1.6), but in the absence of a catalyst this reaction only occurs at high temperatures.[47] Many different CO_2-switchable materials have been reported including switchable polarity solvents,[48] switchable aqueous ionogens,[49] switchable surfactants,[50] and switchable hydrophilicity solvents (SHSs).[51]

Eqn. 1.3

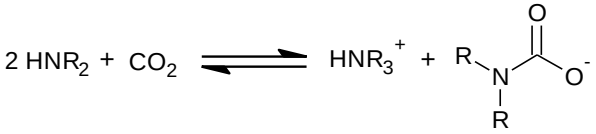

Eqn. 1.4

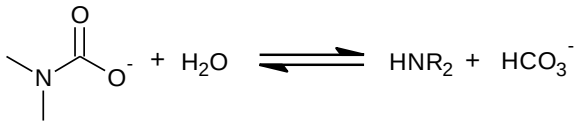

Eqn. 1.5

Eqn. 1.6

SHSs are solvents that are poorly miscible with water in the absence of CO_2 (form biphasic mixtures with water, "hydrophobic"), completely miscible with water in the presence of CO_2 (form monophasic mixtures with water, "hydrophilic"), and can be switched between these two states by the addition or removal of CO_2.[51] Like many other switchable materials, SHSs are amines or amidines that react with CO_2 and water to form bicarbonate salts with different properties than the neutral SHSs.[51,52] This ability to switch between states with different hydrophilicities has been used for such applications as solvent-solute separations,[51–57] water purification by forward osmosis,[58–62] and microextractions for environmental analysis.[63–69]

Miscibility with water is important in "two-component" systems where there is no third component that a SHS could partition into (e.g. a hydrophobic liquid such as 1-octanol). These two-component systems are useful for identifying SHSs. A compound can be tested for switchable hydrophilicity with a three-step experiment. First, the compound is mixed with water. If it forms a biphasic mixture, then CO_2 is bubbled through the mixture. If the two liquids merge to form a monophasic mixture, then CO_2 is subsequently removed from the system. If the two liquids separate to form a biphasic mix, then the compound is a SHS. If the mixture fails to exhibit the desired behaviour (biphasic, monophasic, then biphasic again), then the compound is not a SHS at those conditions. The behaviour of a SHS in the two-liquid system is shown graphically in Fig. 1.2.

One of the most studied applications of SHSs is in solvent-solute separations. Separations based on the switchable behavior of SHSs were first proposed in 2010.[51] Such a process is outlined in Fig. 1.3. A hydrophobic solute such as soybean oil dissolved in a SHS can be separated from the SHS by adding water to the mixture and bubbling CO_2 through the system. The CO_2 facilitates the

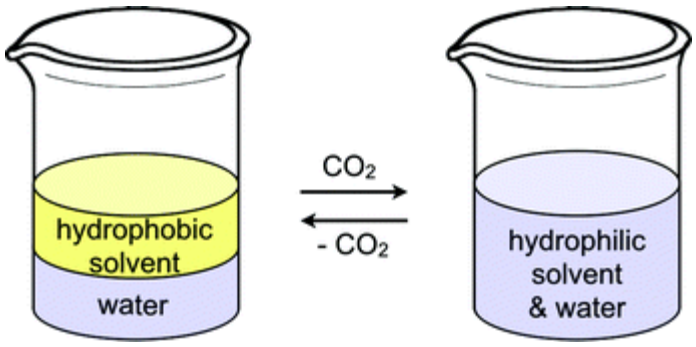

Fig. 1.2 The two-liquid SHS system (image reproduced from Jessop et al., 2011 with permission from the authors).[52]

protonation of the SHS and causes it to enter the aqueous phase while the hydrophobic solute remains in a separate liquid or solid phase, so that it can be isolated by decantation or filtration. The SHS can be recovered from the aqueous phase by heating the mixture and bubbling an inert gas through it to remove the CO_2. This process deprotonates the SHS and reverts it to its hydrophobic state, causing it to phase-separate from water. The two liquid phases can be separated by decantation and both the SHS and water can be reused in further separations. Reports of SHS-based separation processes include the isolation of soybean oil,[51] polystyrene,[52] bitumen,[57] algal lipids,[53,55,56] and lignin-derived phenols.[54]

The critical step in this process is the partitioning of the SHS into the aqueous phase upon addition of CO_2. The organic phase created by the product of the extraction may contain SHS if the SHS does not partition completely into the aqueous phase. If this is the case, the separation will be incomplete. In these "three-component" systems, therefore, the distribution coefficient of the SHS between the aqueous phase and the organic phase becomes an important property rather than the miscibility of the SHS with water, which is important in the two-component system. When a SHS with a favourable distribution coefficient is used, more SHS will partition into the aqueous phase and the organic phase isolated by decantation will contain a low amount of SHS contaminant.

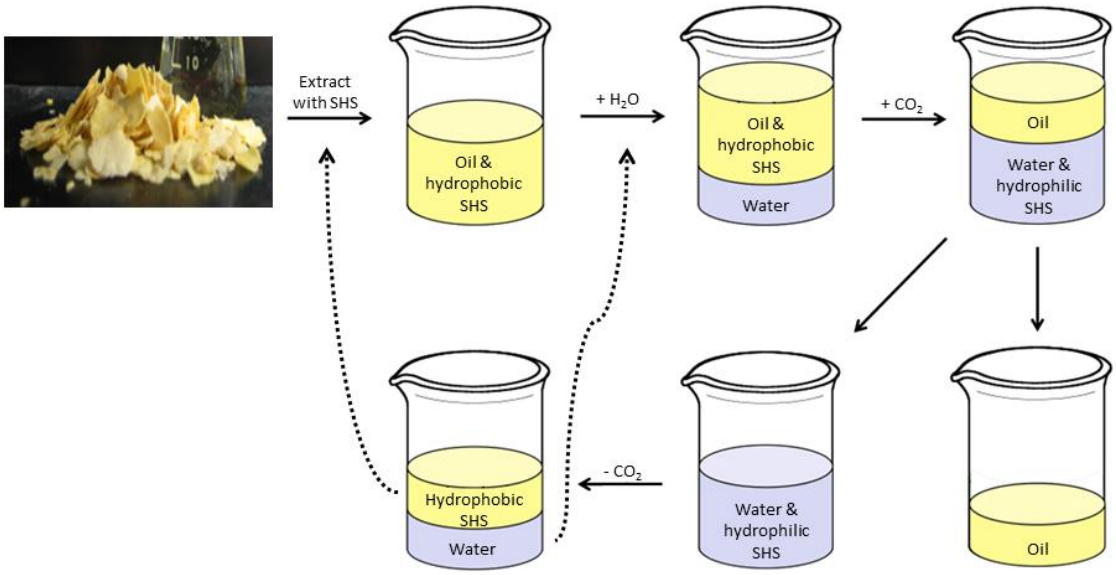

Fig. 1.3 An outline of a process used to isolate lipids from soybean flakes using a SHS. The steps that include mixes of oil, water, and SHS are examples of three-component systems (image reproduced from Vanderveen et al. with permission from the authors).[70]

Solvent-solute based separations are one of the most explored applications of SHSs due to the potential process and safety advantages offered by the technology. Because this separation process does not involve distillation, the solvent does not need to be a volatile liquid. Therefore, using a SHS-based separation process allows for the use of low-volatility, low-flammability solvents that reduce the risk of fires and explosions. By avoiding these hazards and the energy-intensive distillation step, SHSs provide alternatives to traditional solvents and meet the goals outlined in green chemistry principles #5, #6, and #12.

The use of SHSs as a reversible draw solute for water desalination by forward osmosis has also been investigated.[58–62] Aqueous solutions with high osmotic pressures can be generated by the addition of a SHS and CO_2 to the system to create a concentrated SHS-bicarbonate solution. This solution can draw water away from an impure aqueous solution through a semipermeable membrane via forward osmosis. Unlike reverse osmosis processes, no external force must be

supplied to draw water away from the impure aqueous solution. After the osmotic pressure of the two solutions has equalized, the diluted aqueous SHS solution can be isolated and the SHS can be converted to its hydrophobic state by heating the solution and bubbling an inert gas through it. This process causes the SHS to phase-separate from the aqueous phase. The resulting aqueous phase has a low salt content. Therefore, by the action of both switchable hydrophilicity and switchable osmotic pressure, SHSs act as effective reversible draw agents for forward osmosis water desalination.

A third application for SHSs currently being explored is in microextractions for the detection and quantification of environmental contaminants.[63] By creating a homogeneous mixture of SHS and water with CO_2, then phase-separating the two liquids by adding sodium hydroxide, the analyte partitions into the SHS phase as the phase separation occurs. This process is referred to as homogeneous liquid-liquid extraction (HLLE) or switchable solvent liquid phase microextraction (SS LPME) and offers improvements to the dispersive liquid-liquid microextraction (DLLME) technique. In DLLME, an extracting solvent is dispersed into an aqueous sample by the addition of a dispersing agent to improve the kinetics of the extraction and minimize extraction solvent use.[64] The drawbacks of DLLME are the requirement of additional materials (the dispersing agent) and the difficulty in recovering the extracting solvent from the mixture. The SHS-based HLLE technique eliminates the need for a dispersing agent, thereby reducing the material requirements and simplifying the recovery of the extracting solvent. SHSs have been used in HLLE processes for analysis of both organic[63,65] and inorganic[66–69] environmental contaminants.

Efforts to improve SHS technology continue to play an important role in increasing the appeal of processes making use of SHSs. The first reported SHSs contained amidines as the switchable functional groups.[51] Although these SHSs were academically valuable as a first example of the technology, their synthesis was considered too involved to be viable as a solvent in industrial

applications.[52] In response to this concern, several inexpensive tertiary amine-based SHSs were reported and these have become the standard SHSs in use today.[52] *N*,*N*-Dimethylcyclohexylamine (DMCA) in particular has received much attention due to its availability, low cost, and relatively low volatility compared to other trialkylamine SHSs. Further improvements to SHSs have since been made. Wilson and coworkers' research into SHSs as reversible draw agents for forward osmosis led to the identification of 1-cyclohexylpiperidine as an ideal SHS for this purpose.[60] Samorì *et al*. identified SHSs with low toxicity to aquatic organisms.[60,71] My contributions in developing improvements to SHS technology are the subject of this thesis and will be described in the chapters that follow. In the context of green chemistry, it is important to improve SHSs not only in terms of how they influence a given process but also in terms of their effects on the environment and on human health and safety. Identifying new SHSs with improved properties benefits all processes that use SHS and the continued search for better SHSs will benefit this field of study.

1.5 Objectives

The goal of the research presented in this thesis was to advance the understanding of SHSs and apply this knowledge to design SHSs which are safe for both humans and the environment. Identifying new SHSs contributes to a pool of data which details the behaviour of amines or amidines and whether they act as SHSs. A model describing SHS behaviour can be validated by comparing it to this pool of data. The model can then be used to predict the behaviour of untested compounds and guide the search for new SHSs, which in turn provide more data and help to improve the model. This two-pronged approach – understanding SHSs through modelling and identifying new, less-hazardous SHSs – will be used throughout the work and each prong will be used to inform and guide the other.

1.6 References

1) M. Nakamaru, Y. Iwasa and J. Nakanishi, *Chemosphere*, 2003, **53**, 377–387.

2) M. J. Molina and F. S. Rowland, *Nature*, 1974, **249**, 810.

3) J. Hansen, D. Johnson, A. Lacis, S. Lebedeff, P. Lee, D. Rind and G. Russell, *Science*, 1981, **213**, 957–966.

4) US EPA, Basics of Green Chemistry, https://www.epa.gov/greenchemistry/basics-green-chemistry, (accessed 13 December 2017).

5) P. T. Anastas and J. C. Warner, *Green chemistry: theory and practice*, Oxford University Press, Oxford [England] ; New York, 1998.

6) P. T. Anastas and J. B. Zimmerman, *Environ. Sci. Technol.*, 2003, **37**, 94A-101A.

7) 12 Principles of Green Chemistry, https://www.acs.org/content/acs/en/greenchemistry/what-is-green-chemistry/principles/12-principles-of-green-chemistry.html, (accessed 13 December 2017).

8) 12 Principles of Green Engineering, https://www.acs.org/content/acs/en/greenchemistry/what-is-green-chemistry/principles/12-principles-of-green-engineering.html, (accessed 13 December 2017).

9) B. M. Trost, *Science*, 1991, **254**, 1471–1477.

10) R. A. Sheldon, *Green Chem.*, 2007, **9**, 1273–1283.

11) ISO 14040:2006 - Environmental management -- Life cycle assessment -- Principles and framework, https://www.iso.org/standard/37456.html, (accessed 2 January 2018).

12) ISO 14044:2006 - Environmental management -- Life cycle assessment -- Requirements and guidelines, https://www.iso.org/standard/38498.html, (accessed 2 January 2018).

13) M. J. Kamlet, J. L. Abboud and R. W. Taft, *J. Am. Chem. Soc.*, 1977, **99**, 6027–6038.

14) M. J. Kamlet, T. N. Hall, J. Boykin and R. W. Taft, *J. Org. Chem.*, 1979, **44**, 2599–2604.

15) D. Prat, O. Pardigon, H.-W. Flemming, S. Letestu, V. Ducandas, P. Isnard, E. Guntrum, T. Senac, S. Ruisseau, P. Cruciani and P. Hosek, *Org. Process Res. Dev.*, 2013, **17**, 1517–1525.

16) K. Alfonsi, J. Colberg, P. J. Dunn, T. Fevig, S. Jennings, T. A. Johnson, H. Peter Kleine, C. Knight, M. A. Nagy, D. A. Perry and M. Stefaniak, *Green Chem.*, 2008, **10**, 31–36.

17) C. Jiménez-González, D. J. Constable, A. D. Curzons and V. L. Cunningham, *Clean Technol. Environ. Policy*, 2002, **4**, 44–53.

18) C. Jiménez-González, A. D. Curzons, D. J. C. Constable and V. L. Cunningham, *Clean Technol. Environ. Policy*, 2004, **7**, 42–50.

19) R. K. Henderson, C. Jiménez-González, D. J. C. Constable, S. R. Alston, G. G. A. Inglis, G. Fisher, J. Sherwood, S. P. Binks and A. D. Curzons, *Green Chem.*, 2011, **13**, 854–862.

20) C. M. Alder, J. D. Hayler, R. K. Henderson, A. M. Redman, L. Shukla, L. E. Shuster and H. F. Sneddon, *Green Chem.*, 2016, **18**, 3879–3890.

21) D. Prat, A. Wells, J. Hayler, H. Sneddon, C. R. McElroy, S. Abou-Shehada and P. J. Dunn, *Green Chem.*, 2015, **18**, 288–296.

20) ACS Green Chemistry Institute Pharmaceutical Roundtable. Solvent Selection Guide: Version 2.0. March 21, 2011, https://www.acs.org/content/dam/acsorg/greenchemistry/industriainnovation/roundtable/acs-gci-pr-solvent-selection-guide.pdf, (accessed 14 November 2017).

23) D. Prat, J. Hayler and A. Wells, *Green Chem.*, 2014, **16**, 4546–4551.

24) M. Perez-Sanchez, M. Sandoval and M. J. H. and P. D. de María, Biocatalysis in Biomass-derived Solvents, http://www.eurekaselect.com/111692/article, (accessed 14 November 2017).

25) S. Santoro, F. Ferlin, L. Luciani, L. Ackermann and L. Vaccaro, *Green Chem.*, 2017, **19**, 1601–1612.

26) Z. Li, K. H. Smith and G. W. Stevens, *Chin. J. Chem. Eng.*, 2016, **24**, 215–220.

27) M. J. Earle and K. R. Seddon, in *Clean Solvents*, American Chemical Society, 2002, vol. 819, pp. 10–25.

28) Suresh and J. S. Sandhu, *Green Chem. Lett. Rev.*, 2011, **4**, 289–310.

29) Suresh and J. S. Sandhu, *Green Chem. Lett. Rev.*, 2011, **4**, 311–320.

30) H. Zhao, S. Xia and P. Ma, *J. Chem. Technol. Biotechnol.*, 2005, **80**, 1089–1096.

31) E. Ramsey, Q. Sun, Z. Zhang, C. Zhang and W. Gou, *J. Environ. Sci.*, 2009, **21**, 720–726.

32) P. G. Jessop, D. A. Jessop, D. Fu and L. Phan, *Green Chem.*, 2012, **14**, 1245–1259.

33) P. G. Jessop, *Green Chem.*, 2011, **13**, 1391–1398.

34) Y. Zhang, B. R. Bakshi and E. S. Demessie, *Environ. Sci. Technol.*, 2008, **42**, 1724–1730.

35) T. Engel and P. J. Reid, *Physical Chemistry*, Prentice Hall, 2010.

36) C. Housecroft and A. G. Sharpe, *Inorganic Chemistry*, Pearson Higher Ed, 2012.

37) J. M. Berg, J. L. Tymoczko and L. Stryer, *Biochemistry*, W. H. Freeman, 2010.

38) G. W. VanLoon and S. J. Duffy, *Environmental Chemistry: A Global Perspective*, Oxford University Press, 2005.

39) D. M. Etheridge, L. P. Steele, R. L. Langenfelds, R. J. Francey, J.-M. Barnola and V. I. Morgan, *J. Geophys. Res. Atmospheres*, 1996, **101**, 4115–4128.

40) N. US Department of Commerce, ESRL Global Monitoring Division - Global Greenhouse Gas Reference Network, https://www.esrl.noaa.gov/gmd/ccgg/trends/global.html, (accessed 2 January 2018).

41) T. F. Stocker, D. Qin, G.-K. Plattner, M. Tignor, S. K. Allen, J. Boschung, A. Nauels, Y. Xia, V. Bex and P. M. Midgley, Eds., *IPCC, 2013: Summary for Policymakers. In: Climate Change 2013: They Physical Science Basis. Contributions of the Working Group I to the Fifth Assessment Report of the Intergovernmental Panel on Climate Change*, Cambridge University Press, Cambridge, United Kingdom and New York, NY, USA.

42) C. B. Field, V. R. Barros, D. J. Dokken, K. J. Mach, M. D. Mastrandrea, T. E. Bilir, M. Chatterjee, K. L. Ebi, Y. O. Estrada, R. C. Genova, B. Girma, E. S. Kissel, A. N. Levy, S. MacCracken, P. R. Mastrandrea and L. L. White, Eds., *IPCC, 2014: Summary for policymakers. In: Climate Change 2014: Impacts, Adaptation, and Vulnerability. Intergovernmental Panel on Climate Change*,

Cambridge University Press, Cambridge, United Kingdom and New York, NY, USA.

43) B. F. Jacobs, *English: Phase diagram of CO2 (carbon dioxide). X axis is temperature in kelvin; Y axis is pressure in bar.*, 2010.

44) S. E. Hunter and P. E. Savage, *Ind. Eng. Chem. Res.*, 2003, **42**, 290–294.

45) P. G. Jessop, D. J. Heldebrant, X. Li, C. A. Eckert and C. L. Liotta, *Nature*, 2005, **436**, 1102.

46) F. Bougie and M. C. Iliuta, *J. Chem. Eng. Data*, 2012, **57**, 635–669.

47) J. F. Mulvaney and R. L. Evans, *Ind. Eng. Chem.*, 1948, **40**, 393–397.

48) L. Phan, D. Chiu, D. J. Heldebrant, H. Huttenhower, E. John, X. Li, P. Pollet, R. Wang, C. A. Eckert, C. L. Liotta and P. G. Jessop, *Ind. Eng. Chem. Res.*, 2008, **47**, 539–545.

49) S. M. Mercer and P. G. Jessop, *ChemSusChem*, 2010, **3**, 467–470.

50) Y. Liu, P. G. Jessop, M. Cunningham, C. A. Eckert and C. L. Liotta, *Science*, 2006, **313**, 958–960.

51) P. G. Jessop, L. Phan, A. Carrier, S. Robinson, C. J. Dürr and J. R. Harjani, *Green Chem.*, 2010, **12**, 809–814.

52) P. G. Jessop, L. Kozycz, Z. G. Rahami, D. Schoenmakers, A. R. Boyd, D. Wechsler and A. M. Holland, *Green Chem.*, 2011, **13**, 619–623.

53) A. R. Boyd, P. Champagne, P. J. McGinn, K. M. MacDougall, J. E. Melanson and P. G. Jessop, *Bioresour. Technol.*, 2012, **118**, 628–632.

54) D. Fu, S. Farag, J. Chaouki and P. G. Jessop, *Bioresour. Technol.*, 2014, **154**, 101–108.

55) Y. Du, B. Schuur, C. Samorì, E. Tagliavini and D. W. F. Brilman, *Bioresour. Technol.*, 2013, **149**, 253–260.

56) C. Samorì, D. L. Barreiro, R. Vet, L. Pezzolesi, D. W. F. Brilman, P. Galletti and E. Tagliavini, *Green Chem.*, 2013, **15**, 353–356.

57) A. Holland, D. Wechsler, A. Patel, B. M. Molloy, A. R. Boyd and P. G. Jessop, *Can. J. Chem.*, 2012, **90**, 805–810.

58) A. D. Wilson and F. F. Stewart, *RSC Adv.*, 2014, **4**, 11039–11049.

59) A. D. Wilson and C. J. Orme, *RSC Adv.*, 2014, **5**, 7740–7751.

60) C. J. Orme and A. D. Wilson, *Desalination*, 2015, **371**, 126–133.

61) M. L. Stone, C. Rae, F. F. Stewart and A. D. Wilson, *Desalination*, 2013, **312**, 124–129.

62) D. S. Wendt, C. J. Orme, G. L. Mines and A. D. Wilson, *Desalination*, 2015, **374**, 81–91.

63) G. Lasarte-Aragonés, R. Lucena, S. Cárdenas and M. Valcárcel, *Talanta*, 2015, **131**, 645–649.

64) M. Rezaee, Y. Assadi, M.-R. Milani Hosseini, E. Aghaee, F. Ahmadi and S. Berijani, *J. Chromatogr. A*, 2006, **1116**, 1–9.

65) G. Lasarte-Aragonés, R. Lucena, S. Cárdenas and M. Valcárcel, *J. Sep. Sci.*, 2015, **38**, 990–995.

66) E. Yilmaz and M. Soylak, *Anal. Chim. Acta*, 2015, **886**, 75–82.

67) M. Khan and M. Soylak, *RSC Adv.*, 2016, **6**, 24968–24975.

68) M. Soylak, M. Khan and E. Yilmaz, *Anal. Methods*, 2016, **8**, 979–986.

69) E. Yilmaz and M. Soylak, *J. Anal. At. Spectrom.*, 2015, **30**, 1629–1635.

70) J. R. Vanderveen, R. I. Canales, Y. Quan, C. B. Chalifoux, M. A. Stadtherr, J. F. Brennecke and P. G. Jessop, *Fluid Phase Equilibria*, 2016, **409**, 150–156.

71) C. Samorì, L. Pezzolesi, D. L. Barreiro, P. Galletti, A. Pasteris and E. Tagliavini, *RSC Adv.*, 2014, **4**, 5999–6008.

Chapter 2

Design and Evaluation of Switchable-Hydrophilicity Solvents

2.1 Introduction

As described in Section 1.4, one promising application of SHSs is the use of SHS-based separations as an alternative to distillation for solvent-solute separations. Distillation requires the use of volatile solvents which are often associated with hazards such as flammability and smog formation. The SHS-based separation technique described in Section 1.4 does not rely on volatility as a property by which compounds are separated. As such, a process using a SHS rather than a traditional volatile solvent can avoid hazards that are innate to processes using volatile organic compounds.

Prior to the work discussed in this chapter, two series of SHSs were reported: one series of amidine SHSs and one series of tertiary amine SHSs.[1,2] The first reported SHSs were alkyl amidine compounds: *N*,*N*,*N*'-tripropylbutanamidine and *N*,*N*,*N*'-tributylpentanamidine.[1] Among the amidines, only *N*,*N*,*N*'-tributylpentanamidine was reported to switch reliably; *N*,*N*,*N*'-tripropylbutanamidine did not always phase-separate from water after the removal of CO_2, possibly due to a combination of its higher relative hydrophilicity and incomplete removal of CO_2. Several alkyl guanidines were also tested for switchable hydrophilicity, but they did not phase-separate from carbonated water under the conditions used for removing CO_2 from the mixture due to the high basic strength of guanidines. While the amidine SHSs identified in this first publication displayed unique switchable behaviour, they were found to be impractical solvents because they are commercially unavailable and potentially hydrolytically unstable. They also have complex synthetic routes compared to traditional solvents.[2]

In the second reported series of SHSs, eight commercially available trialkylamines were found to display switchable hydrophilicity.[2] The investigation into the switchable hydrophilicity behaviour of tertiary amines was driven by the need to find economically viable alternatives to the

amidine SHSs. Although these solvents are more accessible and practical than the amidine SHSs, some of them have health and safety concerns associated with them, such as toxicity, volatility, or flammability, making them less desirable for industrial purposes. Volatility and flammability in particular are hazards that SHS-based systems are intended to avoid, so the use of a volatile and flammable SHS is counterproductive.

Another property which could be improved on is the rate at which SHSs switch when CO_2 is added to switch them from their hydrophobic states to their hydrophilic states. In a proposed application of trialkylamine SHSs for converting polystyrene foam into polystyrene powder, the resulting powder contained 5 wt% SHS.[2] One hypothesized reason for this contamination was that the SHS did not switch from its hydrophobic state to its hydrophilic state fast enough. As the polystyrene precipitated, some hydrophobic SHS stayed associated with the polystyrene, which encased it and prevented it from entering the aqueous phase. If the switch to the hydrophilic state was more rapid, the SHS might enter the aqueous phase before it became encased in the polystyrene, resulting in a more pure polystyrene powder at the end of the process.

This chapter focuses on designing amine SHSs with beneficial properties and evaluating some of the risks associated with SHSs. The amines were designed to display switchable hydrophilicity and avoid the problems found with previously-identified tertiary amine SHSs. This work had two major foci. The first focus was to develop amine-based SHSs with low volatility and flammability. Amino compounds containing other functional groups were investigated for this purpose. The second focus was to identify SHSs capable of becoming hydrophilic more quickly than other known SHS. Secondary amino compounds were investigated for this purpose.

Prior to searching for new SHSs, the pK_{aH} and log K_{ow} values of compounds previously tested were studied to identify possible correlations between these values and switchable hydrophilicity behaviour. These compounds and their corresponding pK_{aH} and log K_{ow} values are listed in Table 2.1 and shown graphically in Fig. 2.1. The hydrophobicity of a compound, as

Table 2.1 Amines, amidines, and guanidines previously tested for their ability to act as SHSs at room temperature (21 °C).[1,2]

Behaviour	Compound Number	Compound Name	Ratio of Water to Compound (v:v)	Log K_{ow}[a]	pK_{aH}
Monophasic	**2.1**	Triethanolamine	1:1	-1.51	7.85[3]
Monophasic	**2.2**	*N,N,N',N'*-Tetramethylethylenediamine	1:1	0.21	9.28[4]
Monophasic	**2.3**	*N,N,N',N'*-Tetramethylguanidine	2:1	0.30	13.6[5]
Monophasic	**2.4**	*N*-Ethylmorpholine	1:1	0.30	7.70[6]
Monophasic	**2.5**	1,8-Diazabicycloundec-7-ene	2:1	1.73	12[9]
Monophasic	**2.6**	*N*-Hexyl-*N',N'*-dimethylacetamidine	2:1	2.94	12[b]
Irreversible	**2.7**	*N''*-Hexyl-*N,N,N',N'*-tetramethylguanidine	2:1	2.82	13.6[c]
Irreversible	**2.8**	*N''*-Butyl-*N,N,N',N'*-tetraethylguanidine	2:1	3.52	13.6[c]
Irreversible	**2.9**	*N''*-Hexyl-*N,N,N',N'*-tetraethylguanidine	2:1	4.43	13.6[c]
Switchable	**2.10**	Triethylamine	1:1	1.47	10.68[7]
Switchable	**2.11**	*N*,*N*-Dimethylbutylamine	1:1	1.60	10.02[8]
Switchable	**2.12**	*N*-Ethylpiperidine	1:1	1.75	10.45[6]
Switchable	**2.13**	*N*-Methyldipropylamine	1:1	1.96	10.4[9]
Switchable	**2.14**	*N*,*N*-Dimethylcyclohexylamine	1:1	2.04	10.48[10]
Switchable	**2.15**	*N*-Butylpyrrolidine	1:1	2.15	10.36[11]
Switchable	**2.16**	*N*,*N*-Diethylbutylamine	1:1	2.37	10.51[d]
Switchable	**2.17**	*N*,*N*-Dimethylhexylamine	1:1	2.51	10.18[d]
Switchable	**2.18**	*N,N,N'*-Tripropylbutanamidine	2:1	4.20	12[b]
Switchable	**2.19**	*N,N,N'*-Tributylpentanamidine	2:1	5.99	12[b]
Biphasic	**2.20**	*N*,*N*-Dimethylaniline	1:1	2.11	5.06[10]
Biphasic	**2.21**	*N*,*N*-Diisopropylethylamine	1:1	2.28	11.0[12]
Biphasic	**2.22**	Tripropylamine	1:1	2.83	10.70[6]
Biphasic	**2.23**	*N''*-Hexyl-*N,N,N',N'*-tetrabutyguanidine	2:1	7.91	13.6[c]
Biphasic	**2.24**	Trioctylamine	1:1	9.45	10.9[e]

[a]Predicted using ALOGPS software version 2.1.[13–15] [b]Estimated to have a pK_{aH} similar to 1,8-diazabicycloundec-7-ene. [c]Estimated to have a pK_{aH} similar to *N,N,N',N'*-tetramethylguanidine. [d]Measured in this study. [e]Estimated to have a pK_{aH} similar to tributylamine (pK_{aH} 10.89).[6]

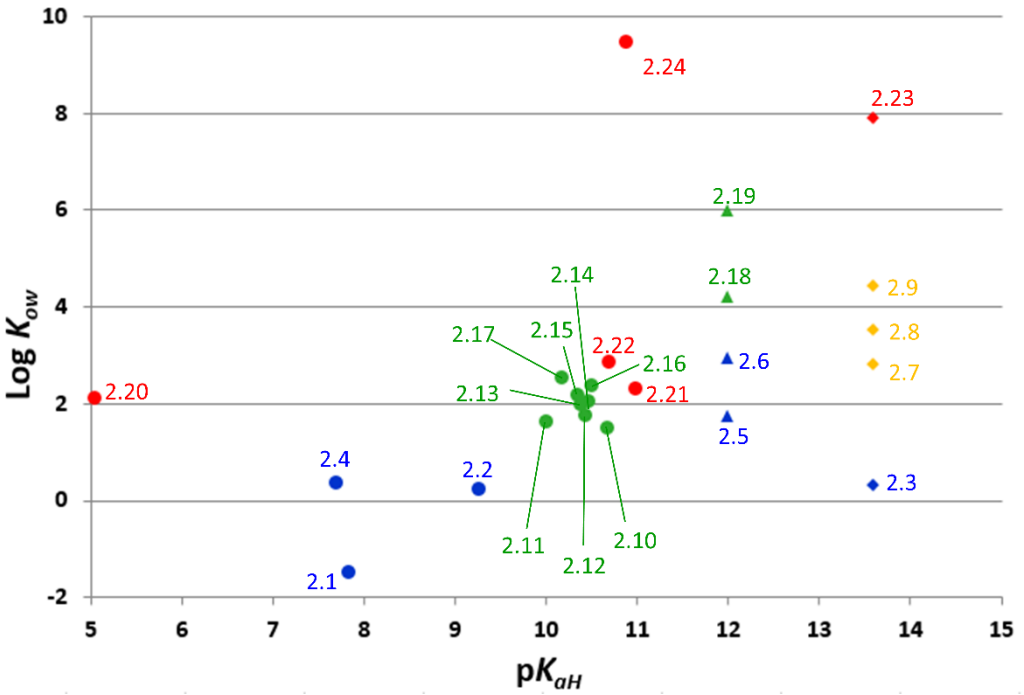

Fig. 2.1 Amines (circles), amidines (triangles), and guanidines (diamonds) listed in Table 2.1, plotted by their log K_{ow} and pK_{aH} and coloured by their observed behaviour: monophasic (blue), irreversible (yellow), switchable (green), and biphasic (red).

measured by log K_{ow}, was already considered to be one of the properties that determined if an amine or amidine displayed switchable hydrophilicity behaviour.[1,2] A very hydrophilic compound would be completely miscible with water even in the absence of CO_2. Conversely, a very hydrophobic compound would be poorly miscible with water even in the presence of CO_2. Only amines and amidines with certain hydrophobicities, as measured by log K_{ow}, should be poorly miscible with water in the absence of CO_2 but become completely miscible with water in the presence of CO_2. For amidines, log K_{ow} values between 3 and 7 were considered to be appropriate for switchable behaviour.[1] For amines, this log K_{ow} range was found to be between 1.2 and 2.5.[2]

The possible relationship between the basicity of an amine or amidine and switchable hydrophilicity had not been discussed in the literature, but such a relationship seemed likely because the switching mechanism for SHSs is an acid-base reaction. Amines and amidines are weak

bases and CO_2 is a weak acid, so the acid-base reaction between the two is an equilibrium. The more basic the amine or amidine is, the more this equilibrium will lie on the side of bicarbonate salt. If an amine or amidine is not sufficiently basic, the equilibrium will not lie far enough on the side of the salt and a switch from neutral amine or amidine to charged ammonium or amidinium will be minimal. Therefore, the basicity of a molecule is likely to affect whether it will display CO_2-switchable behavior.

The compounds in Table 2.1 and Fig 2.1 are separated into four categories based on their behaviours. Compounds with "monophasic" behaviour form monophasic mixtures with water even in the absence of CO_2 (blue dots in Fig 2.1). If a mixture of a compound and water is biphasic both before and after the addition of CO_2, the compound is considered "biphasic" (red dots in Fig 2.1). A compound is considered to have "switchable" behaviour if a mixture of the compound and water is biphasic in the absence of CO_2 and becomes monophasic in the presence of CO_2 (green dots in Fig 2.1). Some guanidine/water mixtures were reported to be biphasic initially and monophasic after the addition of CO_2, but the mixtures could not be reverted to their biphasic state, presumably because of the high basic strength of the guanidines. Compounds which display this behaviour are considered to have "irreversible" behaviour (yellow dots in Fig 2.1). More extreme conditions, such as very high temperatures, may allow these mixtures to become biphasic again but such conditions have not been investigated. Only compounds with switchable behaviour are viable SHSs. Furthermore, the results of these tests are dependent on the volume ratios of water and compound used. The effects of different volume ratios are discussed in detail in Chapter 4. The results shown in Table 2.1 and Fig. 2.1 were reported for 1:1 (v:v) mixtures of water to amine or 2:1 (v:v) mixtures of water to amidine or guanidine.

Based on the data shown in Table 2.1 and Fig. 2.1, insights into the relationship between log K_{ow}, pK_{aH}, and switchable hydrophilicity can be attained. The range of log K_{ow} values for amines with switchable behaviour is between 1.47 and 2.51, which is in good agreement with the proposed range of 1.2-2.5. Amines with monophasic behaviour have log K_{ow} values of 0.30 and below. There

is a range of log K_{ow} values between 0.30 and 1.47 that remains untested. Three amines are reported to have biphasic behaviour. *N*,*N*-Dimethylaniline has an acceptable log K_{ow} (2.11) but it is not a SHS, suggesting that its pK_{aH} (5.06) must be too low for it to exhibit switchable behaviour. Tripropylamine is too hydrophobic with a log K_{ow} value of 2.83. *N*,*N*-Diisopropylethylamine has an acceptable log K_{ow} and a pK_{aH} comparable to the switchable amines, but does not display switchable behaviour. This unexpected result has been attributed to the steric hindrance around the amine center of the molecule that destabilizes ion-pairing of the protonated SHS and the bicarbonate ion.[16] Taken together, the data from Table 2.1 support the proposed requirement of $1.2 < \log K_{ow} < 2.5$ for monoamine SHSs, though refinement on the lower end of the range would be beneficial. With regard to pK_{aH}, the lowest value for a switchable compound is 10.02 and the highest value for a non-switchable compound is 5.06. Some non-SHS amines have pK_{aH} values larger than 5.06 but their non-switchable behaviour can be attributed to their log K_{ow} values instead of their poor basicities. The range of untested pK_{aH} values spans from 5.06 to 10.02; further investigation of this range is required in order to deduce the appropriate pK_{aH} requirements for amines to display switchable hydrophilicity.

In this chapter, several secondary and tertiary amines were tested for switchable hydrophilicity in order to refine the log K_{ow} and pK_{aH} requirements for amine-based SHSs and also to identify SHSs with improved properties relative to the previously identified SHSs listed in Table 2.1, specifically faster switching and lower volatility. This chapter has been reproduced from Vanderveen *et al.*, *Green Chem.*, 2014, **16**, 1187-1197.[17] Various changes have been made to better fit the format and theme of this thesis.

2.2 Results and discussion

A variety of secondary and tertiary amine compounds were tested for switchable behaviour. The amines tested, their behaviours, their predicted log K_{ow} values, and their pK_{aH} values are shown in Table 2.2 and Table 2.3. These amines were selected to help refine the log K_{ow} and pK_{aH}

requirements for amine-based SHSs, but also to identify SHSs with low volatility and rapid switching. Because these SHSs were developed for multiple purposes, the data in the tables will be discussed multiple times in the context of each purpose. However, Table 2.2 contains data focused primarily on SHSs with low volatility and Table 2.3 contains data focused primarily on SHSs with faster switching.

2.2.1 Refining the acceptable pK_{aH} and log K_{ow} ranges for amine SHSs

The amines tested in this study were chosen to help refine the log K_{ow} and pK_{aH} ranges required for amines to display switchable hydrophilicity. Particular focus was placed on the lower limits of each value. By selecting amines with varying lengths of alkyl chains and different hydrophilic functional groups such as alcohols, amines can be chosen to have specific log K_{ow} values.

Based on the data for amines from Tables 2.1, 2.2 and 2.3, also shown graphically in Fig. 2.2a and Fig 2.2b, the most hydrophilic amine with switchable behaviour, as defined in section 2.1, is diisopropylaminoethanol with a log K_{ow} of 1.16. The most hydrophobic amine with switchable behaviour is *N*,*N*-dimethylhexylamine from Table 2.1 with a log K_{ow} of 2.53. In contrast, the most hydrophobic amine with monophasic behaviour, as defined in section 1.1, is diisopropylamine with a log K_{ow} of 1.46 and the most hydrophilic amine with biphasic behaviour (as a result of hydrophobicity and not basicity) is dibutylaminopropanol with a log K_{ow} of 2.56. These data confirm that the range of acceptable log K_{ow} values lies between approximately 1.1 and 2.6, similar to the proposed range in the first report on amine SHSs (1.2-2.5).[2]

The apparent contradiction presented by the monophasic behaviour of diisopropylamine and other monophasic amines with log K_{ow} values greater than 1.2 arises because log K_{ow} is used as a stand-in value for miscibility. Although there is a correlation between log K_{ow} and miscibility with water, they are not equivalent and so some discrepancy in the relationship between log K_{ow} and switchable behaviour is not surprising. Despite this difference, log K_{ow} was used in this study

because log K_{ow} can be predicted more accurately than miscibility or solubility (see Appendix 2). Using predicted log K_{ow} values serves as a convenient and rapid means to characterize SHSs without requiring extensive experimentation.

Tertiary (Table 2.2) and secondary (Table 2.3) amines with additional functional groups (such as alcohols, ketones, esters, acetals, and aromatic rings) were selected to test amines with different pK_{aH} values for switchable behaviour. The electron withdrawing nature of these additional functional groups decreases the electron density at the nitrogen atom and decreases the pK_{aH} value of the amine depending on their distance from the nitrogen atom and the strength of their electron withdrawing effect. *N*,*N*-Dimethylphenethylamine (pK_{aH} = 9.51) is the least basic amine with switchable behaviour using the standard 1:1 (v:v) ratio of water to amine. Propyl 3-(diethylamino)propanoate (pK_{aH} = 9.45) is the most basic amine with an acceptable log K_{ow} value that does not display switchable behaviour using the standard 1:1 (v:v) ratio of water to amine. These results suggest that the lower pK_{aH} limit for an amine to act as a SHS is approximately 9.5. These pK_{aH} and log K_{ow} requirements are shown graphically in Fig. 2.2a and Fig. 2.2b.

An interesting result shown in Table 2.2 is that of *N*,*N*-dimethylbenzylamine. This amine does not display switchable behaviour when mixed with water in a 1:1 (v:v) ratio because it is not a strong enough base (pK_{aH} = 9.03). However, it does display switchable behaviour at a 5:1 (v:v) ratio of water to amine. This result suggests that the pK_{aH} and log K_{ow} ranges identified above are valid at 1:1 (v:v) volume ratios of water to amine, but the ranges might be different at different volume ratios. This notion is discussed in more detail in Chapter 3.

2.2.2 Selecting SHSs with high boiling and flash points

Non-volatile SHSs can be designed to capitalize on the advantages of distillation-free SHS-based separations described in Section 1.4. In order to reduce volatility, SHSs with large molecular weights are preferred. However, increasing the molecular weights by simply extending the alkyl chains would increase the log K_{ow} excessively, hindering the amine's ability to act as a SHS. By

Table 2.2 Tertiary amines including additional functional groups tested for switchable behaviour

Behaviour	Compound Number	Compound Name	Log K_{ow}[a]	pK_{aH}
Monophasic	**2.25**	*N*,*N*-Dimethylaminoethanol	-0.44	9.31[8]
Monophasic	**2.26**	*N*,*N*-Dimethylaminopropanol	-0.08	9.76[18]
Monophasic	**2.27**	*N*,*N*-Diethylaminoethanol	0.41	9.87[8]
Monophasic	**2.28**	*N*,*N*-Diethylglycine methyl ester	0.76	7.75[d]
Monophasic	**2.29**	*N*,*N*-Diethylaminopropanol	0.77	10.39[d]
Monophasic	**2.30**	5-(Diethylamino)pentan-2-one	1.21	10.1[19]
Monophasic	**2.31**	Ethyl 3-(diethylamino)propanoate	1.40	9.35[d]
Switchable	**2.32**	Diisopropylaminoethanol	1.16	10.14[20]
Switchable	**2.33**	4,4-Diethoxy-*N*,*N*-dimethylbutanamine	1.48	9.83[d]
Switchable	**2.34**	Ethyl 4-(diethylamino)butanoate	1.82	10.15[d]
Switchable[b]	**2.35**	*N*,*N*-Dimethylbenzylamine	1.86	9.03[7]
Switchable[c]	**2.36**	5-(Dipropylamino)pentan-2-one	2.15	10.15[d]
Switchable	**2.37**	*N*,*N*-Dimethylphenethylamine	2.18	9.51[21]
Switchable	**2.38**	Dibutylaminoethanol	2.20	9.67[22]
Biphasic	**2.39**	Propyl 3-(diethylamino)propanoate	1.85	9.45[d]
Biphasic	**2.40**	Dibutylaminopropanol	2.56	10.5[d]
Biphasic	**2.41**	Ethyl 3(dipropylamino)propanoate	2.72	9.29[d]
Biphasic	**2.42**	Dibutylaminobutanol	2.93	10.7[d]

[a]Predicted using ALOGPS software version 2.1.[13–15] [b]At a 5:1 volume ratio of water to amine. [c]At a 2:1 volume ratio of water to amine. [d]Measured in this study.

Table 2.3 Secondary amines tested for switchable behaviour

Behaviour	Compound Number	Compound Name	Log K_{ow}[a]	pK_{aH}
Monophasic	**2.43**	Diethylamine	0.71	10.92[3]
Monophasic	**2.44**	Ethyl 3-(*tert*-butylamino)propanoate	1.38	10.09[c]
Monophasic	**2.45**	*tert*-Butylethylamine	1.42	11.35[c]
Monophasic	**2.46**	Diisopropylamine	1.46	11.07[3]
Switchable	**2.47**	Ethyl 3-(*sec*-butylamino)propanoate	1.53	9.73[c]
Switchable	**2.48**	Dipropylamine	1.64	11.05[7]
Switchable	**2.49**	Butyl 3-(isopropylamino)propanoate	1.90	9.77[c]
Switchable[b]	**2.50**	Propyl 3-(*sec*-butylamino)propanoate	1.95	9.80[c]
Switchable	**2.51**	*N*-Propyl-*sec*-butylamine	2.03	11.05[c]
Switchable	**2.52**	Di-*sec*-butylamine	2.43	11.0[23]
Precipitates	**2.53**	Ethyl 3-(isobutylamino)propanoate	1.46	9.45[c]
Precipitates	**2.54**	Ethyl 4-(*tert*-butylamino)butanoate	1.75	10.77[c]
Precipitates	**2.55**	*tert*-Butylisopropylamine	1.84	11.39[c]
Precipitates	**2.56**	Dibutylamine	2.61	11.28[3]
Precipitates	**2.57**	Dihexylamine	4.46	11.0[24]

[a]Predicted using ALOGPS software version 2.1.[13–15] [b]Requires a 2:1 volume ratio of water to amine and solution must be heated to 50 °C. [c]Measured in this study.

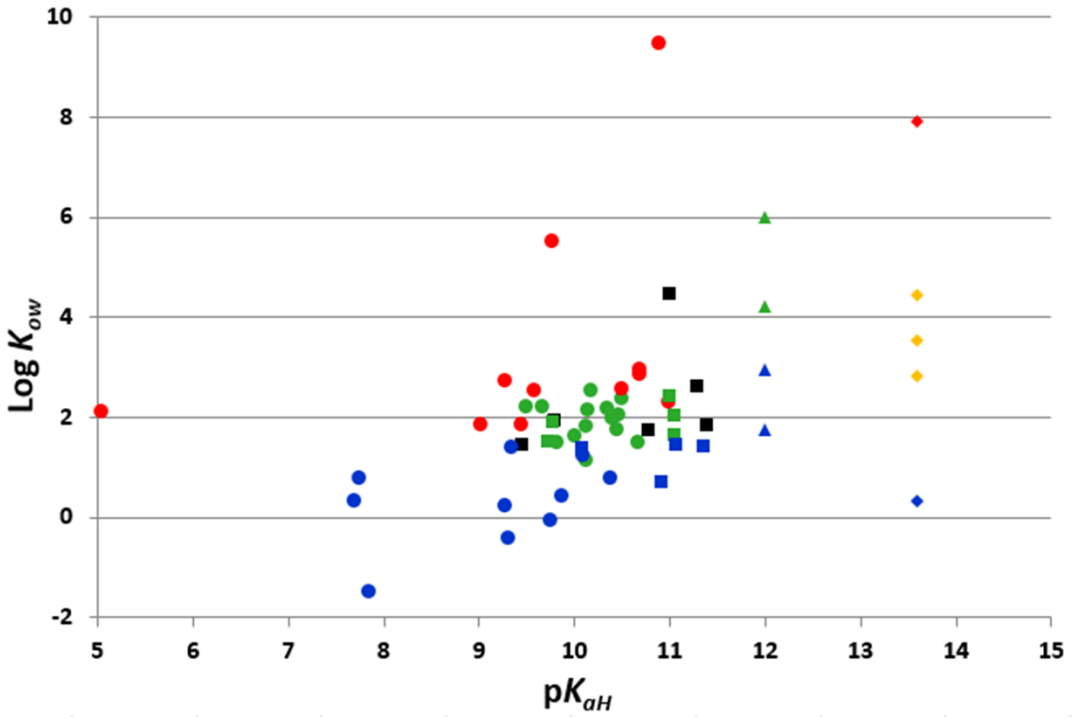

Fig. 2.2a Tertiary amines (circles), secondary amines (squares), amidines (triangles), and guanidines (diamonds) tested for switchable miscibility with water at room temperature (21 °C) from Tables 2.1, 2.2, and 2.3, plotted by their log K_{ow} and pK_{aH} and coloured by their observed behaviour: monophasic (blue), irreversible (yellow), switchable (green), biphasic (red), and precipitation upon CO_2 addition (black). All amine SHSs fall within the green oval. The two green dots outside of the oval correspond to amidine SHSs, which are not expected to have similar log K_{ow} and pK_{aH} ranges as amines. The labels identifying which dots correspond to each compound have been omitted for clarity.

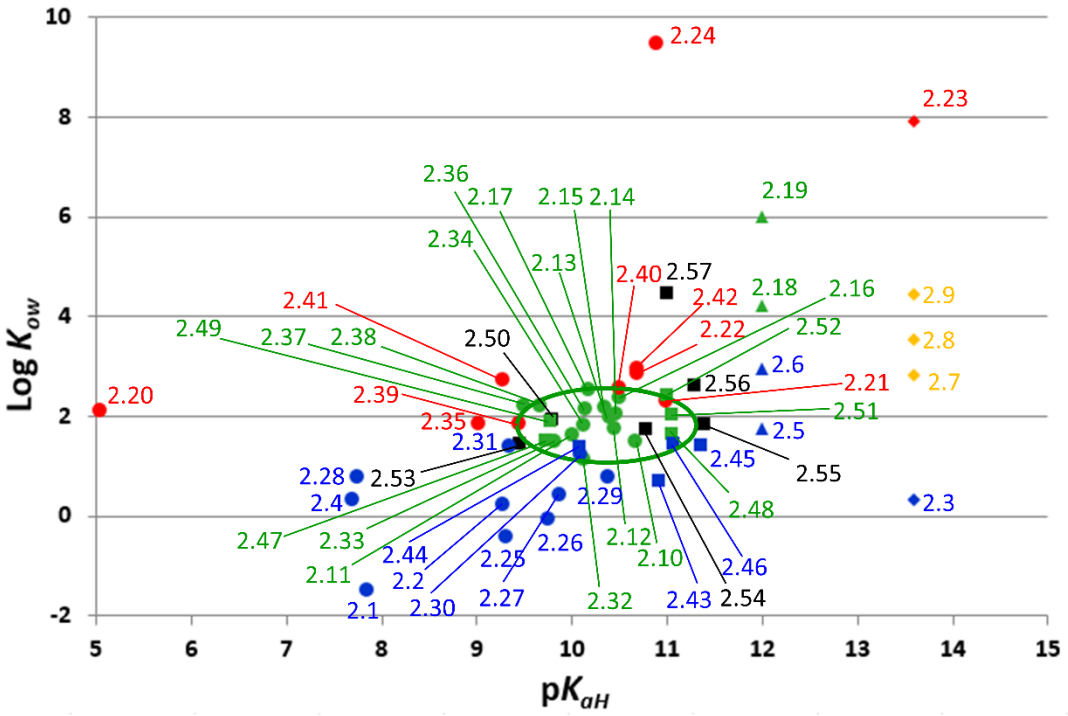

Fig. 2.3b A reproduction of Fig. 2.2a including labels to identify the compounds that are associated with each data point.

including hydrophilic functional groups in the structure of an amine while also increasing the length of the alkyl chains, the solvent can be tailored to be less volatile and yet still fit within the log K_{ow} range required for SHS behaviour.

Hydrophilic functional groups also affect the basicity of the amine. The inductive effects of a functional group can decrease the pK_{aH} of the amine depending on the proximity of the group to the nitrogen centre. When designing a SHS with these functional groups, the exact positions of the amine and the electron withdrawing group must be considered so that the amine will be a sufficiently strong base to act as a SHS. Of the tertiary amines tested which incorporated additional functional groups, six formed monophasic mixtures with water, five formed biphasic mixtures with water, and six displayed switchable behaviour (Table 2.2). Three secondary amines containing other functional groups also displayed switchable behaviour (Table 2.3). These nine new SHSs all followed the log K_{ow} and pK_{aH} criteria suggested in Section 2.2.1 with the noted exception of *N*,*N*-dimethylbenzylamine, which has been discussed in Section 2.2.1.

The different functional groups investigated were alcohols, esters, ketones, acetals, and aromatic rings, each of which will affect the pK_{aH} of the amine differently. Hydroxyl groups placed two carbons away from a tertiary amine do not lower the pK_{aH} of the amine enough to prevent an amino alcohol from displaying switchable behaviour. Aromatic rings must also be two carbons away from a tertiary amine for switchable behaviour to be observed at a 1:1 volume ratio of water to amine. *N*,*N*-Dimethylaniline (pK_{aH} 5.18) is not a strong enough base to have switchable behaviour, while *N*,*N*-dimethylbenzylamine (pK_{aH} 9.03) displays switchable behaviour in a 5:1 volume ratio of water to amine. Finally, *N*,*N*-dimethylphenethylamine (pK_{aH} 9.51) has switchable behaviour at a 1:1 volume ratio of water to amine. Ester groups must be three carbons away from a tertiary amine for an amino ester to display switchable behaviour as evidenced by the glycine derivative and amino propanoates, which are not SHSs, and the amino butanoate, which is a SHS. Secondary amines are more basic than tertiary amines with similar functional groups (e.g.

dipropylamine and tripropylamine), so secondary amino esters with ester groups two carbons away from the amine can still act as SHSs at a 1:1 volume ratio of water to amine.

The boiling points of these SHSs were used to characterize their volatility. The boiling point of a substance is not a direct measurement of volatility, but it is strongly correlated to vapour pressure, which is directly related to volatility. The vapour pressure of a substance is the partial pressure of the vapours from that substance at a given temperature while the normal boiling point of a substance is the temperature at which the vapour pressure of the substance is equal to the atmospheric pressure. Substances with high boiling points have low vapour pressures and substances with low boiling points have high vapour pressures. Given the strong correlation between boiling point and vapour pressure, the use of boiling point to characterize the volatility of SHSs was deemed acceptable for this work.

These nine new SHSs are less volatile than di- and tri-alkylamine SHSs. The SHSs with additional functional groups all have boiling points above 180 °C and predicted flash points above 50 °C (Table 2.4 discussed in section 2.2.4). By comparison, the least volatile trialkylamine SHS, *N*,*N*-dimethylcyclohexylamine, has a boiling point of 162 °C and a flash point of 41 °C. The differences between the boiling and flash points of trialkylamine SHSs and SHSs with additional functional groups shows that the design strategy for less-volatile SHSs was successful.

2.2.3 Secondary amines as faster-switching SHSs

Secondary amines have an alternate reactivity pathway which allows them to uptake CO_2 faster than tertiary amines. Like amidines and tertiary amines, secondary amines can be converted to bicarbonate salts upon exposure to carbon dioxide in the presence of water, but they can also undergo a direct reaction with carbon dioxide to form dialkylammonium *N*,*N*-dialkylcarbamate salts (Equation 2.1). This alternative reaction occurs faster than the bicarbonate salt formation, so secondary amine SHSs are likely to switch faster than tertiary amines.[25] However, the energy and temperature required to remove CO_2 from an aqueous ammonium carbamate solution is much

larger than that required to remove CO_2 from an ammonium bicarbonate solution.[25] Therefore, using a secondary amine SHS based upon the switching reaction shown in equation 2.1 can be more energy-intensive than using a tertiary amine SHS based on the switching reaction shown in equation 2.2.

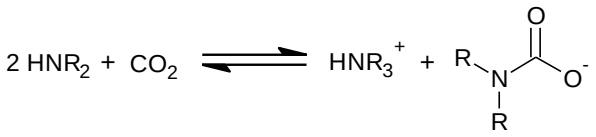

Eqn. 2.1

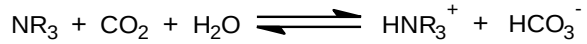

Eqn. 2.2

Although the increased rate of reaction of secondary amines is appealing, the higher energy cost of regeneration is not, so it is important to prevent significant formation of carbamate salts of a SHS. Sterically hindered amines are known to either not form carbamates or form destabilized carbamates which are rapidly hydrolyzed to bicarbonates.[25] Carbamates may form as a kinetic product before being converted to bicarbonates, allowing for rapid uptake of CO_2 without the large energy requirements for decomposing the carbamates.[25] Therefore, a sterically hindered secondary amine SHS may switch rapidly without this increased energy requirement.

Of the secondary amines tested for switchable behaviour, three formed monophasic mixtures with water, five formed biphasic mixtures with water but formed a precipitate upon exposure to CO_2, and six displayed switchable miscibility (Table 2.3). X-ray crystallography of the precipitate formed from dibutylamine confirmed that it was the bicarbonate salt of the amine (Fig. 2.3). This result suggests that the bicarbonate salts of some secondary amines are not sufficiently soluble in water to make the amines useful as SHSs at a 1:1 volume ratio. Compounds that formed solid precipitates upon addition of CO_2 are listed as "precipitates" in the behaviour column of Table 2.3. No precipitates were observed for any tertiary amine tested, which suggests that precipitation is a more prevalent occurrence in secondary amines. One possible explanation for this is that the greater potential for secondary amines to hydrogen bond (via the N-H functionality) causes secondary ammonium bicarbonate salts to aggregate and precipitate out of solution, while

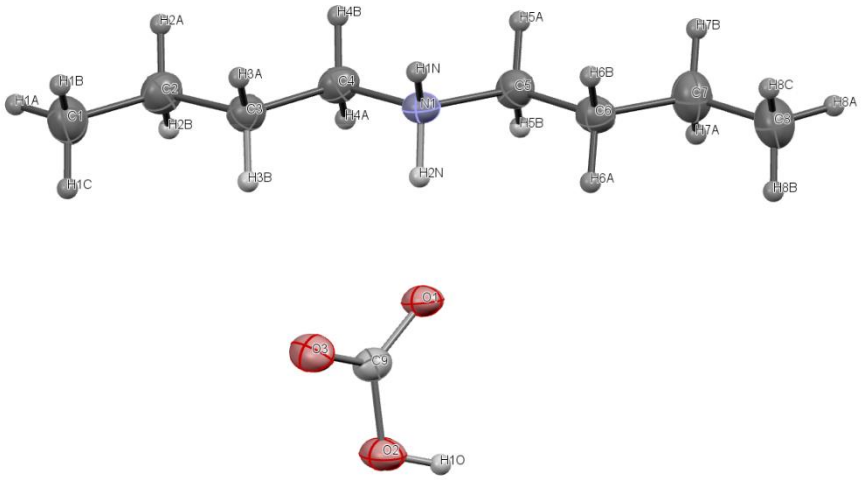

Fig. 2.4 The crystal structure of the precipitate that is formed upon the addition of CO_2 to a mixture containing dibutylamine and water. The crystal structure confirms the identity of the precipitate as dibutylammonium bicarbonate.

---

the tertiary ammonium bicarbonate salts are stabilized more by dissolution than precipitation. Regardless of the reason for this precipitation, compounds which formed precipitates were considered unsuitable for use as SHSs.

Increasing the temperature of the mixture or increasing the volume ratio of water to amine might result in complete dissolution of the bicarbonate salt in the water. A precipitate forms when CO_2 is bubbled through a 1:1 mixture of water and propyl-3-(*sec*-butylamino)propanoate at room temperature (21 °C). If the volume ratio is adjusted to 2:1 (water:amine) a biphasic mixture is obtained. Heating the mixture to 50 °C, and bubbling CO_2 through it results in a monophasic liquid which can be returned to a biphasic mixture if argon is bubbled through it while it is heated to 65 °C. Other secondary amines which form precipitates might display SHS behaviour under different conditions. Some secondary amines, such as *N*-propyl-*sec*-butylamine, form precipitates in carbonated water at room temperature (21 °C) but the heat released from the exothermic reaction

of the amine and carbonated water can warm the solution enough to dissolve the bicarbonate salts completely.

Six secondary amines were confirmed to display SHS behaviour. With the exception of dipropylamine, each of these secondary amine SHSs contained *sec*-butyl or isopropyl groups to destabilize carbamate salts. Converting bicarbonate salts of sterically hindered secondary amine SHSs to CO_2 and neutral amine was achieved at 65 °C while passing N_2 through solution. Dipropylamine/water mixtures became biphasic upon heating to 65 °C even without bubbling N_2 through solution, but the solution became monophasic again when cooled to room temperature (21 °C). The temperature-dependent miscibility of dipropylamine with carbonated water has been observed before but is not the desired behaviour for a SHS.[26] When the solution was heated to 90 °C for 2 h without N_2 passing through it, it became biphasic and remained biphasic when cooled to room temperature (21 °C). The increased temperature requirement to remove CO_2 from the solution is consistent with the formation of carbamate salts, as expected for sterically unhindered secondary amines such as dipropylamine. ^{13}C NMR analysis of carbonated water/dipropylamine solutions confirmed the presence of both bicarbonate salts and carbamate salts in solution, while no carbamates were observed for mixes of carbonated water with sterically-hindered secondary amine SHSs (Fig. 2.4).

Every secondary amine SHS, except di-*sec*-butylamine, switched from a biphasic solution to a monophasic solution after less than 10 min of bubbling CO_2 through the solution, while tertiary amines switch after 20 to 120 min at the same rate of CO_2 addition (50 mL min^{-1}). Di-*sec*-butylamine switched at a pace comparable to tertiary amine SHSs. The two *sec*-butyl groups may either decrease the rate of carbamate formation substantially or prevent carbamate formation completely. Evidently, one branching group near the amine is enough to lower the energy requirements for removing CO_2 while still allowing for a rapid switch from biphasic to monophasic solutions.

2.2.4 Risk evaluation of SHSs

In order for SHSs to be considered for use industrially, it is important to consider their effects on health and the environment, preferably in comparison to the solvents that they would replace. In order to identify the safety and environmental effects of SHSs, various metrics were considered. The LD_{50} (oral, rat), boiling point, flash point, eutrophication potential, skin effects, and log K_{ow} (as a measure of bioaccumulation) of all SHSs identified in this study and previous studies are compared in Table 2.4.[1,2] The reported safety and environmental data reveal trends in the safety risks and environmental impacts of SHSs. We used hexane and toluene as representative conventional (non-switchable) solvents for comparison.

The toxicities of SHSs were compared using oral LD_{50} data (rat). Many SHSs do not have reported LD_{50} values. In these cases, the U.S. Environmental Protection Agency's Toxicity Estimation Software Tool (TEST) was used to predict or estimate oral LD_{50} values.[31] The predicted toxicities of amines were found to be within a factor of 3 of reported LD_{50} values 95% of the time (see Appendix 2). Despite the inherent inaccuracy of toxicity predictions, SHSs with predicted LD_{50} values above 2000 mg/kg are expected to be less toxic than SHSs with LD_{50} values of around

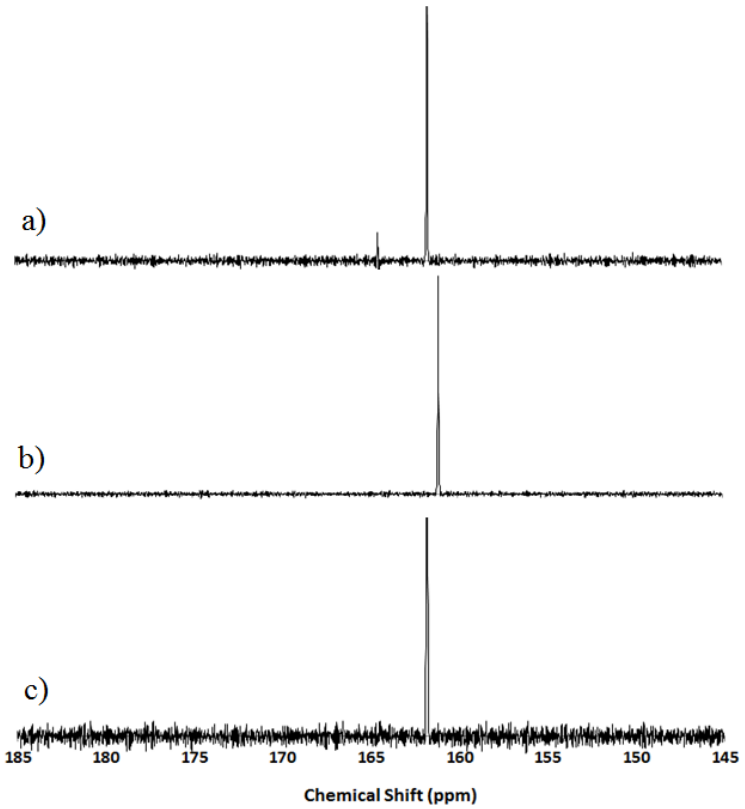

Fig. 2.5 Expansions of the $^{13}C\{^{1}H\}$ NMR spectra of carbonated H_2O and a) dipropylamine, b) sec-butylpropylamine, and c) di-sec-butylamine. The chemical shift associated with carbamate ions typically appears at 165 ppm, while the peak associated with the bicarbonate ion typically appears near 162 ppm.[27–30]

Table 2.4 Properties of known SHSs relating to safety hazards and environmental impacts of solvents.

Substance	LD_{50} (oral, rat) (mg kg^{-1})	Boiling Point (°C)	Flash Point (°C)	Eutrophication Potential[a]	Skin Effects	Log K_{ow}[b]
N,N,N'-Tributylpentanamidine	*4000*[c]	*367*[c]	*176*[c]	*0.17*	n/a	*5.92*
N,N,N'-Tripropylbutanamidine	*700*[c]	*303*[c]	*137*[c]	*0.18*	n/a	*4.20*
N,*N*-Dimethylcyclohexylamine	348[32]	160[33]	43[34]	*0.17*	Corrosive (1B)[35]	*2.04*
N-Ethylpiperidine	280[36]	128[37]	17[36]	*0.17*	Corrosive (1B)[36]	*1.74*
N-Butylpyrrolidine	51[38,d]	156[38]	35[38]	*0.17*	Irritant[39]	*2.15*
N,*N*-Dimethylhexylamine	*500*[c]	148[40]	34[41]	*0.17*	Corrosive (1B)[41]	*2.51*
N,*N*-Dimethylbutylamine	188[42]	95[43]	-5[42]	*0.18*	Corrosive (1A)[42]	*1.60*
N,*N*-Diethybutylamine	*300*[c]	137[44]	24[45]	*0.17*	Corrosive (1B)[45]	*2.37*
N-Methyldipropylamine	*267*[c]	114[46]	3[47]	*0.18*	Corrosive (1B)[47]	*1.96*
Triethylamine	460[32]	89[33]	-9[48]	*0.18*	Corrosive (1A)[49]	*1.47*
N,*N*-Diisopropylaminoethanol	940[50]	190[51,e]	64[52]	*0.15*	Corrosive (1B)[52]	*1.16*
N,*N*-Dibutylaminoethanol	1070[32]	230[53,e]	95[54]	*0.15*	Corrosive (1B)[54]	*2.15*
4,4-Diethoxy-*N*,*N*-dimethylbutanamine	*2000*[c]	270[55,e]	70[56]	*0.13*	n/a	*1.48*
Ethyl 4-(diethylamino)butanoate	*7000*[c]	220[e]	*77*[d]	*0.13*	n/a	*1.82*

Substance	LD_{50} (oral, rat) (mg kg^{-1})	Boiling Point (°C)	Flash Point (°C)	Eutrophication Potential[b]	Skin Effects	Log K_{ow}[c]
N,*N*-Dimethylphenethylamine	*300*[c]	200[57]	71[58]	*0.16*	Irritant[58]	*2.18*
Dipropylamine	460[32]	110[59]	17[48]	*0.18*	Corrosive (1A)[60]	*1.64*
Di-*sec*-butylamine	*300*[c]	133[61]	21[62]	*0.17*	Corrosive (1A)[62]	*2.46*
5-(Dipropylamino)pentanone	*3000*[c]	280[e]	*72*[c]	*0.15*	n/a	*2.14*
Ethyl 3-(*sec*-butylamino)propanoate	*5000*[c]	210[e]	*93*[c]	*0.13*	n/a	*1.53*
Propyl 3-(*sec*-butylamino)propanoate	*3000*[c]	220[e]	*89*[c]	*0.13*	n/a	*1.94*
Butyl 3-(isopropylamino)propanoate	*3000*[c]	230[e]	*105*[c]	*0.13*	n/a	*1.90*
N-Propyl-*sec*-butylamine	*300*[c]	124[63]	*15*[c]	*0.18*	Corrosive (1B)[64]	*2.03*
N,*N*-Dimethylbenzylamine	265[32]	180[65]	53[66]	*0.16*	Corrosive (1B)[66]	*1.86*
Toluene	636-6400[32,67,68,f]	110[69]	4[48]	*0.13*	Irritant[70]	*2.49*
Hexane	28710[32]	69[71]	-22[48]	*0.15*	Irritant[72]	*3.55*

Estimated values are shown in italics. [a] Calculated as mass equivalents of phosphate. [b] Predicted using ALOGPS software version 2.1.[13–15] [c] Predicted using TEST software version 4.1.[31] [d] Oral LD_{50} value for mice. [e] Boiling point at atmospheric pressure extrapolated from boiling point at reduced-pressure. [f] Multiple LD_{50} values have been reported for toluene.[32,67,68] The reported LD_{50} value of 636 mg/kg may be the result of a miscalculation[67,68]

500 mg/kg or lower. Oxygen-containing SHSs have consistently higher predicted LD_{50} values than di-and tri-alkylamine SHSs. While toluene is less toxic than di- and tri-alkylamine SHSs, the varying reports of its LD_{50} and the uncertainty of the predicted LD_{50} values for other SHSs prevent us from drawing further conclusions. Furthermore, multiple different LD_{50} values have been reported for toluene, making its acute toxicity risks less certain. According to the LD_{50} data, hexane is much less toxic than every SHS. However, LD_{50} is a measure of acute toxicity, so solvents with chronic toxicity may appear safe even though they are not. For example, hexane is a known chronic neurotoxin, a serious problem that is not made evident by LD_{50} data.[73–75]

The more volatile SHSs are not advantageous over conventional solvents in terms of inhalation toxicity but the less volatile SHSs are likely to be much safer than conventional solvents by this measure. There are few data regarding this form of toxicity for the SHSs listed in Table 2.4. The inhalation LC_{50} values (rat, 4 h) for triethylamine and dipropylamine are 4.1 g/m^3 and 4.4 g/m^3, respectively,[30] while the corresponding values for toluene and hexane are 30.1 g/m^3 and 169 g/m^3, respectively.[76,77] *N*,*N*-Dimethylcyclohexylamine has a reported LC_{50} (rat, 2 h) of 1.9 g/m^3.[32] Volatile SHSs are expected to have associated inhalation toxicity risks, as evidenced by the inhalation LC_{50} values for triethylamine, dipropylamine, and *N*,*N*-dimethylcyclohexylamine described above. On the other hand, SHSs with low volatility may not pose an inhalation toxicity risk because their vapour pressures may decrease exposure significantly. For example the vapour pressure of propyl-3-(*sec*-butylamino)propanoate at 25 °C was estimated to be 13 Pa using a nomograph. In contrast the vapour pressures of triethylamine, toluene, and hexane at 25 °C are 9670 Pa,[78] 3804 Pa,[79] and 20240 Pa,[80] respectively. Therefore, propyl-3-(*sec*-butylamino)propanoate and other low-volatility SHSs are less likely to be inhaled because of their low vapour pressure, making them less of an inhalation toxicity risk than volatile solvents.

The boiling and flash points of SHSs give an indication of the volatility of the solvents. Flash points also describe the flammability of the solvents. If the boiling point at atmospheric

pressure is not known, a value was estimated by extrapolating from a reduced-pressure boiling point. The TEST program can be used to predict flash points if the flash point of a SHS is not known. These predictions are accurate to within 8 °C 81% of the time if the experimental flashpoint is above 20 °C (see Appendix 2). Almost every SHS is safer than toluene and hexane in terms of volatility and flammability. SHSs containing functional groups in addition to an amine group were designed to be less volatile and less flammable, and the data confirm that they are safer than di- and tri-alkylamine SHSs by these metrics. For example, the amino alcohol *N*,*N*-dibutylaminoethanol has a boiling point of 230 °C[53] and a flash point of 95 °C[54] while the tri-alkylamine *N*,*N*-dimethylcyclohexylamine has a boiling point of 160 °C[33] and a flash point of 43 °C.[34] Under the United Nations Globally Harmonized System of classification, these less-volatile SHSs would be classified as combustible rather than flammable liquids (flash points > 60 °C).[81]

Eutrophication potential is a measurement of the ability of a compound to contribute to eutrophication (excessive growth of algae in water due to high nutrient levels). It quantifies this contribution relative to an equal mass of phosphate. The eutrophication potentials of SHSs were calculated using a modified version of the equation described by Heijungs *et al.*,[82] replacing chemical oxygen demand with theoretical oxygen demand, which was calculated using an equation described by Baker, Milke, and Mihelcic.[83] The implications of these equations are that lower nitrogen content and higher oxygen content in a compound lowers its eutrophication potential. As a result, oxygen containing SHSs have less eutrophication potential than other SHSs, with amino esters having the lowest potential. Indeed, amino ester SHSs have eutrophication potentials similar to toluene and lower than hexane, despite their nitrogen content.

Skin effects are another concern for SHSs; 13 of the SHSs are corrosive. In order to differentiate between different levels of corrosion, different classes of corrosion as defined by the Globally Harmonized System were used where information was available.[81] A class 1A corrosive

substance shows effects after 3 minutes of exposure and less than 1 hour of observation. A class 1B corrosive substance shows effects after 1 hour of exposure and less than 14 days of observation. Class 1A corrosive SHSs should be avoided. By comparison, four of the SHSs and many conventional solvents like toluene and hexane are irritants, rather than corrosive liquids. For many of the SHSs, skin effect data are unavailable.

Bioaccumulation is not a concern for SHSs. Compounds with log K_{ow} values below 3.5 are considered to have low bioaccumulation potential.[84] All known amine SHSs have log K_{ow} between approximately 1.2 and 2.5. The amidine SHSs would not bioaccumulate, despite their high log K_{ow} values, because they are hydrolytically unstable and therefore would not likely persist in the environment long enough to pose a bioaccumulation risk. Some conventional solvents (e.g. hexane) have moderate bioaccumulation potential, while others have low potential (e.g. toluene). Therefore, with respect to bioaccumulation, all SHSs are expected to perform better than solvents that can bioaccumulate and perform comparably to solvents that do not bioaccumulate.

The use of volatile solvents results in volatile organic compound emissions and contributes to smog formation.[85] With regards to this environmental concern, low-volatility solvents are expected to be more benign than high-volatility solvents. SHSs with additional functional groups are much less volatile than conventional solvents like hexane and toluene. While volatile SHSs like triethylamine will have no advantages over conventional solvents, the low-volatility SHSs likely have less potential to contribute to smog formation than conventional solvents.

The persistence of a solvent when it is released into the environment is another concern when evaluating the environmental risks associated with a solvent. Compounds can degrade by a number of different pathways and it can be difficult to predict their persistence. However, some degradation trends relating to chemical structures have been observed.[86] Quaternary carbon centres, extensive branching, heterocycles, and tertiary amines tend to decrease degradability. Features that increase degradability are oxygen atoms (particularly esters), unsubstituted alkyl chains of 4 or

more, and unsubstituted phenyl groups. Although amine biodegradation data are sparse and many exceptions are apparent, secondary amines are typically considered to be more readily biodegradable than tertiary amines.[87–92] For example, dipropylamine is considered biodegradable while triethylamine is not.[92,93] Not all tertiary amines will persist however. The biodegradation of *N*,*N*-dimethylcyclohexylamine is not rapid, but it is considered to be biodegradable in freshwater environments.[94] The available data also indicate that compounds with quaternary carbons are more resistant to biodegradation than straight chain compounds. A common opinion is that any branching will decrease biodegradability. However, Boethling *et al*. report that this is an oversimplification and only extensive branching and quaternary carbons show a trend of decreasing degradability.[86] Many secondary amine SHSs contain a branching group to destabilize carbamate formation. An ideal secondary amine SHS would include one branching group to destabilize the carbamate product without significantly decreasing its biodegradability.

With regard to this information, secondary amino ester SHSs are expected to be the least persistent SHSs, particularly butyl 3-(isopropylamino)propanoate because it contains an n-butyl group. Tertiary amine SHSs containing other functional groups and dialkylamine SHSs are second choices, while trialklyamine SHSs will likely persist longer than the other SHSs. The conventional solvents toluene and hexane contain groups favourable to degradation and no groups resistant to degradation and therefore are both biodegradable.[95,96] With respect to biodegradability, trialkylamine SHSs are expected to be more persistent than conventional solvents, but secondary amine SHSs and tertiary amine SHSs with additional functional groups are expected to have biodegradability comparable to or better than conventional solvents.

From these trends, the most benign types of SHS can be determined. The data available for oxygen-containing SHSs suggest that they are less toxic and less volatile than di- and tri-alkyl amine SHSs. They are also no more corrosive and have lower eutrophication potentials, making them the most benign SHSs identified according to the metrics listed in this study. The amidine

SHSs also have favourable safety and environmental properties apart from their larger eutrophication potentials and their expected corrosive effects, but they are unlikely ever to be used because of their relatively difficult syntheses. No categorical differences between secondary and tertiary amine SHSs are immediately apparent from the data in Table 2.4; The average LD_{50} values, boiling points, and flash points of dialkylamines (300 ± 140 mg kg^{-1}, 122 ± 27 °C, and 18 ± 20 °C, respectively) are all similar to those of trialkylamines (350 ± 90 mg kg^{-1}, 128 ± 12 °C, and 18 ± 3 °C, respectively). However, secondary amine SHSs are likely to be more biodegradable as discussed above.

Carcinogenicity is not accounted for in Table 2.4, but some data are available to allow for some comparisons. For reference, neither hexanes nor toluene are considered carcinogenic.[97,98] Data for triethylamine and *N*,*N*-dimethylcyclohexylamine suggest that trialkylamines are not likely to be carcinogenic either.[94,99] However, secondary amines are capable of forming nitrosamines, many of which are carcinogenic, and so are typically considered to be carcinogens as well.[100,101] Finally, a report on *N*,*N*-dibutylaminoethanol indicates that tertiary amino alcohols should be considered carcinogenic because they are capable of forming nitrosamines as well.[102] These limited data suggest that trialkylamine SHSs are preferable to dialkylamine SHSs and amino alcohol SHSs with respect to carcinogenicity.

Other risks not included in the above discussion should also be considered in order to obtain a more complete assessment of the solvents in consideration. For example, acute toxicity values towards many organisms (e.g. fish, invertebrates) aren't present and risks such as chronic toxicity, developmental toxicity, and mutagenicity are not addressed. These risks and others should be accounted for a more complete assessment of the solvents.

There are other considerations that can also be used to differentiate between SHSs. Some SHSs, such as the amino acetal, the amidines, and the amino esters are prone to hydrolysis and are likely to degrade over time. Dipropylamine forms a stable carbamate salt and more energy must be

put into the system to convert the salt back into CO_2 and neutral amine. Some SHSs switch faster than others as well. In particular, secondary amines switch from biphasic to monophasic mixtures faster than tertiary amines. None of these factors are apparent from the information given in Table 2.4, but they can affect the overall viability of a SHS.

2.3 Conclusions

Several new SHSs have been identified, including secondary amines and amines incorporating an additional functional group. Amines which display SHS behaviour typically have log K_{ow} between 1.2 and 2.5 and pK_{aH} above 9.5. Dimethylbenzylamine is an exception (pK_{aH} 9.03), but is only switchable if the volume of water is much larger than the volume of amine. Some secondary amines can also display switchable behaviour but others can form carbamate salts or precipitate as bicarbonate salts. Secondary amine SHSs can be designed to avoid significant carbamate formation by making them sterically hindered. Amines incorporating other functional groups are more benign than other SHSs, commonly having lower toxicity, volatility, flammability, and eutrophication potential. Compared to toluene, the secondary amine ester SHSs are predicted to be safer for health and the environment in terms of flammability, smog formation, inhalation toxicity, and bioaccumulation (lower K_{ow}). They are comparable to toluene in terms of eutrophication and possibly biodegradation. The variety of compounds identified and their different properties show that can be designed to meet the requirements of an application.

Of the SHS identified in this chapter, *N*,*N*-dibutylaminoethanol is a particularly promising SHS incorporating an alcohol functionality because it is less dangerous than trialkylamine SHSs, is not hydrolytically unstable like amino esters, and is commercially available. As a result, it is readily accessible to researchers and its use improves the safety of SHS-based processes relative to the use of DMCA.

2.4 Experimental Methods

Chemicals were used as received. Amines were commercially available (Sigma-Aldrich, TCI, Fisher) except for amino propanoate/butanoate esters and amino ketones, which were synthesized and characterized as described below. Argon (99.998%) and CO_2 (chromatographic grade) were purchased from Praxair.

2.4.1 Testing amines for switchable behaviour

To confirm the switchable miscibility, amines were mixed with water in a 1:1 volume ratio. If two phases were observed, CO_2 was bubbled into the solution through a gas dispersion tube (Ace Glass, 25-50 micron porosity) for 2 h. If the mixture became monophasic, N_2 was bubbled into the solution through a gas dispersion tube for 2 h while the solution was heated to 65 °C. If the mixture became biphasic again at 65 °C and remained biphasic upon cooling to room temperature (21 °C), the amine was classified as a SHS. Other volume ratios were attempted for some amines.

2.4.2 Evaluation of SHSs

Log K_{ow} values were predicted using ALOGPS 2.1.[13–15] pK_{aH} values were found from literature or determined titrimetrically. Flash points, skin effects, and LD_{50} values were found from literature or MSDS. If flash point or LD_{50} values were unavailable, they were calculated using the TEST program.[31] Eutrophication potentials (EP) were calculated using a variation of the method proposed by Heijungs *et al.*, which calculates the eutrophication potential of a compound based on its molecular weight (MW), the number of phosphorus and nitrogen atoms it contains (ν_P and ν_N), and its theoretical oxygen demand (ν_{ThOD})(equations 2.3 and 2.4).[82] Theoretical oxygen demands were calculated using the method described by Baker, Milke, and Mihelcic (equations 2.5 and 2.6), which assumes that nitrogen atoms are converted to NH_3 and that all carbon atoms are completely oxidized.[83] The reference compound for eutrophication potential is PO_4^{3-}.

$$\nu_{tot,i} = \left(\nu_{P,i} + \nu_{N,i}/16 + \nu_{ThOD,i}/138\right) \quad \text{Eqn. 2.3}$$

$$EP_i = \frac{\nu_{tot,i} \,/\, MW_i}{\nu_{tot,ref} \,/\, MW_{ref}} \quad \text{Eqn. 2.4}$$

$$C_aH_bN_cO_d + nO_2 \rightarrow aCO_2 + \frac{b-3c}{2}H_2O + cNH_3 \quad \text{Eqn. 2.5}$$

$$\nu_{ThOD} = 2n = 2a + \frac{b-3c}{2} - d \quad \text{Eqn. 2.6}$$

2.4.3 Dibutylammonium bicarbonate crystal formation

Dibutylamine (5 mL) and water (5 mL) were combined in a vial. CO_2 was bubbled through the mixture until a large quantity of precipitate formed. The mixture was heated to 40 °C, resulting in a biphasic mixture with no solids. Upon cooling to room temperature (21 °C), needle-like crystals formed at the interface between the liquid phases. The details of the crystallographic analysis are described in Appendix 3.

2.4.4 Observation of secondary amine salt speciation in carbonated water

Amine (dipropylamine, di-*sec*-butylamine, or *sec*-butylisopropylamine, 1 mL) was mixed with 1 mL H_2O in a vial and CO_2 was bubbled through the solution until it became monophasic. CH_3CN (0.2 mL) was added to solution as a reference compound and the solution was characterized by ^{13}C {^1H} NMR spectroscopy.

2.4.5 Measuring the pK_{aH} of amines

For most amines, a ~20 mL solution containing ~0.02 g amine in distilled water was titrated with ~0.1 M HCl. The pH of the solution was recorded after each addition of titrant (Orion 4 Star pH meter, Thermo Scientific). The equivalence point was determined using a derivative plot and the pH at the half equivalence point was taken as the pK_{aH} of the amine. Titrations were performed at least twice.

Dibutylaminobutanol and dibutylaminopropanol were not sufficiently soluble in water to measure their aqueous pK_{aH} directly. The pK_{aH} of these compounds were measured in ethanol-water solutions and extrapolated to a completely aqueous solution using the method described by Gowland and Schmid.[103]

A more detailed description of the methods used to determine pK_{aH} values is presented in Appendix 4.

2.4.6 Synthesis

Amino esters and ketones were synthesized using procedures adapted from literature for similar compounds.[104,105] NMR spectra were collected on a Bruker Avance-500 or a Bruker Avance-300 NMR spectrometer. IR spectra were collected with a Varian 640 FT-IR spectrometer. Mass Spectra were collected with a Perkin Elmer Clarus 600 T mass spectrometer connected to a Perkin Elmer Clarus 680 gas chromatograph.

Ethyl 3-(diethylamino)propanoate. Ethyl acrylate (9.2 g, 0.092 mol) and diethylamine (6.7 g, 0.092 mol) were added to a round bottom flask and stirred for 24 h. Distillation under vacuum afforded the pure product (14.9 g, 94% yield); bp 57-59 °C (4 torr): ^{1}H NMR (300.13 MHz, $CDCl_3$) δ 0.95 (t, *J*=7.2 Hz, 6H), 1.18 (t, *J*=7.2 Hz, 3H), 2.36 (t, *J*=7.4, 2H), 2.44 (q, *J*=7.2 Hz, 4H), 2.71 (t, *J*=7.4 Hz, 2H), 4.05 (q, *J*=7.2 Hz, 2H); ^{13}C NMR (75.47 MHz, $CDCl_3$) δ 12.12, 14.18, 32.49, 46.93, 48.22, 60.34, 172.75; ν_{max} (ATR) cm^{-1} 2972, 2935, 2874, 2806, 1735 (C=O), 1448, 1371, 1198, 1048; *m/z* (EI) 173 (6), 158 (15), 144 (3), 130 (3), 116 (1), 99 (1), 86 (100), 73 (6), 72 (6), 58 (15), 56 (10), 55 (15); Anal. Calcd for $C_9H_{19}NO_2$: C 62.39, H 11.05, N 8.09; found C 62.15, H 11.05, N 8.07. The ^{1}H NMR data match literature values.[104]

Ethyl 3-(dipropylamino)propanoate. Using the same procedure as for ethyl 3-(diethylamino)propanoate but using dipropylamine instead of diethylamine, 4.0 g (0.040 mol) of ethyl acrylate yielded 6.2 g product (77% yield); bp 76-77 °C (4 torr): ^{1}H NMR (300.13 MHz,

$CDCl_3$) δ 0.80 (t, *J*=7.4 Hz, 6H), 1.19 (t, *J*=7.1 Hz, 3H), 1.38 (apparent sextet, *J*=7.4 Hz, 4H), 2.30 (t, *J*=7.4 Hz, 4H), 2.36 (t, *J*=7.4 Hz, 2H), 2.71 (t, *J*=7.4 Hz, 2H), 4.06 (q, *J*=7.1 Hz, 2H); ^{13}C NMR (75.47 MHz, $CDCl_3$) δ 11.65,14.08, 20.31, 32.50, 49.56, 56.06, 60.12, 172.78; ν_{max} (ATR) cm^{-1} 2959, 2937, 2873, 2805, 1736 (C=O), 1463, 1371, 1192, 1053; *m/z* (EI) 201 (9), 172 (100), 156 (2), 144 (12), 130 (4), 114 (59), 101 (6), 86 (13), 84 (27), 72 (26), 70 (12), 56 (10), 55 (26), ; Anal. Calcd for $C_{11}H_{23}NO_2$: C 65.62, H 11.52, N 6.96; found C 65.63, H 11.60, N 6.97. The ^{1}H NMR data match literature values.[104]

Ethyl 4-(diethylamino)butanoate. Ethyl 4-bromobutanoate (5.0 g, 0.026 mol) and diethylamine (8.8 g, 0.12 mol) were added to a round bottom flask containing 20 mL acetonitrile. The mixture was stirred at 65 °C for 24 h. The resulting solution was concentrated by distillation, added to 25 mL 1 M NaOH, and extracted with 3 x 25 mL hexanes. Distillation under vacuum afforded the pure product (3.20 g, 66% yield); bp 65 °C (4 torr): ^{1}H NMR (300.13 MHz, $CDCl_3$) δ 0.94 (t, *J*=7.1 Hz, 6H), 1.19 (t, *J*=7.1 Hz, 3H), 1.70 (p, *J*=7.3 Hz, 2H), 2.26 (t, *J*=7.3 Hz, 2H), 2.37 (t, *J*=7.3 Hz, 2H), 2.4 (q, *J*=7.1 Hz, 4H) 4.07 (q, *J*=7.1 Hz, 2H); ^{13}C NMR (75.47 MHz, DCl_3) δ 11.81, 14.17, 22.39, 32.20, 46.81, 52.08, 60.01, 173.61; ν_{max} (ATR) cm^{-1} 2969, 2936, 2802, 1735 (C=O), 1466, 1472, 1251, 1184; *m/z* (EI) 187 (6), 172 (3), 158 (1), 142 (12), 115 (5), 114 (6), 98 (2), 86 (100), 58 (9), 56 (5); Anal. Calcd for $C_{10}H_{21}NO_2$: C 64.12, H 11.31, N 7.48; found C 64.12, H 11.44, N 7.48.

Ethyl 3-(*sec*-butylamino)propanoate. Ethyl acrylate (4.5 g, 0.045 mol) and *sec*-butylamine (6.6 g, 0.9 mol) were added to a round bottom flask and stirred for 24 h. Distillation afforded the pure product (7.0 g, 89% yield); bp: 65 °C (4 torr): ^{1}H NMR (499.26 MHz, $CDCl_3$) δ 0.77 (t, *J*=7.4 Hz, 3H), 0.91 (d, *J*=6.2 Hz, 3H), 1.14 (t, *J*=7.2 Hz, 3H), 1.20 (m, 1H), 1.35 (m, 1H), 2.37 (t, *J*=6.6 Hz, 2H), 2.44 (apparent sextet, *J*=6.2 Hz, 1H), 2.75 (m, 2H), 4.02 (q, *J*=7.2 Hz, 2H); ^{13}C NMR (125.54 MHz, $CDCl_3$) δ 10.1, 14.1, 19.7, 29.4, 34.8, 42.2, 54.1, 60.1, 172.7; ν_{max} (ATR) cm^{-1} 2963, 2932, 2875, 1731 (C=O), 1463, 1372, 1186, 1028; *m/z* (EI) 172, 158 (7), 144 (94), 130, (5), 112 (7), 98

(65), 86 (56), 84 (7), 70 (37), 56 (100); Anal. Calcd for $C_9H_{19}NO_2$: C 62.39, H 11.05, N 8.09; found C 62.29, H 11.29, N 8.04.

Ethyl 3-(*tert*-butylamino)propanoate. Using the same procedure as for ethyl 3-(*sec*-butylamino)propanoate but using *tert*-butylamine instead of *sec*-butylamine, 1.9 g (0.019 mol) ethyl acrylate and 2.9 g (0.040 mol) *tert*-butylamine yielded 1.7 g product (51% yield); bp 62 °C (4 torr): ^{1}H NMR (300.13 MHz, $CDCl_3$) δ 1.05 (s, 9H), 1.21 (t, *J*=7.1 Hz, 2H), 2.43 (t, *J*=6.6 Hz, 2H), 2.77 (t, *J*=6.6 Hz, 2H), 4.09 (q, *J*=7.1 Hz, 2H); ^{13}C NMR (75.47 MHz, $CDCl_3$) δ 14.1, 28.9, 35.5, 38.0, 50.3, 60.2, 172.9; ν_{max} (ATR) cm^{-1} 2964, 2868, 1731 (C=O), 1479, 1362, 1230, 1174, 1099, 1029; *m/z* (EI), 173 (1), 158 (94), 144 (3), 130 (4), 116 (5), 112 (31), 86 (50), 70 (100), 58 (20), 57 (21), 56 (11), 55 (19); Anal. Calcd for $C_9H_{19}NO_2$: C 62.39, H 11.05, N 8.09; found C 62.28, H 11.13, N 8.07.

Ethyl 3-(isobutylamino)propanoate. Using the same procedure as for ethyl 3-(*sec*-butylamino)propanoate, 1.9 g (0.019 mol) ethyl acrylate and 3.1 g (0.042 mol) isobutylamine yielded 2.4 g product (73% yield); bp: 68 °C (4 torr): ^{1}H NMR (300.13 MHz, $CDCl_3$) δ 0.88 (d, *J*=6.6 Hz, 6H), 1.24 (t, *J*=7.1 Hz, 3H), 1.36 (broad, 1H) 1.71 (apparent nonet, *J*=6.7 Hz, 1H), 2.40 (d, *J*=6.8 Hz, 2H), 2.48 (t, *J*=6.5 Hz, 2H), 2.84 (t, *J*=6.5 Hz, 2H), 4.12 (q, *J*=7.1 Hz, 2H); ^{13}C NMR (75.47 MHz, $CDCl_3$) δ 14.1, 20.6, 28.3, 34.8, 45.1, 57.7, 60.2, 173.1; ν_{max} (ATR) cm^{-1} 2954, 2871, 2821, 1731 (C=O), 1467, 1372, 1186, 1121, 1029; *m/*z (EI) 173 (3), 130 (70), 116 (7), 86 (38), 84 (100), 70 (7), 57 (13), 56 (9), 55 (9); Anal. Calcd for $C_9H_{19}NO_2$: C 62.39, H 11.05, N 8.09; found C 62.26, H 11.23, N 8.04.

5-(diethylamino)pentan-2-one. Using the same procedure as for ethyl 4-(diethylamino)butanoate, 6.35 g (0.0526 mol) 5-chloropentan-2-one and 19.2 g (0.263 mol) diethylamine yielded 0.3488 g of 5-(diethylamino)pentan-2-one (20% yield); bp 66 °C (4 torr): ^{1}H NMR (499.26 MHz, $CDCl_3$) δ 0.95 (t, *J*=7.1Hz, 6H), 1.67 (p, 7.2 Hz, 2H), 2.10 (s, 3H), 2.34 (t, *J*=7.2 Hz, 2H), 2.41 (t, *J*=7.2 Hz,

2H), 2.45 (q, *J*=7.1 Hz, 4H); ^{13}C NMR (125.54 MHz, $CDCl_3$) δ 11.67, 21.24, 29.93, 41.48, 46.71, 51.94, 208.83; ν_{max} (ATR) cm^{-1} 2968, 2800, 1714 (C=O), 1361, 1202, 1175, 1069; *m/z* (EI) 157 (4), 142 (1), 99 (4), 86 (100), 72 (2), 71 (2), 70 (2), 58 (12), 56 (5); HRMS (EI): $C_9H_{19}NO$ for M^+ calculated 157.1467, found 157.1462.

5-(dipropylamino)pentan-2-one. Using the same procedure as for ethyl 4-(diethylamino)butanoate, 3.95 g (0.0328 mol) 5-chloro-pentan-2-one and 11.09 g (0.110 mol) dipropylamine yielded 1.2204 g of 5-(dipropylamino)-pentan-2-one (20% yield); bp 96 °C (4 torr): ^{1}H NMR (499.26 MHz, $CDCl_3$) δ 0.85 (t, *J*=7.4 Hz, 6H), 1.41 (apparent sextet, *J*=7.4 Hz, 4H), 1.68 (p, *J*=7.1 Hz, 2H), 2.12 (s, 3H), 2.32 (multiplet, 6H), 2.37 (t, *J*=7.2 Hz, 2H), 2.45 (t, 2H, *J*=7.2 Hz); ^{13}C NMR (125.54 MHz, $CDCl_3$) δ 11.85, 20.23, 21.36, 29.88, 41.31, 53.14, 56.02, 208.86; ν_{max} (ATR) cm^{-1} 2957, 2872, 2800, 1715 (C=O), 1462, 1362, 1174, 1078; *m/z* (EI) 185 (8), 156 (37), 154 (1), 140 (1), 127 (2), 114 (64), 98 (3), 85 (100), 72 (22), 70 (6), 56 (5); HRMS (EI): $C_{11}H_{23}NO$ for M^+ calculated 185.1780, found 185.1775.

Ethyl 4-(*tert*-butylamino)butanoate. Ethyl 4-bromobutanoate (6.8 g, 0.035 mol) and *tert*-butylamine (5.1 g, 0.070 mol) were added to a round bottom flask containing 20 mL acetonitrile. The mixture was stirred at 70 °C under a nitrogen atmosphere for 48 h. The resulting solution was concentrated by distillation, added to 20 mL 4 M NaOH, and extracted with 3 x 20 mL pentane. Distillation afforded the pure product (3.9 g, 60% yield); bp 72 °C (4 torr): ^{1}H NMR (300.13 MHz, $CDCl_3$) δ 0.51 (broad, 1H), 0.96 (s, 9H), 1.13 (t, *J*=7.1 Hz, 3H), 1.64 (p, *J*=7.2 Hz, 2H), 2.24 (t, *J*=7.3 Hz, 2H), 2.45 (t, *J*=7.1 Hz, 2H), 4.00 (q, *J*=7.1 Hz, 2H); ^{13}C NMR (75.47 MHz, $CDCl_3$) δ 14.10, 26.36, 28.93, 32.20, 41.69, 50.01, 59.99, 173.40; ν_{max} (ATR) 2963, 1732 (C=O), 1447, 1366, 1229, 1159, 1102, 1030; *m/z* (EI) 187 (1), 172 (100), 158 (1), 142 (3), 126 (31), 115 (25), 98 (5), 86 (82), 84 (17), 69 (17), 57 (33); Anal. Calcd for $C_{10}H_{21}NO_2$: C 64.12, H 11.31, N 7.48; found C 63.94, H 11.54, N 7.47.

Propyl 3-(*sec*-butylamino)propanoate. Using the same procedure as for ethyl 3-(*sec*-butylamino)propanoate, 2.1 g (0.021 mol) of propyl acrylate and 2.7 g (0.037 mol) of *sec*-butylamine yielded 3.2 g of product (92.7% yield); bp 74 °C (4 torr): ^{1}H NMR (499.26 MHz, $CDCl_3$) δ 0.87 (t, *J*=7.4 Hz, 3H), 0.93 (t, *J*=7.4 Hz, 3H), 1.01 (d, *J*=6.3 Hz, 3H), 1.30 (m, 1H), 1.46 (m, 1H), 1.64 (apparent sextet, *J*=7.1 Hz, 3H), 2.49 (t, *J*=6.5 Hz, 2H), 2.54 (m, 1H), 2.86 (m, 2H), 4.03 (t, *J*=6.7 Hz, 2H); ^{13}C NMR (125.54 MHz, $CDCl_3$) δ 10.15, 10.37, 19.75, 21.94, 29.43, 34.96, 42.39, 54.25, 66.02, 172.95; ν_{max} (ATR) cm^{-1} 2964, 2878, 1731 (C=O), 1463, 1377, 1356, 1259, 1186, 1063; *m/z* (ESI) 187 (1), 186 (1), 172 (8), 158 (100), 144 (1), 130 (8), 128 (6), 116 (9), 112 (8), 98 (65), 86 (60), 84 (8), 72 (15), 70 (36), 56 (98); Anal. Calcd for $C_{10}H_{21}NO_2$: C 64.12, H 11.31, N 7.48; found C 64.01, H 11.54, N 7.46.

Butyl 3-(isopropylamino)propanoate. Using the same procedure as for ethyl 3-(*sec*-butylamino)propanoate, 4.7 g (0.037 mol) of propyl acrylate and 7.2 g (0.1.221 mol) of *sec*-butylamine yielded 6.5 g of product (94.3% yield); bp 83 °C (4 torr): ^{1}H NMR (499.26 MHz, $CDCl_3$) δ 0.86 (t, *J*= 7.4 Hz, 3H), 0.98 (d, *J*= 6.3 Hz, 6H), 1.31 (apparent sextet, *J*= 7.5 Hz, 2H) 1.54 (p, *J*= 7.1, 2H), 2.43 (t, *J*= 6.6 Hz, 2H), 2.74 (septet, *J*= 6.3 Hz, 1H), 2.80 (t, *J*= 6.6 Hz, 2H), 4.02 (t, *J*= 6.7 Hz, 2H); ^{13}C NMR (125.54 MHz, $CDCl_3$) δ 13.54, 19.10, 22.85, 30.60, 34.87, 42.49, 48.31, 64.20, 172.76; ν_{max} (ATR) cm^{-1} 2960, 2873, 1731 (C=O), 1467, 1379, 1337, 1262, 1173, 1148, 1064; *m/z* (EI) 187 (2), 186 (2), 172 (70), 144 (14), 130 (4), 116 (13), 114 (17), 98 (64), 88 (10), 72 (100), 70 (22), 56 (89); Anal. Calcd for $C_{10}H_{21}NO_2$: C 64.12, H 11.31, N 7.48; found C 64.08, H 11.45, N 7.49.

Propyl 3-(diethylamino)propanoate. Using the same procedure as for ethyl 3-(diethylamino)propanoate, 1.2 g (0.011 mol) propyl acrylate and 1.4 g (0.019 mol) of diethylamine yielded 1.6 g of product (85 % yield); bp 67 °C (4 torr): ^{1}H NMR (499.26 MHz, $CDCl_3$) δ 0.94 (t, *J*= 7.4 Hz, 3H), 1.02 (t, *J*= 7.2 Hz, 6H), 1.64 (apparent sextet, *J*= 7.1 Hz, 2H), 2.44 (t, *J*= 7.5 Hz,

2H), 2.51 (q, *J*= 7.2 Hz, 4H), 2.79 (t, *J*= 7.5 Hz, 2H), 4.03 (t, *J*= 6.7 Hz, 2H); ^{13}C NMR (125.54 MHz, $CDCl_3$) δ 10.36, 11.85, 21.96, 32.30, 46.80, 48.12, 65.94, 172.96; ν_{max} (ATR) cm^{-1} 2968, 2937, 2878, 2805, 1735 (C=O), 1465, 1382, 1198, 1178, 1062; *m/z* (EI) 187 (6), 172 (17), 158 (2), 144 (1), 130 (6), 128 (3), 100 (1), 99 (1), 98 (1), 86 (100), 73 (17), 70 (2), 58 (17), 55 (2); Anal. Calcd for $C_{10}H_{21}NO_2$: C 64.12, H 11.31, N 7.48; found C 63.94, H 11.46, N 7.46.

2.5 References

1) P. G. Jessop, L. Phan, A. Carrier, S. Robinson, C. J. Dürr and J. R. Harjani, *Green Chem.*, 2010, **12**, 809–814.

2) P. G. Jessop, L. Kozycz, Z. G. Rahami, D. Schoenmakers, A. R. Boyd, D. Wechsler and A. M. Holland, *Green Chem.*, 2011, **13**, 619–623.

3) N. F. Hall and M. R. Sprinkle, *J. Am. Chem. Soc.*, 1932, **54**, 3469–3485.

4) P. Paoletti, R. Barbucci, A. Vacca and A. Dei, *J. Chem. Soc. Inorg. Phys. Theor.*, 1971, 310–313.

5) C. Wiles and P. Watts, *Beilstein J. Org. Chem.*, 2011, **7**, 1360–1371.

6) H. K. Hall, *J. Phys. Chem.*, 1956, **60**, 63–70.

7) V. Frenna, N. Vivona, G. Consiglio and D. Spinelli, *J. Chem. Soc. Perkin Trans. 2*, 1985, 1865–1868.

8) M. M. Kreevoy and S.-W. Oh, *J. Am. Chem. Soc.*, 1973, **95**, 4805–4810.

9) R. E. McMahon and N. R. Easton, *J. Med. Pharm. Chem.*, 1961, **4**, 437–445.

10) J. M. Devereux, K. R. Payne and E. R. A. Peeling, J. Chem. Soc., 1957, 2845–2851.

11) L. C. Craig and R. M. Hixon, *J. Am. Chem. Soc.*, 1931, **53**, 4367–4372.

12) S. Jarmelo, N. Maiti, V. Anderson, P. R. Carey and R. Fausto, *J. Phys. Chem. A*, 2005, **109**, 2069–2077.

13) I. V. Tetko and V. Y. Tanchuk, *J. Chem. Inf. Comput. Sci.*, 2002, **42**, 1136–1145.

14) I. V. Tetko, J. Gasteiger, R. Todeschini, A. Mauri, D. Livingstone, P. Ertl, V. A. Palyulin, E. V. Radchenko, N. S. Zefirov, A. S. Makarenko, V. Y. Tanchuk and V. V. Prokopenko, *J. Comput. Aided Mol. Des.*, **19**, 453–463.

15) Virtual Computational Chemistry Laboratory, http://www.vcclab.org/ (accessed September 14, 2016).

16) J. S. McNally, B. Noll, C. J. Orme and A. D. Wilson, *J. Phys. Chem. B*, 2015, **119**, 6766–6775.

17) J. R. Vanderveen, J. Durelle and P. G. Jessop, *Green Chem.*, 2014, **16**, 1187–1197.

18) J. Hine and M. N. Khan, *Indian J. Chem. Sect. B Org. Chem. Med. Chem.*, 1992, **31B**, 427–435.

19) G. M. Steinberg and J. Bolger, *J. Am. Pharm. Assoc. Sci. Ed*, 1957, **46**, 188–191.

20) R. J. Littel, M. Bos and G. J. Knoop, *J. Chem. Eng. Data*, 1990, **35**, 276–277.

21) F. Wang and L. M. Sayre, *J. Am. Chem. Soc.*, 1992, **114**, 248–255.

22) A. Gero, *J. Med. Chem.*, 1963, **6**, 458–459.

23) I. M. Al-Najjar and M. Green, *J. Chem. Soc. Dalton Trans.*, 1979, 1651–1656.

24) C. W. Hoerr, M. R. McCorkle and A. W. Ralston, *J. Am. Chem. Soc.*, 1943, **65**, 328–329.

25) F. Bougie and M. C. Iliuta, *J. Chem. Eng. Data*, 2012, **57**, 635–669.

26) J. Zhang, R. Misch, Y. Tan and D. W. Agar, *Chem. Eng. Technol.*, 2011, **34**, 1481–1489.

27) W. Böttinger, M. Maiwald and H. Hasse, *Fluid Ph. Equilibria*, 2008, **263**, 131–143.

28) Q. Yang, M. Bown, A. Ali, D. Winkler, G. Puxty and M. Attalla, *Energy Procedia*, 2009, **1**, 955–962.

29) F. Barzagli, F. Mani and M. Peruzzini, *Energy Environ. Sci.*, 2010, **3**, 772–779.

30) J. P. Jakobsen, J. Krane and H. F. Svendsen, *Ind. Eng. Chem. Res.*, 2005, **44**, 9894–9903.

31) Toxicity Estimation Software Tool (TEST) v4.1, US EPA. https://www.epa.gov/chemical-research/toxicity-estimation-software-tool-test (accessed January 29, 2018).

32) R. J. Lewis and N. I. Sax, *Sax's dangerous properties of industrial materials*, Van Nostrand Reinhold, New York, 9th ed., 1996.

33) E. J. Gallegos, *Anal. Chem.*, 1981, **53**, 187–189.

34) G. G. Hawley, *The Condensed chemical dictionary*, Van Nostrand Reinhold Co, New York, 10th ed., 1981.

35) N,N-Dimethylcyclohexylamine; MSDS No. 290629; Sigma-Aldrich, http://www.sigmaaldrich.com/MSDS/MSDS/DisplayMSDSPage.do?country=CA&language=en&productNumber=290629&brand=ALDRICH&PageToGoToURL=http%3A%2F%2Fwww.sigmaaldrich.com%2Fcatalog%2Fproduct%2Faldrich%2F290629%3Flang%3Den (accessed September 15, 2016).

36) 1-Ethylpiperidine; MSDS No. 800956; EMD Millipore, http://www.emdmillipore.com/Web-CA-Site/en_CA/-/CAD/ProcessMSDS-Start?PlainSKU=MDA_CHEM-800956&Origin=PDP (accessed September 15, 2016).

37) W. B. Wright, *J. Org. Chem.*, 1962, **27**, 1042–1045.

38) H. Yoshikawa and K. Kawai, *Ind. Health*, 1966, **4**, 63–68.

39) 1-Butylpyrrolidine; MSDS No. 280372; Sigma-Aldrich, http://www.sigmaaldrich.com/MSDS/MSDS/DisplayMSDSPage.do?country=CA&language=en&productNumber=280372&brand=ALDRICH&PageToGoToURL=http%3A%2F%2Fwww.sigmaaldrich.com%2Fcatalog%2Fproduct%2Faldrich%2F280372%3Flang%3Den (accessed September 15, 2016).

40) T. Caronna, A. Citterio, T. Crolla, M. Ghirardini and F. Minisci, *J. Heterocycl. Chem.*, 1976, **13**, 955–960.

41) N,N-Dimethylhexylamine; MSDS No. 308102; Sigma-Aldrich, http://www.sigmaaldrich.com/MSDS/MSDS/DisplayMSDSPage.do?country=CA&language=en&productNumber=308102&brand=ALDRICH&PageToGoToURL

=http%3A%2F%2Fwww.sigmaaldrich.com%2Fcatalog%2Fproduct%2Faldrich%2F308102%3Flang%3Den, (accessed September 15, 2016).

42) N,N-Dimethylbutylamine; MSDS No. 10370; OXEA Corporation, http://www.oxea-chemicals.com/download/wercs/ MTAzNzAjZW4jcHMjYXVzIzE0MzI2MzkyMDMwMDAjb3hlYSMxI0Q=/10370-en-ps-us.pdf (accessed September 15, 2016).

43) W. H. Bell, G. B. Carter and J. Dewing, *J. Chem. Soc. C Org.*, 1969, 352–354.

44) A. R. Lepley and W. A. Khan, *J. Org. Chem.*, 1966, **31**, 2061–2064.

45) N,N-Diethylbutylamine; MSDS No. 460982; Sigma-Aldrich, http://www.sigmaaldrich.com/MSDS/MSDS/DisplayMSDSPage.do?country=CA&language=en&productNumber=460982&brand=ALDRICH&PageToGoToURL=http%3A%2F%2Fwww.sigmaaldrich.com%2Fcatalog%2Fproduct%2Faldrich%2F460982%3Flang%3Den (accessed September 15, 2016).

46) N. C. Deno and R. E. Fruit, *J. Am. Chem. Soc.*, 1968, **90**, 3502–3506.

47) N-Methyldipropylamine; MSDS No. 518824; Sigma-Aldrich, http://www.sigmaaldrich.com/MSDS/MSDS/DisplayMSDSPage.do?country=CA&language=en&productNumber=518824&brand=ALDRICH&PageToGoToURL=http%3A%2F%2Fwww.sigmaaldrich.com%2Fcatalog%2Fproduct%2Faldrich%2F518824%3Flang %3Den (accessed September 15, 2016).

48) G. R. Colonna and A. B. Spencer, *Fire Protection Guide to Hazardous Materials*, National Fire Protection Association, Quincy, MA, 13 edition., 2002.

49) Triethylamine; MSDS No. 471283; Sigma-Aldrich, http://www.sigmaaldrich.com/MSDS/MSDS/DisplayMSDSPage.do?country=CA&language=en&productNumber=471283&brand=SIAL&PageToGoToURL=http%3A%2F%2Fwww.sigmaaldrich.com%2Fcatalog%2Fproduct%2Fsial%2F471283%3Flang%3Den (accessed September 15, 2016).

50) R. E. Watson, A. M. Hafez, J. N. Kremsky and G. O. Bizzigotti, *Int. J. Toxicol.*, 2007, **26**, 503–512.

51) P. A. A. Klusener, L. Tip and L. Brandsma, *Tetrahedron*, 1991, **47**, 2041–2064.

52) 2-(Diisopropylamino)ethanol; MSDS No. 471488; Sigma-Aldrich, http://www.sigmaaldrich.com/MSDS/MSDS/DisplayMSDSPage.do?country=CA

&language=en&productNumber=471488&brand=ALDRICH&PageToGoToURL=http%3A%2F%2Fwww.sigmaaldrich.com%2Fcatalog%2Fproduct%2Faldrich%2F471488%3Flang %3Den (accessed September 15, 2016).

53) W. B. Burnett, R. L. Jenkins, C. H. Peet, E. E. Dreger and R. Adams, *J. Am. Chem. Soc.*, 1937, **59**, 2248–2252.

54) 2-(Dibutylamino)ethanol; MSDS No. 550035; Sigma-Aldrich, http://www.sigmaaldrich.com/MSDS/MSDS/DisplayMSDSPage.do?country=CA&language=en&productNumber=550035&brand=ALDRICH&PageToGoToURL=http%3A%2F%2Fwww.sigmaaldrich.com%2Fcatalog%2Fproduct%2Faldrich%2F550035%3Flang%3Den (accessed September 15, 2016).

55) Pulla, R. M. and Venkaiah, C. N., international pat. app. no. WO2003101931 A2, 2003.

56) 4,4-Diethoxy-N,N-dimethyl-1-butanamine; MSDS No. 647055; Sigma-Aldrich, http://www.sigmaaldrich.com/MSDS/MSDS/DisplayMSDSPage.do?country=CA&language=en&productNumber=647055&brand=ALDRICH&PageToGoToURL=http%3A%2F%2Fwww.sigmaaldrich.com%2Fcatalog%2Fproduct%2Faldrich%2F647055%3Flang%3Den (accessed September 15, 2016).

57) G. W. Gribble and C. F. Nutaitis, *Synthesis*, 2002, **1987**, 709–711.

58) N,N-Dimethylphenethylamine; MSDS No. 523801; Sigma-Aldrich, http://www.sigmaaldrich.com/MSDS/MSDS/DisplayMSDSPage.do?country=CA&language=en&productNumber=523801&brand=ALDRICH&PageToGoToURL=http%3A%2F%2Fwww.sigmaaldrich.com%2Fcatalog%2Fproduct%2Faldrich%2F523801%3Flang%3Den (accessed September 15, 2016).

59) P. G. Stone and S. G. Cohen, *J. Am. Chem. Soc.*, 1982, **104**, 3435–3440.

60) Dipropylamine; MSDS No. D214752; Sigma-Aldrich, http://www.sigmaaldrich.com/MSDS/MSDS/DisplayMSDSPage.do?country=CA&language=en&productNumber=D214752&brand=ALDRICH&PageToGoToURL=http%3A%2F%2Fwww.sigmaaldrich.com%2Fcatalog%2Fproduct%2Faldrich%2Fd214752%3Flang%3Den (accessed September 15, 2016).

61) F. Franks and B. Watson, *Trans. Faraday Soc.*, 1967, **63**, 329–334.

62) Di-sec-butylamine, mixture of (±) and meso; MSDS No. 307351; Sigma-Aldrich, http://www.sigmaaldrich.com/MSDS/MSDS/DisplayMSDSPage.do?country=CA&language=en&productNumber=307351&brand=ALDRICH&PageToGoToURL=http%3A%2F%2Fwww.sigmaaldrich.com%2Fcatalog%2Fproduct%2Faldrich%2F307351%3Flang%3Den (accessed September 15, 2016).

63) D. G. Norton, V. E. Haury, F. C. Davis, L. J. Mitchell and S. A. Ballard, *J. Org. Chem.*, 1954, **19**, 1054–1066.

64) N-sec-Butylpropylamine; MSDS No. B1073; TCI America, http://www.tcichemicals.com/eshop/en/us/commodity/B1073/ (accessed September 15, 2016).

65) D. Redmore, *J. Org. Chem.*, 1978, **43**, 992–996.

66) N,N-Dimethylbenzylamine; MSDS No. 185582; Sigma-Aldrich, http://www.sigmaaldrich.com/MSDS/MSDS/DisplayMSDSPage.do?country=CA&language=en&productNumber=185582&brand=ALDRICH&PageToGoToURL=http%3A%2F%2Fwww.sigmaaldrich.com%2Fcatalog%2Fproduct%2Faldrich%2F185582%3Flang%3Den (accessed September 15, 2016).

67) E. T. Kimura, D. M. Ebert and P. W. Dodge, *Toxicol. Appl. Pharmacol.*, 1971, **19**, 699–704.

68) V. A. Benignus, *Neurotoxicology*, 1981, **2**, 567–588.

69) K. Fukunishi, B. Czech and S. L. Regen, *J. Org. Chem.*, 1981, **46**, 1218–1221.

70) Toluene; MSDS No. 108325; EMD Millipore, http://www.emdmillipore.com/Web-CA-Site/en_CA/-/CAD/ProcessMSDS-Start?PlainSKU=MDA_CHEM-108325&Origin=PDP (accessed September 15, 2016).

71) N. Chang, Z.-Y. Gu and X.-P. Yan, *J. Am. Chem. Soc.*, 2010, **132**, 13645–13647.

72) Hexane; MSDS No. 296090; Sigma-Aldrich, http://www.sigmaaldrich.com/MSDS/MSDS/DisplayMSDSPage.do?country=CA&language=en&productNumber=296090&brand=SIAL&PageToGoToURL=http%3A%2F%2Fwww.sigmaaldrich.com%2Fcatalog%2Fproduct%2Fsial%2F296090%3Flang%3Den (accessed September 15, 2016).

73) Y. Takeuchi, *Environ. Res.*, 1993, **62**, 76–80.

74) O. F. Sendur, Y. Turan, S. Bal and A. Gurgan, *Inhal. Toxicol.*, 2009, **21**, 210–214.

75) D. R. M. Glenn D. Ritchie Kenneth R.Still, William K.Alexander, Alan F.Nordholm, Cody L.Wilson, John Rossi III, *J. Toxicol. Environ. Health Part B*, 2001, **4**, 223–312.

76) R. Snyder, Ed., *Ethel Browning's Toxicity and Metabolism of Industrial Solvents*, Elsevier, New York, 2nd edn., 1987.

77) *Documentation of the Threshold Limit Values and Biological Exposure Indices*, American Conference of Governmental Industrial Hygienists, Inc., Cincinnati, OH, 6th edn., 1991.

78) A. N. Campbell, *Can. J. Chem.*, 1981, **59**, 127–131.

79) L. M. Besley and G. A. Bottomley, *J. Chem. Thermodyn.*, 1974, **6**, 577–580.

80) S. A. Wieczorek and J. Stecki, *J. Chem. Thermodyn.*, 1978, **10**, 177–186.

81) *Globally Harmonized System of Classification and Labelling of Chemicals (GHS)*, United Nations, New York and Geneva, 4th edn., 2011.

82) R. Heijungs, J. B. Guinée, G. Huppes, R. M. Lankreijer, H. A. Udo de Haes, A. Wegener Sleeswijk, A. M. M. Ansems, P. G. Eggels, R. van Duin, H. P. de Goede and I. of E. Sciences, *Environmental life cycle assessment of products: guide and backgrounds (Part 2)*, CML, Leiden, 1992.

83) J. R. Baker, M. W. Milke and J. R. Mihelcic, *Water Res.*, 1999, **33**, 327–334.

84) D. T. Allen and D. R. Shonnard, *Green engineering: environmentally conscious design of chemical processes*, Prentice Hall PTR, Upper Saddle River, NJ, 2002.

85) W. P. L. Carter, *Air Waste*, 1994, **44**, 881–899.

86) R. S. Boethling, E. Sommer and D. DiFiore, *Chem. Rev.*, 2007, **107**, 2207–2227.

87) P. H. Howard, W. M. Stiteler, W. M. Meylan, A. E. Hueber, J. A. Beauman, M. E. Larosche and R. S. Boethling, *Environ. Toxicol. Chem.*, 1992, **11**, 593–603.

88) I. Eide-Haugmo, O. G. Brakstad, K. A. Hoff, K. R. Sørheim, E. F. da Silva and H. F. Svendsen, *Energy Procedia*, 2009, **1**, 1297–1304.

89) I. Eide-Haugmo, H. Lepaumier, A. Einbu, K. Vernstad, E. F. da Silva and H. F. Svendsen, *Energy Procedia*, 2011, **4**, 1631–1636.

90) I. Eide-Haugmo, O. G. Brakstad, K. A. Hoff, E. F. da Silva and H. F. Svendsen, *Int. J. Greenh. Gas Control*, 2012, **9**, 184–192.

91) D. Calamari, R. Da Gasso, S. Galassi, A. Provini and M. Vighi, *Chemosphere*, 1980, **9**, 753–762.

92) M. Kawasaki, *Ecotoxicol. Environ. Saf.*, 1980, **4**, 444–454.

93) K. Kawahara, Y. Yakabe, T. Ohide and K. Kida, *Chemosphere*, 1999, **39**, 2007–2018.

94) Cyclohexyldimethylamine - Registration Dossier - ECHA, https://echa.europa.eu/registration-dossier/-/registered-dossier/13521/5/3/2 (accessed September 16, 2016).

95) E. M. Davis, H. E. Murray, J. G. Liehr and E. L. Powers, *Water Res.*, 1981, **15**, 1125–1127.

96) G. Pasteris, D. Werner, K. Kaufmann and P. Höhener, *Environ. Sci. Technol.*, 2002, **36**, 30–39.

97) N-hexane - Registration Dossier - ECHA, https://echa.europa.eu/registration-dossier/-/registered-dossier/15741/7/8, accessed 10 January 2018.

98) Toluene - Registration Dossier - ECHA, https://echa.europa.eu/registration-dossier/-/registered-dossier/15538/7/8, accessed 10 January 2018.

99) Triethylamine - Registration Dossier - ECHA, https://echa.europa.eu/registration-dossier/-/registered-dossier/14938/7/8, accessed 10 January 2018.

100) R. N. Loeppky, in *Nitrosamines and Related N-Nitroso Compounds*, American Chemical Society, 1994, vol. 553, pp. 1–18.

101) S. S. Mirvish, *Toxicol. Appl. Pharmacol.*, 1975, **31**, 325–351.

102) 2-dibutylaminoethanol - Registration Dossier - ECHA, https://echa.europa.eu/registration-dossier/-/registered-dossier/5336/7/8, accessed 10 January 2018.

103) J. A. Gowland and G. H. Schmid, *Can. J. Chem.*, 1969, **47**, 2953–2958.

104) B. Zou and H.-F. Jiang, *Chin. J. Chem.*, 2008, **26**, 1309–1314.

105) S. R. Cheruku, S. Maiti, A. Dorn, B. Scorneaux, A. K. Bhattacharjee, W. Y. Ellis and J. L. Vennerstrom, *J. Med. Chem.*, 2003, **46**, 3166–3169.

Chapter 3

Modelling the behaviour of switchable hydrophilicity solvents

3.1 Introduction

The data presented in Chapter 2 confirmed that the ability of amines to act as SHSs depends at least in part on their hydrophobicity, represented by log K_{ow}, and their basicities, represented by pK_{aH}. If an amine is too hydrophilic, it will always be completely miscible with water. If an amine is too hydrophobic, it will always be poorly miscible with water. Only amines with intermediate hydrophobicity will switch between being miscible and immiscible with water in the absence and presence of CO_2, respectively. Likewise, if an amine is insufficiently basic, its reaction with CO_2 and water to form ammonium bicarbonate will not proceed far enough to result in a large change in miscibility with water. For amines, the acceptable log K_{ow} range is between 1.1 and 2.6 and the minimum pK_{aH} is 9.5. A similar reliance on log K_{ow} and pK_{aH} is expected for amidines, but the ranges of acceptable values have not been confirmed (a suggested acceptable log K_{ow} range between 3 and 7 has been proposed).[1] If log K_{ow} and pK_{aH} affect whether an amine is a SHS, a mathematical model to describe and predict SHS behaviour can be developed based on these two terms.

The focus of this chapter is on the development of a mathematical description of two systems related to amine SHSs: one where the system consists of two liquids (water and amine), and another where the system consists of three liquids (water, amine, and a hydrophobic liquid). The two-component system serves as an appropriate model for the tests used to confirm if an amine is a SHS (that is, determining if it can switch between poorly miscible with water and highly miscible with water), but also for determining how much SHS can be recovered from a carbonated SHS-water mixture by the removal of CO_2 from the system in a SHS-based separation process. The three-component system serves as an appropriate model to determine how well a SHS can be separated from a liquid solute (e.g. soybean oil) by partitioning into water in a SHS-based

separation process. With the help of an accurate mathematical model, these systems could be optimized in terms of both intrinsic (basicity, hydrophilicity, molecular weight, density) and extrinsic (volume, pressure) parameters. The model described here will be discussed with regards to systems under "standard" conditions (a 1:1 (v:v) mix of water:amine switching between 0 and 1 bar CO_2) and "non-standard" conditions (larger volume ratios of water:amine and/or switching between CO_2 pressures other than 0 and 1 bar).

The models described in this chapter assume that the reactivity of a SHS with CO_2 is limited to the formation of bicarbonate salts. In the search for new examples of SHSs described in Chapter 2, amines that might produce carbamate salts were avoided. Upon bubbling of CO_2 through a mixture of water and either a primary or a non-bulky secondary amine, both bicarbonate and carbamate salts of the amine are produced. Tertiary and bulky secondary amines are unable to produce stable carbamates. Furthermore, carbonate salts are not observed in SHS systems due to the instability of the carbonate ion at the pH ranges observed when comparable volumes of water and amine are carbonated (typically pH ≈ 8). The acidity of the second proton of carbonic acid (pK_{a2} = 10.3) is close to the acidity of the protonated SHS (typically $pK_{aH} \approx 10$).[2] Although systems that can form carbamate or carbonate salts may be viable SHS systems, a different model would likely need to be developed to account for the reactivity of these salts, which are different than the reactivity of bicarbonate salts.

This chapter is partly reproduced from three articles published in *Phys. Chem. Chem. Phys.*, including the initial model development described in Durelle *et al.*, *Phys. Chem. Chem. Phys*., 2014, **16**, 5270-5275 and the improvements made to the model described in Durelle *et al.*, *Phys. Chem. Chem. Phys.*, 2015, **17**, 5308-5313.[3,4] The equations used in the model were derived by Jeremy Durelle with the assistance of Courtney Chalifoux and Julia Kostin. The experimental work in the chapter was performed by Yi Quan under my supervision and the supervision of Jeremy Durelle. I conceived the Ω parameter used to model the three-component system. The equations

used to calculate percent/fraction of protonation are reproduced from a section from Alshamrani *et al.*, *Phys. Chem. Chem. Phys.*, 2016, **18**, 19276-19288.[5] These equations were derived by me. Various changes have been made in these reproductions to better fit the format and theme of this thesis. The derivations of the equations described in this chapter are presented in Appendix 1.

3.2 The two-component system

3.2.1 Model development and comparison to experimental observations under standard conditions

The two-component system consists of water and an amine solvent. This system, shown graphically in Fig. 3.1 and described in detail in Section 1.4, is used when an amine solvent is being tested for suitability as a SHS and when a SHS is being separated from water after the product of a SHS-based separation has been isolated. To qualify as a SHS, the amine must have a low water solubility at low pressures of CO_2 (S, in moles per litre) and a high solubility at high pressures of CO_2 (S′, in moles per litre). In SHS systems, the pressure of CO_2 is typically alternated between ~0 atm (P_{CO2}) and ~1 atm (P_{CO2}'). The term "solubility" used here also includes "miscibility" so that we can include both solid and liquid species. A low S and a high S′ are also required for the

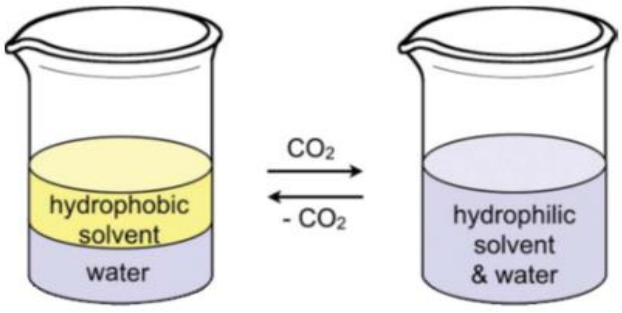

Fig. 3.1 The two-component SHS system consisting of a SHS and water in the absence of CO_2 (left) or the presence of CO_2 (right).

SHS-based separation process described in Section 1.4 to be practical. The solubility of an amine can be related to the number of moles of amine that failed to dissolve in the water:

$$n_{B,undiss} = \frac{\rho}{MW} V_B - S V_w \quad \text{Eqn. 3.1}$$

$$n'_{B,undiss} = \frac{\rho}{MW} V_B - S' V_w \quad \text{Eqn. 3.2}$$

where ρ and MW represent the amine's density and molecular weight, respectively. V_B and V_w represent the volumes of amine and water added to the system, respectively. $n_{B,undiss}$ and $n'_{B,undiss}$ are the moles of amine that remain undissolved in the water after the system has reached equilibrium, respectively. S and S′ are defined to be the total concentration of dissolved amine as either the neutral base or the protonated species, respectively:

$$S \text{ or } S' = [B]_{aq} + [BH^+]_{aq} \quad \text{Eqn. 3.3}$$

Equation 3.3 can be rewritten using equations 3.4-3.6 to substitute for $[BH^+]_{aq}$ to give equations 3.7 and 3.8.

$$K_{aH} = \frac{[B]_{aq}[H^+]_{aq}}{[BH^+]_{aq}} \quad \text{Eqn. 3.4}$$

$$K_1 = \frac{[HCO_3^-]_{aq}[H^+]_{aq}}{K_H P_{CO_2}} \text{ or } \frac{[HCO_3^-]_{aq}[H^+]_{aq}}{K_H P'_{CO_2}} \quad \text{Eqn. 3.5}$$

$$[H^+]_{aq} + [BH^+]_{aq} = [OH^-]_{aq} + [HCO_3^-]_{aq} \quad \text{Eqn. 3.6}$$

$$S = [B]_{aq}\left(1 + \frac{1}{K_{aH}}\sqrt{\frac{K_w + K_1 K_H P_{CO_2}}{1 + [B]_{aq} K_{aH}^{-1}}}\right) \quad \text{Eqn. 3.7}$$

$$S' = [B]_{aq}\left(1 + \frac{1}{K_{aH}}\sqrt{\frac{K_w + K_1 K_H P'_{CO_2}}{1 + [B]_{aq} K_{aH}^{-1}}}\right) \quad \text{Eqn. 3.8}$$

The concentration of neutral amine in the aqueous phase $[B]_{aq}$ is assumed to be equal to the aqueous solubility of the neutral amine at saturation, S_0, and is assumed to remain constant throughout the process. In cases where only a small amount of amine is present such that the total moles of amine is less than S_0, the amine would form a monophasic mixture with water in the

absence of CO_2 and would not be a SHS. Therefore, these cases were not considered in this study. S_0 can be estimated from log K_{ow} using equation 3.9 from Meylan *et al.*[6] which also accounts for the molecular weight and the effect of an aliphatic amine functional group:

$$\log S = 0.796 - 0.854(\log K_{ow}) - 0.00728(MW) + \sum f_i \qquad \text{Eqn. 3.9}$$

where f_i = 1.008 for aliphatic amines. This value of f_i will be used for the model. It is through equation 3.9 that this mathematical model relates to the observed log K_{ow} requirements for amines to be SHSs. For the purposes of this model, the molecular weight, MW, of a typical amine being tested as a SHS was assumed to be 130 g mol^{-1}. Because the assumptions used to estimate f_i and MW are based on values for amine SHSs and not amidine SHSs, only amine SHSs will be discussed in this chapter.

To determine whether S_0 is a constant throughout the process or whether it is affected by the increasing concentration of BH^+ as CO_2 is added, the solubility of *N*,*N*-dimethylcyclohexylamine (DMCA) was measured in increasingly salty aqueous phases. Trimethylcyclohexylammonium iodide ([CyNMe$_3$]I) was added to the mixture to best simulate the system as the protonated amine is drawn into the aqueous phase. *N*,*N*-Dimethylcyclohexylammonium bicarbonate was not used because it can decompose into DMCA, water, and CO_2, thus it would be difficult to control the experiment. Fig. 3.2 shows that the solubility of DMCA increases in aqueous solutions of [CyNMe$_3$]I. A biphasic system could not be attained after the salt concentration reached about 1.0 mol L^{-1} indicating that DMCA is completely miscible with the aqueous phase at such high salt concentrations. This higher solubility is likely due to favourable interactions between neutral amine and the organic cation, which are both relatively hydrophobic species in a hydrophilic environment. Therefore, the solubility of the neutral amine in the aqueous phase would increase as CO_2 is bubbled into the mixture due to the hydrotropic effect of the ammonium cation. As CO_2 is removed from the system, the ammonium salt returns to its neutral form, decreasing the salt concentration in solution and thereby negating

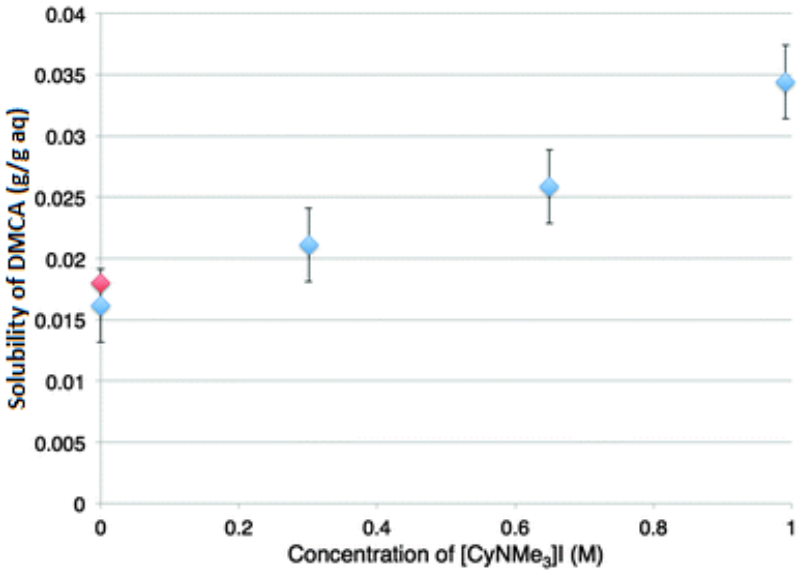

Fig. 3.2 Solubility of DMCA in aqueous solutions of organic salt [CyNMe$_3$]I (standard deviation: ±0.03 g/g from three replicates. The red point corresponds to the reported water solubility of DMCA in the literature.[7]

---

the hydrotropic effect. The increase in solubility of the neutral amine has minimal effect on the model, allowing for switchable behaviour with more hydrophobic amines having slightly lower pK_{aH} values than predicted without this correction.

A good SHS will have S′ >> S. A mapping parameter, Z, which has a value close to 1 when S′ ≫ S and is equal to 0 when S′ = S, is used as a function to determine if an amine will be effective as a SHS:

$$Z = \frac{MW}{\rho} V_{rat}(S' - S) \qquad \text{Eqn. 3.10}$$

where V_{rat} is the amine:water volume ratio (V_B/V_W). The system is restrained by assuming a density and molecular weight typical of SHSs: ρ = 0.85 g mL^{-1} and MW = 130 g mol^{-1}, respectively. Z is used to gauge SHS viability. An amine which has a Z value close to 1 will be an effective SHS whereas an amine with Z ≈ 0 will not.

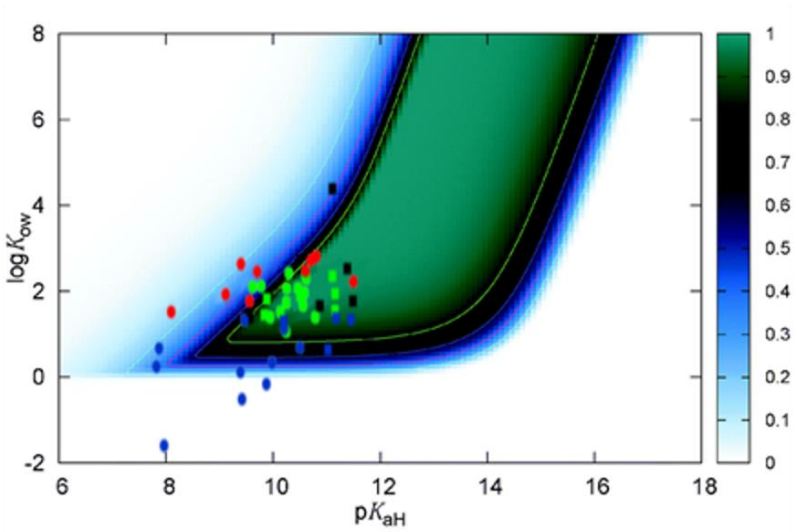

Fig. 3.3 A graph indicating the region of high SHS viability in a two-component system. The z-axis represents Z from equation 3.10. The green dots represent confirmed tertiary and bulky secondary amine SHSs. The red, blue, and black dots represent some tertiary amines that are not SHSs under standard conditions.

The map shown in Fig. 3.3 outlines the ranges of log K_{ow} and pK_{aH} that are optimal for switchable behaviour. The maps were made for 1:1 (v:v) water:amine mixtures switching between CO_2 pressures of 0 and 1 bar. The green area on the graph represents a region where Z is large (> ~0.8), indicating that amines with log K_{ow} and pK_{aH} values in this region should be SHSs. Other regions where Z is small indicate that amines with log K_{ow} and pK_{aH} values in these regions are not likely to be SHSs.

One feature of the graph is a steep increase in the required log K_{ow} at high pK_{aH} values. This steep increase is consistent with the reaction of stronger bases with water to form hydrophilic hydroxide salts. This reaction with water will be more complete for stronger bases than for weaker bases, thereby increasing the amount of hydrophilic salts at lower pressures of CO_2. In order for more basic solvents to be SHSs, they must be more hydrophobic so that the formation of hydroxide salts will not cause them to dissolve in water.

The dots on the graphs represent all of the amine SHSs described in Chapter 2 (green) and amines that are not SHSs under standard conditions (red, blue, and black). The amidine SHSs are not shown because this model was developed for amines and may not be valid for amidines because the value for f_i in equation 3.9 may be different for amidines. This map is in good agreement with the experimental data: most of the SHSs have Z values greater than 0.8 and most of the non-SHSs have Z values less than 0.8. However, the model predicts high Z values for compounds with log K_{ow} values near 1.0 even though the results from Chapter 2 suggest that the minimum log K_{ow} value is approximately 1.2 for SHS behaviour. A likely source of this erroneous result comes from the solubility QSAR in equation 3.9, which uses various assumptions and may be accurate (see Appendix 2 for a discussion of solubility QSAR accuracy). Apart from this difference between the model and the experimental results, the biggest discrepancy between the model and the observed behaviour is that of the *N*,*N*-diisopropylethylamine (DIPEA), represented by the rightmost red dot. DIPEA is not a SHS despite having an appropriate log K_{ow} and pK_{aH}. Its behaviour differs from what is expected due to the steric bulk around the nitrogen center, as determined by McNally *et al.*[8] The model described in this chapter does not account for steric effects on SHSs, therefore it is not unexpected that an amine with significant steric bulk behaves differently than the model predicts.

3.2.2 Application of the model to non-standard conditions and comparison to experimental observations

The two-component system model described above contains two extrinsic variables, water:amine volume ratio and partial pressure of CO_2, that may affect the switchable behaviour of an amine. Section 3.2.1 discusses the model under "standard" SHS conditions: using a 1:1 (v:v) ratio of water:amine and switching between CO_2 partial pressures of 0 bar and 1 bar. In this section, the model will be applied to systems under "non-standard" conditions including increased water:amine volume ratios, switching between different partial pressures of CO_2, or a combination

of the two. Using non-standard conditions may result in different amines displaying SHS behaviour than those observed under standard conditions.

Plots mapping the value of Z as a function of log K_{ow} and pK_{aH} under different pressures of CO_2 but using the same water:amine volume ratio (1:1) are shown in Fig. 3.4. As a comparison to experimental results, the points shown on the graphs represent several known amine SHSs, shown as green dots, as well as five amines that do not act as SHSs under the standard conditions, shown in red. These five amines are *N*,*N*-diethylcyclohexylamine (DECA), tripropylamine (TPA), *N*,*N*-dimethylbenzylamine (DMBA), 1-dimethylamino-2-pentyne (DMAP), and *N*,*N*-diisopropylethylamine (DIPEA).

Fig. 3.4a is a reproduction of Fig. 3.3 and is included to simplify comparisons between it and Figs 3.4b and 3.4c. It shows the range of acceptable log K_{ow} and pK_{aH} values for SHSs when the system is switched between 0 bar CO_2 and 1 bar CO_2. Fig. 3.4b shows the range of acceptable values when the system is switched between 0 bar CO_2 and 10 bar of CO_2. The two ranges are very similar, but the range of acceptable values when using 0 and 10 bar CO_2 extends to lower pK_{aH} values and/or higher log K_{ow} values than when using 0 and 1 bar CO_2. This difference suggests that some amines which are not expected to act as SHSs under the standard conditions may act as SHSs when higher pressures of CO_2 are used to switch the amines to their hydrophilic state, as shown in the Fig 3.4b by the presence of the red dots within the area of large Z values.

The third graph, shown in Fig. 3.4c, illustrates a system where the pressure of CO_2 is adjusted between 1 bar and 10 bar. The range of acceptable log K_{ow} and pK_{aH} values shown in this graph demonstrates the difference between Fig. 3.4a and Fig. 3.4b. This map of Z suggests that some amines can act as SHSs without requiring near-complete removal of CO_2 from the system. Amines that act as SHSs when the system is switched between 1 bar and 10 bar CO_2 ("high-pressure SHSs") can be switched to their hydrophobic, poorly-miscible state simply by depressurizing the system to 1 bar. In contrast, amines that require low CO_2 pressures to switch to their hydrophobic

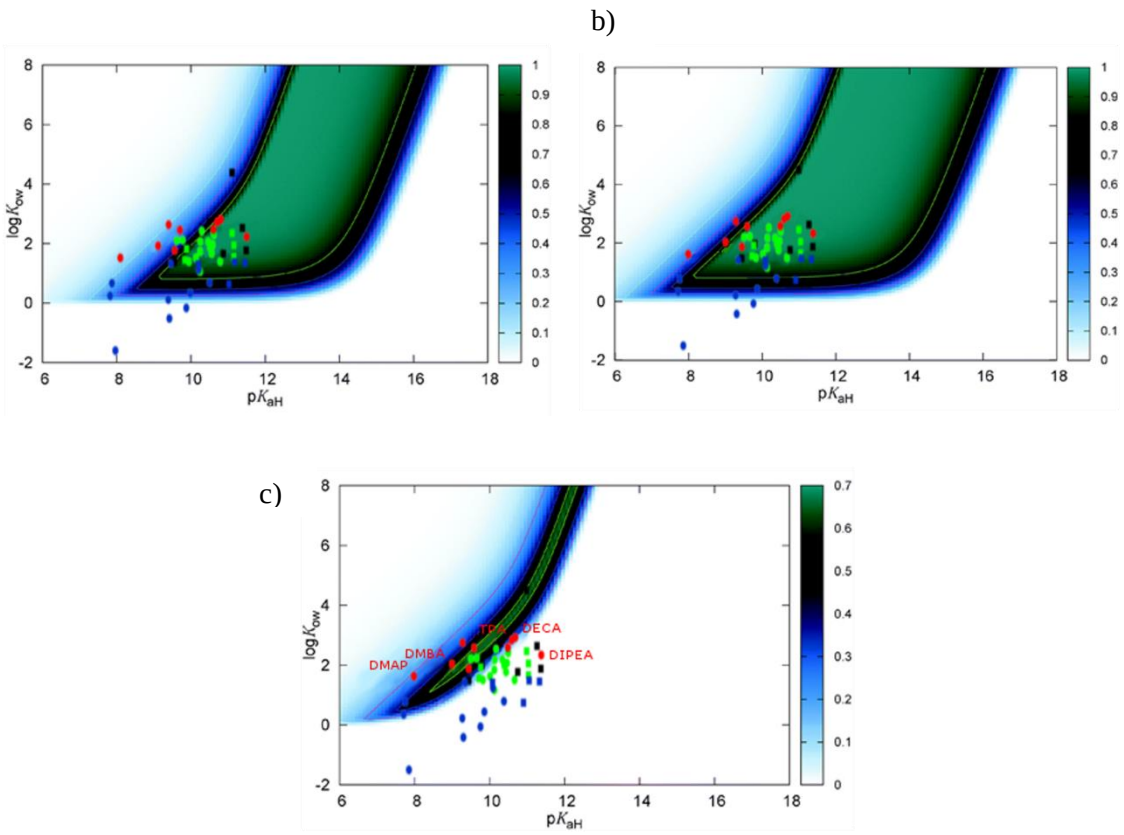

Fig. 3.4 A graph indicating the region of high SHS viability in a two-component system at (a) $P_{CO2}' = 1$ bar and $P_{CO2} = 0$ bar or (b) $P_{CO2}' = 10$ bar and $P_{CO2} = 0$ bar. The region in (c) represents the high pressure SHSs which are water-miscible at $P_{CO2}' = 10$ bar but biphasic at $P_{CO2} = 1$ bar. The amines that lie in the green region of (c) should switch off very easily. Map (c) is also the difference between maps (a) and (b). The green dots represent confirmed amine SHSs. The red, blue, and black dots represent amines that are not SHSs under standard conditions. Five amines that are discussed in this chapter that are not SHSs under standard conditions but are SHSs under nonstandard conditions

state must be heated and have inert gasses bubbled through them in order to remove CO_2 from the system at a reasonable rate. If the switching of high-pressure SHSs to their hydrophobic states can be achieved by simply depressurizing the system, they may be advantageous for processes where heating is undesirable.

In addition to plotting the ranges of acceptable log K_{ow} and pK_{aH} for systems using different pressures of CO_2, equations based on the two-component system model can be used to predict the CO_2 pressure or water:amine volume ratio required for a given amine to become miscible with water. Two new equations can be derived to solve for V_{rat} at a given CO_2 pressure or for P_{CO2}' at a given water:amine volume ratio (equations 3.11 and 3.12). If a system is designed to use specific a)
partial pressures of CO_2 to switch an amine between its hydrophobic and hydrophilic states, then equation 3.11 can be used to identify the minimum water:amine volume ratio required for the amine to act as a SHS. If a system is designed to use a specific water:amine volume ratio, then equation 3.12 can be used to identify the minimum partial pressure of CO_2 required for an amine to become miscible with water (assuming negligible miscibility in the absence of CO_2). Switching between two partial pressures of CO_2, one above this value and one below it, will allow the amine to act as a SHS. Note that in equation 3.11, the P_{CO2} values are included in the S and S′ terms (See Eqns. 3.7 and 3.8).

$$V_{rat} = \frac{\rho Z}{MW(S'-S)} \qquad \text{Eqn. 3.11}$$

$$P'_{CO_2} = \left(\frac{\rho Z K_{aH}}{MW[B]_{aq} V_{rat}}\right)^2 \frac{1+[B]_{aq}{K_{aH}}^{-1}}{K_1 K_H} - \frac{K_w}{K_1 K_H} \qquad \text{Eqn. 3.12}$$

Five tertiary amines that do not act as SHSs under the standard conditions (because they did not form monophasic solutions with water in the presence of 1 atm CO_2) were studied to determine if different partial pressures of CO_2 and/or different water:amine volume ratios can be used to make them act as SHSs. The maps shown in Fig 3.4 suggest that this is the case and equations 3.11 and 3.12 suggest approximate required values for P_{CO2}' and V_{rat} to make an amine completely miscible with water. The five amines used in this study were DECA, TPA, DMBA, DMAP, and DIPEA. Two of these amines (DECA and TPA) failed to act as SHSs under standard conditions because they were too hydrophobic. Another two amines (DMBA and DMAP) failed to act as SHSs under standard conditions because they did not have sufficient basic strength. Finally,

DIPEA does not act as a SHS under standard conditions due to steric hindrance around the nitrogen center. Amines that failed to act as SHSs under standard conditions because they were completely miscible with water (e.g. triethanolamine) were not investigated because increased water:amine volume ratios and increased partial pressure of CO_2 are only expected to improve the miscibility of the amine with water.

Each of these amines was tested for switchable hydrophilicity under nonstandard conditions. In one series of tests, the amines were mixed with increasing amounts of water under 1 atm of CO_2 until they became miscible with the water. In another series of tests, the amines were mixed with water in a 1:1 volume ratio (or a 3:1 water:amine volume ratio for 1-dimethylamine-2-pentyne) and the partial pressure of CO_2 was increased until the amines became miscible with water. The water:amine volume ratios (under 1 atm CO_2) and partial pressures of CO_2 required (with a 1:1 or 3:1 water:amine volume ratio) to observe a monophasic liquid are listed in Table 3.1 for each amine. All of the amines became miscible with water after the water:amine volume ratio or partial pressure of CO_2 was increased sufficiently, confirming the hypothesis that different volume ratios or pressures can allow amines to act as SHSs even if they did not act as SHSs under standard conditions. The predicted V_{rat} and P_{CO2}' values determined from equations 3.11 and 3.12 were typically lower than the experimentally observed values, with the exception of the predicted P_{CO2}' for DMBA. The differences between the experimental and predicted values may be due to the use of assumptions that are only valid at low solute concentrations and pressures or may be due to an insufficient amount of time allowed for the systems to reach equilibrium (see Section 3.6.3). The predicted values for DIPEA are significant outliers because the mathematical model predicts DIPEA to act as a SHS under standard conditions. This incorrect prediction is a result of the model not accounting for the effects of steric hindrance on SHSs.

Because V_{rat} and P_{CO2}' can be changed simultaneously (as opposed to only changing one value from standard conditions) to achieve SHS behaviour from an amine that does not act as a SHS under standard conditions, a plot showing the relationship between these parameters and the mapping parameter Z can be useful for identifying appropriate combinations of V_{rat} and P_{CO2}' to achieve SHS behaviour from an amine. A graph showing the values of V_{rat} and P_{CO2}' that yield the maximum predicted Z values for four amines (using P_{CO2} = 0 bar) is shown in Fig. 3.5 along with the experimentally observed V_{rat} and P_{CO2}' requirements listed in Table 3.1. DIPEA is not shown in this figure due to the inherent inaccuracy of the mathematical model with respect to the behaviour of DIPEA. The figure shows that as V_{rat} increases, less CO_2 pressure is required to achieve SHS behaviour. Conversely, as P_{CO2}' increases, a lower water:amine volume ratio is required.

It was observed that the DIPEA–water system became biphasic once it was depressurized from 7.0 bar of CO_2, whereas amines that act as SHSs under 1 bar CO_2 did not become biphasic unless they were heated and had an inert gas bubbled through them. An amine that only becomes water-miscible under high pressures of CO_2 may require less energy and time to remove CO_2 than amines that become water-miscible at 1 bar of CO_2 because incomplete CO_2 removal would not

Table 3.1 Tertiary amines exhibiting switchable behaviour under non-standard conditions.

Amine	pK_{aH}	log K_{ow}[a]	Predicted V_{rat}[b]	Experimental V_{rat}[b]	Predicted P_{CO2}' (bar)[c]	Experimental P_{CO2}' (bar)[c]
DIPEA	11.4[9]	2.3	0.4	1.5–2.0	0.1	4.0–7.0
DECA	10.7	2.9	1.7	1.5–2.0	2.9	3.0–3.5
TPA	10.6[10]	2.8	1.5	2.5–3.0	2.3	3.5–4.0
DMBA	9.0[11]	2.0	3.6	4.5–5.0	14.9	4.0–7.0
DMAP	7.98[12]	1.6	5.3	6.5–7.0	4.6[d]	4.0–7.0[d]

[a]Predicted using VCCLAB software (ALOGPS).[13–15] [b]The minimum water:amine ratio required to trigger miscibility under 1 bar of CO_2 at 25 °C. [c]The minimum CO_2 pressure required to trigger miscibility in a 1:1 water:amine (v/v) mixture at 25 °C. [d]At a 3:1 volume ratio of water to amine.

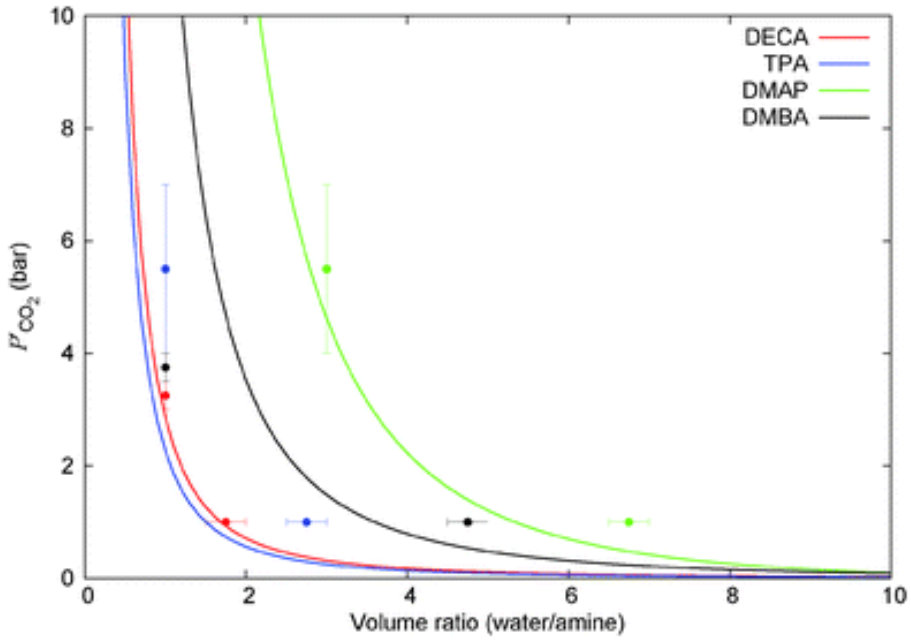

Fig. 3.5 The curves show the values of P_{CO2} which yield a maximum value of Z for DECA, TPA, DMAP and DMBA as a function of V_{rat}, calculated using equation 3.12. The data points indicate the experimentally determined range of pressures needed to achieve a monophasic system. Sudan III dye was used to assist in monitoring the phase switch in the pressure vessel by colouring the organic phase. Each amine–water mix is expected to be monophasic under the conditions above and to the right of the shown curve, and biphasic below and to the left of the curve. The error bars represent the uncertainty of a single measurement (volume ratio: ±0.25 mL/mL, P_{CO2} ±0.025 bar for pressures below 4 bar, ±1.5 bar for pressures above 4 bar).

---

inhibit separation of the amine from the water. To investigate this possibility further, the amount of amine in a carbonated aqueous phase was monitored by GC-TCD as CO_2 was removed over time. This was studied for DMCA–water and DIPEA–water mixtures. DMCA was made miscible with water at 1 bar of CO_2 and DIPEA was made miscible with water at 7 bar of CO_2. Portions of each monophasic solution were sampled and placed in containers open to atmospheric conditions and stirred at room temperature without bubbling an inert gas through them. The composition of the aqueous phase for each sample was observed over time by gas chromatography using a thermal conductivity detector. A plot showing the relative intensity of the amine peak (compared to the

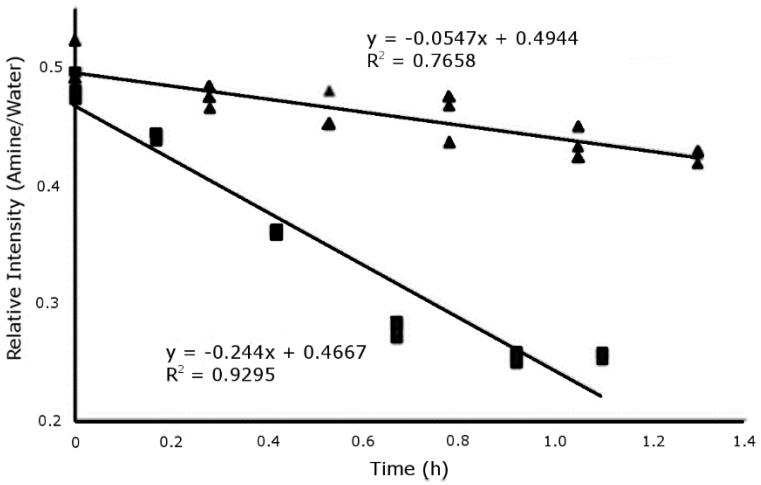

Fig. 3.6 The rate of amine removal from the aqueous phase as shown by relative intensities of amine to water signals measured by GC-TCD. The system changing from 7 bar of CO_2 (DIPEA–water, square points) shows a steeper slope ($-0.22\ h^{-1}$) than the system changing from 1 bar of CO_2 (DMCA–water, triangle points: $-0.055\ h^{-1}$).

water peak) for each sample is shown in Fig. 3.6. The figure indicates that DIPEA separates from water faster than DMCA does under these conditions. This result suggests that the separation of high-pressure SHSs from water is more rapid than that of standard SHSs under the same conditions.

3.3 The three-component system

3.3.1 Model development and comparison to experimental observations under standard conditions

In practice, SHS technology is used to separate a hydrophobic product from a solvent, such as the separation of a water-immiscible organic oil from the amine solvent that it is dissolved in. Such processes are described in Section 1.4, but a conceptual separation is also shown visually in Fig 3.7. The separation of SHS from the hydrophobic product occurs by the pH-dependent distribution of SHS between the hydrophobic product phase and an added aqueous phase. At low pH (caused by the addition of CO_2), the SHS will partition more completely into the aqueous phase

and be separated from the product. For the model being described, the hydrophobic product in consideration is a liquid organic product such as an oil.

The product oil layer complicates the SHS phase behaviour by adding a third component to the mixture. In such a system there is partitioning of neutral amine (K_{ow}) and charged ammonium bicarbonate (K_{ow}') species between the aqueous and organic layers. Strictly speaking, K_{ow} refers to the partitioning of a compound between 1-octanol and water. A different partition coefficient should be used depending on the nature of the organic phase, K_P and K_P' are used here to represent the partition coefficients of neutral and charged amines, respectively, between water and an unspecified organic phase. However, the equations described below remain the same regardless of the nature of the organic phase apart from substituting K_{ow} and K_{ow}' with K_P and K_P'. In this model, 1-octanol is used for the organic phase as a representative generic hydrophobic liquid product and so K_{ow} and K_{ow}' are used.

Eqn. 3.13

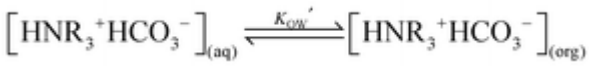

Eqn. 3.14

$$K_{ow} = \frac{[B]_{org}}{[B]_{aq}} \qquad \text{Eqn. 3.15}$$

$$K'_{ow} = \frac{[BH^+]_{org}}{[BH^+]_{aq}} \qquad \text{Eqn. 3.16}$$

To simplify matters, it is assumed that the load of amine present in the water–organic solvent system will not affect the properties of either phase and thus the partition coefficients remain constant, although in the future it would be desirable to develop a model that does not make this assumption.

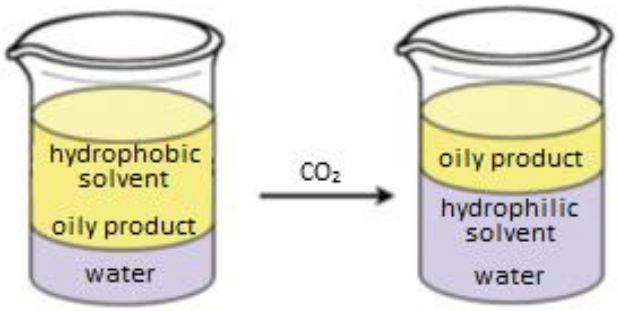

Fig. 3.7 The removal of SHS from an oily product by the addition of CO_2 in a three-component system consisting of SHS, water, and an oily liquid product.

The pH-dependent distribution of neutral and charged species between two immiscible liquid phases is described by the distribution coefficient, *D*, which is defined as the ratio of concentration of species contained in the organic layer to the concentration of species in the aqueous layer.[16]

$$D = \frac{[B]_{org}+[BH^+]_{org}}{[B]_{aq}+[BH^+]_{aq}} \qquad \text{Eqn. 3.17}$$

Following derivations found in Appendix 1, it follows that:

$$\log D = \log K_{ow} + \log\left(1 + 10^{pK_{aH}-pH-\Delta \log K_{ow}}\right) - \log(1 + 10^{pK_{aH}-pH}) \qquad \text{Eqn. 3.18}$$

given that $\Delta\log K_{ow} = \log K_{ow} - \log K_{ow}'$.[17] The term $\Delta\log K_{ow}$ represents the difference in distribution coefficients of the neutral and charged amine and is assumed to be a constant for species belonging to the same family.[18,19] At high pH levels, most of the amine is unprotonated and $\log D \approx \log K_{ow}$, whereas at low pH levels, most of the amine is protonated and thus $\log D \approx \log K_{ow}'$. Equation 3.18 follows these approximations at extreme pH levels. $\Delta\log K_{ow}$ was calculated for DMCA in systems containing water and 1-octanol by measuring its distribution coefficients at varying pH levels (Fig. 3.8). The results are consistent with equation 3.16 and also show that $\Delta\log K_{ow} \approx 2.8$. A similar experiment was performed using toluene as the organic phase and $\Delta\log K_P \approx 2.8$ in this system as well.

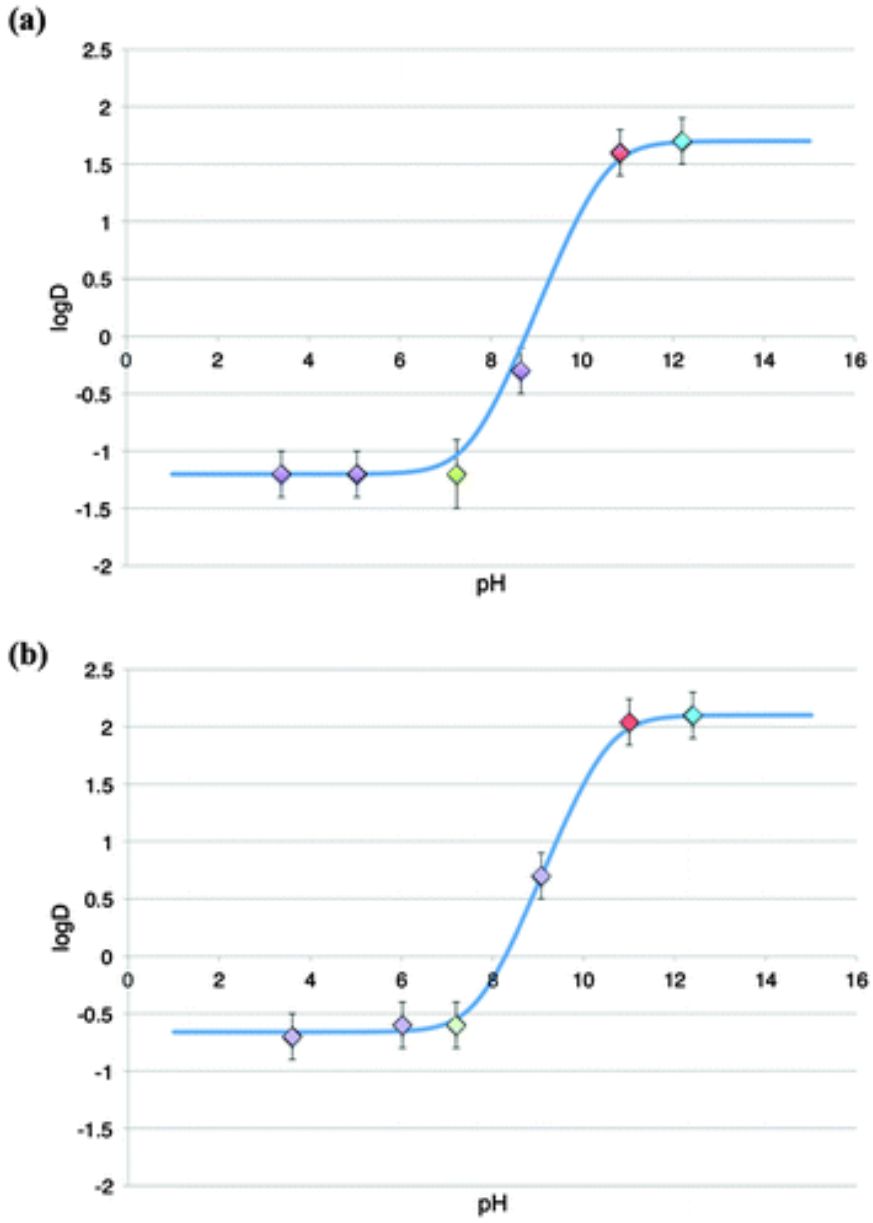

Fig. 3.8 Distribution coefficient of DMCA (a) between toluene and water and (b) between 1-octanol and water. The distribution of 3.3 mmol of amine between the organic solvent and water (5 mL each) at ambient temperature is represented by the red point. The distribution after saturation of the mixture with CO_2 at 1.0 atm is represented by the green point. To adjust the pH, 0.5, 1.0, and 2.0 mole equivalents of glycolic acid (purple points) or 1.0 equivalent of NaOH (blue point) were used. The curve predicted by equation 18 is overlaid to show agreement with the data. The standard deviation of the log *D* measurements was ±0.2 from three replicates.

Another way to represent equation 3.18 is by substituting the pH variable with a ratio of charged to neutral species. One arrives at the following relationship:

$$\log(D) = \log\left(\frac{K_{ow}}{K'_{ow}} + \frac{[BH^+]_{aq}}{[B]_{aq}}\right) - \log\left(\frac{1}{K'_{ow}} + \frac{1}{K'_{ow}}\frac{[BH^+]_{aq}}{[B]_{aq}}\right) \quad \text{Eqn. 3.19}$$

which has the fraction $[BH^+]_{aq}/[B]_{aq}$ being the only term that changes between systems at low and high pressures of CO_2. The charge balance equation of this system can be used to determine the fraction $[BH^+]_{aq}/[B]_{aq}$ using equation 3.20.

$$\frac{[BH^+]_{aq}}{[B]_{aq}} = \frac{1}{K_{aH}}\left(\frac{K_w + K_1 K_H P_{CO_2}}{1 + [B]_{aq} K_{aH}{}^{-1}}\right)^{1/2} \quad \text{or} \quad \frac{[BH^+]_{aq}}{[B]_{aq}} = \frac{1}{K_{aH}}\left(\frac{K_w + K_1 K_H P'_{CO_2}}{1 + [B]_{aq} K_{aH}{}^{-1}}\right)^{1/2} \quad \text{Eqn. 3.20}$$

A mapping parameter Ω is defined as the negative of the product of log D_1 and log D_2 (Equation 3.21), where D_1 and D_2 represent the distribution coefficients of the amine at low and high pressures of CO_2, respectively. An effective SHS will have a positive number for log D_1 as a requirement that the solvent be hydrophobic enough to make a biphasic mixture with water. The amine solvent should partition preferentially into the aqueous phase rather than the organic product phase after CO_2 has been bubbled through the system, as represented by a negative value for log D_2. Thus the product of log D_1 and log D_2 will be negative for effective SHSs. To create a positive map, we multiply the product by (−1):

$$\Omega = -\log D_1 \times \log D_2 \quad \text{Eqn. 3.21}$$

Fig. 3.9 shows the map produced by equation 3.21 using CO_2 pressures of P_{CO2} = 0 bar and $P_{CO2}{}'$ = 1 bar. The green dots represent the dataset of confirmed tertiary and bulky secondary amine SHSs discussed in Chapter 2. Fig. 3.9 is in good agreement with all of the confirmed amine SHSs. The figure suggests that for a three-component system where the liquid product is 1-octanol, amines with a log K_{ow} > ~3 will not function as desired because their log D_2 will be too large. Likewise, amines with log K_{ow} < ~1 will not function as desired because their log D_1 will be too low. Unlike the two-component system, this discrepancy between the predicted minimum log K_{ow} and the minimum reported in Chapter 2 (log K_{ow} = 1.2) may not be erroneous. The values identified in

Chapter 2 were determined using two-component systems. In the context of three-component systems, it makes sense that an amine with a log K_{ow} value of 1.0 would partition more into an organic phase (a concentration ratio of 10:1 organic:aqueous) in the absence of CO_2 and then partition very favourably into the aqueous upon the addition of CO_2, which is the desired behaviour for a SHS in this context. Amines with low pK_{aH} values will not be sufficiently protonated by CO_2 and thus log D_2 will not be different enough from log D_1 to result in an adequate change in behaviour. The graph also predicts that amines with pK_{aH} values as large as 16 might act as SHSs, but amines typically do not have pK_{aH} values much larger than 11, so there is no experimental evidence to support this prediction.

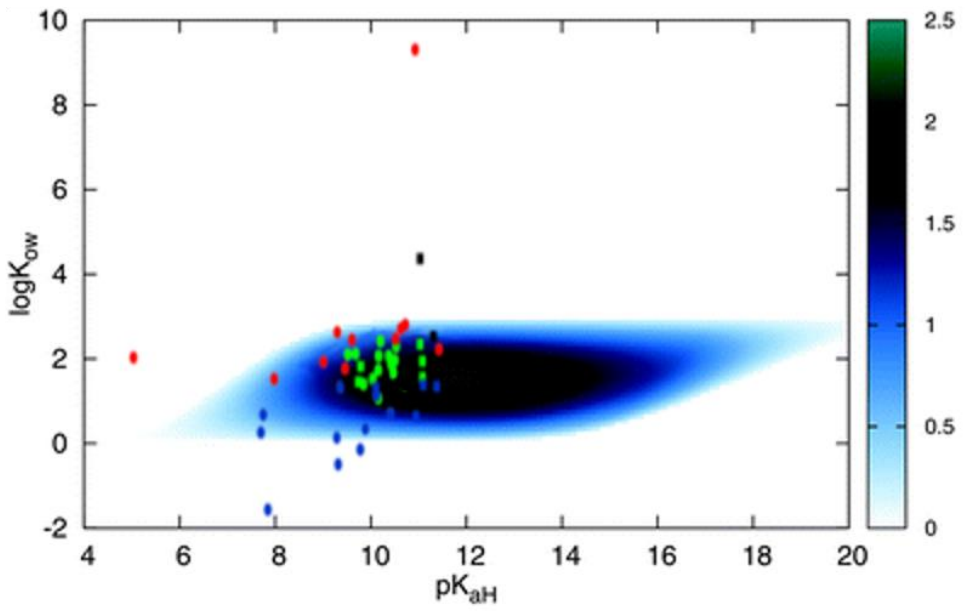

Fig. 3.9 A map of Ω, indicating the region of high SHS viability in a three-component system, assuming that Δlog K_{ow} = 2.8. The green dots represent the confirmed amine SHSs. The red, blue and black dots represent amines that are not SHSs under standard conditions.

3.3.2 Application of the model to non-standard conditions

Just as with the two-component system, the behaviour of an amine in the three-component system may be changed when non-standard conditions are used. Amines that are expected to partition poorly into the aqueous phase under standard conditions might partition more favourably into the aqueous phase under non-standard conditions. The model for the three-component system is based on the distribution coefficients of amines between an organic phase and an aqueous phase. Because distribution coefficient is independent of the water:amine volume ratio, only changes in the partial pressures of CO_2 used in a system will change the value of the mapping parameter, Ω. Therefore, only the effect of different partial pressures of CO_2 will be discussed in this section. However, it should be noted that increasing the volume of water relative to the volume of the organic phase will result in more amine present in the aqueous phase relative to the organic phase because more amine must be present in the aqueous phase to bring the aqueous concentration of amine up to its equilibrium value.

Fig. 3.10 shows the log *D* values of amines in systems containing an aqueous phase and a 1-octanol phase under different partial pressures of CO_2, as calculated by equation 3.19. Three amines that act as SHSs under standard conditions: DMCA, *N*,*N*-diisopropylaminoethanol (DIPAE), and triethylamine (TEA); and four amines that do not act as SHSs under standard conditions (DECA, TPA, DMAP, and DMBA) are shown in the figure. DIPEA was not included in this graph because, as discussed previously, the model does not predict its behaviour accurately. The log *D* values for all amines are predicted to decrease as the partial pressure of CO_2 increases. This trend is expected because higher pressures of CO_2 should increase the percent protonation of an amine, making the log *D* value of the amine closer to log K_{ow}' than log K_{ow}. Each curve also levels off as the value for log *D* approaches its lower limit of log D = log K_{ow}'.

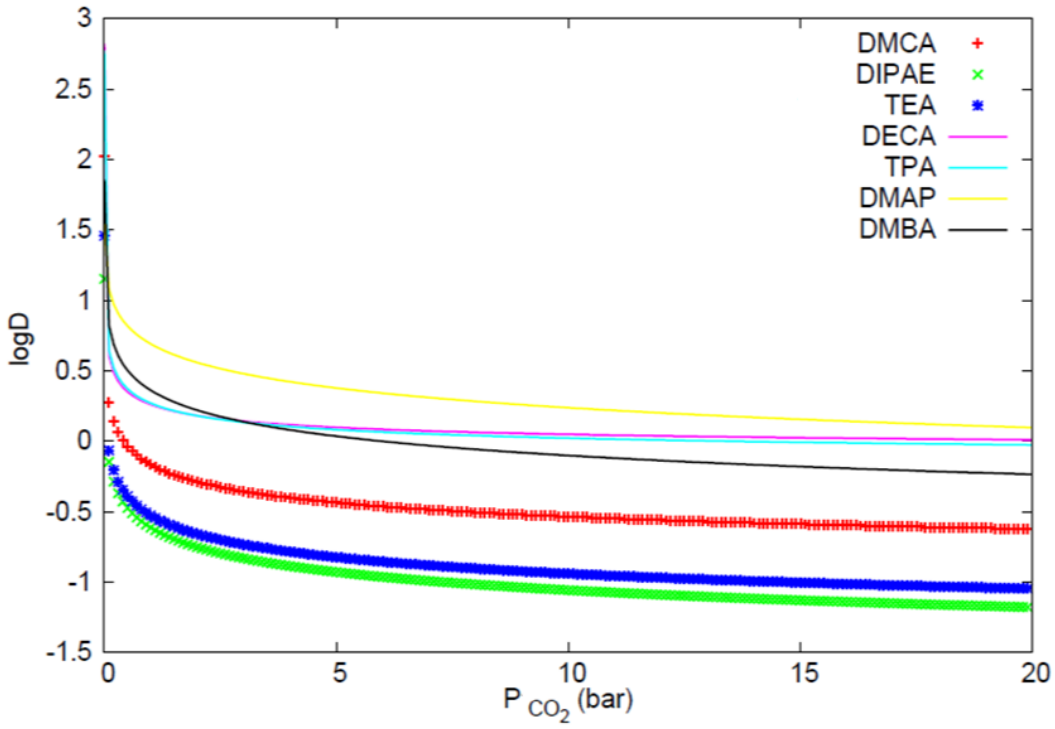

Fig. 3.10 Calculated distribution coefficient curves for standard SHSs (DMCA, DIPAE, and TEA) and non-standard SHSs (DECA, TPA, DMBA and DMAP) as a function of P_{CO2}. Amines that function as SHSs under standard conditions have lower log D values than amines that require non-standard conditions at all CO_2 pressures shown. Therefore, standard SHSs require can be more completely separated from liquid products than non-standard SHSs using similar CO_2 pressures.

The bicarbonate salts of DMBA and DMAP are assumed to partition favourably into the aqueous layer due to their low log K_{ow}' values. However, due to their low pK_{aH} values (pK_{aH} = 9.0 and 8.1, respectively), a high CO_2 pressure is needed to quantitatively protonate these compounds.

In practice, it is typically desirable for the organic phase in the three-component system to contain little SHS after the addition of CO_2. The organic phase is typically a hydrophobic product, such as soybean oil, and should be free of impurities such as residual SHS. Therefore, lower log *D* values are desirable. Using higher pressures of CO_2 in the three-component system should improve the separation of SHS from the organic phase because the log *D* value of every amine is expected

to decrease as the pressure of CO_2 increases. However, the benefits of CO_2 pressures above ~5 bar may be limited if the log *D* value of the SHS is already similar to the log K_{ow}' value of the SHS-bicarbonate salt. Furthermore, amines with log K_{ow}' values greater than 0 for their bicarbonate salts are not recommended for use as SHSs because they will not partition favourably into the aqueous phase, even under high pressures of CO_2.

3.4 Fraction of protonation of amines in three-component systems

Protonation/deprotonation is the "switch" that triggers a change between the two states of a CO_2-switchable compound. Therefore, determining the fraction of protonated SHS is a useful measure of how completely a SHS is switched from one state to another and so equations to calculate the fraction of protonated species are useful for estimating how effective the switch is. Because unprotonated SHS molecules are likely to partition into the organic liquid product, the fraction of protonated SHS governs the ability of the SHS to be separated from the liquid product. In order to have effective switching of the SHS into its hydrophilic form and efficient removal of the SHS from the organic product layer, the addition of CO_2 must be sufficient to bring the pH down well below the system midpoint (i.e. the pH at which P = 0.5). When an amine is completely soluble in water and no organic phase is present, the fraction of protonated species, P, can be calculated using equation 3.20 and the system midpoint is at pH = pK_{aH}.

$$P = \frac{[H^+]_{aq}}{[H^+]_{aq} + K_{aH}} \qquad \text{Eqn. 3.22}$$

However, when an organic layer present, one must account for the partitioning between the layers. Fundamentally, P is the ratio of protonated amine in both the aqueous and organic layers to the total amount of amine (neutral and protonated) in the system:

$$P = \frac{n_{BH^+,org} + n_{BH^+,aq}}{n_{B,tot}} \qquad \text{Eqn. 3.23}$$

The mass balance for the amine states that $n_{B,tot} = n_{B,org} + n_{B,aq} + n_{HB^+,org} + n_{HB^+,aq}$. Using this relationship, the expression for P in a biphasic system can be derived:

$$P = \frac{[H^+]_{aq}}{[H^+]_{aq} + K_{aH}\left(\frac{K_P V_{rat}+1}{K_P' V_{rat}+1}\right)} \qquad \text{Eqn. 3.24}$$

where $V_{rat} = V_{org}/V_{aq}$ and K_P and K_P' are the partition coefficients for the amine and the ammonium bicarbonate salts, respectively, between the aqueous phase and the organic phase. K_P is used here instead of K_{ow} to allow the equation to be used for systems containing organic phases other than 1-octanol. The difference between log K_p and log K_P' (Δlog K_P) is still assumed to be 2.8, equivalent to Δlog K_{ow}. With only an aqueous phase, equation 3.24 reduces to equation 3.22. The exchange between aqueous and organic layers results in a decrease of protonated species at a particular pH. Fig. 3.11 shows that the presence of an organic layer makes it necessary to have a much more acidic environment in order to substantially protonate the base. Given that the acid being used to protonate the solvent is carbonic acid (apparent pK_{a1} = 6.4), it is wise to use a low V_{rat} in order to ensure a greater fraction of protonated amine.

In order to use the fraction of protonated amine to help guide the choice of compound to use as a SHS, equations must be developed to answer two questions. First, what log K_{ow} and pK_{aH} values will result in low fractions of protonation (e.g. <0.05) in the absence of CO_2 at the volume ratio of organic phase to aqueous phase being used? Second, what log K_{ow} and pK_{aH} values will result in high fractions of protonation (e.g. >0.95) in the presence of CO_2 at the volume ratio of organic phase to aqueous phase being used? Any amine with a set of log K_{ow} and pK_{aH} values that results in low fractions of protonated species in the absence of CO_2 and high fractions of protonated species in the presence of CO_2 should be effective as a switchable compound.

Equation 3.24 can be used to answer these questions if the pH of the aqueous phase is known. Using equation 3.25, the pH of the aqueous phase can be calculated for systems containing an aqueous phase, an organic phase, an organic base, and CO_2. The pH of the aqueous phase is

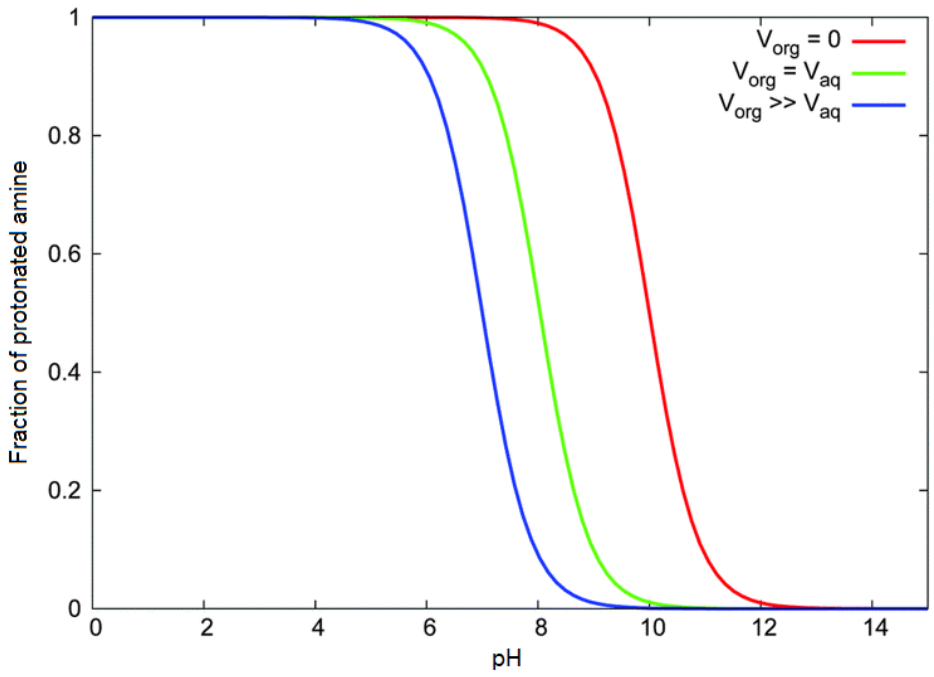

Fig. 3.11 The effect of the organic layer volume on the fraction of protonated base. If V_{rat} is nearly zero (red line), then the system midpoint is essentially the p of the amine. If V_{rat} is much larger than 1, then the system midpoint is shifted down by about 3 pH units (blue line). K_{ow}, K_{ow}', and the acid dissociation constant are assumed to be 10^{2}, $10^{-0.8}$, and 10^{-10}, respectively.

---

calculated by solving this 3rd-order polynomial equation for $[H_3O^+]_{aq}$ and converting $[H_3O^+]_{aq}$ to pH. In equation 3.25, $[B]_0$ is defined as the total moles of amine present in the system (both aqueous and organic phases) divided by the volume of the aqueous phase.

$$0 = [H^+]_{aq}^3(K_P'V_{rat} + 1) + [H^+]_{aq}^2(K_{aH}(K_PV_{rat} + 1) + [B]_0) - [H^+]_{aq}K_w(K_P'V_{rat} + 1) - K_{aH}K_w(K_PV_{rat} + 1) \quad \text{Eqn. 3.25}$$

Fig. 3.12 shows upper and lower limits for log K_P and pK_{aH} to achieve good switchability (≤5% protonation in the absence of CO_2 and ≥95% protonation in the presence of CO_2) in systems with V_{rat} = 0.5 and different $[B]_0$. Three sets of lines, each with different colours, show different limits for compounds with different log K_P values. The broken lines are for systems in the absence

of CO_2 and show the pK_{aH} values that result in 5% protonation in the absence of CO_2 for compounds with the given log K_P value. Compounds with pK_{aH} values below these lines will be less than 5% protonated in the absence of CO_2. Compounds with pK_{aH} values above these lines will be more than 5% protonated in the absence of CO_2 and may not be ideal choices as switchable compounds. Likewise, the solid lines are for systems in the presence of 1 atm CO_2 and show the pK_{aH} values that result in 95% protonation in the presence of 0.1 MPa CO_2 for compounds with the given log K_P. Compounds with pK_{aH} values above these lines will be more than 95% protonated in the presence of 0.1 MPa CO_2. Compounds with pK_{aH} values below these lines will be less than 95% protonated in the present of 0.1 MPa CO_2 and may not be ideal choices as switchable compounds. Therefore, a compound with a given log K_P will be an effective switchable compound (that is, it

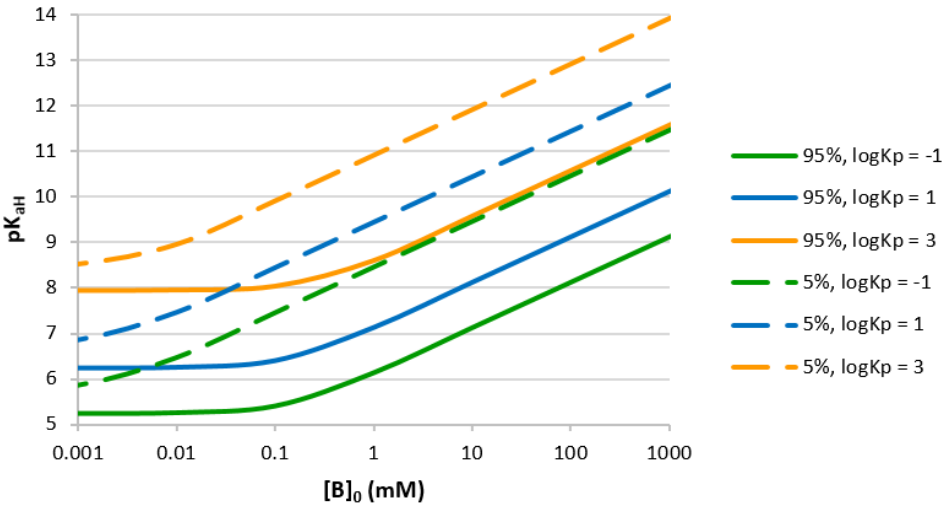

Fig. 3.12 The pK_{aH} required for a base to be 5% protonated when placed in a water:organic biphasic mixture under air (dashed lines) or 95% protonated in the biphasic mixture under 0.1 MPa CO_2 (solid lines), for bases having a log K_P value of −1, (green), 1 (blue) or 3 (orange), at 25 °C. A base having a pK_{aH} between the dashed and solid lines, at the concentration desired, should be selected. A Δlog K_P of 2.8 and a V_{rat} of 0.5 was assumed.

switches between mostly unprotonated and mostly protonated) if it has a pK_{aH} value between the two lines.

For applications involving SHSs, the amount of base in the system is very large, so the relevant portions of the graph are at $[B]_0$ = 1000 mM. Based on the graph, SHSs will be switched effectively if they have pK_{aH} values between approximately 10 and 14 (using the lower limit for the line representing log K_P = 1 and the upper limit for the line representing log K_P = 3, which roughly corresponds to the observed log K_P range for SHSs (1.1-2.6). As discussed earlier, compounds with pK_{aH} values as low as 9.5 can act as SHSs. The implication of Fig. 3.12 is that these compounds might not switch as completely from their deprotonated states to their protonated states, even though they act as SHSs.

SHSs can have even higher $[B]_0$ than what is shown in Fig. 3.12, but these high concentrations can introduce significant errors in the calculations due to the non-ideal behaviour of the solution. The equations make use of concentrations as substitutes for activities and concentrations deviate significantly from activities at high concentrations. Furthermore, constants such as K_P and K_{aH} are only reliable at low concentrations. Because of the likely inaccuracy of the equations at high concentrations, the graph only shows concentrations as high as 1000 mM.

3.5 Conclusions

A mathematical model describing the switching process for tertiary and bulky secondary amine SHSs for the two- and three-component systems has been developed. The basicity and hydrophilicity ranges are correlated and can be optimized by maximizing the mapping parameters Z and Ω. Plots of these two mapping functions indicate a narrow range of acceptable log K_{ow} and pK_{aH} values, which matches the values of known amine SHSs. One of these mapping functions indicates values expected for amines that will switch readily between water-miscible and forming a biphasic mixture with water. The other mapping function indicates those amines that will switch

from partitioning into an oil layer to partitioning into an aqueous layer. The two mapping functions indicate similar but not identical ranges of pK_{aH} and log K_P. An ideal amine SHS would perform well by both criteria and would therefore fit within the ranges predicted by both mapping functions.

Another set of equations was developed to calculate the percent protonation of a base in a biphasic organic-aqueous mixture. These equations can be used to determine how much of the base is protonated in both the absence and presence of CO_2 and thereby quantify how effectively the base can be switched between its deprotonated state and its protonated state. The larger the change in percent protonation is, the larger the change in the properties of a switchable compound will be.

Furthermore, the aqueous solubility of the neutral amine was found to increase as more protonated amine enters the aqueous phase as a bicarbonate salt. This is likely due to favourable hydrophobic–hydrophobic attractions between the neutral amine and the organic cations. In the three-component system, both log K_P and log K_P' change if the organic layer is changed from 1-octanol to toluene. The difference between these two partition coefficients, $\Delta\log K_P$, however, is not significantly affected.

3.6 Experimental

All chemicals were used as received. CO_2 (4.8, supercritical fluid chromatography grade) was purchased from Praxair. *N*,*N*-Dimethylcyclohexylamine (99%), *N*,*N*-diisopropylethylamine (≥99%), tripropylamine (≥98%), *N*,*N*-dimethylbenzylamine (≥99%), glycolic acid (99%), and acetophenone (99%) were purchased from Sigma-Aldrich. *N*,*N*-Diethylcyclohexylamine (>98%) was purchased from TCI America. 1-Dimethylamino-2-pentyne (98%) was purchased from Alfa Aesar. *N*,*N*,*N*-trimethylcyclohexylammonium iodide was synthesized from DMCA and iodomethane (≥99%, Sigma-Aldrich).

3.6.1 Measuring the solubility of DMCA

Four samples of distilled water (average of 5 g accurate to 0.1 mg) were placed in 20 mL vials. To each vial, an average of 0.0, 450.0 , 900.0, and 1350.0 mg of *N*,*N*,*N*-trimethylcyclohexylammonium iodide salt ([$CyNMe_3$]I, a white powder) was added to make 0.0000, 0.3343, 0.6686 and 1.0030M aqueous solutions, respectively. DMCA was then added to each solution until a biphasic mixture was observed. It should be noted that this biphasic mixture could not be attained for salt solutions with concentrations greater than 1.0 M. The mixtures were stirred for 30 min and allowed to settle for 3 h at which point it was assumed that equilibrium had been established. A sample from each aqueous layer was taken (450.0 mg average) and placed in a 50 mL volumetric flask. Acetophenone (20.0 μL) was added to each flask as an internal standard and then each flask was filled with HPLC-grade methanol to the 50 mL mark. These samples were then analyzed by gas chromatography with flame-ionization detection (GC-FID). The weight of DMCA was calculated by a calibration curve of weight ratio (of acetophenone to DMCA) to peak area ratio (of acetophenone to DMCA). This was repeated in triplicate.

3.6.2 Measuring $\Delta\log K_{ow}$

DMCA (450 mg) was added to a mixture of water (5 g) and 1-octanol (4.5 g) at room temperature. The mixture was stirred for 30 min and was left to settle for 3 h. The pH of the aqueous layer was then measured using an Orion 4-Star pH meter (Thermo Scientific). A sample of the aqueous layer (500 mg) was drawn from the mixture and placed in a 50 mL volumetric flask. Acetophenone (20 μL) was added as an internal standard. The solution was diluted to the mark with HPLC-grade methanol and analyzed by GC-FID. The weight of DMCA was calculated by a calibration curve of weight ratio (of acetophenone to DMCA) to peak area ratio (of acetophenone to DMCA). Another mixture of DMCA, water, and 1-octanol was prepared and the pH was measured after CO_2 was bubbled through the system for 1 h under 101.3 kPa. Again, a sample from

the aqueous layer (100 mg) was taken and treated with excess base (to deprotonate the ammonium salt). Acetophenone (20 μL) was added and the sample was diluted with methanol to the 50 mL mark.

Three more mixtures were prepared as described above. Glycolic acid was added to each mixture in 0.5, 1, and 2 molar equivalents to DMCA, respectively. Glycolic acid was chosen because its conjugate base is more stable than the bicarbonate anion and yet similar in size and hydrogen-bonding ability. The pH of each aqueous layer was measured. A 100 mg sample from each aqueous layer was taken and acetophenone (20 μL) was added. The sample was treated with base, diluted with methanol to the 50 mL mark, and analyzed by GC-FID. Finally, another mixture was prepared and treated with NaOH (1 mol equivalent to DMCA). The pH of the aqueous layer was measured and 500 mg of the aqueous layer was analyzed by GC-FID as described above. Each sample was prepared in triplicate. This procedure was repeated with toluene in place of 1-octanol.

3.6.3 Determining the minimum water:amine volume ratio and CO_2 pressure required to switch non-standard SHSs

To determine the minimum water:amine volume ratio required for a water:amine mix to become monophasic under 1 atm of CO_2, an amine was mixed with water in a 1:1 volume ratio in a graduated cylinder. CO_2 was bubbled through the mixture using a gas dispersion tube (5 mm i.d., 25-50 μL porosity) for 60 min, after which it was assumed that the mixture was at equilibrium. If the mixture remained biphasic, another 0.5 volume equivalents of water was added to the mixture and CO_2 was bubbled through the mixture for another 60 min. This process was repeated until the mixture was observed to be monophasic.

To determine the minimum pressure of CO_2 required for a 1:1 (v:v) mix of water:amine to become monophasic, water and an amine were mixed in a high-pressure vessel with a viewing window. A small amount of Sudan III dye, which colours the organic phase, was added to improve the visual contrast between the two phases. A magnetic stir bar was also added and the contents of

the vessel were stirred gently to improve the mixing of the two phases. CO_2 was passed through the vessel to ensure that the headspace in the vessel contained only CO_2 and then the vessel was placed under 1 bar CO_2 for 60 min, after which it was assumed that the mixture was at equilibrium. After 60 min the mixture was observed while it was still under pressure to determine if it was monophasic or biphasic. If the mixture was biphasic, the pressure of CO_2 was increased by 0.05 MPa and allowed to equilibrate for another 60 min. This process was repeated until the mixture was observed to be monophasic.

3.6.4 Monitoring the phase separation of carbonated water:amine mixes over time

A 1:1 (v:v) mixture of water:DMCA was prepared in a vial. CO_2 was bubbled through the mixture for 60 min, resulting in a monophasic liquid. A 4 mL portion of the solution was transferred to a 10 mL graduated cylinder with a stir bar. A 1:1 (v:v) mixture of water:DIPEA was also prepared in a high pressure vessel, which was then pressurized to 0.7 MPa with CO_2 and allowed to equilibrate for 60 min, resulting in a monophasic liquid. The DIPEA mixture was then depressurized to atmospheric pressure (~0.1 MPa) and a 4 mL portion of the solution was transferred to a 10 mL graduated cylinder with a stir bar.

The mixtures were stirred (200 rpm) at room temperature (21 °C) and atmospheric conditions, allowing CO_2 to evolve from the solution. An organic phase appeared and increased in volume over time. The aqueous phase of each mixture was sampled periodically and analyzed by gas chromatography using a thermal conductivity detector. The ratio of the integrations of the amine peak and the water peak for each chromatogram was determined to characterize the changes in the composition of the aqueous phases over time.

3.7 References

1) P. G. Jessop, L. Phan, A. Carrier, S. Robinson, C. J. Dürr and J. R. Harjani, *Green Chem.*, 2010, **12**, 809–814.

2) H. S. Harned and S. R. Scholes, *J. Am. Chem. Soc.*, 1941, **63**, 1706–1709.

3) J. Durelle, J. R. Vanderveen and P. G. Jessop, *Phys. Chem. Chem. Phys.*, 2014, **16**, 5270–5275.

4) J. Durelle, J. R. Vanderveen, Y. Quan, C. B. Chalifoux, J. E. Kostin and P. G. Jessop, *Phys. Chem. Chem. Phys.*, 2015, **17**, 5308–5313.

5) A. K. Alshamrani, J. R. Vanderveen and P. G. Jessop, *Phys. Chem. Chem. Phys.*, 2016, **18**, 19276–19288.

6) W. M. Meylan, P. H. Howard and R. S. Boethling, *Environ. Toxicol. Chem.*, 1996, **15**, 100–106.

7) P. G. Jessop, L. Kozycz, Z. G. Rahami, D. Schoenmakers, A. R. Boyd, D. Wechsler and A. M. Holland, *Green Chem.*, 2011, **13**, 619–623.

8) J. S. McNally, B. Noll, C. J. Orme and A. D. Wilson, *J. Phys. Chem. B*, 2015, **119**, 6766–6775.

9) T. Fujii, H. Nishida, Y. Abiru, M. Yamamoto and M. Kise, *Chem. Pharm. Bull. (Tokyo)*, 1995, **43**, 1872–1877.

10) Z. Pawelka and T. Zeegers-Huyskens, *Can. J. Chem.*, 2003, **81**, 1012–1018.

11) V. Frenna, N. Vivona, G. Consiglio and D. Spinelli, *J. Chem. Soc. Perkin Trans. 2*, 1985, 1865–1868.

12) I. M. Koshkina, L. A. Remizova, E. V. Ermilova and I. A. Favorskaya, *Reaktsionnaya Spos. Organicheskikh Soedin.*, 1970, **7**, 944–952.

13) I. V. Tetko and V. Y. Tanchuk, *J. Chem. Inf. Comput. Sci.*, 2002, **42**, 1136–1145.

14) I. V. Tetko, J. Gasteiger, R. Todeschini, A. Mauri, D. Livingstone, P. Ertl, V. A. Palyulin, E. V. Radchenko, N. S. Zefirov, A. S. Makarenko, V. Y. Tanchuk and V. V. Prokopenko, *J. Comput. Aided Mol. Des.*, **19**, 453–463.

15) Virtual Computational Chemistry Laboratory, http://www.vcclab.org (accessed October 1, 2014)

16) G. Caron, F. Reymond, P.-A. Carrupt, H. H. Girault and B. Testa, *Pharm. Sci. Technol. Today*, 1999, **2**, 327–335.

17) C. Silva, M. Mor, F. Vacondio, V. Zuliani and P. Vincenzo Plazzi, *Il Farm.*, 2003, **58**, 989–993.

18) J. R. Seward and T. W. Schultz, *SAR QSAR Environ. Res.*, 1999, **10**, 557–567.

19) A. D. James, J. M. Wates and E. Wyn-Jones, *J. Colloid Interface Sci.*, 1993, **160**, 158–165.

Chapter 4

Development of a Virtual Screening Process to Identify Benign Switchable Hydrophilicity Solvents

4.1 Introduction

Switchable hydrophilicity solvents have potential workplace health and safety advantages over traditional organic solvents. As described in Section 1.4, SHSs, unlike traditional organic solvents, do not need to be highly volatile because they can be separated from dissolved hydrophobic products without distillation. Volatile organic solvents tend to be health and safety hazards due to their flammability, their potential to cause smog formation, and their toxic effects upon inhalation. SHSs can be considered safe alternatives to traditional organic solvents because they do not need to be volatile and can avoid the hazards associated with solvent volatility.

Given the potential for SHSs to be safer than traditional organic solvents, minimizing the environmental impacts and human health and safety risks of SHSs is desirable in order to further distinguish SHSs from traditional solvents beyond simply being less volatile. The work presented in Chapter 2 focused in part on identifying SHSs that pose fewer risks to the environment and to human health and safety. Some of the SHSs identified in Chapter 2 were developed specifically to have low volatility and flammability. All of the SHSs discussed in Chapter 2 were also evaluated and compared to some traditional solvents in terms of other environmental risks and human health and safety risks, such as acute oral toxicity and eutrophication potential. Some SHSs were found to pose fewer risks than others, but continued searches for SHSs with the lowest possible risk are likely to identify SHSs with even fewer risks.

The use of computational chemistry and virtual screening processes to identify SHSs with few risks provides significant advantages over the use of human intellect alone. Computers are capable of generating thousands of possible molecular structures and, through the use of

quantitative structure-activity relationships (QSARs), predicting their physical and chemical properties. Virtual screening involves generating thousands of potential structures and, based on their predicted properties, screening them to identify which structures are predicted to have the most desired properties. Collecting data from QSARs and analyzing the results with a virtual screening process allows for thousands of molecular structures to be tested rapidly *in silico*, far more and far faster than can be tested experimentally. These virtual screening processes can be used to identify target molecules that are likely to be ideal for the purpose they were screened for. The target molecules can then be tested experimentally to confirm the predictions made by the software.

This virtual screening method is common practice in the pharmaceutical industry for identifying molecules that are likely to display drug-like behaviour,[1–4] but it is rarely used in other fields of chemistry. In the field of green chemistry, a virtual screening approach would be valuable to help researchers identify materials that will not only meet performance criteria but will also be safe for human use and have little environmental impact. Öberg screened 50 000 small molecules for only two criteria (lifetime and baseline (narcosis) toxicity) but not for a specific application.[5] Studies on ionic liquids, spurred by the proposed use of thinking in structure–activity relationships (T-SAR, making use of known structure-activity relationships to design compounds with properties desirable for a particular use),[6,7] have also been performed to screen specifically for cytotoxicity,[8] or only for applications to chemical separations.[9–11] The development of virtual screening methods designed for use in green chemistry would create useful tools for identifying ideal candidates for a given application, candidates that not only perform their tasks well, but also pose few risks to the environment or to human health and safety.

In this chapter, a virtual screening method is developed with the intention of identifying the greenest compounds for a given task. This approach is applied to identifying SHSs that are expected to be relatively benign (compared to other SHSs) with respect to environmental impacts

and to human health and safety (herein referred to as "EH&S properties"). More than 30 000 structures are screened and several structures that are predicted to be SHSs with preferable EH&S properties are identified. Four of these molecules were synthesized and tested to confirm that they are SHSs. Although the method was applied to find safe SHSs, the same methodology could be used to identify the greenest compounds for any given task.

The work presented in this chapter is reproduced from Vanderveen *et al*., *Green Chem.*, 2015, **17**, 5182-5188.[12] Various changes have been made in these reproductions to better fit the format and theme of this thesis. The virtual combinatorial software was developed and implemented by Dr. Luc Patiny. The accuracy of the QSAR predictions was investigated with the help of Courtney Chalifoux and Michael Jessop.

4.2 Description of the virtual screening approach

4.2.1 Overview

The virtual screening method described in this chapter consists of three components: structure generation, property prediction, and structure evaluation.

The structure generation was performed using the open source Script platform[13] and the OpenChemLib library.[14,15] The generated structures were visualized using the NPellet Visualizer.[16] An online version of this software can be accessed via http://www.cheminfo.org.[17] The procedure used to generate the structures is known as virtual combinatorial chemistry and result in a virtual combinatorial library of structures that can be studied using computational chemistry. The virtual combinatorial chemistry approach identifies a "scaffold" structural fragment and several additional "R-group" fragments. The software generates molecules by attaching the R-group fragments to the scaffold fragment in every possible combination. A more detailed description of virtual combinatorial chemistry is given by Leland *et al.*[18]

The property prediction component calculates the relevant properties of each structure generated by the structure generation component. The properties that must be predicted depend on which properties are important in assessing the viability of a compound for use in a given task. For example, an amine must have a log K_{ow} between 1.2 and 2.5 and a pK_{aH} (pK_a of the conjugate acid) > 9.5 in order to act as a SHS (under standard conditions). Therefore, the log K_{ow} and pK_{aH} of a compound must be calculated to determine if it is a SHS. In this chapter, property predictions apart from log K_{ow} and pK_{aH} were performed using the Toxicity Estimation Software Tool (TEST) developed by the U.S. EPA.[19] Predicted values include LC_{50} (fathead minnow, 96 h; and daphnia magna, 48 h), LD_{50} (oral, rat), bioaccumulation factor, boiling point, vapour pressure, melting point, and flash point. More reliable toxicity predictions are available but they are more processor-time intensive and therefore less suitable for the screening of thousands of structures. Log K_{ow} values were predicted using the OpenChemLib library.[14,15] pK_{aH} values were predicted using ACD/Percepta software.[20] A list of SMILES from the structure generator was used as input for these calculations. A more complete description of the property prediction methods is presented in Appendix 2 The structures generated from the virtual combinatorial software, along with the predicted properties calculated as described above, were then transferred to the structure evaluation component of the virtual screening method.

The evaluation component of the virtual screening method reads the values outputted from the prediction software, applies acceptability functions to the data, and generates acceptability values for each molecular structure. Acceptability functions and acceptability values were used to account for inaccuracies in the predicted values. Without accounting for inaccuracies in the predictions, the performance of the virtual screening process will decrease; some compounds that are acceptable may be considered unacceptable and some compounds that are unacceptable may be considered acceptable due to inaccurate predictions. The calculations of acceptability values were performed within the NPellet visualizer using a calculator programmed with JavaScript.

4.2.2 Acceptability functions

Acceptability functions were generated to estimate the probability that a predicted value corresponds with an experimental value that meets or exceeds the desired value for the property in consideration. An acceptability value close to 1 implies that the compound is almost certain to be acceptable given its predicted value. Likewise, an acceptability value close to 0 implies that a compound is almost certain to be unacceptable given its predicted value. An acceptability value of 0.5 implies that there is a 50% chance that the compound is acceptable based on its predicted value.

In order to develop an acceptability function, the accuracy of the predictions must be known. To determine the accuracy of the predicted values, they must be compared to experimental values. A list of amines with experimentally determined values was collected for each of the properties we studied. These experimental values were compared to values predicted by the software (e.g. Figure 4.1a) and the deviations of the predicted values from the experimental values

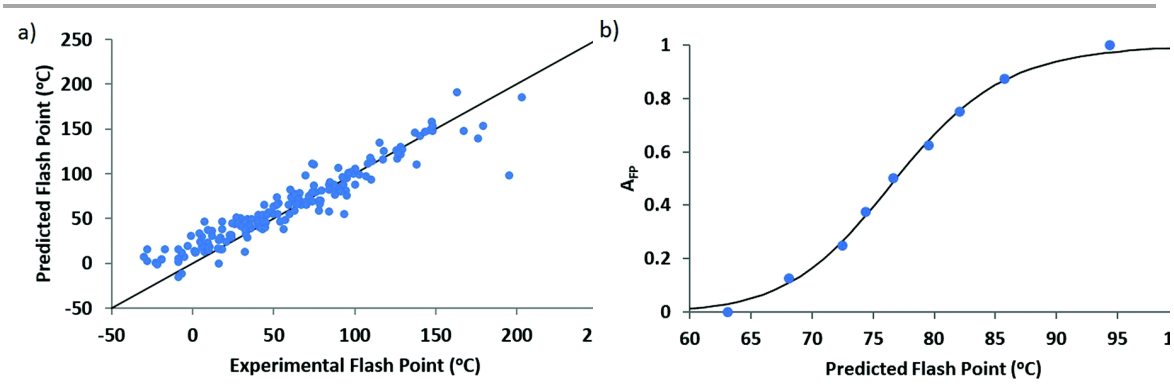

Fig. 4.1 (a) A comparison of predicted and experimentally determined flash points. The black line represents a perfect prediction. (b) the sigmoidal acceptability function (black line) fit to the flash point acceptability values (A_{FP}) assigned to every 10^{th} deviation-percentile (10^{th}-90^{th}) away from the target value of 80 °C (blue dots). See Appendix 2 for plots regarding other properties.

were calculated. Only amines with structural similarities to the structures being generated by the virtual combinatorial process were used to determine the accuracy of the predictions. By avoiding dissimilar compounds, the accuracy of the predictions made on the structures of interest may be more appropriately characterized. For this reason, compounds containing heteroatoms apart from nitrogen and oxygen, compounds containing carboxylic acid functional groups, and compounds not containing an amine functional group were not included in the reliability analysis.

The deviations of the predicted values from the experimental values were considered in order to determine how acceptable certain predicted values would be. The 10^{th}, 20^{th}, 30^{th} … 90^{th} percentiles of the deviations were identified (herein referred to as "deviation-percentiles"). The flash point data shown in the histogram in Fig. 4.2 can be used as an example. The 10^{th} percentile of the deviation between predicted and experimental flash points was -14.4, while the 90^{th} percentile was 16.9. These values indicate that there is only a 10% chance that the experimental value is more than 14.4 °C lower than the predicted value and only a 10% chance that the experimental value is more than 16.9 °C higher than the predicted value. The 50^{th} percentile was 3.3, so there is a 50% chance that the experimental value is at least 3.3 °C higher than the predicted value and a 50% chance that the experimental value is less than the predicted value plus 3.3 °C.

These deviation-percentiles were applied to the target value to determine the probability that a predicted value meets or exceeds the target value. Continuing to use flash point as an example (target value = 80 °C), a predicted value of 76.7 °C has a 50% chance of meeting the target value because the 50^{th} deviation-percentile is 3.3. If the predicted value is 76.7 °C, there is a 50% chance that the experimental value is at least 3.3 °C greater than that, so there is a 50% chance that the experimental value is at least 80.0 °C. Likewise, a predicted value of 63.1 °C only has a 10% chance of meeting the target value based on the 90^{th} deviation-percentile (only a 10% chance that the deviation is greater than 16.9) and a predicted value of 94.4 °C has a 90% chance of meeting the

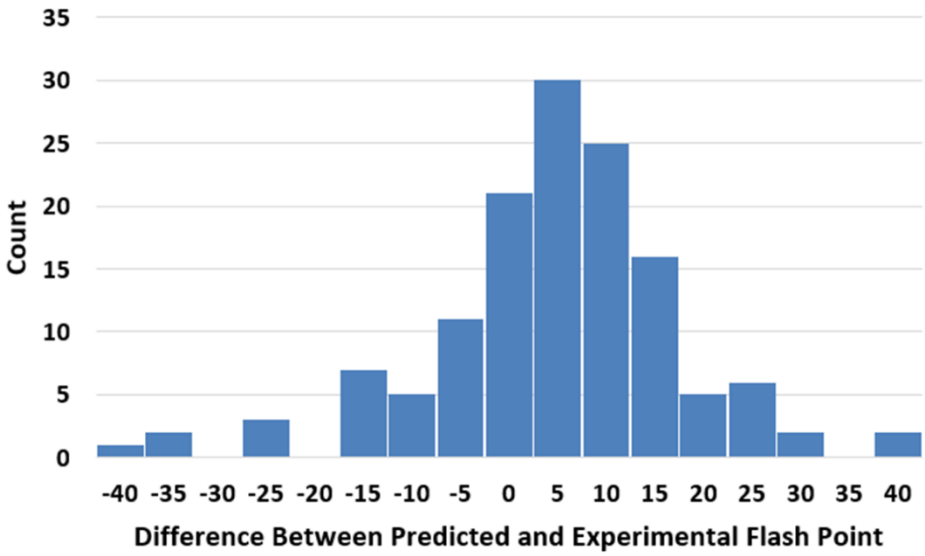

Fig. 4.2 A histogram of the differences between experimental flash point values and the flash point values predicted by TEST. These deviations from perfect predictions were used to create acceptability functions.

target value based on the 10th deviation-percentile (only a 10% chance that the deviation is less than -14.4).

Acceptability values were assigned to each deviation-percentile difference from the target value according to the likelihood that these predictions correspond to experimental values that meet or exceed the target value. Therefore, the predicted value that was at the 50th deviation-percentile difference from the target value (76.7 °C using the flash point example) was assigned an acceptability value of 0.5 because it has a 50% chance of meeting or exceeding the target value. The predicted value that was at the 90th deviation-percentile difference from the target value (only 10% chance that it meets or exceeds the target value) was assigned an acceptability value of 0. The predicted value that was at the 10th deviation-percentile difference from the target value (90% chance that it meets or exceeds the target value) was assigned an acceptability value of 1. The predicted values at every 10th deviation-percentile difference from the target value (10th, 20th, 30th

… 90th) were assigned acceptability values decreasing in increments of 1/8 (e.g. 0.875 for 20th percentile, 0.75 for 30th percentile, etc.).

Acceptability functions were created by fitting a sigmoidal function to a graph of acceptability value vs. predicted value using the data for each of the deviation-percentiles described above (Figure 4.1b). The sigmoidal function was defined to include acceptability values between 0 to 1 following equation 4.1, where A_x is the acceptability value for property x and P_x is the predicted value for property x. The sigmoidal function was fit to the data by altering the constants C, D, and E to minimize the sum of the root mean square deviation of the calculated acceptability from the assigned acceptability of each data point using Microsoft Excel's Solver tool.

$$A_x = \frac{1}{1+\left(\frac{C}{P_x+E}\right)^D} \qquad \text{Eqn. 4.1}$$

Acceptability values and acceptability functions were determined for every property prediction made on a structure and were typically calculated using similar methods as described above. The exact method depends on if a low value is desired instead of a high value, in which case the deviation-percentiles would be assigned opposite acceptability values (increasing from 0 to 1 instead of decreasing from 1 to 0), or if relative deviation instead of absolute deviation were used, in which case comparisons would be made by multiplication and division instead of addition and subtraction. For some properties, there was insufficient experimental data available to determine the accuracy of the predictions (bioaccumulation factor, LC_{50} (daphnia magna, 48 h)) or else a different method of defining acceptability values was used (vapour pressure), so acceptability functions were approximated for these properties.

An example graph of the comparison of experimental and predicted values as well as an example graph showing the acceptability function derived from these data are shown in Fig. 4.2 for the flash point of an amine. For graphs of comparisons and acceptability functions for all of the properties discussed in this chapter, see Appendix 2.

In addition to the individual acceptability values, two overall acceptability values are given: one for properties related to performance and one for properties related to environmental impact, health, and safety (EHS). The performance acceptability is the sum of all acceptability values related to the performance requirements being screened for. Larger performance acceptability corresponds to an increased likelihood that the structure works for the desired application (e.g. it is a SHS). The EHS acceptability is the sum of all acceptability values related to EHS properties. Larger EHS acceptability corresponds to an increased likelihood that the chemical meets the desired EHS requirements. These overall acceptability values can be used to screen for ideal structures; the user can select minima for each acceptability value and be given a list of structures which are predicted to meet or exceed these minima.

4.3 Applying the software

4.3.1 Defining the context and target values

This virtual screening approach to identifying the greenest compounds for a task was applied to SHS technology. The previous experimental approach to identifying less-hazardous SHSs, described in Chapter 2, was only partly successful. Each of the SHSs that were identified had at least one problem that prevented it from being entirely satisfactory, such as toxicity, flammability, or instability. The disadvantage of this experimental approach is its inability to test large numbers of compounds rapidly. The virtual screening approach overcomes this disadvantage and can be used to identify compounds of interest that can then be tested experimentally. In this study, the virtual screening methodology was used to identify tertiary amines that are likely both to act as SHSs and to have few hazards. Amidines and secondary amines that act as SHSs have been reported before but were not screened for in this study.[21,22]

In order to identify what properties are of interest and what values can be considered acceptable, a specific task for which the compounds will be used must be given. In a hypothetical

scenario we used for our study, a company is interested in using a SHS in one of its processes (e.g. the extraction of soybean oil or water purification via forward osmosis), but it wants the SHS to meet certain globally harmonized system (GHS) requirements for aquatic toxicity, acute toxicity, and bioaccumulation so that it will not be considered a significant risk.[23] Additionally, the SHS should have a flash point significantly greater than the operating temperatures of the process (25–70 °C). Finally, the SHS should have a low vapour pressure so that its odour is minimized. Based on this scenario, the properties of interest and acceptable values were determined. These properties and values are discussed below and summarized in Table 4.1.

The log K_{ow}, pK_{aH}, and melting point predictions were included to identify whether or not a compound is a SHS. As discussed in Chapters 2 and 3, only amines with log K_{ow} values between 1.2 and 2.5 and pK_{aH} above 9.5 act as SHSs under standard conditions (1 : 1 v/v ratio of water to amine, 1 atm of CO_2). Amines with lower pK_{aH} and higher log K_{ow} can act as SHSs under modified conditions (higher pressure of CO_2 and/or larger volume ratio of amine to water) as discussed in Chapter 3, but solvent-solute separations using SHSs with higher log K_{ow} are expected to be less complete than more hydrophilic SHSs.[24] For this study, we limited our search to only amines with log K_{ow} between 1.2 and 2.5. Amines with pK_{aH} between 9.0 and 9.5 may not function as SHSs at 1 atm but can act as SHSs at CO_2 pressures up to 10 atm and were considered viable candidates in this study. In addition to having acceptable log K_{ow} and pK_{aH} values, the amine must be a liquid under operating conditions because it must act as a solvent. Therefore, it must have a melting point less than 25 °C. Melting point, log K_{ow}, and pK_{aH} acceptability functions were applied to the software to identify structures that are likely to meet these criteria.

The EHS requirements for the compounds were selected to match various regulatory standards described by the GHS.[23] According to the GHS, a compound is not considered to bioaccumulate significantly if it has a bioconcentration factor less than 500. TEST predicts

Table 4.1 The properties used in the application of the virtual screening process to identify possible SHSs for use in a hypothetical application, the target values for each property, and the reasoning for choosing these target values.

Property	Target value	Reasoning
Log K_{ow}	$1.2 < \log K_{ow} < 2.5$	Required for SHS behaviour
pK_{aH}	≥ 9.0	Required for SHS behaviour
Melting point	< 25 °C	Solvents should be liquid at room temperature
LD_{50} (oral, rat)	> 2000 mg kg^{-1}	Meet GHS definition of low acute toxicity risk[23]
LC_{50} (fathead minnow, 96 h)	> 100 mg L^{-1}	Not classified as toxic by GHS[23]
LC_{50} (daphnia magna, 48 h)	> 100 mg L^{-1}	Not classified as toxic by GHS[23]
Flash point	> 80 °C	Low risk of fire at upper operating temperature
Boiling point	≥ 180 °C	Less volatile compounds should have less odour
Vapour pressure	≤ 30 mtorr	Less volatile compounds should have less odour
Bioaccumulation factor	< 500	Indicates low levels of bioaccumulation according to GHS[23]

bioaccumulation factor (BAF) rather than bioconcentration factor, so BAF was used in this study instead of bioconcentration factor, but the target value of <500 was still employed. Compounds with LC_{50} values above 100 mg L^{-1} for both fathead minnow (96 h) and daphnia magna (48 h) are not categorized as acutely toxic to aquatic life by the GHS. Compounds with LD_{50} (oral, rat) higher than 2000 mg kg^{-1} are considered category 5 substances for acute toxicity: relatively low hazard.

An ideal SHS would meet or exceed these values. The SHS should also not be flammable at or near its upper operating temperature, so for our hypothetical application the flash point should be ≥80 °C. Acceptability functions for each of these criteria were applied to screen for compounds that are likely to meet these requirements.

Two other requirements were implemented into the software to account for volatility in an attempt to apply a filter to select only SHSs that do not have an odour. A previously identified SHS that has no detectable odour has a vapour pressure of approximately 0.03 torr at 25 °C, estimated using a nomograph.[22] Therefore, to select only SHSs which do not have noticeable odours, a filter was applied to screen for amines with vapour pressures below 0.03 torr at 25 °C. However, more volatile amines might have mild smells which, while not preferred, might be acceptable. Therefore, a linear function for vapour pressure acceptability was used instead of a sigmoidal function, where compounds with vapour pressures lower than 0.03 torr would be considered completely acceptable and compounds with vapour pressures above 0.5 torr would be considered completely unacceptable as they would likely have strong odours. The latter value was chosen because it is one fifth of the vapour pressure of *N*,*N*-dimethylcyclohexylamine, a SHS with a strong odour. The acceptability of compounds increases linearly from 0 to 1 between these two values. Boiling point was used as an additional measure of volatility. The software was set to assign boiling point acceptability values to screen for compounds with boiling points above 180 °C.

4.3.2 Structure generation and property prediction

Tertiary amine structures were generated via the virtual combinatorial approach using a trimethylamine scaffold fragment and functionalizing the carbon atoms with 6 R-group fragments outlined in Fig. 4.3. Some fragments could be further substituted with additional R-groups. Some common functional groups, such as esters, carboxylic acids, and phenols, are not represented in the list because of their incompatibility within SHS structures: SHSs with ester groups are

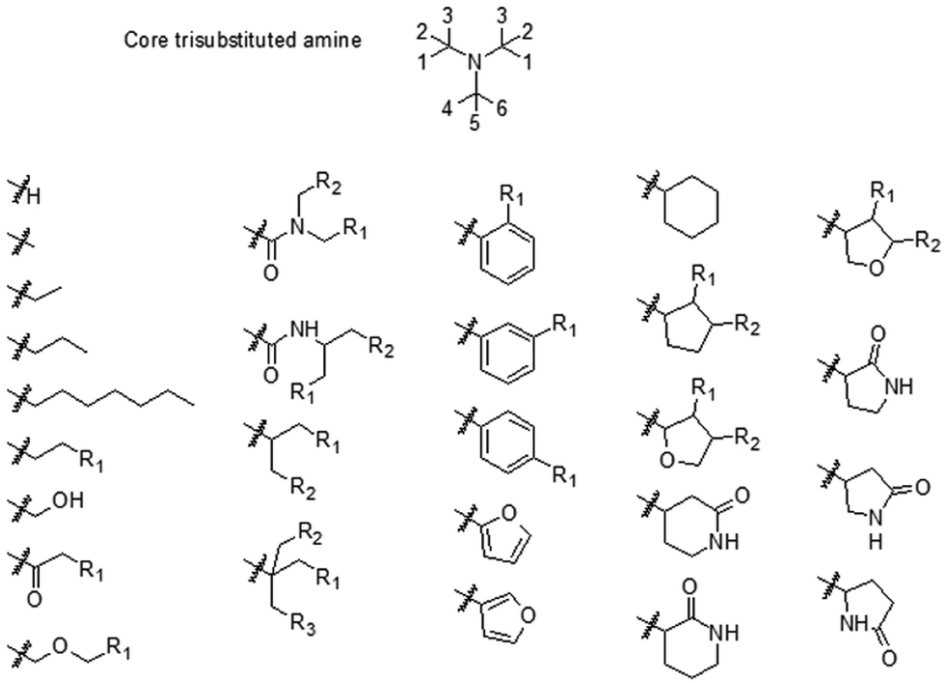

Fig. 4.3 Fragments used to generate molecular structures, including the trimethylamine scaffold showing its 9 substitution sites for up to 6 different fragments.

hydrolytically unstable (see Chapter 2) while carboxylic acids and phenols are acidic and can interfere with the reversible protonation of an amine by the addition of CO_2. To prevent an overwhelming number of structures from being generated, the scope of this study was limited to substituents having ≤7 heavy atoms (C or O). Furthermore, 2 of the 3 carbon atoms on the scaffold fragment were functionalized identically to decrease the synthetic difficulty of the generated structures. Finally, structures with branching groups on all 3 of the carbons on the trimethylamine scaffold fragment were rejected due to the likely synthetic difficulty of preparing such sterically hindered amines (e.g. triisopropylamine). Using this method with the restrictions described above, 33856 tertiary amine structures were created. These structures were then transferred to the property prediction component of the virtual screening approach.

In order to decrease the number of predictions required, the compounds were screened for log K_{ow} before any other property predictions were made. Only compounds with predicted log K_{ow}

values between 0.9 and 2.6 were kept for further study. As mentioned previously, amines require log K_{ow} values between 1.2 and 2.5 in order to act as SHSs, so compounds with log K_{ow} values outside this range were disregarded. However, the initial screening requirements were made more lenient to minimize the number of false negatives being rejected. After applying this initial screening step, 5213 tertiary amine structures remained out of the original 33856.

The properties of interest for the remaining structures were calculated and the acceptability values for each property were determined for each structure. The overall performance acceptability values were the sum of the log K_{ow}, pK_{aH}, and melting point acceptability values. The overall EHS acceptability values were the sum of the LD_{50} (oral, rat), LC_{50} (fathead minnow, 96 h), LC_{50} (daphnia magna, 48 h), flash point, boiling point, vapour pressure, and bioaccumulation factor acceptability values.

The overall acceptability values were screened to identify compounds that are likely to be SHSs that meet the EHS requirements described in the hypothetical scenario. The screening filters for both performance acceptability and EHS acceptability were adjusted, starting with strict requirements and relaxing those requirements until synthetically viable structures were identified. Viable structures were identified with performance acceptability values ≥2.5 out of 3 and EHS acceptability values ≥5 out of 7. Twelve example structures proposed by the software is shown in Fig. 4.4. Although some structures identified by the software might have high acceptability, many of them are also difficult to obtain synthetically, making them unviable options.

4.3.3 Confirming the successful identification of switchable-hydrophilicity solvents

To confirm that the structures generated from the software are indeed SHSs, four easily-prepared amines (compounds **4.1**–**4.4**, Fig. 4.5), proposed by the software that were predicted to be most likely to meet our design criteria, were synthesized and tested for their ability to display switchable miscibility with water. Amines are considered to be SHSs if they are miscible with water

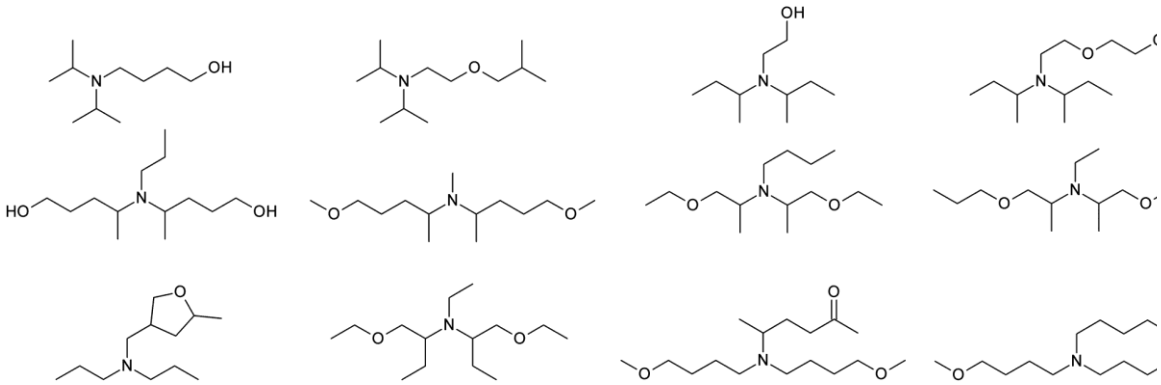

Fig. 4.4 Examples of molecular structures identified by the software as SHSs with a high probably of meeting the design criteria.

in the presence of CO_2 and immiscible with water in the absence of CO_2. Compounds **4.1–4.3** all displayed the desired behaviour, but compound **4.4** did not. It was found to be completely miscible with water, even in the absence of CO_2. This false positive is likely due to the fact that log K_{ow} was used as a proxy measurement for solubility in the software. Solubility predictions were not implemented into the software due to their poor performance at predicting complete miscibility for amines (see Appendix 2). Despite this false positive, most of the structures identified by the software are likely to be SHSs.

Of all the structures identified by the software as good candidates, none of the amines were given a perfect EHS acceptability value of 7. In most cases, the predicted LC_{50} values for both fathead minnow, 96 h, and daphnia magna, 48 h, did not meet the requirements for the study. Although the compounds investigated did not meet all of the design goals, the SHSs identified in this study met all 3 of our performance criteria and 5 of 7 EHS criteria. These SHSs are therefore reasonable candidates for use in the process they were designed for. The predicted properties for the three confirmed SHSs (compounds **4.1–3**) are shown in Table 4.2. Additionally, compounds **4.1–3** have very mild odours. These SHSs could be recommended to the hypothetical company for use in their process.

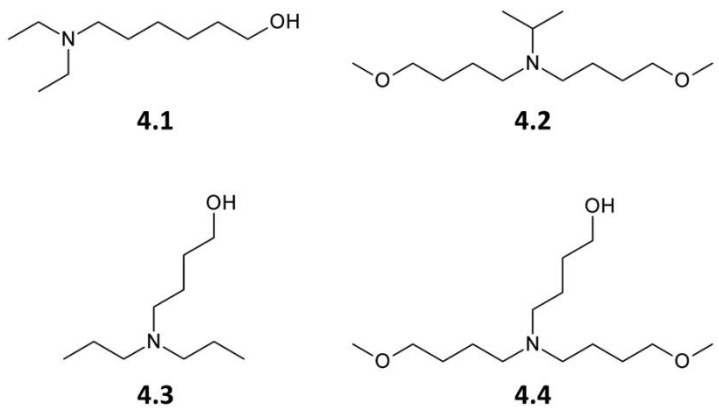

Fig. 4.5 Four compounds identified by the screening method that were synthesized for confirmation of the method's success.

The successful identification of 3 amines with preferable properties demonstrates the efficacy of this type of virtual screening. Although no structures were identified which meet all of the criteria we implemented, the scope of the study did not encompass all possible structures. With a larger scope, the likelihood of finding a structure that meets all of the requirements increases because more compounds can be screened.

In the future, this method can be improved to identify the most desirable compounds. This may include adding additional predictions for other EHS related properties and/or investigating more structures. Predicted values for carcinogenicity and mutagenicity could be considered for example. Additionally structures with substituents larger than 7 heavy atoms could be added to the study or secondary amines could be screened for their potential to act as SHSs. With a larger scope, it is more likely that ideal SHSs will be identified. Furthermore, the current iteration of the screening method may overemphasize the importance of low volatility relative to other EHS properties. Flash point, boiling point, and vapour pressure are all properties that relate to volatility and are correlated with each other. Therefore, a compound with a high flash point acceptability will also likely have high boiling point and volatility acceptabilities. As a result, structures that are

Table 4.2 Acceptability values and predicted properties for the SHSs identified by the virtual screening method and confirmed by experimental testing.

Property	Desired value	Compound		
		4.1	**4.2**	**4.3**
Performance acceptability	3	2.72	2.97	2.76
EHS acceptability	7	5.14	5.31	5.03
Log K_{ow}	$1.2 < \log K_{ow} < 2.5$	1.97	2.26	1.97
pK_{aH}	≥ 9	9.7	9.7	10.6
Melting point (°C)	< 25	0	-48	-3
LD_{50} (oral, rat) (mg kg^{-1})	> 2000	2600	1600	2400
LC_{50} (fathead minnow, 96 h) (mg L^{-1})	> 100	27	97	19
LC_{50} (daphnia magna, 48 h) (mg L^{-1})	> 100	46	11	38
Bioaccumulation factor	< 500	65	32	31
Flash point (°C)	≥ 80	97	103	106
Boiling point (°C)	≥ 180	225	254	227
Vapour pressure (mtorr)	≤ 30	6	1	5

predicted to have low volatility meet three design requirements while structures that are predicted to have high fathead minnow LC_{50} values only meet one design requirement. This bias towards low volatility was not intended and future iterations of the screening method might identify SHSs with higher toxicity acceptability values if the correlation between the volatility-related acceptability values is accounted for. By making alterations to the screening method, different structures might be identified as the most likely candidates to meet the design requirements and these different structures might be more preferable than those identified in this first iteration of the screening process.

Despite the success of this method, it has some disadvantages. The synthetic feasibility of the structures generated by the software is not accounted for, so the chemist using the software must decide which compounds are synthetically viable. The software also does not take into account the environmental and health impacts associated with manufacturing the compounds identified. Finally, some properties, such as solubility in water or the propensity of amines to form nitrosamines, cannot be predicted reliably; new QSAR models must be made before these properties can be incorporated into the screening process.

4.4 Conclusions

A general strategy for identifying compounds with desired EHS and performance properties was described. If the properties required for good performance are known, then predictions of those properties can be performed on a large number of molecular structures generated in silico. Various environmental, human health, and safety (EHS) parameters can also be predicted to describe which of the structures are likely to be the greenest choice. By applying both EHS and performance based filters, compounds combining good performance with minimal risk can be identified. We believe that virtual screening can be used to identify any type of reagent if the chemical or physical properties that are required for performance are known. Additionally, the acceptability functions used in the software are entirely modular, so predicted properties can be added or removed from the software to fit the needs of the user. Therefore, the software can be altered to work for any given application. Using this method for virtual screening of compounds allows for a high throughput, rapid identification of potential compounds that not only function in the manner desired, but also pose little threat to human health and safety or the environment.

This approach to molecular design has been applied to identify SHSs with properties that match the requirements for a given application. Using the knowledge of the properties that relate to SHS behaviour, gained from previous work described in Chapters 2 and 3, this virtual screening

approach was successful in identifying several tertiary amines that are likely to act as SHSs. Furthermore, by screening for EHS related properties, SHSs with very few hazards were identified. Four of the compounds identified by the virtual screening process were tested experimentally to determine if they are SHSs. Three of the four compounds displayed the behaviour characteristic of a SHS. In addition to confirming the success of this virtual screening approach, these three compounds are expected to be among the safest known SHSs. Among the three identified, compounds **4.1** is likely to be the most interesting candidates for further research because its synthesis as more successful than those of compounds **4.2** and **4.3**, making it more readily accessible to researchers. However, improved synthetic methods could result in one of the other SHS being the most available (and least expensive) option.

4.5 Experimental Methods

All chemicals were used as received. Diethylamine (99.5%), isopropylamine (99.5%), dipropylamine (99%), diisopropylethylamine (99%), 4-chloro-1-butanol (~85%), and 4-amino-1-butanol (98%) were purchased from Sigma-Aldrich. 6-Bromo-1-hexanol (95%) was purchased from Combi-Blocks. 1-Bromo-4-methoxybutane (95+%) was purchased from Matrix Scientific. Acetonitrile (reagent grade) and diethyl ether (reagent grade) were purchased from ACP Chemicals. Sodium hydroxide pellets were purchased from Acros Organics. Anhydrous magnesium sulfate (99.5%) and concentrated aqueous hydrochloric acid (reagent grade) were purchased from Fisher Scientific. Argon (99.998%) and supercritical fluid chromatography grade CO_2 were purchased from Praxair.

4.5.1 Evaluating an amine to determine if it is a SHS

Approximately 1 mL of an amine was mixed with approximately 1 mL of water in a 10 mL graduated cylinder. If the mixture was biphasic, CO_2 was bubbled through the mixture using a gas dispersion tube until the mixture became monophasic or for up to 2 h. If the mixture became

monophasic within 2 h, CO_2 was removed from the system by heating it to 60 °C and bubbling argon through the mixture using a gas dispersion tube until the amine phase-separated from the water or for up to 2 h. If the mixture displayed all of the desired behaviour (biphasic initially, monophasic after addition of CO_2, and biphasic after removal of CO_2), the amine in the mixture was considered a SHS, otherwise it is not a SHS under these conditions.

4.5.2 Synthesis of 6-(diethylamino)-1-hexanol (4.1)

A 100 mL round bottom flask equipped with a stir bar and reflux condenser was charged with 5 mL of 6-bromo-1-hexanol (38 mmol), 16 mL of diethylamine (150 mmol), and 20 mL of acetonitrile. The mixture was stirred and refluxed overnight, cooled to room temperature, then added to 20 mL of 20% aqueous NaOH. The mixture was extracted with diethyl ether (3 x 20 mL) and the combined organic phase was dried with magnesium sulfate, decanted, and then concentrated under reduced pressure to afford the crude product. Distillation under vacuum yielded the pure product as a colourless liquid (4.2 g, 60% yield); BP 77 °C (0.2 torr); ^{1}H NMR (400.13 MHz, $CDCl_3$) δ 1.01 (t, *J*= 7.1 Hz, 6H), 1.25-1.40 (m, 4H), 1.46 (p, *J*= 7.5 Hz, 2H), 1.56 (p, *J*= 6.8 Hz, 2H), 2.40 (t, *J*= 7.6 Hz, 2H), 2.51 (q, *J*= 7.1 Hz, 4H), 3.61 (t, *J*= 6.7 Hz, 2H); ^{13}C NMR (100.61 MHz, $CDCl_3$) δ 11.4, 25.7, 26.8, 27.4, 32.7, 46.8, 52.8, 62.5; ν_{max} (ATR) 3320, 2968, 2930, 2857, 2804, 1467, 1378, 1293, 1201, 1059, 769; *m*/*z* (EI) 173 (8), 158 (7), 86 (100), 72 (24), 58 (26), 55 (10); HRMS $C_{10}H_{23}NO$ for M^+ calculated: 173.1780, found: 173. 1788.

The ^{1}H NMR data do not match a literature report (the peaks at 2.40 ppm and 2.51 ppm are reported at 2.73 and 2.86, respectively), but are consistent with an experimental spectrum from Bio-Rad Laboratories present in the SciFinder database, which shows signals at 2.4 ppm and 2.5 ppm.[25,26]

4.5.3 Synthesis of *N*,*N*-di-(4-methoxybutyl)isopropylamine (4.2)

A 50 mL round bottom flask equipped with a stir bar and reflux condenser was charged with 1 mL of isopropylamine (12 mmol), 5 g of 1-bromo-4-methoxybutane (30 mmol), and 5.3 mL of diisopropylethylamine (30 mmol). The mixture was stirred for 6 h at room temperature (21 °C), then for 18 h in an oil bath heated to 40 °C, and finally for another 24 h in an oil bath heated to 100 °C. The mixture was then cooled to room temperature and 20 mL of 20% aqueous NaOH was added. The mixture was extracted with diethyl ether (3 x 20 mL) and the combined organic phase was dried with magnesium sulfate, decanted, and then concentrated under reduced pressure to afford the crude product. Distillation under vacuum yielded the pure product as a colourless liquid (1.9 g, 40% yield); BP 73 °C (0.2 torr); ^{1}H NMR (499.12 MHz, $CDCl_3$) δ 0.88 (d, *J*= 6.4 Hz, 6H), 1.37 (p, *J*= 6.6 Hz, 4H), 1.49 (p, *J*= 6.6 Hz, 4H), 2.29 (t, *J*= 6.6 Hz, 4H), 2.83 (septet, *J*= 6.4 Hz, 1H), 3.25 (s, 6H), 3.30 (t, *J*= 6.6 Hz, 4H); ^{13}C NMR (125.50 MHz, $CDCl_3$) δ 18.0, 25.5, 27.5, 49.6, 49.8, 58.4, 72.8; ν_{max} (ATR) 2961, 2930, 2864, 2823, 2806, 1461, 1385, 1360, 1318, 1222, 1192, 1164, 1117, 1087, 949, 898; *m*/*z* (EI) 231 (3), 216 (18), 158 (100), 98 (9), 87 (60), 84 (23), 55 (23); HRMS $C_{13}H_{29}NO_2$ for M^+ calculated: 231.2198, found: 231.2191.

4.5.4 Synthesis of 4-(dipropylamino)-1-butanol (4.3)

A 50 mL round bottom flask equipped with a stir bar and a reflux condenser was charged with 5 mL of 4-chlorobutanol (50 mmol) and 17 mL of dipropylamine (125 mmol). The mixture was stirred in an oil bath heated to 100 °C for 96 h, then cooled to room temperature. The mixture was then added to 40 mL of 1 M aqueous HCl and extracted with 40 mL of ether. The pH of the isolated aqueous phase was adjusted by adding solid sodium hydroxide until the pH was >12, then the aqueous phase was extracted with diethyl ether (3 x 40 mL). The combined organic phase was dried with magnesium sulfate, decanted, and then concentrated under reduced pressure to afford the crude product. Distillation under vacuum yielded the pure product as a colourless liquid (2.5 g,

30 % yield); BP 52 °C (0.1 torr); ^{1}H NMR (499.12 MHz, $CDCl_3$) δ 0.78 (t, *J*= 7.5 Hz, 6H), 1.39 (sextet, *J*= 7.6 Hz, 4H), 1.53 (m, 4H), 2.30 (m, 6H), 3.44 (t, *J*= 4.9 Hz, 2H), 6.39 (broad, 1H); ^{13}C NMR (125.50 MHz, $CDCl_3$) δ 11.8, 19.2, 26.0, 32.5, 54.7, 55.7, 62.4; ν_{max} (ATR) 3379, 2956, 2933, 2872, 2801, 1460, 1378, 1297, 1190, 1066, 1023; *m*/*z* (EI) 173 (14), 144 (87), 114 (100), 100 (8), 86 (30), 72 (60), 55 (21); HRMS $C_{10}H_{23}NO$ for M^+ calculated: 173.1780, found: 173.1784.

4.5.5 Synthesis of 4-(di-(4-methoxybutyl)amino)-1-butanol (4.4)

A 50 mL round bottom flask equipped with a stir bar and a reflux condenser was charged with 1 mL of 4-amino-1-butanol (10 mmol), 4.2 mL of 4-bromo-1-methoxybutane (30 mmol), and 3.8 mL of diisopropylamine (20 mmol). The mixture was stirred in an oil bath heated to 100 °C for 48 h. The mixture was then cooled to room temperature and 10 mL of concentrated aqueous HCl was slowly added to it. The resulting mixture was extracted with diethyl ether (2 x 20 mL). The pH of the isolated aqueous phase was adjusted by adding solid NaOH until its pH was >12. The aqueous phase was then extracted with diethyl ether (3 x 10 mL). The combined organic phase was dried with magnesium sulfate, decanted, and concentrated under reduced pressure to afford the crude product. Distillation under vacuum yielded the pure product as a colourless liquid (0.7 g, 25%); BP 89 °C (0.1 torr); ^{1}H NMR (400.13 MHz, $CDCl_3$) δ 1.54 (m, 8H), 1.65 (m, 4H), 2.46 (m, 6H), 3.33 (s, 6H), 3.38 (t, *J*= 6.0 Hz, 4H), 3.55 (t, *J*= 4.7 Hz, 2H), 6.20 (broad, 1H); ^{13}C NMR (100.61 MHz, $CDCl_3$) δ 22.7, 26.2, 27.7, 32.6, 53.4, 54.6, 58.5, 62.7, 72.6; ν_{max} (ATR) 3421, 2932, 2863, 2824, 2807, 1461, 1385, 1223, 1192, 1116, 1085, 850, 808, 737; *m*/*z* (EI) 261 (3), 246 (5), 202 (32), 188 (80), 116 (8), 87 (100), 84 (22), 55 (26); HRMS $C_{14}H_{31}NO_3$ for M^+ calculated: 261.2304, found: 261.2309.

4.6 References

1) S. Kar and K. Roy, *Expert Opin. Drug Discov.*, 2012, **7**, 877–902.

2) A. Tropsha, *Mol. Inform.*, 2010, **29**, 476–488.

3) L. B. Salum and A. D. Andricopulo, *Mol. Divers.*, 2009, **13**, 277–285.

4) W. M. Berhanu, G. G. Pillai, A. A. Oliferenko and A. R. Katritzky, *ChemPlusChem*, 2012, **77**, 507–517.

5) T. Öberg, *Environ. Toxicol. Chem.*, 2006, **25**, 1178–1183.

6) B. Jastorff, R. Störmann and J. Ranke, *CLEAN – Soil Air Water*, 2007, **35**, 399–405.

7) J. Ranke, S. Stolte, R. Störmann, J. Arning and B. Jastorff, *Chem. Rev.*, 2007, **107**, 2183–2206.

8) M. Cruz-Monteagudo, E. Ancede-Gallardo, M. Jorge and M. N. Dias Soeiro Cordeiro, *Toxicol. Sci.*, 2013, **136**, 548–565.

9) S. Mortazavi-Manesh, M. A. Satyro and R. A. Marriott, *AIChE J.*, 2013, **59**, 2993–3005.

10) Y. Zhang, X. Ji, Y. Xie and X. Lu, *Appl. Energy*.

11) X. Zhao, Q. Yang, D. Xu, Z. Bao, Y. Zhang, B. Su, Q. Ren and H. Xing, *AIChE J.*, 2015, **61**, 2016–2027.

12) J. R. Vanderveen, L. Patiny, C. B. Chalifoux, M. J. Jessop and P. G. Jessop, *Green Chem.*, 2015, **17**, 5182–5188.

13) cheminfo/script, https://github.com/cheminfo/script (accessed May 8, 2015).

14) Actelion/openchemlib, https://github.com/Actelion/openchemlib (accessed May 8, 2015).

15) P. Ertl, L. Patiny, T. Sander, C. Rufener and M. Zasso, *J. Cheminformatics*, 2015, **7**, 10.

16) NPellet/visualizer, https://github.com/NPellet/visualizer (accessed July 16, 2015).

17) Chemical library (large), http://www.cheminfo.org/Chemistry/Cheminformatics/Chemical_library__large_.html (accessed July 16, 2015).

18) B. A. Leland, B. D. Christie, J. G. Nourse, D. L. Grier, R. E. Carhart, T. Maffett, S. M. Welford and D. H. Smith, *J. Chem. Inf. Comput. Sci.*, 1997, **37**, 62–70.

19) Toxicity Estimation Software Tool (TEST) v4.1, US EPA. https://www.epa.gov/chemical-research/toxicity-estimation-software-tool-test (accessed Jan. 29, 2018).

20) *ACD/Percepta, version 12.0*, Advanced Chemistry Development, Inc., Toronto, ON, Canada, www.acdlabs.com, 2014.

21) P. G. Jessop, L. Phan, A. Carrier, S. Robinson, C. J. Dürr and J. R. Harjani, *Green Chem.*, 2010, **12**, 809–814.

22) J. R. Vanderveen, J. Durelle and P. G. Jessop, *Green Chem.*, 2014, **16**, 1187–1197.

23) *Globally Harmonized System of Classification and Labelling of Chemicals (GHS)*, United Nations, New York and Geneva, 4th edn., 2011.

24) J. Durelle, J. R. Vanderveen, Y. Quan, C. B. Chalifoux, J. E. Kostin and P. G. Jessop, *Phys. Chem. Chem. Phys.*, 2015, **17**, 5308–5313.

25) T. Ikawa, Y. Fujita, T. Mizusaki, S. Betsuin, H. Takamatsu, T. Maegawa, Y. Monguchi and H. Sajiki, *Org. Biomol. Chem.*, 2011, **10**, 293–304.

26) SciFinder, Chemical Abstracts Service: Columbus, OH. 1H NMR spectrum, spectrum ID HB_11234, RN 6947-12-2, https://scifinder.cas.org (accessed January 25, 2018).

Chapter 5

Non-Random Two-Liquid Modelling of a Switchable-Hydrophilicity Solvent System: *N*,*N*-Dimethycyclohexylamine, Water, and Toluene

5.1 Introduction

Of the applications discussed in Section 1.4, the use of SHSs as a solvent for hydrophobic organic products has been the primary focus of the work described thus far. In this application, a SHS is used to dissolve a hydrophobic organic material (e.g. from an extraction, for a chemical reaction, or for facile transportation through a pipeline). When it comes time to separate the dissolved material from the solvent, water and CO_2 are added to the mixture. The CO_2 causes the SHS to enter the aqueous phase, leaving behind the hydrophobic organic product as a separate phase that can be isolated by decantation or filtration. The CO_2 is driven out of the remaining SHS-water mixture, causing the SHS to phase-separate from the water. Both the SHS and the water can be isolated by decantation and reused for further use. This process was outlined in Chapter 1, but due to its relevance in this chapter is also outlined in Fig. 5.1.

In the ideal scenario, this process would result in complete separation of every component. The hydrophobic product that remains after the addition of water and CO_2 would be free of both SHS and water. Likewise, the aqueous phase of this mixture would not contain any of the hydrophobic material. After CO_2 is removed from the aqueous phase, the resulting SHS phase would be free of water and the aqueous phase would not contain any SHS.

In practice, it is unlikely that any of the separations described above will be complete. Some water and SHS will contaminate the product, some water and product will contaminate the SHS, and some SHS and product will contaminate the water. Of these non-ideal situations, the contamination of the product phase is the primary concern. Both the SHS and the water are recycled in this process, so any contamination of either phase by any of the three components (water, SHS,

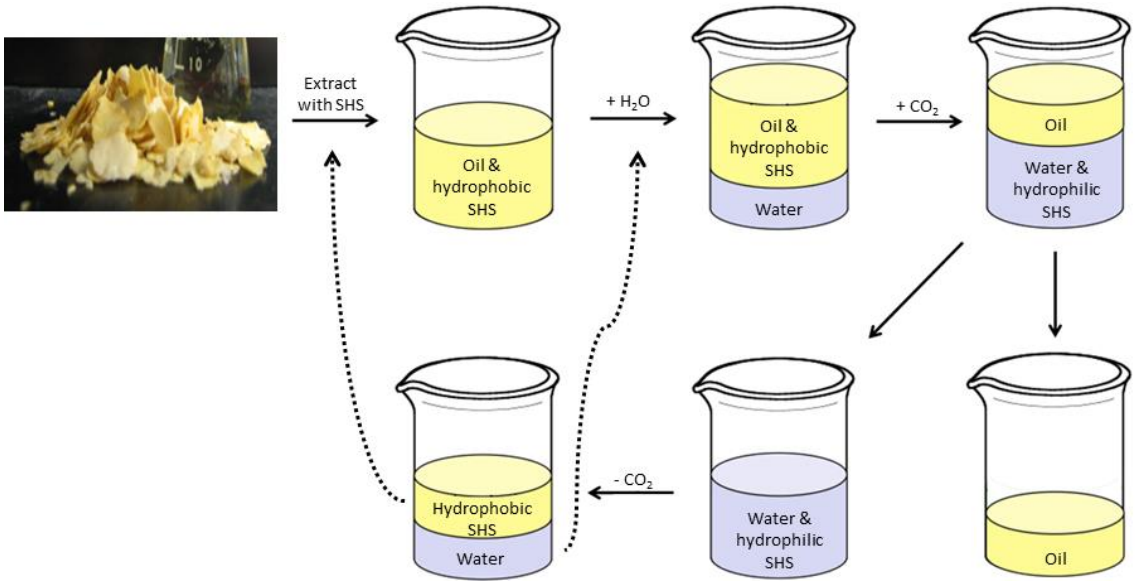

Fig. 5.1 The process used for the extraction and subsequent isolation of soybean oil using a SHS. Image adapted from *Green Chem.*, 2010, **12**, 809-814 with permission of the authors.[1]

or product) results in no loss of material. Furthermore, these phases will be mixed again in subsequent process cycles, so partial cross contamination may not be a concern. Contaminants other than water, SHS, or product may become a concern if they accumulate in the system, but they will not be discussed in this chapter. Unlike the contamination of water or SHS, contamination of the product results in the loss of water and SHS from the system, so these materials will need to be replaced. More significantly, additional purification steps may need to be added to the process if the contamination of the product is too great.

In this chapter, the liquid-liquid equilibrium (LLE) phase compositions of a representative system containing SHS, water, and hydrophobic product is discussed in the context of product contamination. The compositions of each phase at equilibrium provides insight into the contamination of the product. The ternary or quaternary phase diagram created from the data can be used to estimate the composition of the product-rich phase for mixtures with any given composition of SHS, water, and hydrophobic product, thereby determining the level of product

contamination. Furthermore, the data are correlated to a Non-Random Two-Liquid (NRTL) Gibb's energy model to confirm the thermodynamic consistency of the data and to offer a mathematical means of predicting phase compositions.

Data were collected for two systems at 303.15 K: one under atmospheric conditions and another under 1 atm CO_2. Because the product isolation step occurs in the presence of CO_2, data obtained for the system under 1 atm CO_2 are relevant for describing product contamination. The system under atmospheric conditions was investigated to aid in fitting the data to the NRTL model.

The work presented in this chapter is reproduced from Vanderveen *et al.*, *Fluid Ph. Equilibria*, 2016, **409**, 150-156.[2] Experimental data were collected by Yi Quan, Courtney Chalifoux, and myself. The data were correlated and fit to the NRTL model by Roberto Canales at the University of Notre Dame. Various changes have been made to better fit the format and theme of this thesis.

5.2 Experimental

5.2.1 Materials

N,*N*-Dimethylcyclohexylamine ("DMCA", 99%) and 2-hydroxyethanoic acid ("glycolic acid", 99%) were purchased from Sigma-Aldrich. Toluene (>99.5%) was purchased from ACP Chemicals. Carbon dioxide (supercritical fluid chromatography grade, 4.8) was purchased from Praxair. Deionized water from municipal sources was purified using a Synergy™ UV ultrapure water system (EMD Millipore). Acetonitrile (Drisolv, 99.8%) was purchased from EMD Millipore. The purity of the chemicals was checked by gas chromatography using a flame ionization detector (FID, detection limit: 1 ppm) and checked again using a thermal conductivity detector (TCD, detection limit: 100 ppm) to detect the presence of water. No impurities were detected by these methods and the materials were used without further purification. A summary of the purity of each compound and the purification steps used for each compound is given in Table 5.1.

5.2.2 Procedure

Ternary mixtures of water + DMCA + toluene were prepared in closed vials. Their compositions were calculated from the mass of each component. The total weight of each mixture was approximately 14 g. For samples pertaining to the quaternary system, carbon dioxide was passed through the mixture (10 mL/min) at 1 atmosphere for 8 h using a needle. The mixtures were sealed and agitated briefly and then allowed to equilibrate over 16 h, during which time 2 clear phases developed. The mixtures were maintained

at 303.15 K in a constant temperature bath (Cannon Instrument Company). Afterward, samples of both phases of each mixture were collected to determine their compositions.

5.2.3 Analytical Method

Samples were analyzed by gas chromatography using a Clarus 680 gas chromatograph (Perkin Elmer) coupled to a thermal conductivity detector. Separation was carried out with a CP-volamine capillary column (30 m length, 0.32 ID, Agilent Technologies). The column temperature

Table 5.1 The purity and purification steps used for the compounds in this study.

Chemical Name	Source	Initial Mass Fraction Purity	Purification Method	Final Mass Fraction Purity	Analysis Method
DMCA	Sigma-Aldrich	0.99	None	-	GC[a]
Toluene	ACP Chemicals	0.995	None	-	GC
Carbon dioxide	Praxair	0.99998	None	-	GC
Water	Deionized municipal water	-	UV, deionization & membrane filtration	>0.9999	GC
Glycolic acid[c]	Sigma-Aldrich	0.99	None	-	GC

[a]Gas chromatography

was maintained at 343.15 K for 2 min, then increased to 513.15 K at 40 K min^{-1} and held at that temperature for 3 min. Helium flowing at 1 mL min^{-1} was used as a carrier gas. Injection volumes of the samples were 0.5 μL unless otherwise stated and the split ratio was 50:1. Each sample was analyzed four times and the results were averaged to determine the mass fractions of the components in the sample.

The compositions of the samples taken from the lower phase of the mixtures prepared without CO_2 were not reliable using gas chromatography (GC) alone. Due to the high concentration of water, the peaks corresponding to water could not be integrated accurately without diluting the samples, but diluting the samples would obscure the peaks corresponding to DMCA and toluene. When enough sample was injected to detect the DMCA and toluene, significant fronting of the water peaks occurred. When the injection volume was decreased to minimize peak fronting, the DMCA and toluene peaks were below the limit of quantification. More reliable results were obtained by using GC to determine the mass of DMCA and toluene in samples of known total mass. A known quantity of acetonitrile was added to the samples as an internal standard. Injection volumes for these samples were 5.0 μL. The mass fraction of water was then calculated based on the results of the GC analysis such that the sum of the mass fractions of the components was 1.000 as described in equation 5.1, where w_{11}, w_{21}, and w_{31} are the mass fractions of water, DMCA, and toluene, respectively, in the aqueous phase.

$$w_{11} = 1 - w_{21} - w_{31} \qquad \text{Eqn. 5.1}$$

In samples pertaining to the quaternary system, GC analysis cannot differentiate between DMCA and protonated DMCA ($DMCAH^+$) or water + CO_2 and bicarbonate due to the thermal decomposition of the ammonium bicarbonate salt (equation 5.2). Instead, GC analysis shows three peaks for the five species: one for water and bicarbonate salt of DMCA (DMCAH-bicarbonate) that decomposed to water, one for DMCA and DMCAH-bicarbonate salt that decomposed to

DMCA, and one for toluene. The peak corresponding to CO_2 was not used for quantification due to the volatility of CO_2, which increased the uncertainty of measurements made using this peak.

$$DMCAH^+ + HCO_3^- \rightarrow DMCA + H_2O + CO_2 \qquad \text{Eqn. 5.2}$$

To determine the amount of DMCA and DMCAH-bicarbonate in the aqueous phase of each of the samples pertaining to the quaternary system, the pH of the aqueous phase was measured using an Orion 4-Star benchtop pH-conductivity meter (Thermo Scientific). The pH of the solution was used to calculate the fraction of protonated DMCA (equation 5.3), where *P* is the fraction of protonated species, pK_a is the pK_a of the conjugate acid of the amine, and pH is the pH of the aqueous phase. The pK_a of $DMCAH^+$ is 10.48.[3] *P* indicates what fraction of the DMCA + DMCAH-bicarbonate peak from the TCD corresponds to DMCAH-bicarbonate in the aqueous phase, while the remaining fraction of the peak corresponds to DMCA in the aqueous phase. The amount of DMCAH-hydroxide in solution was assumed to be negligible at the pH range measured in the aqueous phase of each sample. The use of pH and pK_a to determine *P* may not give accurate results for solutions with large concentrations of DMCA and DMCAH. To validate this pH method, it was compared to an alternative method for the determination of *P* for DMCA using quantitative ^{13}C NMR reported by Wilson and Stewart.[4] In this method, the mole ratio of bicarbonate and DMCA can be used to calculate *P* by calculated the quotient of the moles of bicarbonate and the moles of DMCA as determined by quantitative ^{13}C NMR (equation 5.4, where A_{HCO3-} and A_{DMCA} are the areas under peaks in ^{13}C NMR corresponding to the bicarbonate ion or to the methanetriyl carbon in DMCA, respectively). The value from the pH method (P = 0.955) was comparable to the value using the NMR method (P = 0.952, reported by Wilson and Stewart) for samples containing only water and DMCA under 1 atm CO_2.[4] This result suggests that the pH method is acceptable despite being used at high concentrations of DMCA and DMCAH.

$$P = \frac{10^{(pK_a - pH)}}{1 + 10^{(pK_a - pH)}} \qquad \text{Eqn. 5.3}$$

$$P = \frac{A_{HCO_3^-}}{A_{DMCA}}$$ Eqn. 5.4

The amount of DMCAH-bicarbonate in the aqueous phase was also used to determine the amount of water in the aqueous phase. The moles of water in each sample was determined by the TCD signal corresponding to water + decomposed DMCAH-bicarbonate. The moles of DMCAH-bicarbonate in the sample was subtracted from this value to account for water created from the decomposed DMCAH-bicarbonate. The remainder corresponds to the moles of water in the aqueous phase and was converted to mass of water.

A similar process was used to determine the amount of water, DMCA, and DMCAH-bicarbonate in the organic phase. However, the amount of DMCAH-bicarbonate could not be determined using equation 5.3. Instead, the value was determined from the concentration of the salt in the aqueous phase and its partition coefficient, K_P (equation 5.5). The log of the partition coefficient was experimentally determined to be -3.1 ± 0.1.

$$[DMCAH^+ \cdot HCO_3^-]_{org} = K \times [DMCAH^+ \cdot HCO_3^-]_{aq}$$ Eqn. 5.5

To determine the partition coefficient of DMCAH-bicarbonate between toluene and water, a mixture containing 5 mL of water, 20 mL of toluene, 5 mL of DMCA, and 2.5 g of glycolic acid (1 molar equivalent to DMCA) was prepared. The mixture was prepared with a significant mass fraction of DMCA to more accurately model the quaternary system (water + DMCA + toluene + DMCAH-bicarbonate), which often contains a large mass fraction of DMCA. Glycolic acid was used as a substitute for "carbonic acid" (meaning the mixture of H_2CO_3 and hydrated CO_2 that is obtained when CO_2 is dissolved in water) because the glycolate anion is structurally similar to the bicarbonate anion but glycolic acid is a stronger acid than carbonic acid, which ensures more complete protonation of the DMCA, and it does not readily decompose to a gas. The mixture was agitated briefly, then allowed to equilibrate over 16 h at a temperature of 303.15 K. The organic

phase was sampled without dilution. A sample from the aqueous phase was diluted 1000-fold with methanol. The concentration of DMCA in each phase was determined by GC-FID.

It should be noted that the partition coefficient measured in this experiment differs from the toluene-water distribution coefficient for DMCA at low pH (where partition coefficient and distribution coefficient are expected to be approximately equivalent) reported in Chapter 3. This difference likely arises from different experimental procedures used in the measurements. The procedure used in this chapter was chosen to measure the partition coefficient in systems with high concentrations of aqueous DMCAH-bicarbonate, which are more relevant to the systems studied in this chapter. Therefore, the value of $K_P = -3.1 \pm 0.1$ is used in this chapter.

For all mixtures, the mass fraction of dissolved CO_2 and bicarbonate derived from dissolved CO_2 was assumed to be negligible compared to other components in the mixtures, based on previously reported values for the solubility of CO_2 in water and in toluene near 303.15 K and atmospheric pressure.[5,6] Therefore, these species were not considered in either the experimental data or the NRTL model.

5.3 Results and Discussion

5.3.1 Ternary system (water + DMCA + toluene)

The equilibrium compositions of the phases in each sample for the ternary system (the system under atmospheric conditions) are given in Table 5.2, where w_{i1} and w_{i3} are the mass fractions of component i in the aqueous phase and the organic phase, respectively. The experimental tie-lines and the tie-lines fit by the NRTL model are plotted in Fig 5.2. In all samples, the aqueous phase contains very little DMCA and toluene. The organic phase contains primarily DMCA and toluene, but water is present in increasing portions as the ratio of DMCA to toluene is increased. The tie-line data were fit using the Othmer-Tobias equation (Equation 5.6),[7] the Hand equation (Equation 5.7),[8] and the Bachman equation (Equation 5.8).[9] The correlated results are

Table 5.2 Compositions of initial mixtures and experimental tie lines for the ternary system [water(1) + DMCA(2) + toluene(3)] at 303.15 K.[a]

Initial composition			Aqueous phase			Organic phase		
w_1	w_2	w_3	w_{11}	w_{21}	w_{31}	w_{13}	w_{23}	w_{33}
0.5441	0.4559	0.0000	0.988	0.012	0.0000	0.180	0.820	0.0000
0.5335	0.3995	0.0670	0.9918	0.0081	0.0001	0.0935	0.7765	0.1300
0.5423	0.3266	0.1311	0.9921	0.0078	0.0001	0.0471	0.6896	0.2633
0.5430	0.2607	0.1963	0.9939	0.0059	0.0002	0.0253	0.5679	0.4068
0.5442	0.1942	0.2616	0.9962	0.0036	0.0002	0.0148	0.4328	0.5522
0.5429	0.1282	0.3289	0.9970	0.0028	0.0002	0.0083	0.2872	0.7045
0.5339	0.0622	0.4039	0.9980	0.0017	0.0003	0.0061	0.1429	0.8510
0.5353	0.0000	0.4647	0.9997	0.0000	0.0003	0.005	0.0000	0.995

[a] Standard uncertainties, u, are $u(w) = 0.002$ and $u(T) = 0.1$ K.

shown numerically in Table 5.3 and graphically in Fig 5.3. These equations show empirical correlations in the experimental results, but they do not guarantee thermodynamic consistency.[10]

$$\ln\left(\frac{1-w_{11}}{w_{11}}\right) = A\ln\left(\frac{1-w_{33}}{w_{33}}\right) + B \qquad \text{Eqn. 5.6}$$

$$\ln\left(\frac{w_{21}}{w_{11}}\right) = A\ln\left(\frac{w_{23}}{w_{33}}\right) + B \qquad \text{Eqn. 5.7}$$

$$w_{23} = A\left(\frac{w_{23}}{w_{11}}\right) + B \qquad \text{Eqn. 5.8}$$

This ternary system corresponds to a stage in a SHS-based separation process immediately before separating the SHS from a dissolved liquid product (Fig. 5.1, top center beaker). Based on the distribution ratio of SHS between the two phases, no significant separation of SHS from the product would have occurred at this stage. The next stage in the separation process is to introduce CO_2 into the system, which should cause the SHS to separate from the product. While the information gained from this ternary system is not essential to understanding the separation process,

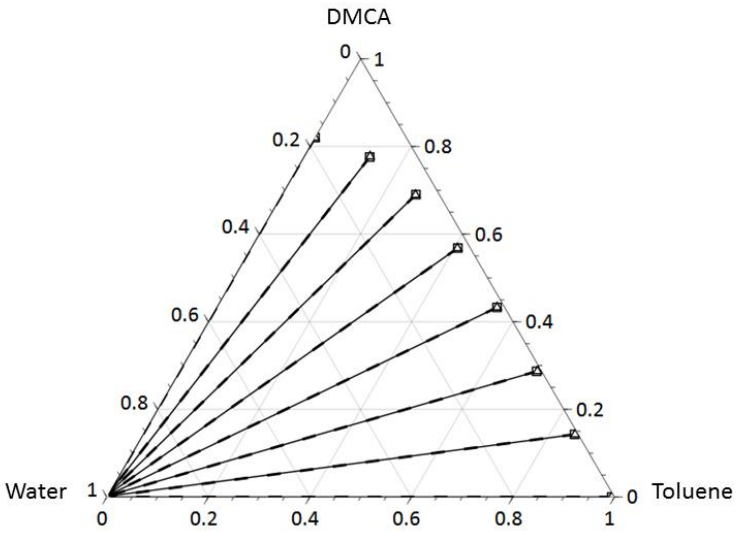

Fig. 5.2 Ternary diagram for the LLE of [water + DMCA + toluene] at 303.15 K. The values displayed are mass fractions. (Δ ─) experimental tie-line data, (□ - -) NRTL tie-line data.

the interaction parameters determined by the NRTL model for this system were used in fitting the parameters in a model of the desired quaternary system, as discussed below.

5.3.2 Quaternary system (water + DMCA + toluene + DMCAH-bicarbonate)

The equilibrium compositions of the phases in each sample for each quaternary system (the system under 1 atm CO_2) are given in Table 5.4. The initial compositions of the mixtures are given before the addition of CO_2, but do not represent the global compositions of the equilibrated mixtures. Portions of each sample evaporated during the addition of CO_2 and bicarbonate ions were

Table 5.3 Constants of Othmer-Tobias, Hand, and Bachman equations

Equation	A	B	R^2
Othmer-Tobias	0.423	5.419	0.945
Hand	0.473	5.455	0.948
Bachman	0.990	0.002	>0.999

a)

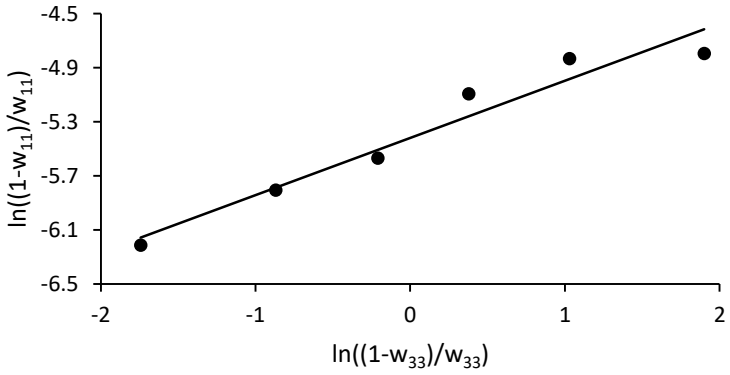

b)

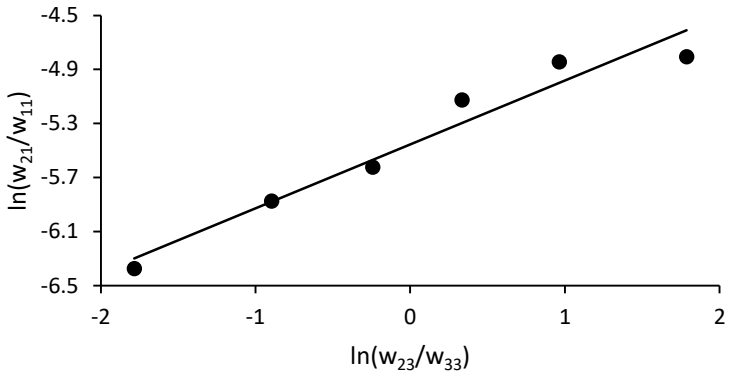

c)

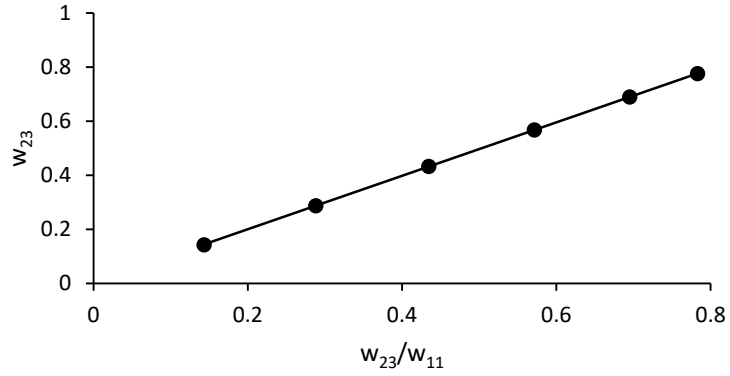

Fig. 5.3 Plots for the empirical correlation of tie-line data for the system [water(1) + DMCA(2) + toluene(3)] at 303.15 K, including: a) an Othmer-Tobias plot, b) a Hand plot, and c) a Bachman plot.

Table 5.4 Compositions of initial mixtures, pH of aqueous phase, and experimental tie-lines for the quaternary system [water(1) + DMCA(2) + toluene(3) + DMCAH-bicarbonate(4)] at 303.15 K.[a]

Initial composition[b]			Aqueous phase					Organic phase			
w_1	w_2	w_3	pH	w_{11}	w_{21}	w_{31}	w_{41}	w_{13}	w_{23}	w_{33}	w_{43}
0.245	0.755	0	9.15	0.226[c]	0.024[c]	0.000	0.750[c]	0.021	0.978	0.000	0.001
0.083	0.845	0.072	9.17	0.229	0.024	0.001	0.746	0.022	0.923	0.054	0.001
0.164	0.693	0.143	8.91	0.229	0.014	0.002	0.755	0.020	0.839	0.140	0.001
0.242	0.547	0.211	8.90	0.279	0.013	0.003	0.705	0.017	0.685	0.297	0.001
0.313	0.414	0.273	8.75	0.347	0.008	0.003	0.642	0.014	0.401	0.584	0.001
0.395	0.266	0.339	8.51	0.485	0.004	0.001	0.510	0.012	0.134	0.854	0.000
0.466	0.130	0.404	8.11	0.697	0.001	0.000	0.302	0.010	0.035	0.955	0.000

[a] Standard uncertainties, u, for mass fractions in the organic phase are $u(w_{i3}) = 0.002$. Standard uncertainties, u, for mass fractions in the aqueous phase are $u(w_{11}) = u(w_{31}) = 0.002$ and $u(w_{21}) = u(w_{41}) = 0.007$. Standard uncertainties, u, for temperature and pH are $u(T) = 0.1$ K and $u(pH) = 0.05$, respectively.

[b] Before addition of CO_2.

[c] The combined mass fraction of DMCA and DMCAH-bicarbonate has been reported for the aqueous phase of a ternary system [water + DMCA + DMCAH-bicarbonate]. The reported value is 0.770 with an unspecified uncertainty at an unspecified temperature. This value is similar to the combined value in the present study, 0.774.[4]

formed from CO_2, changing the global composition of the samples. The carbonated samples were used as-prepared and the evaporation was not investigated. In all mixtures, the organic phase contains primarily toluene and DMCA. Likewise, the aqueous phase contains primarily water and DMCAH-bicarbonate. A quaternary plot showing the experimental tie-lines and tie-lines predicted by the NRTL model is shown in Fig 5.4. The tie-line data were not fit to the Othmer-Tobias, Hand, or Bachman equations because these equations deal with ternary systems and may not be appropriate for quaternary systems or pseudo-ternary systems.

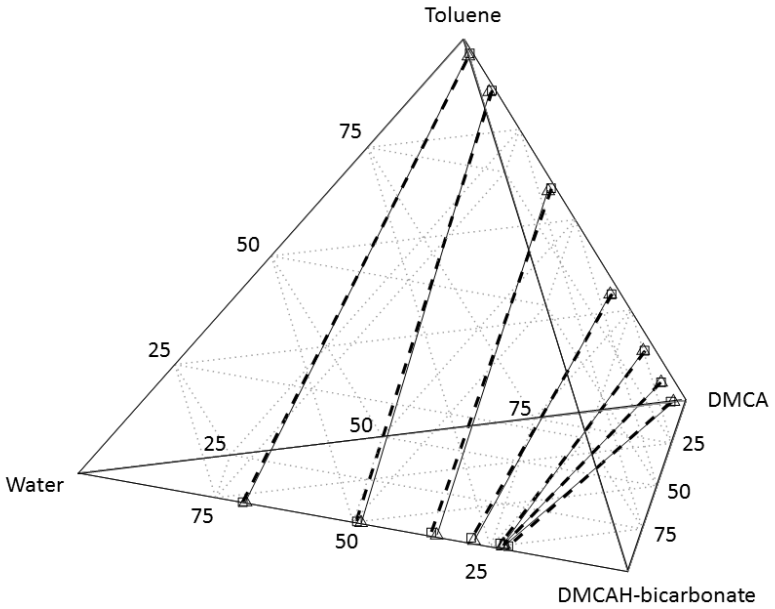

Fig. 5.4 Quaternary diagram for the LLE of [water + DMCA + toluene + DMCAH-bicarbonate] at 303.15 K. (Δ ─) experimental tie-line data, (□ - -) NRTL tie-line data.

Due to the intrinsic relationship between DMCA and DMCAH-bicarbonate, a more practical phase diagram would consider DMCA and DMCAH-bicarbonate as a single component. With regard to the process shown in Fig. 5.1, no distinction between DMCA and DMCAH-bicarbonate needs to be made. Any DMCAH-bicarbonate present in the product oil (the organic phase, Fig. 5.1, bottom right beaker) will decompose to DMCA, water, and CO_2 over time as described by Equation 5.2. Likewise, the DMCAH-bicarbonate present in the aqueous phase will thermally decompose back to DMCA, water, and CO_2 when the SHS is regenerated (Fig. 5.1, bottom left beaker). Therefore, a more practical treatment of the data would combine DMCA and DMCAH-bicarbonate using an appropriate method.

A pseudo-ternary plot was created by treating DMCAH-bicarbonate as if it was a 1:1:1 mole ratio mixture of its degradation products, DMCA, water, and CO_2 (Fig. 5.5). The CO_2 fraction was not considered, but the mass fractions of DMCA and water that would be created as a result of

DMCAH-bicarbonate degradation were added to the measured mass fractions of DMCA and water. Because this degradation occurs during GC analysis, the signal corresponding to DMCA is a result of both DMCA present in the initial sample and DMCA that was created from the decomposition of DMCAH-bicarbonate. The same is true for the signal corresponding to water. Because the signals were already the sum of the initial component and the component from DMCAH-bicarbonate degradation, the data from the GC could be analyzed in the same way as the data for the ternary system [water + DMCA + toluene]. No distinction was made between DMCA and DMCAH-bicarbonate, so the fraction of protonation did not need to be determined. These experimental mass fractions used in Fig. 5.5 are shown in Table 5.5.

The fitted NRTL tie-line data for the quaternary system could be altered to fit the pseudo-ternary data. To perform this alteration, the mass fraction of each component was converted to a mole fraction (n_{ij}, equation 5.9). The mole fraction of DMCAH-bicarbonate was treated as a 1:1:1 mole ratio mixture of DMCA, water, and CO_2 (equation 5.10, where n^*_{ij} indicates the mole ratio of component *i* in phase *j* that forms as a result of DMCAH-bicarbonate degradation). The CO_2 mass fraction was not considered in this study. "Combined" mole fractions (n'_{ij}) for water and DMCA were calculated by adding the moles of each substance with their corresponding mole fractions resulting from DMCAH-bicarbonate degradation (equation 5.11). These combined mole fractions were converted to mass fractions (m'_{ij}), then normalized (w'_{ij}) such that their sum was 1.000 (equations 5.12 & 5.13).

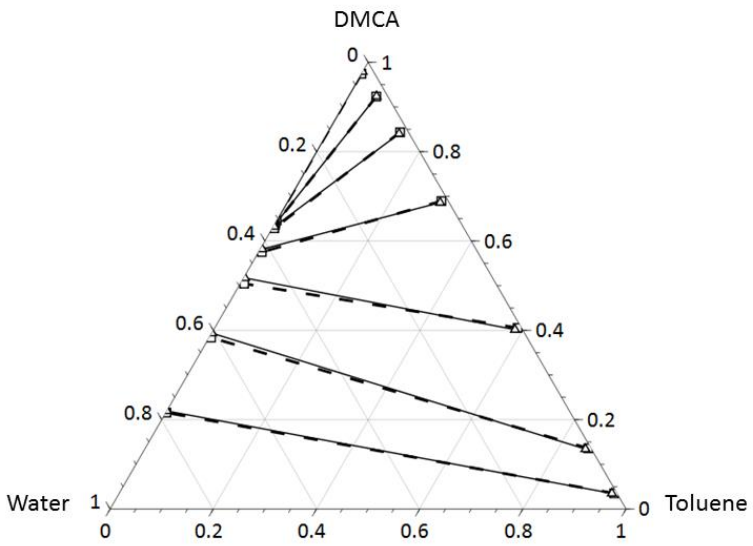

Fig. 5.5 Pseudo-ternary diagram for the LLE of (water + DMCA + toluene + DMCAH-bicarbonate) at 303.15 K. (Δ ─) experimental tie-line data, (□ - -) NRTL tie-line data.

Table 5.5 Compositions of initial mixtures, experimental tie lines, DMCA distribution coefficients, *D*, and selectivity, *s*, for the pseudo-ternary system [water(1) + DMCA(2) + toluene(3)] at 303.15 K.[a]

Initial composition[b]			Aqueous phase			Organic phase			*D*	*s*
w_1	w_2	w_3	w'_{11}	w'_{21}	w'_{31}	w'_{13}	w'_{23}	w'_{33}		
0.245	0.755	0	0.361	0.639	0.000	0.021	0.979	0.000	1.53	-
0.083	0.845	0.072	0.363	0.636	0.001	0.022	0.924	0.054	1.45	36.7
0.164	0.693	0.143	0.366	0.632	0.002	0.020	0.840	0.140	1.33	44.5
0.242	0.547	0.211	0.414	0.582	0.004	0.017	0.686	0.297	1.18	64.7
0.313	0.414	0.273	0.480	0.517	0.003	0.014	0.402	0.584	0.776	272
0.395	0.266	0.339	0.606	0.394	0.001	0.012	0.134	0.854	0.341	4200
0.466	0.130	0.404	0.780	0.219	0.000	0.010	0.035	0.955	0.160	22300

[a] Standard uncertainties, *u*, are $u(w) = 0.002$ and $u(T) = 0.1$ K.

[b] Before addition of CO_2.

$$n_{ij} = \frac{w_{ij}}{MW_{ij}} \quad \text{Eqn. 5.9}$$

$$n_{1j}^{*} = n_{2j}^{*} = n_{CO_2 j}^{*} = n_{4j}\ ;\ n_{3j}^{*} = 0 \quad \text{Eqn. 5.10}$$

$$n_{ij}' = n_{ij} + n_{ij}^{*} \quad \text{Eqn. 5.11}$$

$$m_{ij}' = n_{ij}' \times MW_{ij} \quad \text{Eqn. 5.12}$$

$$w_{ij}' = \frac{m_{ij}'}{m_{1j}' + m_{2j}' + m_{3j}'} \quad \text{Eqn. 5.13}$$

The differences between Fig 5.5 and Fig. 5.2 highlight the effect CO_2 has on the water + DMCA + toluene system. Very little DMCA is present in the aqueous phase in the absence of CO_2, but in the presence of CO_2, DMCA (in the form of either DMCA or DMCAH-bicarbonate) can account for over 60 wt% of the aqueous phase. In fact, depending on the global composition of the mixture, DMCA may distribute preferentially into the aqueous phase when placed under 1 atm of CO_2, as evidenced by the low distribution coefficients for DMCA in mixtures with a small global mass fraction of DMCA. Furthermore, the organic phase contains less water in the presence of CO_2 when there is a large global mass fraction of DMCA present. The removal of water from the organic phase is likely facilitated by the formation of DMCAH-bicarbonate in the aqueous phase, creating a highly concentrated and hygroscopic salt solution.

The selectivity, s, and distribution ratio, D, for the extraction of DMCA from toluene into water were calculated for each tie-line using Equations 5.14 and 5.15.

$$s = \frac{w_{21}' \times w_{33}'}{w_{23}' \times w_{31}'} \quad \text{Eqn. 5.14}$$

$$D = \frac{w_{23}'}{w_{21}'} \quad \text{Eqn. 5.15}$$

where w'_{21} and w'_{23} are the normalized mass fractions of DMCA in the aqueous and organic phases, respectively, and w'_{31} and w'_{33} are the normalized mass fractions of toluene in the aqueous and organic phases, respectively, after performing the same alterations used to plot the quaternary liquid-liquid equilibria on a ternary diagram to combine the DMCA and DMCAH-bicarbonate fractions. Larger selectivities and lower distribution ratios are preferable for this type of separation

because they indicate that more DMCA is extracted from the organic phase while less toluene contaminates the aqueous phase. However, small amounts of toluene in the aqueous phase may not be detrimental to the separation process because the aqueous phase is reused in the SHS-based application, resulting in a working load of toluene that gets carried over between individual cycles of the process shown in Fig. 1. Therefore, lower selectivities are not ideal, but they are also not prohibitive.

Another indicator of the efficacy of a SHS-based separation is the composition of the organic phase. The quaternary system models a stage in a SHS-based separation process immediately before isolating the product by decantation (top right beaker in Fig. 5.1). Therefore, the composition of the organic phase corresponds to the composition of the product. For an ideal separation, the organic phase should contain the product (modelled by toluene) and very little water and SHS. Lower global fractions of DMCA yield organic phases with higher compositions of toluene according to the data presented here (lowest two rows in Table 5.5).

The data presented in this chapter for the quaternary system apply specifically to systems containing only water, DMCA, and toluene under 1 atm of CO_2 and at 303.15 K, but some general insights can be made. The product-rich phase will contain less SHS if there is less SHS in the global composition. This conclusion is supported by the increasing selectivities, decreasing distribution coefficients, and increasing fractions of toluene in the toluene-rich phases that are observed in systems containing smaller fractions of DMCA in their global compositions. Therefore it is beneficial to use as little SHS as possible to dissolve the product prior to the separation of the two by the addition of water and CO_2. However, the SHS:product ratio is likely to be decided not by the separation step, but by prior processing steps. For example, when using a SHS to extract oil from soybeans, the process would be optimized to extract as much oil as possible in the most cost-effective manner. The resulting solution would have a fixed composition of SHS and oil.

A more appropriate means of obtaining a more complete separation of SHS and product is to use more water in the separation process. By adding more water to the system, the fraction of SHS in the global composition will decrease and the product-rich phase will contain less SHS as a result. Alternatively, multiple extraction steps with small amounts of water can be used to obtain an organic phase with larger fractions of product for every extraction performed. In a similar fashion to separatory funnel extractions, which are typically performed using multiple extractions steps with small portions of extracting solvent, using multiple small portions of water would likely result in higher product purity than using an equivalent volume of water in a single extraction step. Another option is a liquid-liquid countercurrent extraction process to maximize the efficiency of SHS removal without increasing the amount of water used. It should be noted that using more water for extraction can be detrimental to the overall process because the water must be heated in a later step to remove CO_2 and recover the SHS. If more water is present, the energy cost to heat it will be greater.

5.3.3 NRTL correlation model

The ternary [water + DMCA + toluene] and quaternary [water + DMCA + toluene + DMCAH-bicarbonate] systems were modeled using the Non-Random Two-Liquid NRTL activity coefficient method proposed by Renon and Prausnitz.[11]

The NRTL model is an activity coefficient model based on concepts established in the field of thermodynamics: activity and Gibbs energy. Unlike the Hand, Othmer-Tobias, and Bachman correlations, which are empirical in nature, the NRTL model can be used to determine the thermodynamic consistency of LLE data because it has been developed from thermodynamic equations. Another activity coefficient model that is often used to describe LLE data is the Universal Quasi-Chemical model, or UNIQUAC. This study makes use of NRTL, so only NRTL will be discussed here.

A system containing two phases is said to be at equilibrium when it has met the condition of isofugacity (equation 5.16). In this equation, x_i^{α} and x_i^{β} are the mole fractions of component i in the aqueous phase (α) and the organic phase (β), respectively, while γ_i^{α} and γ_i^{β} are the activity coefficients of component i in the aqueous and organic phases, respectively. When this condition is met, the chemical potentials of each phase are the equivalent. The NRTL model attempts to correlate LLE data by fitting parameters such that the experimental data are in agreement with the condition of isofugacity. To do this, the activity coefficients of each component in the system must be determined. Activity coefficients are related to the excess Gibbs energy of a system by equations 5.17 and 5.18, where i and k are components of a mixture.[12]

$$x_i^{\alpha}\gamma_i^{\alpha} = x_i^{\beta}\gamma_i^{\beta} \qquad \text{Eqn. 5.16}$$

$$g^E = RT\sum_i \ln(\gamma_i) \qquad \text{Eqn. 5.17}$$

$$\ln(\gamma_i) = \frac{g^E}{RT} - \sum_{k\neq i} x_k \frac{\delta(g^E/RT)}{\delta x_k} \qquad \text{Eqn. 5.18}$$

The NRTL model considers the residual Gibbs energy, $g^{(j)}$, of a molecule j surrounded by other molecules in a solution containing two compounds, where J=1 or 2 for compound 1 or 2, respectively. The residual Gibbs energy of this molecule is the sum of the Gibbs energies for the interactions of compounds 1 and 2 with each other in solution (g_{11}, g_{22}, or g_{12}, which is equivalent to g_{21},), normalized by the local mole fractions of 1 and 2, (χ_{ij}) in solution (that is, the mole fraction of 1 and 2 around molecule j):

$$g^{(j)} = x_{1j}g_{1j} + x_{2j}g_{2j} \qquad \text{Eqn. 5.19}$$

Note also that the sum of the mole fractions must equal one:

$$x_{11} + x_{21} = 1 \qquad \text{Eqn. 5.20}$$

$$x_{12} + x_{22} = 1 \qquad \text{Eqn. 5.21}$$

The excess Gibbs energy, g^E, is the difference between $g^{(j)}$ and the residual Gibbs energy of the solution if it were surrounded purely by other molecules of the same type, $g^{(j)}_{pure}$, where

$g^{(j)}_{pure}=g_{jj}$. The total excess Gibbs energy of a mixture of two compounds is the sum of the excess Gibbs energies of each component, normalized by the mole fractions of the components:

$$g^E = x_1\left(g^{(1)} - g^{(1)}_{pure}\right) + x_2\left(g^{(2)} - g^{(2)}_{pure}\right) \quad \text{Eqn. 5.22}$$

The nonrandomness of the mixture of compounds 1 and 2 is accounted for using equations 5.23 and 5.24, which relates the local mole fractions around molecule j to the strength of the interactions between molecule j and compounds 1 and 2, g_{1j} and g_{2j}, as well as a nonrandomness parameter α_{ij}:

$$\frac{x_{21}}{x_{11}} = \frac{x_2}{x_1}\frac{e^{(-\alpha_{12}g_{21}/RT)}}{e^{(-\alpha_{12}g_{11}/RT)}} \quad \text{Eqn. 5.23}$$

$$\frac{x_{12}}{x_{22}} = \frac{x_1}{x_2}\frac{e^{(-\alpha_{12}g_{12}/RT)}}{e^{(-\alpha_{12}g_{22}/RT)}} \quad \text{Eqn. 5.24}$$

Equations 5.23 and 5.24 combine with equation 5.22 to give equation 5.25.

$$g^E = x_1x_{21}(g_{21} - g_{11}) + x_{2x_{12}}(g_{12} - g_{22}) \quad \text{Eqn. 5.25}$$

Four parameters, τ_{12}, τ_{21}, G_{12}, and G_{21} are defined for simplicity, where:

$$\tau_{12} = \frac{g_{12}-g_{22}}{RT} \quad \text{Eqn. 5.26}$$

$$\tau_{12} = \frac{g_{21}-g_{11}}{RT} \quad \text{Eqn. 5.27}$$

$$G_{12} = e^{-\alpha_{12}\tau_{12}} \quad \text{Eqn. 5.28}$$

$$G_{21} = e^{-\alpha_{12}\tau_{21}} \quad \text{Eqn. 5.29}$$

These parameters are combined with equation 5.25 to form the NRTL excess Gibbs energy equation for a binary system (equation 5.30). This equation can then be used in equation 5.18 to determine activity coefficients, resulting in equations 5.31 and 5.32. Experimental data for binary systems (e.g. water + DMCA or water + toluene) can be fit to this equation by identifying appropriate values for τ_{12}, τ_{21}, and α_{12}.

$$g^E = x_1x_2\left(\frac{\tau_{21}G_{21}}{x_1+x_2G_{21}} + \frac{\tau_{12}G_{12}}{x_2+x_1G_{12}}\right) \quad \text{Eqn. 5.30}$$

$$\ln(\gamma_1) = {x_2}^2 \left[\tau_{21}\left(\frac{G_{21}}{x_1+x_2G_{21}}\right)^2 + \left(\frac{\tau_{12}G_{12}}{(x_2+x_1G_{21})^2}\right)\right] \quad \text{Eqn. 5.31}$$

$$\ln(\gamma_2) = {x_1}^2 \left[\tau_{12}\left(\frac{G_{12}}{x_2+x_1G_{12}}\right)^2 + \left(\frac{\tau_{21}G_{21}}{(x_1+x_2G_{21})^2}\right)\right] \quad \text{Eqn. 5.32}$$

In the case of systems with three or more components, the equations become larger, but the derivations remain the same. Equation 5.33 is used to calculate the activity coefficient of component i in a mixture containing n components.

$$\ln \gamma_i = \frac{\sum_{j=1}^{n} x_j \tau_{ji} G_{ji}}{\sum_{k=1}^{n} x_k G_{ki}} + \sum_{j=1}^{n} \frac{x_j G_{ij}}{\sum_{k=1}^{n} x_k G_{kj}} \left(\tau_{ij} - \frac{\sum_{m=1}^{n} x_m \tau_{mj} G_{mj}}{\sum_{k=1}^{n} x_k G_{kj}}\right) \quad \text{Eqn. 5.33}$$

The NRTL model was not developed for electrolyte solutions. Nonetheless, it has been successfully applied to a wide variety of systems, including ionic liquids.[13–16] In this context, the model parameters should not be assigned any meaning in terms of intermolecular interactions. Rather, the NRTL model should be viewed only as a fitting equation.

For the three component system (water, DMCA and toluene), there are three sets of binary interaction parameters (τ_{ij} and τ_{ji}) and nonrandomness factors ($\alpha_{iJ=}\ \alpha_{ji}$) to be fit to experimental data. For the four component system (water, DMCA, toluene and DMCAH-bicarbonate), this rises to six. Our approach to developing the NRTL model for these system was to fit the parameters to the simplest systems possible. Since water + DMCA and water + toluene are both partially miscible at the temperature of interest, their binary interaction parameters were fit to the experimental binary liquid-liquid equilibrium (LLE) data. The water + DMCA and water + toluene binary data LLE were taken in this study and are shown in Table 5.2. For a fixed value of the nonrandomness factor, the τ_{ij} parameters for a binary system can be determined directly from the mutual solubility data by solving the isofugacity equations (equation 5.16), thus providing an exact "fit" to the experimental data. However, this equation system may have multiple solutions, not all of which correspond to a stable binary equilibrium. Thus, to determine these τ_{ij} values, we used the interval method implemented by Simoni et al.,[17] which guarantees that all possible parameter solutions are found

and that only those yielding stable binary equilibria are considered. These τ_{ij} parameter values were determined at 303.15 K, using α_{ij} values between 0.1 and 0.4, with increments of 0.05, as possibilities. Since DMCA and toluene are completely miscible at 303.15 K, the parameters for this pair had to be fit to the ternary data, fixing the binary interaction parameters for water/toluene and water/DMCA to the values determined from the binary data. The same set of values for α_{ij} were considered for determining the DMCA/toluene parameters. For each set of α_{ij} values, a minimization was performed with the Nelder-Mead simplex direct search[18] and the objective function shown in equation 5.34, where *m* is the number of components and *n* the number of tie lines.

$$OF = \sum_{i=1}^{n}\sum_{j=1}^{m}\left(x_{ij}^{\alpha} - x_{ij}^{\alpha,calculated}\right)^2 + \left(x_{ij}^{\beta} - x_{ij}^{\beta,calculated}\right)^2 \qquad \text{Eqn. 5.34}$$

After the minimizations were completed, several different combinations of values for the α_{ij} and τ_{ij} parameters for the three pairs of compounds that gave low values of the objective function were determined and sorted by objective value. Potentially optimal parameter sets were then tested for phase stability using an interval method, as discussed by Simoni et al.[13] and Tessier et al.[19] Using this method the number and composition of phases predicted by the NRTL model for a particular set of parameter values can be determined with certainty. Parameter combinations that mistakenly predicted a single phase or more than two phases were discarded. For remaining parameter sets, the root mean square deviation (RMSD) was calculated according to equation 5.35 using the predicted compositions from the interval method. The parameter combination with the smallest value of RMSD was then selected as optimal.

$$RMSD = \sqrt{\sum_{i=1}^{n}\sum_{j=1}^{m}\frac{\left(x_{ij}^{\alpha} - x_{ij}^{\alpha,calculated}\right)^2 + \left(x_{ij}^{\beta} - x_{ij}^{\beta,calculated}\right)^2}{2 \cdot m \cdot n}} \qquad \text{Eqn. 5.35}$$

For the quaternary system, three additional sets of binary parameters, corresponding to the water + DMCAH-bicarbonate, DMCA + DMCAH-bicarbonate and toluene + DMCAH-

bicarbonate binary systems, are needed. These three new sets of τ_{ij} and α_{ij} parameters were fit to the experimental LLE data for the quaternary system, keeping the values of the NRTL parameters for the other three binaries fixed at the ones found to best model the ternary system. The parameter estimation and modeling of the compositions for the quaternary system was done using the same methodology as described for the ternary system. The optimized τ_{ij} parameters obtained from these procedures are shown in Table 5.6 with their respective α_{ij}.

As shown in Figs. 5.2, 5.4, and 5.5, the NRTL model results are virtually indistinguishable from the experimental tie-lines. The RMSD of the NRTL model for the compositions of the ternary system is 0.0026 and for the quaternary system it is 0.0114, showing that the NRTL method is appropriate for modeling the mixtures presented in this work and demonstrating that the experimental results are thermodynamically consistent. In additions, the NRTL model can be used to predict the compositions of both phases in a mixture of with a known global composition of water, DMCA, and toluene at 303.15 K. This predictive ability is not directly useful for systems using any different components or any different temperatures. However, the development of an NRTL model for this system demonstrates that such modelling is possible and provides the groundwork for developing models for other systems that may be more relevant to specific applications.

Table 5.6 NRTL nonrandomness factors (α_{ij}) and binary parameters (τ_{ij}) for the quaternary system [water(1) + DMCA(2) + toluene(3) + DMCAH-bicarbonate(4)] at 303.15 K and 1 atm.

Component	NRTL parameters		
i-j	α_{ij}	τ_{ij}	τ_{ji}
1-2	0.35	5.8360	-0.1711
1-3	0.10	9.6133	0.0084
2-3	0.15	2.7314	-2.8351
1-4	0.10	-6.6749	-5.3309
2-4	0.15	5.8249	1.2239
3-4	0.30	7.2289	-2.0146

5.4 Conclusions

Liquid-liquid equilibrium data for the ternary system (water + DMCA + toluene) and the quaternary system (water + DMCA + toluene + DMCAH-bicarbonate) were obtained at 303.15 K and atmospheric pressure. Toluene and DMCA are miscible in all proportions in both systems. In the quaternary system, DMCAH-bicarbonate was never observed to precipitate. The ternary system could be properly correlated using the NRTL model. The NRTL parameters used to correlate the ternary system could also be used to properly correlate the quaternary system using the collected data to identify the other necessary NRTL parameters. The quaternary system (water + DMCA + toluene + DMCAH-bicarbonate) models a stage in a SHS-based separations immediately prior to isolating the organic product by decantation. Therefore, the purity of the isolated organic product can be determined by the composition of the organic phase. The results suggest that a more pure product phase can be obtained through the use of more water in an extraction step or by performing multiple extraction steps. The LLE data can be used as reference data and the methods employed to study the system can be modified to study other SHS systems.

5.5 References

1) P. G. Jessop, L. Phan, A. Carrier, S. Robinson, C. J. Dürr and J. R. Harjani, *Green Chem.*, 2010, **12**, 809–814.

2) J. R. Vanderveen, R. I. Canales, Y. Quan, C. B. Chalifoux, M. A. Stadtherr, J. F. Brennecke and P. G. Jessop, *Fluid Ph. Equilibria*, 2016, **409**, 150–156.

3) J. M. Devereux, K. R. Payne and E. R. A. Peeling, *J. Chem. Soc.*, 1957, 2845–2851.

4) A. D. Wilson and F. F. Stewart, *RSC Adv.*, 2014, **4**, 11039–11049.

5) L. W. Diamond and N. N. Akinfiev, *Fluid Ph. Equilibria*, 2003, **208**, 265–290.

6) H.-J. Ng and D. B. Robinson, *J. Chem. Eng. Data*, 1978, **23**, 325–327.

7) D. Othmer and P. Tobias, *Ind. Eng. Chem.*, 1942, **34**, 693–696.

8) D. B. Hand, *J. Phys. Chem.*, 1929, **34**, 1961–2000.

9) I. Bachman, *Ind. Eng. Chem. Anal. Ed.*, 1940, **12**, 38–39.

10) P. Carniti, L. Cori and V. Ragaini, *Fluid Ph. Equilibria*, 1978, **2**, 39–47.

11) H. Renon and J. M. Prausnitz, *AIChE J.*, 1968, **14**, 135–144.

12) S. M. Walas, *Phase Equilibria in Chemical Engineering*, Butterworth-Heinemann, 2013.

13) L. D. Simoni, Y. Lin, J. F. Brennecke and M. A. Stadtherr, *Ind. Eng. Chem. Res.*, 2008, **47**, 256–272.

14) A. Chapeaux, L. D. Simoni, T. S. Ronan, M. A. Stadtherr and J. F. Brennecke, *Green Chem.*, 2008, **10**, 1301–1306.

15) I. Domínguez, E. J. González, R. González and Á. Domínguez, *J. Chem. Eng. Data*, 2011, **56**, 3376–3383.

16) S. García, M. Larriba, J. García, J. S. Torrecilla and F. Rodríguez, *J. Chem. Thermodyn.*, 2011, **43**, 1641–1645.

17) L. D. Simoni, Y. Lin, J. F. Brennecke and M. A. Stadtherr, *Fluid Ph. Equilibria*, 2007, **255**, 138–146.

18) J. Lagarias, J. Reeds, M. Wright and P. Wright, *SIAM J. Optim.*, 1998, **9**, 112–147.

19) S. R. Tessier, J. F. Brennecke and M. A. Stadtherr, *Chem. Eng. Sci.*, 2000, **55**, 1785–1796.

Chapter 6

Diamines as Switchable Hydrophilicity Solvents with Improved Phase Behaviour

6.1 Introduction

The previous chapters in this thesis have focused on studying the behaviour of monoamine SHSs and developing new monoamine SHSs with improved properties. The studies first identified properties required for SHS behaviour, pK_{aH} and log K_{ow}, and modelled SHS behaviour using those properties. After understanding the behaviour, new SHSs were developed with a focus on making them safer for humans and the environment. The increased understanding of SHS technology and the corresponding development of new SHSs helped to improve the technology and increase its viability.

However, as revealed in the last chapter, the organic phase resulting from a single-stage SHS-based separation remains contaminated with a large amount of SHS. The lowest level of contamination found in the compositions that were tested for the water-DMCA-toluene system (under 1 atm of CO_2) in the previous chapter was 3.5 wt%. More energy must be expended in the form of additional separation stages in order to decrease the level of SHS contamination. If additional water is used, even more energy is required to remove the CO_2 from the resulting aqueous phase because additional heat is needed to warm a larger volume of water. These extra energy inputs that are required to obtain a pure product from a SHS-based separation process are undesirable because they make the process less appealing as an alternative to distillation. Further developments are necessary to improve the separation efficiency of SHS from the organic phase without using prohibitive amounts of energy.

Inspiration for alterations to current SHSs that solve this separation problem can be found from improvements made to other switchable materials. “Switchable water” additives, which are

used to switch aqueous solutions between low and high ionic strength, can be used to "salt out" water-miscible organic solvents like tetrahydrofuran and acetonitrile.[1–4] However, some of the switchable additive in these systems may be removed from the aqueous phase by partitioning into the organic phase, causing a loss of additive over time. Diamine and polyamine additives were found to be retained in the aqueous phase much more than monoamine SHSs.[1] While this advantage of diamines and polyamines over monoamines was not discussed, one explanation of this result is that the greater ionic charge on the poly-cationic additives make them more hydrophilic than mono-cations, allowing them to be more completely retained in the aqueous phase. In addition to reports of diamines as switchable water additives, there is also a report of diamines as switchable amine surfactants, compounds that only act as surfactants in the presence of acids such as CO_2.[5] These diamine surfactants have more hydrophilic head groups than their monoamine counterparts due to the increased charge in the head groups. As a result, the diamine surfactants can be used at higher temperatures and higher pH without forming clouded solutions.[5] Given the successful use of diamines as switchable water additives and switchable surfactants with increased hydrophilicity, diamine SHSs may also display increased hydrophilicity in the presence of CO_2 that causes them to partition more completely out of organic phases.

This chapter focuses on the development of diamine SHSs and demonstrating their superior separation properties over monoamine SHSs. Several diamines were tested for SHS behaviour to determine the log K_{ow} and pK_{aH1} (the pK_a of the monoprotonated diamine) values required for diamines to act as SHSs. Unlike monoamines, diamines also have pK_{aH2} values (the pK_a of the diprotonated species) that must be also be considered in the context of CO_2-switchable behaviour. The diamine SHSs that were identified were compared to monoamine SHSs in terms of their switching speed, their distributions between aqueous and organic phases, and their possible harmful effects to humans and the environment. The results show that diamine SHSs can separate more

completely from hydrophobic organic products than monoamines, though they have some drawbacks as well.

The work presented in this chapter was performed with the help of Jialing Geng and Susanna Zhang, who synthesized the diamines and tested them for switchable hydrophilicity.

6.2 Results and Discussion

6.2.1 Identification of Diamine SHSs

Fourteen diamines were tested for switchable hydrophilicity (Scheme 6.1). As with the identifications of SHSs described in previous chapters, a compound is considered to have switchable hydrophilicity if it passes three tests. First, it must create a biphasic mixture with water (typically an equal volume of water) in the absence of CO_2. Second, the same mixture from the first test must become monophasic upon exposure to 1 atm of CO_2. Third, the mixture from the second test must revert to a biphasic mixture when CO_2 has been thoroughly removed from the system. If a diamine/water mixture displays all three of these behaviours, the diamine is considered a SHS.

The compounds tested in this study were selected to have specific log K_{ow}, pK_{aH1}, and pK_{aH2} values in order to determine the required values for each property for diamine SHSs. The log K_{ow} and pK_{aH} values of monoamines were shown in Chapters 2 and 3 to be determining factors for switchable hydrophilicity and they are expected to be so for diamines as well. The pK_{aH2} value of a diamine is also expected to play a role in the switchability of diamines. The length of the hydrocarbon link between the two amine groups was varied as a means of adjusting a compound's pK_{aH2} value to determine how low it can be without preventing the compound's switchable behaviour. The proximity of the amine groups has an effect on the compound's pK_{aH2} (pK_a of the diprotonated species).[6] When two equivalent amine groups are closely connected, pK_{aH2} is much lower than pK_{aH1}, but when the two groups are distant, pK_{aH2} is only about 0.8 units below pK_{aH1}. If a compound's pK_{aH2} is too small, the compound will not be sufficiently di-protonated by CO_2 in

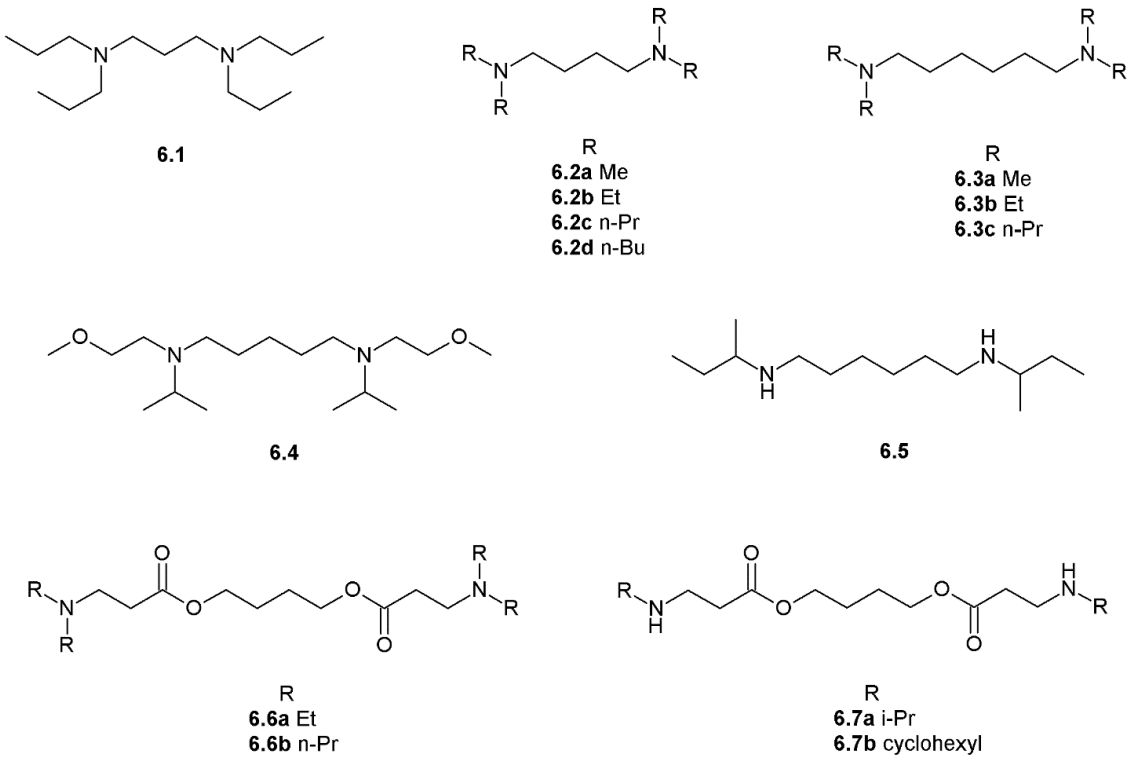

Scheme 6.1 Diamines used in this study.

water and will therefore not exhibit a sufficient change in hydrophilicity. By testing diamines with a variety of low K_{ow}, pK_{aH1}, and pK_{aH2} values, a clear picture can be formed of the properties required for a diamine to have switchable hydrophilicity.

The phase behaviours of these compounds when mixed with water are shown in Table 6.1 and represented graphically in Fig. 6.1. The behaviours are reported for 1:1 (v:v) mixtures of water:diamine and for 1 atm of CO_2. Three compounds were too hydrophilic and were completely miscible with water, even in the absence of CO_2 ("monophasic" in Table 6.1 and blue dots in Fig. 6.1). Five compounds formed biphasic mixtures with water, even in the presence of CO_2 ("biphasic" in Table 6.1 and red dots in Fig. 6.1). These compounds are either too hydrophobic to enter the aqueous phase as salts (e.g. compound **6.2d**) or not basic enough and therefore not sufficiently protonated by CO_2 to switch (e.g. compound **6.6b**). Finally, 5 compounds displayed

Table 6.1 The behaviours of diamines when mixed with an equal volume of water or carbonated water as well as their predicted log K_{ow}, pK_{aH1}, and pK_{aH2} values.

Behaviour[a]	Compound	Log K_{ow}[b]	pK_{aH1}[c]	pK_{aH2}[c]
Monophasic	**6.2a**	0.7	10.0	8.5
Monophasic	**6.3a**	1.7	10.1	9.3
Monophasic	**6.7a**	2.2	9.5[d]	8.5[d]
Switchable	**6.2b**	2.7	10.8	10.0
Switchable	**6.2c**	4.7	10.2	9.3
Switchable	**6.3b**	3.7	10.9	10.2
Switchable	**6.4**	2.5	9.3	8.6
Switchable	**6.7b**	4.9	9.5[e]	8.5[e]
Biphasic	**6.1**	4.2	10.2	7.5
Biphasic	**6.2d**	6.6	10.2	9.3
Biphasic	**6.3c**	5.6	10.2	9.6
Biphasic	**6.6a**	2.8	9.0[d]	8.1[d]
Biphasic	**6.6b**	4.7	9.0[e]	8.1[e]
Precipitates	**6.5**	4.1	11.2	10.6

[a] "Monophasic": the compound forms a monophasic mixture with water in both the absence and presence of CO_2. "Biphasic": the compound forms a biphasic mixture with water in both the absence and presence of CO_2. "Switchable": the compound forms a biphasic mixture with water in the absence of CO_2 and a monophasic mixture with water in the presence of CO_2. "Precipitates": A solid forms upon the addition of CO_2 to a mixture of the compound and water. [b]Predicted using EPISUITE (KOWWIN v1.68) software.[7] [c]Predicted using Advanced Chemistry Development's ACD/Percepta v12.0 software, unless otherwise specified.[8] [d]Experimentally determined. [e]Estimated from experimental values of an analogous compound.

the desired switchable behaviour: poorly miscible with water in the absence of CO_2 and completely miscible with water in the presence of CO_2 ("switchable" in Table 6.1 and green dots in Fig. 6.1). Compound **5** is poorly miscible with water in the absence of CO_2, but it does not form a monophasic liquid when CO_2 is added. Instead, the mixture solidifies ("precipitates" in Table 6.1 and black dot in Fig. 6.1). The amine precipitates as a salt and, because no liquids were visible in the sample, water is likely either incorporated in the solid as a hydrate or trapped inside the solid. This behaviour was observed for secondary monoamines in Chapter 2 and the precipitate was identified as an ammonium bicarbonate salt.

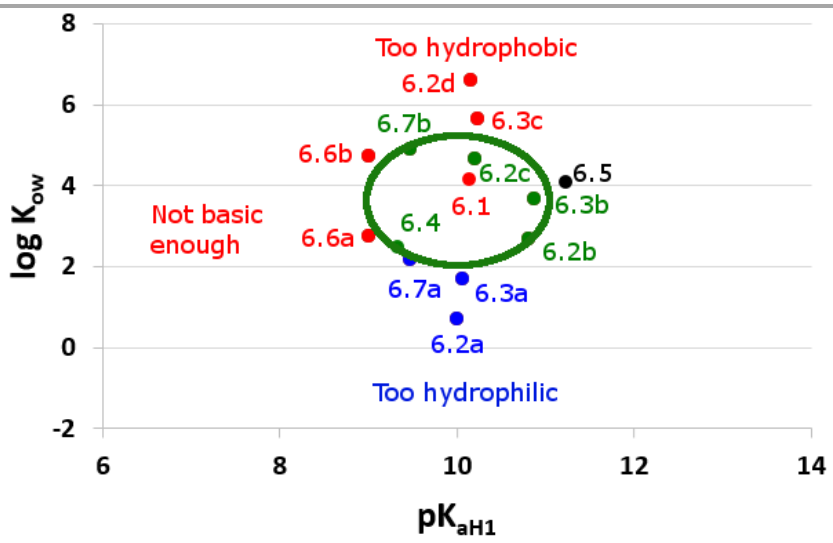

Fig. 6.1 A plot of log K_{ow} vs. pK_{aH1} of the diamines tested for switchable hydrophilicity. Green dots represent compounds with switchable hydrophilicity. Red dots represent compounds that always form biphasic mixtures with water. Blue dots represent compounds that always form monophasic mixtures with water. Black dots represent compounds that form a solid when CO_2 is added. The area within the green oval shows the approximate range of log K_{ow} and pK_{aH1} values required for a diamine to be a SHS, although there are insufficient data to determine the upper limit of the range of acceptable pK_{aH1} values.

The predicted log K_{ow} value of every diamine in Table 6.1 was calculated as a means of determining the correct hydrophobicity required for a diamine to have switchable hydrophilicity. If a diamine is too hydrophilic, then it will always be miscible with water, even in the absence of CO_2. If a diamine is too hydrophobic, then any change in hydrophilicity brought about by the addition of CO_2 will not be enough make the diamine miscible with water. Only diamines with intermediate log Kow values and intermediate hydrophobicities will act as SHSs. In the case of diamines, it appears that successful SHSs have a log K_{ow} between approximately 2.5 and 5. Diamines with lower log K_{ow} values, such as compounds 6.2a, 6.3a, and 6.7a, are too hydrophilic to be SHSs because they form monophasic mixtures with water under air. On the other hand, diamines with log $K_{ow} > 5$, such as compounds 6.2d and 6.3c are too hydrophobic to be SHSs because they form biphasic mixtures with water under 1 atm CO_2. The standard deviation of the log K_{ow} predictions is stated to be ± 0.48 and this value is supported by our analysis (see Appendix 2).[7] Therefore, only diamines with log K_{ow} values between 2.5 and 5 have the intermediate hydrophobicity required for switchable hydrophilicity behaviour.

As with monoamine SHSs, diamine SHSs must have sufficient basicity, measured by pK_{aH1}, in order to act as SHSs. If an amine is too weak a base, it will not be sufficiently protonated in the presence of CO_2 to become hydrophilic. Based on the experimental and predicted pK_{aH1} values for diamines used in this study, a pK_{aH1} value of 9.5 is sufficient, but a value of 9.0 is not. Thus, compounds **6.6a** and **6.6b** are not SHSs, but compound **6.7b** is. Predicted pK_{aH1} values were used for most diamines, but for diamines with pK_{aH1} values near 9.0-9.5 (compounds **6.6a**, **6.6b**, **6.7a**, and **6.7b**), experimental pK_{aH1} and pK_{aH2} values were determined. The experimental values were all lower than the predicted values by between 0.2 and 1.3 units. The pK_{aH1} and pK_{aH2} values for compound **6.4** could not be determined experimentally (see section 6.4.6), so its predicted pK_{aH1} and pK_{aH2} values were used. Compound **6.4** has a predicted pK_{aH1} value of 9.3 and it is a SHS. Therefore, the minimum pK_{aH1} value required for a diamine to be a SHS may be lower

than 9.5, or the predicted pK_{aH1} for compound **6.4** may differ from its real value by 0.2 units. The uncertainty of the prediction is stated to be ± 0.4.[8] Because the uncertainty of predicted pK_{aH1} values is relatively large, the predicted pK_{aH1} value of compound **6.4** was not used to determine the acceptable pK_{aH1} range. The upper limit of the pK_{aH1} range was not determined because amines typically do not have pK_{aH} values much higher than 11 in water. Therefore, diamines with p$K_{aH1} \geq$ 9.5 are sufficiently basic to act as SHSs (unless pK_{aH2} is low, discussed later), but diamines with p$K_{aH1} \leq 9.0$ are not.

In addition to log K_{ow} and pK_{aH1}, the effect of pK_{aH2} on SHS behaviour was characterized. In a similar manner to pK_{aH1}, if the monoprotonated diamine is not sufficiently basic, it will not be protonated to the extent required to become miscible with water. In order to compare the effects of pK_{aH2} on switchable hydrophilicity behaviour, three diamines with different alkyl chain lengths between the two nitrogen atoms were compared: compounds **6.1**, **6.2c**, and **6.3b**. The degree of separation between the two protonatable sites has been shown to affect the basicity of the second protonatable site.[6] If the sites are too close, pK_{aH2} will be too low, the second site may not be sufficiently protonated by CO_2, and the compound may not become water-miscible under a CO_2 atmosphere. Compounds **6.1**, **6.2c**, and **6.3b** all fit the log K_{ow} and pK_{aH1} requirements discussed above and should all display switchable hydrophilicity if pK_{aH2} is not a factor. However, compound **6.1** does not act as a SHS. It has a shorter chain length (3 carbons) connecting the nitrogen atoms than compounds **6.2c** and **6.3b** (4 and 6 carbons, respectively) and a lower pK_{aH2} (7.5 compared to 9.3 and 10.2, respectively) as a result. It appears that a diamine must not have a pK_{aH2} as low as 7.5 and therefore must have a minimum of 4 carbon atoms separating the two nitrogen atoms in order to act as a SHS.

These acceptable log K_{ow} and pK_{aH1} ranges, as well as the minimum 4 carbon atom separation requirement, apply to systems that contain a 1:1 (v:v) mix of water:diamine and are switched between ~0 atm and ~1 atm of CO_2. Diamines that are too hydrophobic (log $K_{ow} > 5$) or

not basic enough (pK_{aH1} < ~9.5) to act as SHSs under these conditions and diamines that have 3 or fewer carbons separating the two amine groups may act as SHSs if more water or a higher pressure of CO_2 is used, as was demonstrated for monoamines in Chapter 3.

The requirements for diamines to act as SHSs are different from those for monoamines. The data presented in Chapter 2 revealed that a monoamine must have a log K_{ow} value between 1.2 and 2.5 to act as a SHS (using 1 atm of pressure and equal volumes of amine and water). It appears that diamines must be more hydrophobic than monoamines in order to act as SHSs. Furthermore, Wilson and Stewart proposed that tertiary amines containing only hydrocarbon functionalities (in addition to the amine group) should have a carbon:nitrogen ratio between 6:1 and 12:1 in order for it to display switchable miscibility with water.[9] Based on the results of the hydrocarbon-functionalized diamines used in this study, the appropriate carbon:nitrogen ratio for diamines is between 6:1 (compound **6.2b**) and 8:1 (compound **6.2c**). Compound **6.3c** had a carbon:nitrogen ratio of 9:1 and did not display the desired behaviour. Therefore, diamines require different properties than monoamines in order to act as SHSs.

Another difference between monoamine and diamine SHSs is in the time required to switch the two between their hydrophilic and hydrophobic states. First, diamine SHSs generally required more time than monoamines to switch from their hydrophobic state to their hydrophilic states (Fig 6.2a). The times required to switch compound **6.3b** and a monoamine SHS, *N*,*N*-dimethylcyclohexylamine (DMCA), were compared. When CO_2 was passed through mixtures of each compound with water with the same volumes of SHS and water (2 mL each) and the same CO_2 flow rate (10 mL/min), it took DMCA 80 min to become monophasic with water but 260 min for diamine **6.3b** to become monophasic with water. Therefore, DMCA merged with water faster than diamine **6.3b**.

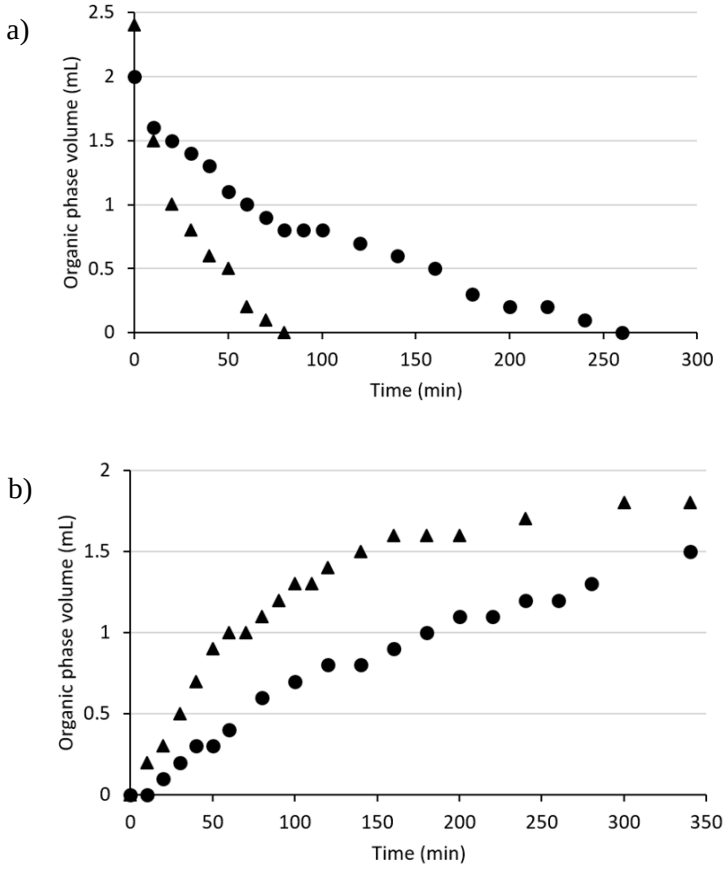

Fig. 6.2 The volume of the organic phase in systems containing 2 mL water and 2 mL SHS (triangles = DMCA, circles = compound **6.3b**) over time while bubbling gasses through the mixture (a = CO_2 at room temperature, b = Ar at 60 °C).

DMCA also separated from water faster than diamine **6.3b** at 60 °C with argon bubbled through the mixture at 15 mL/min (Fig. 6.2b). Although both SHSs began to separate from water within 20 min under these conditions, the organic phase increased in volume faster in the case of DMCA than it did for compound **6.3b**. After heating and argon-bubbling continued overnight, the volume of the organic phase containing compound **6.3b** was restored to 2 mL the next day while the aqueous phase had decreased to 1.4 mL, indicating the loss of water from the system. When the experiment continued overnight for the system containing DMCA, the volume of the organic phase was only 1.7 mL, as opposed to the 2.4 mL that would be expected (more than 2 mL because water

is soluble in DMCA up to 21.4 wt% at 20 °C),[10] and the volume of the aqueous phase was 1.6 mL. It is likely that both DMCA and water are lost from this system overnight, but this could also indicate a less complete separation of DMCA from water than that of diamine **6.3b** from water. Despite the uncertainty over the completeness of the separation of DMCA from water, the diamine SHS separated more slowly than the monoamine SHS.

Diamine SHSs tend to form foams more readily than monoamines when gasses are bubbled through their mixtures with water. This tendency to foam is likely caused by the surfactant behaviour of the mono-protonated diamine that forms as a reaction intermediate during the protonation process. These mono-protonated species have hydrophilic head groups, composed of the protonated nitrogen, and hydrophobic tails, composed of the alkylene linker and the substituents on the unprotonated nitrogen. During the experiments described above, mixtures of diamine SHS and water created substantially more foam than mixtures of monoamine SHS and water.

The increased tendency of diamines to form foams presents a greater difficulty when working with diamine SHSs than with monoamine SHSs. In the context of switching speeds, the conditions described above were used to limit foaming for diamine **6.3b** to simplify quantification of volumes and to prevent the loss of material that would have resulted from the foam expanding beyond the capacity of the vessel. Differences in gas flow rates can affect the switching speeds of SHSs. For example, DMCA has been reported to become monophasic with an equal volume of water within 16 min using a CO_2 flow rate of 100 mL/min.[11] Therefore, both diamines and monoamines can be switched faster than is represented in Fig. 6.2 if a faster CO_2 flow rate is used, but the increased flow rate would also cause the diamine mixture to foam considerably. In applications using diamine SHSs, foam formation must be accounted for even when monoamine SHSs would not foam significantly.

6.2.2 Phase behaviour of diamine SHSs

In order to determine whether diamine SHSs can be more completely removed from hydrophobic phases than monoamine SHSs, log *D* values (log of the distribution coefficient) were measured to determine how a SHS would distribute between water (aqueous phase) and 1-octanol (representing a typical organic phase) at different pH values (Fig. 6.3). A low distribution coefficient suggests that the species tends to partition more into the aqueous phase while a high distribution coefficient suggests that the species tends to partition more into the organic phase. An ideal SHS would have a high distribution coefficient in its neutral form at high pH conditions and a low distribution coefficient in its charged form at low pH conditions. Overall, a SHS with good switchable behaviour would have a large change in log *D* (Δlog *D*) between protonated and unprotonated forms. This behaviour would improve the separation of the SHS from a dissolved product when CO_2 and water are added to the mixture, such as in the process outlined in Section 1.4. By decreasing the amount of SHS in the product-rich phase immediately prior to the filtration/decantation step, a more pure product is obtained after the mechanical separation is performed, post-separation purification steps are minimized, and SHS loses are reduced. A comparison of log *D* values between monoamines and diamines would support or refute the hypothesis that diamine SHSs can be separated more completely from organic phases than monoamine SHSs.

The distribution coefficients, *D*, of compounds **6.2c** and **6.3b** at different pH levels have been measured and compared to the distribution coefficients for DMCA measured in Chapter 3. In their fully protonated forms, compounds **6.2c** and **6.3b** exhibit log *D* values of -4.2 and -2.9 respectively, compared to -0.7 for DMCA. These results suggest that diamine SHSs partition more favourably into the aqueous phase in their fully protonated forms than monoamine SHSs, causing them to separate more completely from a hydrophobic material when CO_2 is introduced. This property would result in a more pure isolated hydrophobic product as well as more complete

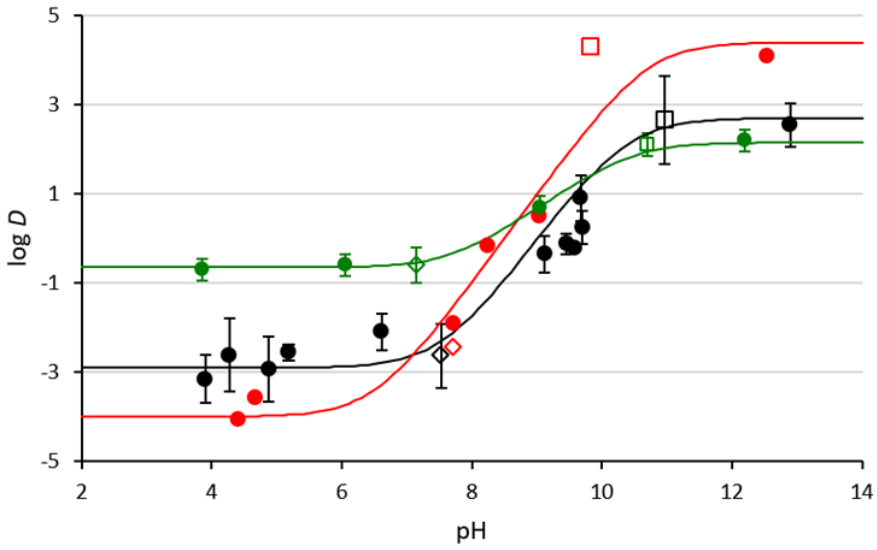

Fig. 6.3 1-Octanol/water distribution coefficients of compounds **6.3b** (black), **6.2c** (red) and DMCA (green) at room temperature at varying aqueous pH values. pH values were either not adjusted (empty squares), adjusted with CO_2 (empty diamonds), or adjusted with glycolic acid or NaOH (filled in circles). Values for compound **6.3b** were measured in triplicate and the error bars are shown (maximum standard deviation: ±1.0). The lines represent the log *D* curve estimated from the data (see SI for details). The data and estimated curve for DMCA (green) were taken from Chapter 3.

---

reusability of the SHS since less SHS would be lost by association with the isolated hydrophobic product. In their neutral forms, compounds **6.2c** and **6.3b** exhibit log *D* values of 4.1 and 2.6 respectively, compared to 2.1 for DMCA, which means that in basic conditions, diamines partition more favourably into the organic phase than monoamines. Overall, compounds **6.2c** and **6.3b** have much larger Δlog *D* between carbonated and uncarbonated solutions (Δlog *D* = 5.9 and 8.2, respectively) than DMCA (Δlog *D* = 2.8). The fact that Δlog *D* is dramatically larger for diamine SHSs could create significant process advantages.

Although the log *D* curves of diamines suggests that they have more favourable partitioning than monoamines, more evidence is needed to confirm the anticipated practical advantages of diamine SHSs. First, log *D* may be dependent on concentration and differences between

monoamine and diamine might be minimized at higher concentrations than those represented in Fig 6.3. Second, the log *D* curves show that diamines partition more favourably into the aqueous phase only if the pH of the aqueous phase is sufficiently low. More experiments under conditions similar to those used in a SHS-based separation process are required to demonstrate the practical advantages of diamine SHSs.

The liquid-liquid equilibria (LLE) of mixtures of SHS, toluene, and carbonated water were prepared in order to compare the removal of monoamine and diamine SHSs from a hydrophobic liquid more directly (Table 6.2). Toluene acted as a representative hydrophobic liquid product that was to be isolated. To determine the extent to which it was contaminated with SHS, the mass ratio of SHS/toluene in the organic phase was determined. Data were collected for mixtures using diamine **6.3b** as the SHS and these results were compared to values reported in Chapter 5 for mixtures of similar compositions using DMCA as the SHS. The data confirm that contamination of the hydrophobic product (toluene) is lower with the diamine than the monoamine, but only when the total amount of SHS is small. In mixtures with higher fractions of SHS, diamine **6.3b** and DMCA contaminate the toluene to similar extents because the higher pH in the presence of the diamine prevents the log *D* of the diamine from being sufficiently low; in such situations a higher CO_2 pressure would be useful. In mixtures with lower fractions of SHS, however, the toluene is contaminated with approx. 0.1 wt% diamine **6.3b** compared to approx. 4 wt% DMCA, representing an approx. 40-fold decrease in contamination when using diamine **6.3b**.

The effects of pH on the effective separation of the diamine SHS from toluene is in agreement with the log D data reported in Fig 6.3. In the LLE experiments, diamine **6.3b** showed no advantage over DMCA in mixtures with aqueous pH values near 9.0, but it did show an advantage over DMCA in the mixture with an aqueous pH value near 8.0. When considering the log *D* values of DMCA and diamine **6.3b** at these pH values, it is apparent that the difference in log *D* between the two is small at pH values near 9.0. At pH values near 8.0, however, the difference

Table 6.2 Comparison of the contamination of toluene with monoamine (DMCA) and diamine (Compound **6.3b**) SHS in systems with different compositions of SHS, water, and toluene at 30.0 °C.

SHS:Water:Toluene	SHS/Toluene (g/g)		Aqueous pH	
(mass percent)	Compound **6.3b**	DMCA[a]	Compound **6.3b**	DMCA[a]
42:31:27	0.66±0.006	0.69±0.004	9.05±0.05	8.75±0.05
27:39:34	0.22±0.003	0.16±0.003	8.99±0.05	8.51±0.05
13:47:40	0.0015±0.001	0.037±0.002	8.05±0.05	8.11±0.05

[a]Data from Chapter 5.

in log *D* is substantial, almost 2 log-scale units. This comparison of the log *D* curves suggests that no significant advantages are obtained from using diamine SHSs if the separation process occurs at pH values near 9.0, but that a large advantage is gained from using diamine SHSs if the process occurs at pH values near 8.0. In order to make use of the potential separation advantages of diamines, the separation must be carried out at sufficiently low pH values to minimize the log *D* of the diamine. These inferences from the log *D* curves match the LLE data from Table 6.2. The pH of the aqueous phase during a SHS-based extraction is governed by parameters such as the pK_{aH} values of the SHS, the SHS concentration, and the pressure of CO_2. These variables should be carefully considered when using a diamine SHS to achieve lower log *D* values to ensure that the pH is low enough. Fortunately, either multistage or countercurrent liquid-liquid extraction would likely ensure that the pH is sufficiently low at the final decantation.

As final evidence of the improved separation of diamines from hydrophobic materials, diamine **6.3b** and DMCA were compared in their separation from soybean oil, mimicking the separation step in a previously tested application of SHSs for extracting and isolating lipids from soybeans.[12] Mixtures of SHS, soybean oil, and water were prepared in a 1:1:2 volume ratio and

CO_2 was passed through the solutions until the pH of the aqueous phase was ~8.0. Afterwards, the amount of SHS remaining in the organic phase was measured. DMCA was present in the soybean oil at concentrations of 7.5 ± 2.8 g/L, while diamine **6.3b** could not be detected in the oil (limit of detection: 1.2 g/L). These results demonstrate that a diamine SHS can be more completely removed from a hydrophobic product than a monoamine SHS without requiring the use of additional water.

Given that diamine SHSs have higher log K_{ow} values than monoamine SHSs, they may also have lower solubility in water than monoamine SHSs. If this is the case, then diamine SHSs could be separated from water more completely than monoamine SHSs, allowing them to be reused more efficiently for a given application since less SHS would be lost in the aqueous phase. This increased reusability would be in addition to the increased reusability obtained by losing less SHS to the hydrophobic product. The solubility of compound **6.3b** in water was measured and found to be 2.7±0.6 g L^{-1} at 20 °C. By comparison, the reported aqueous solubilities of four monoamine SHSs range from 1.9 g/L to 44 g/L.[11] Although compound **6.3b** is less soluble in water than some monoamine SHSs, it is not less soluble than all of them. A more hydrophobic diamine SHSs such as compound **6.2c** might be less soluble in water than all monoamine SHSs, but given the already low solubility of some monoamine SHSs, the benefits would be minimal. Instead, the recovery of SHS from the aqueous phase is more likely governed by how completely CO_2 is removed from the system.

6.2.3 Mathematical comparison of the percent of protonation of monoamine and diamine SHSs

It is important to develop mathematical models describing the behaviour of diamine switchable materials, as has been done for monoamine switchable materials in Chapter 3 and more broadly in a literature model.[13] These models provide insight into how changes in molecular properties (specifically partition coefficients and pK_{aH} values) affect the performance of a

switchable compound. These models also aid in the selection of an appropriate molecule for a given application.

A first approximation of the difference between monoamines and diamines can be made by comparing the percent of unprotonated species in carbonated water. Unprotonated species are hydrophobic and will partition into the organic phase, which is undesirable in processes where carbonated water is used to extract SHS from the organic phase. Therefore, the amount of unprotonated species is a first indicator of performance. In an aqueous solution with pH = 8, a monoamine with pK_{aH} = 10 will be 99.0% protonated and 1.0% unprotonated. In a similar environment (pH = 8), a diamine with pK_{aH1} = 10 and pK_{aH2} = 9.4 will only have 98.05% of its basic sites protonated, but the ratio of diprotonated/monoprotonated/unprotonated species is 96.13/3.83/0.04, so only 0.04% of the diamine is expected to be unprotonated at pH = 8 (see Appendix 1 for the equations used in these calculations). Therefore, diamines are expected to have a much lower percent of unprotonated species than monoamines in carbonated water at the same pH.

A more detailed calculation of the fraction of protonation of diamine SHSs and monoamine SHSs can be made using a more complicated systems of equations. This series of equations is similar to the model described in Section 3.4. The switch between the hydrophilic and hydrophobic states of a SHS is caused by protonation of the basic sites. Therefore, an effective switchable material will have a small fraction of protonated sites in the absence of CO_2 (e.g. < 0.05) and a large fraction of protonated sites in the presence of CO_2 (e.g. > 0.95). For diamines, this fraction includes both sites on the molecule. Unlike the corresponding model from Chapter 3 used to describe monoamines, which is simple enough to describe in a single equation, the fraction of protonated sites for diamine SHSs is best described using a series of equations. These equations and their derivations are described in the supplementary information. Although a single equation could be derived, it would be large and unwieldy.

Fig 6.4 compares monoamines and diamines in terms of fraction of protonated sites (in the entire system) for a system containing water and 1-octanol at different amine or diamine concentrations. The term $[B]_0$ is the amount of monoamine or diamine added to the system divided by the volume of water in the system. The fraction of protonated sites is a function of concentration, the log K_{ow} value of the neutral amine, the pK_{aH1} values of the amines, the octanol:water volume ratio, and the partial pressure of CO_2. The log K_{ow} values of the monoprotonated species (log K_{ow}') and diprotonated species (log K_{ow}'') are assumed to be related to the log K_{ow} of the neutral species by a constant, $\Delta\log K_{ow}$, which is the difference between log K_{ow} and log K_{ow}' as well as the difference between log K_{ow}' and log K_{ow}''. The $\Delta\log K_{ow}$ value used for monoamines was 2.8 as reported in Chapter 3. The $\Delta\log K_{ow}$ value for diamines was 3.0, based on the log D curves shown in Fig 6.3. Furthermore, the pK_{aH2} value of a diamine was assumed to be related to its pK_{aH1} value by a constant, ΔpK_{aH}, which is the difference between pK_{aH1} and pK_{aH2}. The ΔpK_{aH} value was 0.8 based on the data shown in Table 6.1, though some diamines have larger ΔpK_{aH} values. In order to simplify the comparison, only one log K_{ow} value each was used for the monoamine and diamine. The chosen values represent the proposed lowest log K_{ow} value necessary for a compound to act as a SHS (1.2 for monoamines, 2.5 for diamines). The pK_{aH} of the monoamine and the pK_{aH1} of the diamine were both 10.0. Furthermore, only an octanol:water volume ratio of 0.5 and CO_2 pressures of 0 and 0.1 MPa were considered.

The graph details two environments: one where the SHS should be in its neutral, hydrophobic state (dotted lines), and one where it should be in its charged, hydrophilic state (solid lines). When CO_2 is absent from the system (dotted lines, CO_2 pressure = 0 MPa), the SHS should have a low fraction of protonation. The dotted lines represent the pK_{aH} (or pK_{aH1} for diamines) values at which the SHS will have 5% of its basic sites protonated. Any SHS with smaller pK_{aH} (i.e. below the dotted line) values will be less than 5% protonated and fit the description of an ideal switchable compound in the absence of CO_2. Any SHS with larger pK_{aH} values (above the dotted

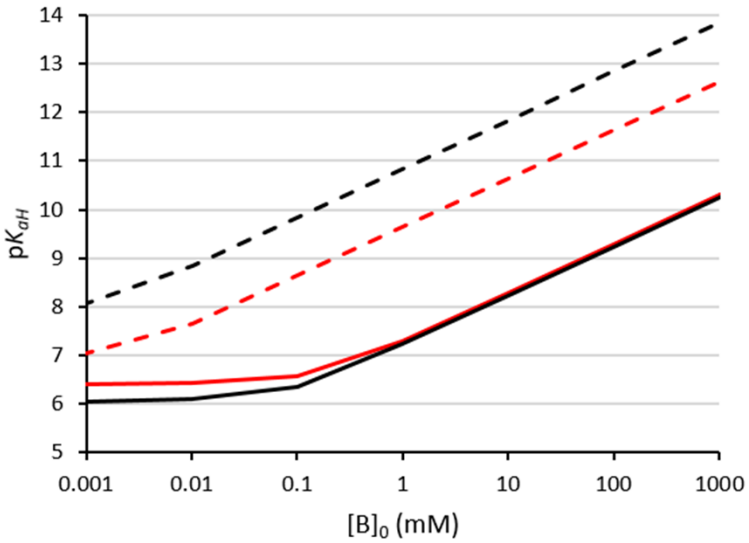

Fig. 6.4 The pK_{aH} (of a monoamine, log K_{ow} = 1.2, red lines) or pK_{aH1} (of a diamine, log K_{ow} = 2.0 black lines) required to have 5% (in the absence of CO_2, dashed lines) or 95% (in the presence of 0.1 MPa CO_2, solid lines) of its basic sites protonated in a 1:2 (v:v) mixture of 1-octanol and water as a function of amine concentration ($[B]_0$ = millimoles of amine per litre of water). Amines with pK_{aH} or pK_{aH1} values between the solid and dashed lines will be less than 5% protonated in the absence of CO_2 and more than 95% protonated under 0.1 MPa CO_2, indicating that they can be almost completely switched between their protonated and unprotonated states by the addition or removal of CO_2.

---

line) will be more than 5% protonated and fail to meet this criterion. In the presence of CO_2 (solid lines, CO_2 pressure = 0.1 MPa), the SHS should have a large fraction of protonation. The solid line represents the pK_{aH} or pK_{aH1} values at which the SHS will have 95% of its basic sites protonated. Any SHS with a larger pK_{aH} value (above the solid line) will be more than 95% protonated and fit the description of an ideal switchable compound in the presence of CO_2. Any SHS with a smaller pK_{aH} value (below the solid line) will be less than 95% protonated and fail to meet this criterion.

The area between the respective solid and dotted lines represents the range of pK_{aH} values that will result in ideal switching behaviour at a given concentration of SHS. This area is larger for the diamine than for the monoamine, meaning that a wider range of pK_{aH} values is possible for diamine SHSs than for monoamine SHSs. In practice, this difference is likely not significant

because amines typically do not have pK_{aH} values greater than 11, so the difference between the upper pK_{aH} limits for monoamines and diamines (dotted lines) is not of practical significance, particularly at the concentrations typical when SHSs are used ($[B]_0 > 1$ M). Apart from the likely unimportant difference of the upper pK_{aH} limits, monoamine and diamine SHSs have similar pK_{aH} ranges for ideal switching behaviour.

The equations used to generate the graph shown in Fig. 6.4 use many approximations and assumptions and should be used as guidelines only. Values such as K_{ow} and pK_{aH} are measured at low concentrations and may not be accurate for solutions with high concentrations of SHSs. The partition coefficients of SHS-bicarbonate salts were estimated based on the results shown in Fig. 6.3 and the differences between the partition coefficients of neutral, monoprotonated, and diprotonated were assumed to be the same for all monoamine SHSs and for all diamine SHSs. Despite these limitations, the predictions are useful in determining general trends in the behaviour of monoamine and diamine SHSs.

6.2.4 Virtual screening for safe diamine SHSs

In order to increase the benefits of diamine SHSs, it is important to make them as safe for humans and the environment as possible. SHSs are of interest because they can be separated from solutes without distillation, so solvent volatility can be minimized without impacting the energy requirements for separation. However, a lack of volatility is not sufficient to make a solvent "green". In the context of green chemistry, a solvent should be as safe as possible for humans and the environment in addition to performing its task well. Diamine SHSs have better performance than monoamine SHSs, but they may have environmental, health, or safety hazards that make them less desirable to use. Many of the diamines used in the study were selected for their log K_{ow} and pK_{aH} values rather than for their environmental impacts. Identifying safe diamine SHSs would increase the value of this class of solvent in the context of green chemistry.

One strategy for designing safe compounds is a virtual screening approach, such as the one described in Chapter 4. This approach uses a virtual combinatorial library to create many molecular structures and then uses QSARs to predict the properties of those structures. Based on the predicted properties, the structures can then be screened to identify those structures that can both perform a task well and have few associated hazards. As described in Chapter 4, this strategy has been used to identify less-hazardous monoamine SHSs. By adjusting the property requirements to match those for diamine SHSs, the virtual screening process was modified for use in identifying diamine SHSs that are likely to be less hazardous than the experimentally identified diamines (see Appendix 2.3 for details). Compound **6.4** was identified as a promising diamine SHS using this strategy.

Table 6.3 shows the predicted values for the environmental, human health, and safety hazards of some diamine SHSs used in this study and some reported monoamine SHSs for comparison. Values were predicted using the U.S. Environmental Protection Agency's Toxicity Estimation Software Tool v4.1 (TEST).[14] The limitations of using predicted properties for screening were discussed in Chapter 4. Despite the inaccuracies of some predictions made by the software, the accuracy is still sufficient to distinguish highly toxic compounds from those that are not particularly toxic. Furthermore, acceptability functions were used as a means of minimizing the number of false positives and false negatives in the screening process. The predicted toxicity values and vapour pressures can be used as indicators of which SHSs are safer relative to other SHSs if the values are different by an order of magnitude.

The screening process is useful for identifying molecules that are likely to perform as desired, but it does not guarantee success. The predicted values of each property may differ significantly from experimental values. Furthermore, the process does not screen for all hazards. Carcinogenicity, mutagenicity, and chronic toxicity are some examples of hazards that are not considered in the screening process. Finally, the effects of synthesizing the compounds on the environment and on human health and safety are not considered. Nevertheless, the screening

process is useful for identifying molecules with a higher probability of being a SHS with few associated hazards.

The usefulness of the virtual screening process is demonstrated by a comparison of the predicted properties of several diamine SHSs, shown in Table 6.3. Compound **6.4**, which was identified from the virtual screening process, is predicted to be less hazardous than diamine SHSs identified without the assistance of virtual screening for every hazard being considered except for daphnia magna LC_{50} (48h), where it is comparable to those diamine SHSs. In particular, it is predicted to be an order of magnitude less hazardous in the case of fathead minnow LC_{50} (96h) and rat LD_{50} (oral). Taking the predictions at face value and using the definitions described by the Globally Harmonized System (GHS) of classification, compound **6.4** would be unclassified with

Table 6.3 Toxicology parameters for diamine and monoamine (DMCA, triethylamine, and **4.2**) SHSs calculated from TEST.

Compound	Fathead minnow LC_{50} (mg/L)	Daphnia magna LC_{50} (mg/L)	Oral rat LD_{50} (mg/kg)	Boiling Point (°C)	Vapour pressure (mTorr)	Flash point (°C)	Bioaccumulation Factor
6.2b	64	4.0	400	226	15	79	17
6.2c	3.3	2.5	630	270	3	117	86
6.3b	42	4.9	340	249	40	96	29
6.4	150	4.0	3000	318	$6.8_{E^{-2}}$	145	55
DMCA	100	38	320	159	3100	38	9.6
Triethylamine	470	140	1300	85	62000	5	4.1
4.2	97	11	1600	254	1	103	32

respect to acute fathead minnow toxicity (the highest classified LC_{50} is 100 mg/L as a category 3

acute toxic substance).[15] With regard to oral toxicity, it would be a category 5 acute toxic substance (LD_{50} between 2000 and 5000 mg/kg, compounds which "may present a danger to vulnerable populations").[15] In comparison, the other diamine SHSs would be classified as category 2 or 3 toxic substances for acute fathead minnow toxicity ($LC_{50} \leq 10$ or 100 mg/L, respectively) and as category 4 toxic substances for oral toxicity (LD_{50} between 300 and 200 mg/kg).[15]

Table 6.3 can also be used to compare diamine SHSs to monoamine SHSs. Diamine SHSs are predicted to be more hazardous than monoamine SHSs with regard to daphnia magna LC_{50} (48h), but less hazardous with regard to flammability and volatility. The two types of SHSs are comparable with regard to rat LD_{50} (oral) and fathead minnow LC_{50} (96h). Furthermore, in all categories except daphnia magna LC_{50} (48h), compound **6.4** is comparable to compound **4.2**, a monoamine SHS identified in Chapter 4 using the same virtual screening approach.

None of the diamine SHSs shown in Table 6.3 have desirable predicted LC_{50} values for daphnia magna toxicity, but this does not mean that there are no diamine SHSs that are predicted to be safe with respect to this environmental hazard. The virtual screening process identified several diamines which are predicted to be quite acceptable in terms of toxicity toward daphnia magna (LC_{50} (48h) > 100 mg/L, according to GHS classifications).[15] One such example is the structure shown in Scheme 6.2, with a predicted daphnia magna LC_{50} of 230 mg/L. Although this compound

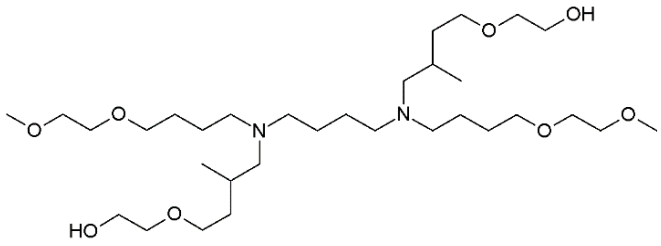

Scheme 6.2 A diamine that was predicted to act as a SHS and pose little risk to daphnia magna.

has other expected hazards, it suggests that diamine SHSs are not categorically toxic to daphnia magna and it is possible to design such molecules to avoid this hazard as well.

Another environmental concern that must be considered is bioaccumulation. According to the GHS, a bioconcentration factor (BCF) less than 500 indicates low levels of bioaccumulation. Additionally, log K_{ow} can be used as a surrogate measure of bioaccumulation with log $K_{ow} < 4$ indicating low levels of bioaccumulation. Given that the log K_{ow} range required for diamines to act as SHSs is approximately 2.5-5, some diamine SHSs might have the potential to bioaccumulate. However, it has been shown that the BCF of ionizable compounds depend on the pH of the environment, with bases having lower BCFs at lower pH,[16] and that log D may be a better surrogate for bioaccumulation than log K_{ow}.[17] Given the pK_{aH1} and pK_{aH2} values of the diamine SHSs, they are likely to have low log D values in environments with pH < 9 and therefore have low risk of bioaccumulation. This hypothesis is supported by the predictions for diamines made by TEST, which all have predicted bioaccumulation factors less than 100, despite compound **6.2c** having a predicted log K_{ow} of 4.7.

6.3 Conclusions

The first CO_2-switchable diamine SHSs were identified and these SHSs were compared to monoamine SHSs. Diamines require larger log K_{ow} values to be SHSs than monoamines. The carbon:nitrogen atom ratios required for diamines with only alkyl functionalities to act as SHSs are also different than those for trialkyl monoamine SHSs. Diamine SHSs partitioned more favourably into water than monoamine SHSs if the pH of the aqueous phase is sufficiently low (pH ~8). This enhanced partitioning was shown to decrease the contamination of toluene and soybean oil (as representative hydrophobic products) at the end of a SHS-based separation process. The enhanced partitioning also improves the recyclability of the SHS because less SHS will be lost as contaminant in the organic product. These observations are supported by mathematical models, which indicate

that diamines will be more completely protonated and have lower log *D* values than monoamines in the presence of CO_2.

Two results disfavour the use of diamines. First, the time required for diamine SHSs to switch between their hydrophobic and hydrophilic states is longer than for monoamine SHSs. Second, diamine SHSs tend to produce foam during the switching process, a phenomenon that does not occur significantly when switching monoamine SHSs.

The safety of diamines and monoamines were also compared using predicted values. In general, some but not all diamine SHSs are predicted to have greater ecotoxicity to daphnia magna but higher flash points than monoamine SHSs. A virtual screening approach can be used to identify diamine SHSs that are predicted to have reduced risks.

Of the diamines tested, the most promising candidate for further research is compound **6.3b**. This SHS can be prepared with the least difficulty, making it much more accessible to researchers than the other diamine SHSs identified in this chapter. Although it is not predicted to be as safe for humans and the environment as compound **6.4**, the relatively involved preparation of compound **6.4** makes it less desirable for future studies. Even if it were readily obtainable, the financial costs of using compound **6.4** would likely render any process using it too expensive to be commercially viable.

6.4 Experimental Methods

All chemicals were used as received. Compounds **6.2a** and **6.3a** were purchased from TCI and Sigma-Aldrich, respectively. Glycolic acid, potassium carbonate, and *N*,*N*-dimethylcyclohexylamine were purchased from Sigma-Aldrich. CO_2 (4.8, supercritical fluid chromatography grade) and argon (4.8) were purchased from Praxair. The equations used to create Figs 6.3, 6.4, and 6.5 and information pertaining to the virtual screening process are also described in Appendix 2.

6.4.1 Testing diamines for switchable hydrophilicity

To test if a diamine displays switchable hydrophilicity, a mixture containing an equal volume of water and the diamine was prepared at room temperature, about 20 °C. If the resulting mixture was monophasic, the diamine was not considered a SHS. If the mixture was biphasic, CO_2 was bubbled into the mixture using a gas dispersion tube (Ace Glass, 5 mm i.d., 25-50 μm porosity) until it became monophasic or for up to 6 h. If the mixture remained biphasic, the diamine was not considered a SHS. If the mixture became monophasic, CO_2 was removed by heating the mixture to 60 °C and then sparging it with argon using a gas dispersion tube (Ace Glass, 5 mm i.d., 25-50 μm porosity) until the mixture became biphasic again or for up to 6 h. If the mixture remained monophasic, the diamine was not considered to be a SHS. If the mixture became biphasic again, the diamine was considered to be a SHS.

6.4.2 Monitoring the switching of SHSs over time

A mixture of 2 mL water and 2 mL SHS (either DMCA or compound **6.3b**) was prepared in a 10 mL graduated cylinder covered with a septum. The mixture was agitated briefly and then the volume of the organic phase was recorded. A needle was inserted into the septum as a vent and another needle was inserted into the septum and lowered into the SHS/water mixture. CO_2 was bubbled through the solution via the second needle at a rate of 10 mL/min, measured using an Intelligent Digital Flowmeter (Varian). The needle used to bubble CO_2 was removed from the mixture briefly at intervals to record the volume of the organic phase. The needle was inserted back into the mixture after the volume of the organic phase was recorded. The CO_2 bubbling was allowed to continue until no organic phase was visible.

After the organic phase disappeared, the CO_2 being bubbled through the solution was replaced with Ar (flow rate = 15 mL/min) and the graduated cylinder was placed in an oil bath heated to 60 °C. The needle used to bubble Ar was removed from the mixture and the graduated

cylinder was raised out of the oil bath briefly at intervals to record the volume of the organic phase. The needle was inserted back into the mixture and the graduated cylinder was lowered back into the oil bath after the volume of the organic phase was recorded. The volume of the organic phase was monitored for 340 min, then Ar bubbling at 60 °C was continued overnight. The Ar bubbling and heating were stopped the next day and the final volume of the organic phase was recorded.

6.4.3 Measuring log *D* and aqueous solubility

For log *D* measurements, diamine (**6.2c** or **6.3b**, 0.40 mL) was added to a mixture of 4.00 mL water and 4.00 mL 1-octanol into a vial at room temperature. Glycolic acid, CO_2, or NaOH was added to the mixture to adjust the pH of the solution. For samples containing glycolic acid, the acid was added in specific molar equivalences relative to the diamine (compound **6.3b**: 0.25, 0.50, 0.75, 1.00, 1.25, 1.50, 1.75, 2.00, 2.50, and 3.00 equivalents; compound **6.2c**: 0.50, 1.00, 1.50, 2.00, and 3.00 equivalents). For samples containing CO_2, CO_2 was bubbled through the mixture at a rate of 50 mL min^{-1} for 1 h using a gas dispersion tube (Ace Glass, 5 mm i.d., 25-50 μm porosity). For samples containing NaOH, 1.00 molar equivalent of NaOH relative to the diamine was added to the mixture. The mixture was stirred overnight and allowed to settle for 2 h. The pH of the aqueous phase was tested and both the aqueous layer and the organic layer were sampled separately and diluted with methanol as required for analysis (e.g. at high pH, the organic phase required substantial dilution, but the aqueous phase required very little). Toluene (10 μL) was added as an internal standard. The concentration of diamine in each solution was measured using GC-FID and used to calculate log *D* for the diamine at the measured pH. Samples for compound **6.3b** were made in triplicate and averaged.

For aqueous solubility measurements, 0.200 mL of compound **6.3b** was added to 10.0 mL of water. The mixture was stirred vigorously for 2 h, then allowed to equilibrate overnight at room temperature (20 °C). A 1.50 mL portion of aqueous phase was sampled and weighed. To this sample was added a weighed 10 μL portion of acetonitrile as an internal standard. The concentration of compound **6.3b** was determined using GC-FID. This procedure was performed in triplicate and the average value was reported as the solubility of compound **6.3b** in water.

6.4.4 Measuring the amount of SHS contaminant in toluene after a SHS-based separation

Mixtures containing different mass fractions of compound **6.3b**, water, and toluene were prepared to match the proportions of some of the mixtures studied in Chapter 5 that used DMCA instead of compound **6.3b**. CO_2 was bubbled through the mixtures for 8 h using a needle, then the mixtures were heated to 30.0 °C in a constant temperature bath for 16 h. After this time, the organic phase of each mixture was sampled and the amount of toluene and SHS in that phase was determined by GC-FID. The pH of the aqueous phase of each sample was measured using an Orion 4-Star benchtop pH-conductivity meter (Thermo Scientific). The experiments for each sample with different mass fractions were performed in triplicate and the averaged results were reported as the mass ratio of SHS:toluene in the organic phase of each mixture.

6.4.5 Measuring the amount of SHS contaminant in soybean oil after a SHS-based separation

Mixtures containing 5.00 mL SHS (either diamine **6.3b** or DMCA), 5.00 mL soybean oil, and 10.0 mL deionized water were prepared. CO_2 was bubbled through the mixtures until the pH of the aqueous phase was ~8.0 as measured by an Orion 4-Star benchtop pH-conductivity meter (Thermo Scientific). Afterward, 2.00 mL of the organic phase was sampled and extracted with 6.00

mL of 10% aqueous glycolic acid. 1.00 mL of the aqueous phase was diluted to 5.00 mL using methanol and the amount of SHS in the aqueous phase was determined by GC-FID. Experiments using each SHS were performed in triplicate and averaged results were reported as the amount of SHS remaining in the soybean oil.

6.4.6 Measuring pK_{aH1} and pK_{aH2}

The ionization constants of compounds **6.6a** and **6.7a** at room temperature (20 °C) were determined using a procedure analogous to that described by Speakman for diprotic acids.[18] A known amount of diamine was dissolved in water and the solution was titrated with a 0.1 M solution of HCl standardized by titrating potassium carbonate. The pH of the solution was measured after every addition of HCl using an Orion 4-Star benchtop pH-conductivity meter (Thermo Scientific). The data were interpreted using the Fortran code described by Albert and Serjeant to determine the pK_a values of diprotic acids, adapted for analysis of dibasic compounds and translated to operate in MATLAB.[19] The MATLAB code and its use are described in detail in Appendix 4. The pK_{aH} values for compounds **6.6b** and **6.7b** could not be accurately measured by this method due to their limited solubility in water. Their values were assumed to be equivalent to those of compounds **6.6a** and **6.7a**, respectively. Compound **6.4** was not sufficiently soluble in water to measure its pK_{aH} values accurately and no suitable similar molecule was identified to measure the values indirectly as was done for compound **6.6b** and **6.7b**. The pK_{aH} values of the remaining diamines were not experimentally determined because their pK_{aH1} values were expected to be greater than those of the ester-containing diamines and, therefore, meet the pK_{aH1} requirement for displaying switchable hydrophilicity. The unmeasured pK_{aH} values were predicted using ACD/Labs Percepta software rather than being determined experimentally.

The accuracy of the predicted values from ACD/Labs Percepta software is discussed in Appendix 2. The software itself reports a standard deviation of ±0.4 for each pK_{aH} value and the

data in Appendix 2 supports this reported standard deviation. Diamines with predicted pK_{aH1} values greater than 10 are expected to have experimental pK_{aH1} values greater than 9.5 and therefore have acceptable basicity to be SHSs.

6.4.7 Synthesis

6.4.7.1 Synthesis and characterization of compounds 6.6a, 6.6b, 6.7a, and 6.7b

The following procedure was adapted from the procedure for conversion of mono-acrylates by Zou and Jiang.[20] A weighed mixture of 10.6 mmol 1,4-butanediol diacrylate and 40 mmol of a primary or secondary amine was stirred overnight at room temperature in a round bottom flask. Afterwards, the product was purified by heating the mixture to 50 °C under vacuum for 4 h to remove volatile compounds. No further purification was performed.

1,4-Butanediol di-(3-(diethylamino)propanoate) (6.6a) Using 4.1 mL diethylamine. Isolated yield: 95%. ^{1}H NMR (499.12 MHz, $CDCl_3$): δ = 1.01 (t, *J*= 7.1 Hz, 12H), 1.71 (broad triplet, 4H), 2.42 (t, *J*= 7.3 Hz, 4H), 2.53 (q, *J*= 7.1 Hz, 8H), 2.79 (t, *J*= 7.3 Hz, 4H), 4.11 (broad triplet, 4H); ^{13}C NMR (125.50 MHz, $CDCl_3$) 11.8, 25.3, 32.3, 46.8, 48.1, 63.8, 172.8; ν_{max} (ATR-FTIR) cm^{-1}: 744, 1172, 1466, 1732 (C=O), 2806, 2968; HRMS (ESI): calculated for $C_{18}H_{37}O_4N_2$ (MH^+): 345.27478, found: 345.27420.

1,4-Butanediol di-(3-(dipropylamino)propanoate) (6.6b) Using 5.5 mL dipropylamine. Isolated yield: 95%. ^{1}H NMR (499.12 MHz, $CDCl_3$) δ = 0.85 (t, 12H, *J*= 7.4), 1.42 (sextet, 8H, *J*= 7.4), 1.71 (broad triplet, 4H), 2.34 (t, 8H, *J*= 7.4), 2.41 (t, 4H, *J*= 7.3), 2.75 (t, 4H, *J*= 7.3), 4.10 (broad triplet, 4H); ^{13}C NMR (125.50 MHz, $CDCl_3$): δ = 11.8, 20.3, 25.3, 32.5, 49.5, 55.9, 63.7, 172.9; ν_{max} (ATR-FTIR) cm^{-1}: 745, 1048, 1188, 1239, 1461, 1735 (C=O), 2805, 2873, 2958; HRMS (EI): calculated for $C_{22}H_{45}O_4N_2$ (MH+): 401.33738, found: 401.33700.

1,4-Butanediol di-(3-(isopropylamino)propanoate) (6.7a) Using 3.5 mL isopropylamine. Isolated yield: 95%. ^{1}H NMR (499.12 MHz, $CDCl_3$): δ = 1.07 (d, *J*= 6.3 Hz, 12H), 1.39 (b, 2H),

1.71 (broad triplet, 4H), 2.49 (t, *J*= 6.6 Hz, 4H), 2.82 (septet, *J*= 6.3 Hz, 2H), 2.89 (t, *J*= 6.6 Hz, 4H), 4.12 (broad triplet, 4H); ^{13}C NMR (125.50 MHz, $CDCl_3$) δ = 22.9, 25.2, 34.9, 42.5, 48.4, 63.8, 172.7; ν_{max} (ATR-FTIR) cm^{-1}: 745, 1170, 1469, 1729 (C=O), 2871, 2961, 3326 (N-H); HRMS (ESI): calculated for $C_{16}H_{33}O_4N_2$ (MH^+): 317.24348, found: 317.24282.

1,4-Butanediol di-(3-(cyclohexylamino)propanoate) (6.7b) Using 4.6 mL cyclohexylamine. Isolated yield: 95%. ^{1}H NMR (499.12 MHz, $CDCl_3$): δ = 1.03 (qt (apparent), 4H), 1.15 (tt, J^1 = 12.3 Hz, J^2 = 6.1 Hz, 2H), 1.23 (qt, J^1 = 12.3 Hz, J^2 = 6.8 Hz, 4H) 1.31 (b, 2H), 1.61 (dt, J^1 = 12.3 Hz, J^2 = 6.8 Hz, 2H) 1.64-1.80 (m, 8H), 1.93 (d, *J*= 12.5 Hz, 4H), 2.42 (tt, J^1 = 10.4 Hz, J^2 = 3.7 Hz, 2H), 2.48 (t, *J*= 6.6 Hz), 2.92 (t, *J*= 6.6 Hz), 4.11 (broad triplet, 4H), ^{13}C NMR (125.50 MHz, $CDCl_3$): δ = 25.0, 25.3, 26.1, 33.6, 35.1, 42.1, 56.5, 63.8, 172.8; ν_{max} (ATR-FTIR) cm^{-1}: 744, 1167, 1449, 1730 (C=O), 2851, 2923, 3326 (N-H); HRMS (ESI): calculated for $C_{22}H_{41}O_4N_2$ (MH^+): 397.30608, found: 397.30527.

6.4.7.2 Synthesis and characterization of compounds 6.2b, 6.2c, and 6.2d

Succinyl chloride was converted to *N,N,N',N'*-tetraalkylsuccinamide following a procedure adapted from Peng *et al.* for conversion of mono-acyl chlorides.[21] A solution containing amine (100 mmol) in 55 mL dichloromethane was stirred at 0 °C. A second solution containing succinyl chloride (20 mmol) in 20 mL dichloromethane was added to the first solution dropwise over the course of 1 h. Afterwards, the mixture was allowed to warm to room temperature with stirring. The mixture was stirred overnight, then a 1 M aqueous solution of $HCl_{(aq)}$ (70 mL) was added and the product was extracted with 3 x 70 mL dichloromethane. The organic layer was dried with $MgSO_4$, filtered, and then concentrated under reduced pressure to yield the crude succinamide intermediate.

The reduction of the succinamide intermediate was performed following a procedure adapted from Knapick et al.[22] A mixture of lithium aluminium hydride (80 mmol) in 25 mL

tetrahydrofuran was prepared under inert conditions in a 2-neck round bottom flask equipped with a reflux condenser. The crude succinamide intermediate was dissolved in 50 mL tetrahydrofuran and slowly added to the lithium aluminium hydride solution. The mixture was refluxed overnight, then cooled to 0 °C in an ice bath. Water was slowly added to the mixture until all of the remaining lithium aluminium hydride had reacted. The mixture was filtered via vacuum filtration and the filtrate was concentrated under reduced pressure. A 50 mL solution of 10% $NaOH_{(aq)}$ was added to the concentrated mixture, after which the product was extracted with 3 x 50 mL diethyl ether. The combined organic phase was dried with $MgSO_4$, filtered, and then concentrated under reduced pressure. The crude product was purified by vacuum distillation.

***N,N,N',N'*-Tetraethyl-1,4-butanediamine (6.2b)** Using diethylamine. Isolated yield: 50%, bp: 63 °C (1 torr). ^{1}H NMR (499.12 MHz, $CDCl_3$): δ = 0.95 (t, 12H, *J*= 7.2 Hz), 1.39 (broad triplet, 4H), 2.38 (broad triplet, 4H), 2.47 (q, 8H, *J*= 7.2 Hz); ^{13}C NMR (125.50, $CDCl_3$): δ = 11.7, 20.31, 25.1, 46.8, 52.9; ν_{max} (ATR-FTIR) cm^{-1}: 765, 1069, 1202, 1292, 1381, 1468, 2795, 2871, 2933, 2967. *m*/*z* (EI): 200 (4) [M$^+$], 171 (13), 128 (7), 126 (10), 114 (4), 98 (30), 86 (100), 84 (15), 73 (15), 58 (26), 56 (16) ; HRMS (EI) calculated for $C_{12}H_{29}N_2$ (MH^+): 201.23253; found: 201.23297.

***N,N,N',N'*-Tetrapropyl-1,4-butanediamine (6.2c)** Using dipropylamine. Isolated yield: 55%, bp: 50 °C (0.2 torr). ^{1}H NMR (499.12 MHz, $CDCl_3$): δ = 0.86 (t, *J*= 7.4 Hz, 12H), 1.36-1.54 (m, 12H), 2.36 (t, *J*= 7.5 Hz, 8H), 2.40 (broad triplet, 4H); ^{13}C NMR (125.50 MHz, $CDCl_3$): 12.0, 20.3, 25.1, 29.3, 54.2, 56.3; ν_{max} (ATR-FTIR) cm^{-1}: 746, 1076, 1190, 1378, 1463, 2796, 2871, 2933, 2956; *m*/*z* (EI): 256 (4) [M$^+$], 213 (4), 156 (10), 154 (27), 128 (29), 126 (23), 114 (100), 112 (37), 101 (10), 98 (11), 86 (8), 84 (21), 72 (32), 70, (15), 55 (7); HRMS (EI): calculated for $C_{16}H_{36}N_2$ (M^+): 256.2878; found: 256.2871.

***N,N,N',N'*-Tetrabutyl-1,4-butanediamine (6.2d)** Using dibutylamine. Isolated yield: 35%, bp: 89 °C (0.2 torr) (lit. 107-108 °C at 0.3 mm Hg).[23] ^{1}H (499.12 MHz, $CDCl_3$) δ = 0.90 (t, *J*= 7.3 Hz, 12H), 1.30 (sextet, *J*= 7.3 Hz, 8H), 1.36-1.46 (m, 12H), 2.30-2.47 (m, 12H); ^{13}C NMR (125.50

MHz, $CDCl_3$) 14.1, 21.7, 25.1, 29.3, 53.9, 54.2; ν_{max} (ATR-FTIR) cm^{-1}: 732, 1084, 1179, 1376, 1465, 2795, 2861, 2929, 2954; *m/z* (EI): 312 (3), 255 (5), 184 (11), 182 (21), 142 (100), 128 (10), 126 (32), 112 (18), 100 (14), 98 (8), 92 (8), 86 (29), 84 (26), 71 (18), 57 (10), 55 (9); HRMS (EI): calculated for $C_{20}H_{44}N_2$ (M^+): 312.3504, found: 312.3508. This compound has been reported before but only information regarding its boiling point was presented.[23]

6.4.7.3 Synthesis and characterization of compounds 6.1, 6.3b, 6.3c, and 6.5

A mixture containing 3 g of dibromoalkane and 8 equivalents of amine was stirred and refluxed overnight. The mixture was allowed to cool to room temperature, then 30 mL water was added to it and solid NaOH was dissolved in the water until the pH of the aqueous phase was >12. The product was extracted with 3 x 30 mL diethyl ether. The combined organic fractions were dried with $MgSO_4$, filtered, and then the diethyl ether was evaporated using a rotary evaporator to afford the crude product. The product was purified by vacuum distillation.

***N*,*N*,*N*',*N*'-Tetrapropyl-1,3-propanediamine (6.1)** Using 1,3-dibromopropane and dipropylamine. Isolated yield: 25%, bp: 49 °C (0.2 torr) (lit. 120-130 °C at 10 torr).[24] ^{1}H NMR (499.12 MHz, $CDCl_3$): δ = 0.86 (t, *J*= 7.5 Hz, 12H), 1.43 (sextet, *J*= 7.5 Hz, 8H), 1.57 (p, *J*= 7.5 Hz, 2H), 2.35 (t, *J*= 7.5 Hz, 8H), 2.40 (t, *J*= 7.5 Hz, 4H); ^{13}C NMR (125.50 MHz, $CDCl_3$): δ = 12.0, 20.2, 24.7, 52.4, 56.3; ν_{max} (ATR-FTIR) cm^{-1}: 745, 1078, 1191, 1378, 1462, 2797, 2872, 2933, 2956; *m*/*z* (EI): 242 (3) [M^+], 141 (33), 126 (13), 114 (100), 112 (99), 98 (24), 86 (53), 72 (25), 70 (56), 58 (8), 56 (11); HRMS (EI): calculated for $C_{15}H_{35}N_2$ (MH^+): 243.27948, found: 243.27895. This compound has been reported before but only information regarding its boiling point was presented.[24]

***N*,*N*,*N*',*N*'-Tetraethyl-1,6-hexanediamine (6.3b)** Using 1,6-dibromohexane and diethylamine. Isolated yield: 80%, bp: 80 °C (0.2 torr) (lit. 88 °C at 1 mm Hg).[25] ^{1}H NMR (499.12 MHz, $CDCl_3$): δ = 0.95 (t, 12H, *J*= 7.1 Hz), 1.24 (broad pentet, 4H, *J*= 6.9 Hz), 1.40 (broad pentet, 4H), 2.35 (t,

4H), 2.45 (q, 8H, *J*= 7.1 Hz); ^{13}C NMR (125.50 MHz, $CDCl_3$): δ = 11.70, 27.05, 27.73, 46.93, 53.02; ν_{max} (ATR-FTIR) cm^{-1}: 770, 1069, 1203, 1292, 1381, 1467, 2795, 2858, 2930, 2967; *m*/*z* (EI): 228 (43) [M^+], 199 (33), 142 (36), 112 (22), 86 (23), 58 (14); HRMS (EI): calculated for $C_{14}H_{33}N_2$ (MH^+): 229.26383, found: 229.26464. This compound has been reported before but only information regarding its boiling point was presented.[25]

***N*,*N*,*N*',*N*'-Tetrapropyl-1,6-hexanediamine (6.3c)** Using 1,6-dibromohexane and dipropylamine. Isolated yield: 40%, bp: 90 °C (0.2 torr). ^{1}H NMR (499.12 MHz, $CDCl_3$) δ 0.87 (t, *J*=4 Hz, 12H), 1.28 (broad pentet, 4H), 1.35-1.52 (m, 12H), 2.30-2.45 (m, 12H); ^{13}C NMR (125.50 MHz, $CDCl_3$) δ 11.9, 20.2, 27.1, 27.6, 54.2, 56.3; ν_{max} (ATR-FTIR) cm^{-1}: 745, 1077, 1191, 1378, 1464, 2796, 2871, 2931, 2956; *m*/*z* (EI): 284 (44) [M^+], 256 (42), 241 (42), 182 (37), 154 (40), 114 (28), 86 (23); HRMS (EI): calculated for $C_{18}H_{41}N_2$ (MH^+): 285.32643, found: 285.32686.

***N*,*N*'-Di-*sec*-butyl-1,6-hexanediamine (6.5)** Using 1,6-dibromohexane and sec-butylamine. Isolated yield: 50%, bp: 90 °C (1 torr) (lit. 95 °C at 0.5 torr)[26]. ^{1}H NMR (499.12 MHz, $CDCl_3$): δ = 0.89 (t, *J*= 7.5 Hz, 6H), 1.01 (d, *J*= 6.3 Hz, 6H), 1.20-1.40 (m, 6H), 1.40-1.55 (m, 6H), 2.53 (m, 4H), 2.60 (m, 2H); ^{13}C NMR (125.50 MHz, $CDCl_3$) 10.2, 19.9, 27.5, 29.6, 30.5, 47.4, 54.6; ν_{max} (ATR-FTIR) cm^{-1}: 710, 1099, 1164, 1372, 1461, 2806, 2854, 2925, 2960. *m*/*z* (EI): 228 (3) [M^+], 213 (4), 199 (41), 171 (7), 156 (7), 154 (24), 140 (11), 128 (24), 126 (100), 114 (25), 112 (4), 100 (25), 98 (61), 92 (7), 86 (51), 81 (7), 72 (12), 70 (12), 56 (21); HRMS (ESI): calculated for $C_{14}H_{33}N_2$ (MH^+): 229.26383, found: 229.26369. This compound has been reported before but only information regarding its boiling point was presented.[26]

6.4.7.4 Synthesis and characterization information for compound 6.4

A mixture of 16 mL 2-bromo-1-methoxyethane (170 mmol) and 30 mL isopropylamine (370 mmol) was stirred and refluxed overnight. The mixture was cooled, 25 mL water was added, and solid NaOH was added until the pH of the water was >12. The mixture was extracted with 3 x

25 mL diethyl ether. The combined organic phase was dried with $MgSO_4$, filtered, and then concentrated under reduced pressure. The resulting liquid was distilled, isolating three fractions at temperatures of 52 °C, 93 °C, and 134 °C. The fractions were collected separately and analyzed by ^{1}H NMR spectroscopy. The third fraction contained the desired reaction intermediate (*N*-(2-methoxyethyl)isopropylamine, 9.6 g, 50% yield).

The reaction intermediate was used as the amine reactant in a reaction with glutaryl chloride, following the same procedure as that described above in Section 2. The resulting amide was reduced with lithium aluminium hydride, again following the procedure described in Section 2. The product was purified by distillation.

***N,N'*-Dimethoxyethyl-*N,N'*-diisopropyl-1,5-pentanediamine (6.4)** Yield: 65%, bp: 120 °C (1 torr). ^{1}H NMR (499.12 MHz, $CDCl_3$): 0.99 (d, *J*= 6.6 Hz), 12H), 1.26 (p, *J*= 7.6 Hz, 2H), 1.43 (p, *J*= 7.6 Hz, 4H), 2.40 (t, *J*= 7.6 Hz, 4H), 2.59 (t, *J*= 6.8 Hz, 4H), 2.93 (septet, *J*= 6.6 Hz, 2H), 3.35 (s, 6H), 3.40 (t, *J*= 6.8 Hz, 4H); ^{13}C NMR (125.50 MHz, $CDCl_3$): δ = 18.2, 25.3, 29.0, 49.3, 51.2, 51.4, 58.8, 72.7; ν_{max} (ATR-FTIR) cm^{-1}: 965, 1119, 1175, 1360, 1461, 2811, 2870, 2928, 2965; *m*/*z* (EI): 301 (1), 287 (3), 270 (5), 257 (100), 239 (239), 186 (37), 172 (8), 156 (11), 153 (23), 142 (95), 140 (53), 138 (17), 130 (53), 126 (15), 112 (38), 106 (17), 100 (54), 98 (51), 88 (31), 86 (11), 84 (16), 72 (10), 70 (12), 59 (24), 56 (24); HRMS: calculated for $C_{17}H_{39}N_2O_2$ (MH^+): 303.30060, found: 303.30105.

6.5 References

1) S. M. Mercer and P. G. Jessop, *ChemSusChem*, 2010, **3**, 467–470.

2) Jessop, P. G., Mercer, S. M., Brown, R.S., and Robert, T., US Patent No. 20130105377, 2013.

3) Jessop, P. G., Mercer, S. M., Robert, T., Brown, R. S., Clark, T. J., Mariampillia, T. J., Resendes, R., and Wechsler, D., US Patent No. 20140076810, 2014.

4) S. M. Mercer, T. Robert, D. V. Dixon, C.-S. Chen, Z. Ghoshouni, J. R. Harjani, S. Jahangiri, G. H. Peslherbe and P. G. Jessop, *Green Chem.*, 2012, **14**, 832–839.

5) A. S. Elhag, Y. Chen, P. P. Reddy, J. A. Noguera, A. M. Ou, G. J. Hirasaki, Q. P. Nguyen, S. L. Biswal and K. P. Johnston, *Energy Procedia*, 2014, **63**, 7709–7716.

6) V. Frenna, N. Vivona, G. Consiglio and D. Spinelli, *J. Chem. Soc. Perkin Trans. 2*, 1985, 1865–1868.

7) *Estimation Programs Interface Suite for Microsoft Windows*, US EPA, Washington, DC, USA, 2012.

8) *ACD/Percepta, version 12.0*, Advanced Chemistry Development, Inc., Toronto, ON, Canada, www.acdlabs.com, 2014.

9) A. D. Wilson and F. F. Stewart, *RSC Adv.*, 2014, **4**, 11039–11049.

10) R. M. Stephenson, *J. Chem. Eng. Data*, 1993, **38**, 634–637.

11) P. G. Jessop, L. Kozycz, Z. G. Rahami, D. Schoenmakers, A. R. Boyd, D. Wechsler and A. M. Holland, *Green Chem.*, 2011, **13**, 619–623.

12) P. G. Jessop, L. Phan, A. Carrier, S. Robinson, C. J. Dürr and J. R. Harjani, *Green Chem.*, 2010, **12**, 809–814.

13) A. K. Alshamrani, J. R. Vanderveen and P. G. Jessop, *Phys. Chem. Chem. Phys.*, 2016, **18**, 19276–19288.

14) Toxicity Estimation Software Tool (TEST) v4.1, US EPA. https://www.epa.gov/chemical- research/toxicity-estimation-software-tool-test (accessed Jan. 29, 2018).

15) *Globally Harmonized System of Classification and Labelling of Chemicals (GHS)*, United Nations, New York and Geneva, 4th edn., 2011.

16) C. Rendal, K. O. Kusk and S. Trapp, *Environ. Toxicol. Chem.*, 2011, **30**, 2395–2406.

17) W. Fu, A. Franco and S. Trapp, *Environ. Toxicol. Chem.*, 2009, **28**, 1372–1379.

18) J. C. Speakman, *J. Chem. Soc.*, 1940, 855–859.

19) A. Albert and E. P. Serjeant, *The determination of ionization constants: a laboratory manual*, Chapman and Hall, London ; New York, 3rd ed., 1984.

20) B. Zou and H.-F. Jiang, *Chin. J. Chem.*, 2008, **26**, 1309–1314.

21) B. Peng, D. Geerdink, C. Farès and N. Maulide, *Angew. Chem. Int. Ed.*, 2014, **53**, 5462–5466.

22) E. G. Knapick, P. Ander and J. A. Hirsch, *Synthesis*, 1985, 58–60.

20) Reynolds, D. D. and Laasko, T. T. M., US Patent No. 2716134, 1955.

21) Hansen, J. C. and Moore, G. G. I., US Patent No. 5104034, 1992.

25) R. S. Davidson and J. W. Goodin, *Eur. Polym. J.*, 1982, **18**, 597–606.

23) Lassila, K. R. and Casey, J. P., US Patent No. 5371288, 1994.

Chapter 7

Conclusions and Recommendations

7.1 Summary

This thesis has described contributions to the improvement of SHS technology. Prior to these findings, only initial studies on SHSs had been performed. First, amidine SHSs were used to demonstrate the concept of SHS-based separations and the potential to replace volatile solvents and distillation with a different technique. However, these initial SHSs were considered impractical for general use because of their relatively difficult synthesis and their hydrolytic instability. Afterwards, more practical tertiary amine SHSs were identified but many of these solvents were as volatile as traditional solvents, limiting the benefits of SHS technology. The task undertaken in this work was to improve SHSs beyond these initial studies and identify new SHSs with many advantages over traditional solvents.

This research employed a two-pronged approach to achieving these goals. The first prong was exploratory experimental work with the goal of identifying new SHSs with different properties (Chapters 2, 4, and 6). The second prong was a mathematical modelling approach with the goal of understanding the behaviour of SHSs (Chapters 3 and 5). Exploratory investigations led to new discoveries regarding SHS behaviour which were used to develop mathematical models. The modelling in turn suggested new possibilities that could be investigated experimentally. These two approaches complimented each other, giving a deeper understanding of SHSs and their behaviour and aiding in the identification of new SHSs.

Over the course of this research improvements have been made to SHS technology. Both the performance of SHSs and their safety to humans and the environment were addressed by identifying three new classes of SHS: tertiary amines containing aromatic and/or oxygen-containing functional groups, secondary amines, and diamines. First, amines that contain other

functional groups were confirmed to behave as SHSs. Of these SHSs, the ones functionalized with oxygen-containing groups such as alcohols, ethers, and esters were found to be less volatile than trialkylamine SHSs. Furthermore, these SHSs were predicted to be less harmful to humans and the environment than trialkylamine SHSs. A virtual screening process can be used to identify SHSs that are predicted to have as few risks as possible; three new SHSs with few risks were identified using this process. The second new class of SHS, secondary amines, were found to switch from their hydrophobic state to their hydrophilic state more rapidly than tertiary amine SHSs. It is postulated that this increased switching speed is due to the formation of carbamate salts as intermediates to the formation of bicarbonate salts. There is an increased energy cost associated with eliminating CO_2 from carbamate salts. Fortunately, this cost can be decreased or eliminated by using sterically hindered amines to destabilize the carbamates. Finally, diamine SHS were identified as a third new class of SHS that can partition more favourably into water in the presence of CO_2 than monoamine SHSs, improving their separation from hydrophobic materials. The wide range of SHSs we identified – monoamines and diamines, secondary amines and tertiary amines, unfunctionalized or functionalized – provide many options for those who develop processes that use SHSs so that they can select one that best fits the specific process to maximize performance and to minimize risk.

The understanding of the behaviour of SHSs has also improved over the course of this research, providing a guide to follow when developing new SHSs or processes that use SHSs. The log K_{ow} and pK_{aH} values of amines were found to be good predictors of SHS behaviour. The required values for log K_{ow} and pK_{aH} change depending on the relative amounts of water and amine as well as on the pressure of CO_2 used to induce a switch. Additionally, diamines have different log K_{ow} requirements than monoamines. Liquid amines that fit within the required values for these parameters (pK_{aH} > ~9.5, ~1.2 < log K_{ow} < ~2.5 for monoamines or ~2 < log K_{ow} < ~5 for diamines) are likely to be SHSs. Other properties can then be designed for the solvent to make it safer (e.g.

high flash point, high LD_{50}, high LC_{50}, low bioaccumulation factor). Furthermore, a liquid-liquid equilibrium study of a representative SHS-based separation process gave insight into the effect that the composition of a system has on the degree of separation of a SHS from a hydrophobic liquid. In general, it was found that using less SHS (as a percent of the total composition of the system) resulted in more complete separations of the SHS from hydrophobic liquids. These insights will help to design SHS-based separation processes for maximum separation efficiency. The knowledge gained and the models constructed for SHS as a result of these findings will aid future researchers in their efforts to improve technologies and make new discoveries.

The development of a virtual screening process to identify SHSs with favourable properties is an excellent example of two prongs of the research coming together (Chapter 4). This virtual screening process uses the modelling and knowledge obtained from previous results to screen many molecules for properties ideal for SHSs and for minimal risk to the environment and to human health and safety. The molecules that pass the screening process are ideal candidates to test experimentally because they have a high probability of being SHSs that pose few threats to human health and safety and to the environment. Four candidate compounds were tested experimentally and three of them were confirmed to be SHSs. The models that were created based on past observations were used to design new SHSs with improved properties, thus combining the two branches of the research.

Three SHSs are recommended for use in SHS-based processes: *N*,*N*-dibutylaminoethanol, compound **4.1**, and compound **6.3b**. *N*,*N*-Dibutylaminoethanol is likely to be among the safest commercially available SHSs at this time, making it readily accessible to researchers. Compound **4.1** is predicted to offer safety improvements over *N*,*N*-dibutylaminoethanol and would be preferred for use, but it is not currently commercially available. However, its synthesis is not challenging and the added effort to obtain it may be worthwhile to use a SHS that is likely to be among the safest

known SHS. Finally, compound **6.3b** is recommended as a diamine SHS, again due to its easy preparation relative to other known diamine SHSs.

7.2 Recommendations for future areas of study

While this research has successfully improved the design of SHSs, the results so far suggest further work that can be done in this area. First, secondary amine SHSs have not been investigated to the same extent as tertiary amine SHSs. Furthermore the exploration and testing of new examples of secondary amine SHSs could be valuable to furthering the understanding of SHSs. More detailed investigations of the kinetics and equilibria of neutral SHSs, SHS-bicarbonate salts, and SHS-carbamate salts in carbonated water could provide improvements to the steric hindrance recommendations made in Chapter 2 and provide more detailed guidelines to the amount of steric hindrance required to obtain a desired switching rate. Second, because diamine SHSs can partition more favourably into the aqueous phase in the presence of CO_2 than monoamine SHSs, SHSs with more amine groups may have even more favourable partitioning. Compounds like triamines and tetramines may add too much synthetic complexity too be worth their cost as solvents, but liquid polymeric amines with switchable hydrophilicity may be an interesting area of research provided that the viscosity of the polymers does not inhibit their practicality as solvents. Finally, there is even the possibility of identifying SHSs that use functional groups other than amines. For example, octanoic acid has been reported as a solvent with CO_2-switchable miscibility with water in the presence of a water-soluble amine.[1] All of these types of SHS (secondary amines, polymeric amines, carboxylic acids) have different properties that could make them superior to mono-tertiary amine SHSs in certain applications or even open up new applications that are not possible for tertiary-amine SHSs (e.g. processes using acidic organic solvents, enamine/iminium catalysis). Therefore, further development of these classes of SHS has the potential to result in improvements

to SHS technology as well as new applications for SHSs where tertiary mono-amines are not suitable.

Beyond improving the design of SHSs, there are many opportunities to investigate potential applications of SHSs. SHSs have already been applied to a wide range of processes such as biomass extractions, water purification, and catalyst recycling. However, each extraction process poses unique challenges, so a SHS-based extraction of lipids from soybeans might require different ideal conditions than an SHS-based extraction of lipids from microalgae. Furthermore, most reported applications of SHSs use DMCA exclusively, but other SHSs with different properties (e.g. polarity, hydrogen bond donating ability) may be better suited for that application. One application which has been well-explored by Wilson and coworkers is the use of SHSs as reversible draw agents for forward osmosis. Over several studies, they have improved the process both in terms of the conditions used as well as the amine selected as the draw agent.[2–8] Another example of an improvement made to an application is by Samorì *et al.*, who improved on the extraction of algal lipids using SHSs first reported by Boyd *et al.* by using a polyethoxylated amine SHSs that allowed for a more complete separation of lipids from the amine than the process using DMCA could.[9,10] These improvements illustrate that not all SHSs are equal from a process perspective, and so if using DMCA does not result in a viable process, using a different SHS might make the process viable. Therefore, investigating the use of several different SHSs in many applications, even similar ones, will be useful to demonstrate the versatility of this class of solvent.

A challenge associated with the use of SHSs relates to their reactivity. Solvent reactivity is often undesirable because it can alter solutes in unintended ways and can itself degrade, complicating the mixtures and decreasing process efficiency through product and solvent losses. Because SHSs require some basicity to function, they are inherently reactive towards base-sensitive compounds. Furthermore, many SHSs are nucleophilic as well and can also react with electrophiles. This reactivity inherent to many SHSs limits the applications that they may be used in.

One field of study to which SHSs have not yet been applied, and could actually use their reactivity as an advantage, is in base-catalyzed reactions. SHSs have been reported as a reaction solvent, but not for a base-catalyzed reaction.[11] Base-catalyzed reactions are particularly interesting in this instance because a SHS may be capable of playing a double role as both a solvent and catalyst, thereby decreasing the number of different reagents required in a reaction and simplify the reaction system. For example, the Knoevenagel condensation is catalyzed by amines and may be facile to perform using a SHS as combination solvent/catalyst.[12] Other base-catalyzed reactions, such as transesterifications and aldol condensations, might also occur in a SHS without requiring a catalyst in addition to the SHS. A SHS-catalyzed transesterification reaction may be valuable to eliminate the use of additional materials in the conversion of lipids to biodiesel. The extraction of lipids from soybeans and algae has already been reported and using the SHS present in the mixture to catalyze the transesterification of triacylglycerides into fatty acid methyl esters would eliminate the need for an additional transesterification catalyst. Secondary amine SHSs may be even more potent as catalysts than tertiary amine SHSs because of their ability to form activated enamine and iminium species. Enamine/iminium catalysis, particularly using proline as a catalyst, has received much attention and has been successfully applied to aldol reactions, Michael additions, Mannich reactions, and many others (for two reviews on enamine and iminium catalysis, see Erkkilä *et al.* and Mukherjee *et al.*).[13,14] Secondary amine SHSs capable of this type of catalysis could be valuable solvents for use in synthetic applications.

7.3 Closing thoughts

I joined the Jessop group in 2012 because the idea of CO_2 switchable materials appealed to me. These technologies were simple, creative, and practical. They also pointed to bold aspirations; replacing a centuries-old technology like distillation is not a simple task. Potentially transformative and disruptive ideas like these are rewarding to investigate because they seek first

and foremost to improve the current state of our society and create a brighter future for the world. I am proud of the work I have done and excited about the improvements to SHS technology that have been made by all researchers that chose to get involved with SHSs so far. Even if SHS technology does not become anything more than a scientific curiosity, the attempt at impacting the world for the better has been made.

Positive impacts on society should be the primary goal of all scientists, researchers, and inventors. Not scientific publications, not patents, not awards or professional recognition. If your work is successful and offers improvements to current processes and technologies, all of these will follow. Not that these other goals should be neglected, but science is at its best when it is motivated primarily by positive progress. If this remains true, then by the combined efforts of the scientific community we can turn the problems of today into the problems of yesterday.

7.4 References

1) Q. Chen, L. Wang, G. Ren, Q. Liu, Z. Xu and D. Sun, *J. Colloid Interface Sci.*, 2017, **504**, 645–651.

2) A. D. Wilson and F. F. Stewart, *RSC Adv.*, 2014, **4**, 11039–11049.

3) M. L. Stone, C. Rae, F. F. Stewart and A. D. Wilson, *Desalination*, 2013, **312**, 124–129.

4) D. S. Wendt, C. J. Orme, G. L. Mines and A. D. Wilson, *Desalination*, 2015, **374**, 81–91.

5) C. J. Orme and A. D. Wilson, *Desalination*, 2015, **371**, 126–133.

6) A. D. Wilson and C. J. Orme, *RSC Adv.*, 2014, **5**, 7740–7751.

7) K. K. Reimund, B. J. Coscia, J. T. Arena, A. D. Wilson and J. R. McCutcheon, *J. Membr. Sci.*, 2016, **501**, 93–99.

8) B. Adhikari, M. G. Jones, C. J. Orme, D. S. Wendt and A. D. Wilson, *J. Membr. Sci.*, 2017, **527**, 228–235.

9) C. Samorì, L. Pezzolesi, D. L. Barreiro, P. Galletti, A. Pasteris and E. Tagliavini, *RSC Adv.*, 2014, **4**, 5999–6008.

10) A. R. Boyd, P. Champagne, P. J. McGinn, K. M. MacDougall, J. E. Melanson and P. G. Jessop, *Bioresour. Technol.*, 2012, **118**, 628–632.

11) C. Tao, P. Tan, X. Wang, Z. Mao, C. Lai, J. Li and Q. Chen, Chinese Patent No. 104557488 A, 2015.

12) E. Knoevenagel, *Berichte Dtsch. Chem. Ges.*, 1898, **31**, 2596–2619.

13) S. Mukherjee, J. W. Yang, S. Hoffmann and B. List, *Chem. Rev.*, 2007, **107**, 5471–5569.

14) A. Erkkilä, I. Majander and P. M. Pihko, *Chem. Rev.*, 2007, **107**, 5416–5470.

Appendix 1

Derivations of equations

A1.1 The solubility of a SHS in water, accounting for partial pressure of CO_2 (Eqn. 3.7)

$$K_w = [H^+]_{aq}[OH^-]_{aq} \quad \text{Eqn. A1.1}$$

$$[OH^-]_{aq} = \frac{K_w}{[H^+]_{aq}} \quad \text{Eqn. A1.2}$$

$$K_{aH} = \frac{[B]_{aq}[H^+]_{aq}}{[BH^+]_{aq}} \quad \text{Eqn. A1.3}$$

$$[BH^+]_{aq} = \frac{[B]_{aq}[H^+]_{aq}}{K_{aH}} \quad \text{Eqn. A1.4}$$

$$K_H = \frac{[CO_2]_{aq}}{P_{CO_2}} \quad \text{Eqn. A1.5}$$

$$[CO_2]_{aq} = K_H P_{CO_2} \quad \text{Eqn. A1.6}$$

$$K_1 = \frac{[H^+]_{aq}[HCO_3^-]_{aq}}{[CO_2]_{aq}} \quad \text{Eqn. A1.7}$$

$$K_1 = \frac{[H^+]_{aq}[HCO_3^-]_{aq}}{K_H P_{CO_2}} \quad \text{Eqn. A1.8}$$

$$[HCO_3^-]_{aq} = \frac{K_1 K_H P_{CO_2}}{[H^+]_{aq}} \quad \text{Eqn. A1.9}$$

$$[H^+]_{aq} + [BH^+]_{aq} = [OH^-]_{aq} + [HCO_3^-]_{aq} \quad \text{Eqn. A1.10}$$

$$[H^+]_{aq} + \frac{[B]_{aq}[H^+]_{aq}}{K_{aH}} = \frac{K_w}{[H^+]_{aq}} + \frac{K_1 K_H P_{CO_2}}{[H^+]_{aq}} \quad \text{Eqn. A1.11}$$

$$[H^+]_{aq}{}^2 + \frac{[B]_{aq}[H^+]_{aq}{}^2}{K_{aH}} = K_w + K_1 K_H P_{CO_2} \quad \text{Eqn. A1.12}$$

$$[H^+]_{aq}{}^2 \left(1 + \frac{[B]_{aq}}{K_{aH}}\right) = K_w + K_1 K_H P_{CO_2} \quad \text{Eqn. A1.13}$$

$$[H^+]_{aq}{}^2 = \frac{K_w + K_1 K_H P_{CO_2}}{\left(1 + [B]_{aq} K_{aH}^{-1}\right)}$$ Eqn. A1.14

$$[H^+]_{aq} = \sqrt{\frac{K_w + K_1 K_H P_{CO_2}}{\left(1 + [B]_{aq} K_{aH}^{-1}\right)}}$$ Eqn. A1.15

$$S = [B]_{aq} + [BH^+]_{aq}$$ Eqn. A1.16

$$S = [B]_{aq} + \frac{[B]_{aq}[H^+]_{aq}}{K_{aH}}$$ Eqn. A1.17

$$S = [B]_{aq}\left(1 + \frac{[H^+]_{aq}}{K_{aH}}\right)$$ Eqn. A1.18

$$S = [B]_{aq}\left(1 + \frac{1}{K_{aH}}\sqrt{\frac{K_w + K_1 K_H P_{CO_2}}{1 + [B]_{aq} K_{aH}^{-1}}}\right)$$ Eqn. A1.19

A1.2 The pressure of CO_2 required for an amine to become miscible with water (Eqn. 3.12)

$$Z = \frac{MW * V_{rat}(S' - S)}{\rho}$$ Eqn. A1.20

$$S' - S = \frac{\rho Z}{MW * V_{rat}}$$ Eqn. A1.21

$$[B]_{aq}\left(1 + \frac{1}{K_{aH}}\sqrt{\frac{K_w + K_1 K_H P'_{CO_2}}{1 + [B]_{aq} K_{aH}^{-1}}}\right) - [B]_{aq}\left(1 + \frac{1}{K_{aH}}\sqrt{\frac{K_w + K_1 K_H P_{CO_2}}{1 + [B]_{aq} K_{aH}^{-1}}}\right) = \frac{\rho Z}{MW * V_{rat}}$$ Eqn. A1.22

$$P_{CO_2} = 0$$

$$1 + \frac{1}{K_{aH}}\sqrt{\frac{K_w + K_1 K_H P'_{CO_2}}{1 + [B]_{aq} K_{aH}^{-1}}} - 1 - \frac{1}{K_{aH}}\sqrt{\frac{K_w}{1 + [B]_{aq} K_{aH}^{-1}}} = \frac{\rho Z}{MW [B]_{aq} V_{rat}}$$ Eqn. A1.23

$$\frac{1}{K_{aH}}\sqrt{\frac{K_w + K_1K_HP'_{CO_2}}{1+[B]_{aq}K_{aH}^{-1}}} - \frac{1}{K_{aH}}\sqrt{\frac{K_w}{1+[B]_{aq}K_{aH}^{-1}}} = \frac{\rho Z}{MW[B]_{aq}V_{rat}} \quad \text{Eqn. A1.24}$$

$$\sqrt{\frac{K_w + K_1K_HP'_{CO_2}}{1+[B]_{aq}K_{aH}^{-1}}} - \sqrt{\frac{K_w}{1+[B]_{aq}K_{aH}^{-1}}} = \frac{\rho Z K_{aH}}{MW[B]_{aq}V_{rat}} \quad \text{Eqn. A1.25}$$

$$\sqrt{\frac{1}{1+[B]_{aq}K_{aH}^{-1}}}\left(\sqrt{K_w + K_1K_HP'_{CO_2}} - \sqrt{K_w}\right) = \frac{\rho Z K_{aH}}{MW[B]_{aq}V_{rat}} \quad \text{Eqn. A1.26}$$

$$\sqrt{K_w + K_1K_HP'_{CO_2}} - \sqrt{K_w} = \frac{\rho Z K_{aH}}{MW[B]_{aq}V_{rat}}\sqrt{1+[B]_{aq}K_{aH}^{-1}} \quad \text{Eqn. A1.27}$$

Assume $K_w + K_1K_HP'_{CO_2} \gg K_w$

$$\sqrt{K_w + K_1K_HP'_{CO_2}} - 0 \cancel{\sqrt{K_w}} = \frac{\rho Z K_{aH}}{MW[B]_{aq}V_{rat}}\sqrt{1+[B]_{aq}K_{aH}^{-1}} \quad \text{Eqn. A1.28}$$

$$K_w + K_1K_HP'_{CO_2} = \left(\frac{\rho Z K_{aH}}{MW[B]_{aq}V_{rat}}\right)^2\left(1+[B]_{aq}K_{aH}^{-1}\right) \quad \text{Eqn. A1.29}$$

$$K_1K_HP'_{CO_2} = \left(\frac{\rho Z K_{aH}}{MW[B]_{aq}V_{rat}}\right)^2\left(1+[B]_{aq}K_{aH}^{-1}\right) - K_w \quad \text{Eqn. A1.30}$$

$$P'_{CO_2} = \left(\frac{\rho Z K_{aH}}{MW[B]_{aq}V_{rat}}\right)^2\frac{1+[B]_{aq}K_{aH}^{-1}}{K_1K_H} - \frac{K_w}{K_1K_H} \quad \text{Eqn. A1.31}$$

A1.3 Calculating log *D* as a function of pH (Eqn. 3.18)

$$K_{ow} = \frac{[B]_{org}}{[B]_{aq}} \quad \text{Eqn. A1.32}$$

$$[B]_{org} = K_{ow}[B]_{aq} \quad \text{Eqn. A1.33}$$

$$K'_{ow} = \frac{[BH^+]_{org}}{[BH^+]_{aq}} \quad \text{Eqn. A1.34}$$

$$[BH^+]_{org} = K'_{ow}[BH^+]_{aq} \quad \text{Eqn. A1.35}$$

$$\Delta log K_{ow} = log K_{ow} - log K'_{ow} = \log\left(\frac{K_{ow}}{K'_{ow}}\right)$$ Eqn. A1.36

$$D = \frac{[B]_{org} + [B^+]_{org}}{[B]_{aq} + [B^+]_{aq}}$$ Eqn. A1.37

$$D = \frac{[B]_{org}/[B]_{aq} + [B^+]_{org}/[B]_{aq}}{1 + [B^+]_{aq}/[B]_{aq}}$$ Eqn. A1.38

$$D = \frac{K_{ow} + [B^+]_{org}/[B]_{aq}}{1 + [H^+]_{aq} K_{aH}^{-1}}$$ Eqn. A1.39

$$D = \frac{K_{ow}K_{aH} + K_{aH}[B^+]_{org}/[B]_{aq}}{K_{aH} + [H^+]_{aq}}$$ Eqn. A1.40

$$D = \frac{K_{ow}K_{aH} + [H^+]_{aq}[B^+]_{org}/[BH^+]_{aq}}{K_{aH} + [H^+]_{aq}}$$ Eqn. A1.41

$$D = \frac{K_{ow}K_{aH} + [H^+]_{aq}K'_{ow}}{K_{aH} + [H^+]_{aq}}$$ Eqn. A1.42

$$D = \frac{10^{-pK_{aH}}K_{ow} + 10^{-pH}K'_{ow}}{10^{-pK_{aH}} + 10^{-pH}}$$ Eqn. A1.43

$$D = \frac{K_{ow} + 10^{pK_{aH}-pH}K'_{ow}}{1 + 10^{pK_{aH}-pH}}$$ Eqn. A1.44

$$D = K_{ow}\left(\frac{1 + 10^{pK_{aH}-pH}K'_{ow}/K_{ow}}{1 + 10^{pK_{aH}-pH}}\right)$$ Eqn. A1.45

$$D = K_{ow}\left(\frac{1 + 10^{pK_{aH}-pH}10^{-\Delta log K_{ow}}}{1 + 10^{pK_{aH}-pH}}\right)$$ Eqn. A1.46

$$\log D = \log K_{ow} + \log\left(1 + 10^{pK_{aH}-pH-\Delta \log K_{ow}}\right) - \log(1 + 10^{pK_{aH}-pH})$$ Eqn. A1.47

A1.4 Calculating log *D* as a function of protonation ratio (Eqn. 3.19)

$$K_{aH} = \frac{[B]_{aq}[H^+]_{aq}}{[BH^+]_{aq}}$$ Eqn. A1.3

$$[H^+]_{aq} = \frac{K_{aH}[BH^+]_{aq}}{[B]_{aq}}$$ Eqn. A1.48

$$D = \frac{K_{ow}K_{aH} + [H^+]_{aq}K'_{ow}}{K_{aH} + [H^+]_{aq}} \quad \text{Eqn. A1.42}$$

$$D = \frac{K_{ow}K_{aH} + K_{aH}[BH^+]_{aq}K'_{ow}/[B]_{aq}}{K_{aH} + K_{aH}\,[BH^+]_{aq}K'_{ow}/[B]_{aq}} \quad \text{Eqn. A1.49}$$

$$D = \frac{K_{ow} + [BH^+]_{aq}K'_{ow}/[B]_{aq}}{1 + [BH^+]_{aq}K'_{ow}/[B]_{aq}} \quad \text{Eqn. A1.50}$$

$$D = \frac{K_{ow}/K'_{ow} + [BH^+]_{aq}/[B]_{aq}}{1/K'_{ow} + [BH^+]_{aq}K'_{ow}/[B]_{aq}} \quad \text{Eqn. A1.51}$$

$$\log(D_1\ or\ D_2) = \log\left(\frac{K_{ow}}{K'_{ow}} + \frac{[BH^+]_{aq}}{[B]_{aq}}\right) - \log\left(\frac{1}{K'_{ow}} + \frac{1}{K'_{ow}}\frac{[BH^+]_{aq}}{[B]_{aq}}\right) \quad \text{Eqn. A1.52}$$

A1.5 Calculating the fraction of protonation as a function of CO_2 pressure (Eqn. 3.20)

$$K_{aH} = \frac{[B]_{aq}[H^+]_{aq}}{[BH^+]_{aq}} \quad \text{Eqn. A1.3}$$

$$[H^+]_{aq} = \frac{K_{aH}[BH^+]_{aq}}{[B]_{aq}} \quad \text{Eqn. A1.48}$$

$$[H^+]_{aq} + [BH^+]_{aq} = [OH^-]_{aq} + [HCO_3^-]_{aq} \quad \text{Eqn. A1.10}$$

$$\frac{K_{aH}[BH^+]_{aq}}{[B]_{aq}} + [BH^+]_{aq} = \frac{[B]_{aq}K_w}{K_{aH}[BH^+]_{aq}} + \frac{[B]_{aq}K_1K_HP_{CO_2}}{K_{aH}[BH^+]_{aq}} \quad \text{Eqn. A1.53}$$

$$\frac{K_{aH}[BH^+]_{aq}}{[B]_{aq}} + [BH^+]_{aq} = \frac{[B]_{aq}K_w}{K_{aH}[BH^+]_{aq}} + \frac{[B]_{aq}K_1K_HP_{CO_2}}{K_{aH}[BH^+]_{aq}} \quad \text{Eqn. A1.54}$$

$$\frac{K_{aH}^2[BH^+]_{aq}^2}{[B]_{aq}} + K_{aH}[BH^+]_{aq}^2 = [B]_{aq}K_w + [B]_{aq}K_1K_HP_{CO_2} \quad \text{Eqn. A1.55}$$

$$\frac{K_{aH}^2[BH^+]_{aq}^2}{[B]_{aq}^2} + \frac{K_{aH}[BH^+]_{aq}^2}{[B]_{aq}} = K_w + K_1K_HP_{CO_2} \quad \text{Eqn. A1.56}$$

$$K_{aH}{}^2\left(\frac{[BH^+]_{aq}}{[B]_{aq}}\right)^2 + \frac{K_{aH}{}^2[B]_{aq}[BH^+]_{aq}^2}{K_{aH}[B]_{aq}^2} = K_w + K_1K_HP_{CO_2} \quad \text{Eqn. A1.57}$$

$$K_{aH}{}^2\left(\frac{[BH^+]_{aq}}{[B]_{aq}}\right)^2\left(1+\frac{[B]_{aq}}{K_{aH}}\right)=K_w+K_1K_HP_{CO_2} \quad \text{Eqn. A1.58}$$

$$K_{aH}{}^2\left(\frac{[BH^+]_{aq}}{[B]_{aq}}\right)^2=\frac{K_w+K_1K_HP_{CO_2}}{1+[B]_{aq}K_{aH}{}^{-1}} \quad \text{Eqn. A1.59}$$

$$\left(\frac{[BH^+]_{aq}}{[B]_{aq}}\right)^2=\frac{1}{K_{aH}{}^2}\left(\frac{K_w+K_1K_HP_{CO_2}}{1+[B]_{aq}K_{aH}{}^{-1}}\right) \quad \text{Eqn. A1.60}$$

$$\frac{[BH^+]_{aq}}{[B]_{aq}}=\frac{1}{K_{aH}}\left(\frac{K_w+K_1K_HP_{CO_2}}{1+[B]_{aq}K_{aH}{}^{-1}}\right)^{1/2} \quad \text{Eqn. A1.61}$$

A1.6 Calculating the fraction of protonated monoamine (Eqn. 3.24)

$$n_{B,tot}=n_{B,org}+n_{B,aq}+n_{BH^+,org}+n_{BH^+,aq} \quad \text{Eqn. A1.62}$$

$$P=\frac{n_{BH^+,org}+n_{BH^+,aq}}{n_{B,tot}} \quad \text{Eqn. A1.63}$$

$$P=\frac{n_{BH^+,org}+n_{BH^+,aq}}{n_{B,org}+n_{B,aq}+n_{BH^+,org}+n_{BH^+,aq}} \quad \text{Eqn. A1.64}$$

$$P=\frac{[BH^+]_{org}V_{org}+[BH^+]_{aq}V_{aq}}{[B]_{org}V_{org}+[B]_{aq}V_{aq}+[BH^+]_{org}V_{org}+[BH^+]_{aq}V_{aq}} \quad \text{Eqn. A1.65}$$

$$\frac{1}{P}=\frac{[B]_{org}V_{org}+[B]_{aq}V_{aq}+[BH^+]_{org}V_{org}+[BH^+]_{aq}V_{aq}}{[BH^+]_{org}V_{org}+[BH^+]_{aq}V_{aq}} \quad \text{Eqn. A1.66}$$

$$\frac{1}{P}=\frac{[BH^+]_{org}V_{org}+[BH^+]_{aq}V_{aq}}{[BH^+]_{org}V_{org}+[BH^+]_{aq}V_{aq}}+\frac{[B]_{org}V_{org}+[B]_{aq}V_{aq}}{[BH^+]_{org}V_{org}+[BH^+]_{aq}V_{aq}} \quad \text{Eqn. A1.67}$$

$$\frac{1}{P}=1+\frac{[B]_{org}V_{org}+[B]_{aq}V_{aq}}{[BH^+]_{org}V_{org}+[BH^+]_{aq}V_{aq}} \quad \text{Eqn. A1.68}$$

$$\frac{1}{P}=1+\frac{\left([B]_{org}/[B]_{aq}\right)V_{org}+V_{aq}}{\left([BH^+]_{org}/[B]_{aq}\right)V_{org}+\left([BH^+]_{aq}/[B]_{aq}\right)V_{aq}} \quad \text{Eqn. A1.69}$$

$$\frac{1}{P}=1+\frac{\left([B]_{org}/[B]_{aq}\right)\left(V_{org}/V_{aq}\right)+1}{\left([BH^+]_{org}/[B]_{aq}\right)\left(V_{org}/V_{aq}\right)+\left([BH^+]_{aq}/[B]_{aq}\right)} \quad \text{Eqn. A1.70}$$

$$\frac{1}{P} = 1 + \frac{K_P V_{rat} + 1}{\left([BH^+]_{aq}/[B]_{aq}\right)K'_P V_{rat} + \left([BH^+]_{aq}/[B]_{aq}\right)}$$ Eqn. A1.71

$$\frac{1}{P} = 1 + \frac{K_P V_{rat} + 1}{\left([BH^+]_{aq}/[B]_{aq}\right)(K'_P V_{rat} + 1)}$$ Eqn. A1.72

$$\frac{1}{P} = 1 + \frac{K_P V_{rat} + 1}{[H^+]_{aq} K_{aH}^{-1}(K'_P V_{rat} + 1)}$$ Eqn. A1.73

$$P = \frac{[H^+]_{aq} K_{aH}^{-1}(K'_P V_{rat} + 1)}{[H^+]_{aq} K_{aH}^{-1}(K'_P V_{rat} + 1) + K_P V_{rat} + 1}$$ Eqn. A1.74

$$P = \frac{[H^+]_{aq}(K'_P V_{rat} + 1)}{[H^+]_{aq}(K'_P V_{rat} + 1) + K_{aH}(K_P V_{rat} + 1)}$$ Eqn. A1.75

$$P = \frac{[H^+]_{aq}}{[H^+]_{aq} + K_{aH}\left(\frac{K_P V_{rat} + 1}{K'_P V_{rat} + 1}\right)}$$ Eqn. A1.76

A1.7 Calculating the pH of the aqueous phase at a given $[B]_0$ for a monoamine (Eqn 3.25)

$$[BH^+]_{aq} + [H^+]_{aq} = [OH^-]_{aq} + [HCO_3^-]_{aq}$$ Eqn. A1.10

$$[BH^+]_{aq} = [OH^-]_{aq} + [HCO_3^-]_{aq} - [H^+]_{aq}$$ Eqn. A1.77

$$[BH^+]_{aq} = \frac{K_w}{[H^+]_{aq}} + [HCO_3^-]_{aq} - [H^+]_{aq}$$ Eqn. A1.78

$$[BH^+]_{aq} = \frac{K_w}{[H^+]_{aq}} + \frac{K_1 K_H P_{CO_2}}{[H^+]_{aq}} - [H^+]_{aq}$$ Eqn. A1.79

$$n_{B,0} = [B]_{org} V_{org} + [B]_{aq} V_{aq} + [BH^+]_{org} V_{org} + [BH^+]_{aq} V_{aq}$$ Eqn. A1.80

$$[B]_0 = \frac{B_0}{V_{aq}}$$ Eqn. A1.81

$$[B]_0 = [B]_{org} V_{rat} + [B]_{aq} + [BH^+]_{org} V_{rat} + [BH^+]_{aq}$$ Eqn. A1.82

$$[B]_0 = [B]_{aq} K_P V_{rat} + [B]_{aq} + [BH^+]_{aq} K'_P V_{rat} + [BH^+]_{aq}$$ Eqn. A1.83

$$[B]_0 = [B]_{aq}(K_P V_{rat} + 1) + [BH^+]_{aq}(K'_P V_{rat} + 1)$$ Eqn. A1.84

$$0 = [B]_{aq}(K_P V_{rat} + 1) + [BH^+]_{aq}(K'_P V_{rat} + 1) - [B]_0 \quad \text{Eqn. A1.85}$$

$$0 = \frac{K_{aH}[BH^+]_{aq}}{[H^+]_{aq}}(K_P V_{rat} + 1) + [BH^+]_{aq}(K'_P V_{rat} + 1) - [B]_0 \quad \text{Eqn. A1.86}$$

$$0 = \frac{K_{aH}}{[H^+]_{aq}}\left(\frac{K_w}{[H^+]_{aq}} + \frac{K_1 K_H P_{CO_2}}{[H^+]_{aq}} - [H^+]_{aq}\right)(K_P V_{rat} + 1) \quad \text{Eqn. A1.87}$$
$$+ \left(\frac{K_w}{[H^+]_{aq}} + \frac{K_1 K_H P_{CO_2}}{[H^+]_{aq}} - [H^+]_{aq}\right)(K'_P V_{rat} + 1) - [B]_0$$

$$0 = \left(\frac{K_{aH}K_w}{[H^+]_{aq}^2} + \frac{K_{aH}K_1 K_H P_{CO_2}}{[H^+]_{aq}^2} - K_{aH}\right)(K_P V_{rat} + 1) \quad \text{Eqn. A1.88}$$
$$+ \left(\frac{K_w}{[H^+]_{aq}} + \frac{K_1 K_H P_{CO_2}}{[H^+]_{aq}} - [H^+]_{aq}\right)(K'_P V_{rat} + 1) - [B]_0$$

$$0 = \left(K_{aH}K_w + K_{aH}K_1 K_H P_{CO_2} - K_{aH}[H^+]_{aq}^2\right)(K_P V_{rat} + 1) \quad \text{Eqn. A1.89}$$
$$+ \left(K_w[H^+]_{aq} + K_1 K_H P_{CO_2}[H^+]_{aq} - [H^+]_{aq}^3\right)(K'_P V_{rat} + 1)$$
$$- [B]_0[H^+]_{aq}^2$$

$$0 = \left(K_{aH}K_w + K_{aH}K_1 K_H P_{CO_2} - K_{aH}[H^+]_{aq}^2\right)(K_P V_{rat} + 1) \quad \text{Eqn. A1.90}$$
$$+ \left(K_w[H^+]_{aq} + K_1 K_H P_{CO_2}[H^+]_{aq} - [H^+]_{aq}^3\right)(K'_P V_{rat} + 1)$$
$$- [B]_0[H^+]_{aq}^2$$

$$0 = K_{aH}K_w(K_P V_{rat} + 1) + K_{aH}K_1 K_H P_{CO_2}(K_P V_{rat} + 1) \quad \text{Eqn. A1.91}$$
$$- K_{aH}[H^+]_{aq}^2(K_P V_{rat} + 1) + K_w[H^+]_{aq}(K'_P V_{rat} + 1)$$
$$+ K_1 K_H P_{CO_2}[H^+]_{aq}(K'_P V_{rat} + 1) - [H^+]_{aq}^3(K'_P V_{rat} + 1)$$
$$- [B]_0[H^+]_{aq}^2$$

$$0 = -K_{aH}K_w(K_PV_{rat}+1) - K_{aH}K_1K_HP_{CO_2}(K_PV_{rat}+1) \quad \text{Eqn. A1.92}$$
$$+ K_{aH}[H^+]_{aq}^2(K_PV_{rat}+1) - K_w[H^+]_{aq}(K_P'V_{rat}+1)$$
$$- K_1K_HP_{CO_2}[H^+]_{aq}(K_P'V_{rat}+1) + [H^+]_{aq}^3(K_P'V_{rat}+1)$$
$$+ [B]_0[H^+]_{aq}^2$$

$$0 = [H^+]_{aq}^3(K_P'V_{rat}+1) + [H^+]_{aq}^2(K_{aH}(K_PV_{rat}+1)+[B]_0) \quad \text{Eqn. A1.93}$$
$$- [H^+]_{aq}\left(K_w + K_1K_HP_{CO_2}\right)(K_P'V_{rat}+1)$$
$$- K_{aH}\left(K_w + K_1K_HP_{CO_2}\right)(K_PV_{rat}+1)$$

A1.8 Estimating log *D* curves of compounds 2c and 3b for Fig. 6.3

The distribution coefficient, *D*, of a diamine at a given pH is defined by equation A1.94. Concentrations of the different species in the organic phase can be calculated from their concentrations in the aqueous phase and their partition coefficients, K_{ow}, K_{ow}', and K_{ow}'' (equations A1.33, A1.35, and A1.95). Replacing the organic phase concentrations using these equations gives equation A1.96. The concentrations of the protonated species can be calculated from the pH of the solution and their K_a values (equivalent to K_{aH} of the conjugate base) (equations A1.97-A1.101). Replacing the concentrations of protonated species using these equations gives equation A1.102. Finally, $[B]_{aq}$ can be cancelled from all terms and the numerator and denominator multiplied by K_{aH1}*K_{aH2} to give equation A1.103.

Equation A1.103 can be solved for *D* at a given pH if the base's pK_{aH1}, pK_{aH2}, K_{ow}, K_{ow} K_{ow}', and K_{ow}' values are known. The pK_{aH1} and pK_{aH2} values for compounds **2c** and **3b** were predicted using ACD/Percepta v12.0 software. The K_{ow} values for each compound were estimated based on their measured distribution coefficients at high pH, where $D \approx K_{ow}$. The K_{ow}' values for each compound were estimated based on their measured distribution coefficients at low pH, where $D \approx K_{ow}''$. Finally, the K_{ow}' values for each compound were assumed to be the midpoint value between K_{ow} and K_{ow}' on the log scale. All the relevant values for compounds **2c** and **3b** are shown

in Table A1.1. These values were used in equation A1.103 to generate the lines shown in Fig. 6.3. The log *D* curves used for monoamines in that figure were calculated using Eqn. A1.47.

Table A1.1 Values used in the calculation of the log *D* curves shown in Fig. 6.3.

Compound	**pK_{aH1}**	**pK_{aH2}**	**log K_{ow}**	**log K_{ow}'**	**log K_{ow}''**
2c	10.20	9.34	4.4	0.2	-4.0
3b	10.87	10.24	2.7	-0.1	-2.9

$$D = \frac{[B]_{org} + [BH^+]_{org} + [BH_2^{2+}]_{org}}{[B]_{aq} + [BH^+]_{aq} + [BH_2^{2+}]_{aq}} \quad \text{Eqn. A1.94}$$

$$[B]_{org} = K_{ow}[B]_{aq} \quad \text{Eqn. A1.33}$$

$$[BH^+]_{org} = K'_{ow}[BH^+]_{aq} \quad \text{Eqn. A1.35}$$

$$[BH_2^{2+}]_{org} = K''_{ow}[BH_2^{2+}]_{aq} \quad \text{Eqn. A1.95}$$

$$D = \frac{K_{ow}[B]_{aq} + K'_{ow}[BH^+]_{aq} + K''_{ow}[BH_2^{2+}]_{aq}}{[B]_{aq} + [BH^+]_{aq} + [BH_2^{2+}]_{aq}} \quad \text{Eqn. A1.96}$$

$$K_{aH1} = \frac{[B]_{aq}[H^+]_{aq}}{[BH^+]_{aq}} \quad \text{Eqn. A1.97}$$

$$[BH^+]_{aq} = \frac{[B]_{aq}[H^+]_{aq}}{K_{aH1}} \quad \text{Eqn. A1.98}$$

$$K_{aH2} = \frac{[BH^+]_{aq}[H^+]_{aq}}{[BH_2^{2+}]_{aq}} \quad \text{Eqn. A1.99}$$

$$[BH_2^{2+}]_{aq} = \frac{[BH^+]_{aq}[H^+]_{aq}}{K_{aH2}} \quad \text{Eqn. A1.100}$$

$$[BH_2^{2+}]_{aq} = \frac{[B]_{aq}[H^+]_{aq}^{\ 2}}{K_{aH1}K_{aH2}} \quad \text{Eqn. A1.101}$$

$$D = \frac{K_{ow}[B]_{aq} + \frac{K'_{ow}[B]_{aq}[H^+]_{aq}}{K_{aH1}} + \frac{K''_{ow}[B]_{aq}[H^+]_{aq}^{\ 2}}{K_{aH1}K_{aH2}}}{[B]_{aq} + \frac{[B]_{aq}[H^+]_{aq}}{K_{aH1}} + \frac{[B]_{aq}[H^+]_{aq}^{\ 2}}{K_{aH1}K_{aH2}}} \quad \text{Eqn. A1.102}$$

$$D = \frac{K_{ow}K_{aH1}K_{aH2} + K'_{ow}K_{aH2}[H^+]_{aq} + K''_{ow}[H^+]_{aq}^{\ 2}}{K_{aH1}K_{aH2} + K_{aH2}[H^+]_{aq} + [H^+]_{aq}^{\ 2}} \quad \text{Eqn. A1.103}$$

A1.9 Equation for the graph in Fig. 6.4

The equations described in Section 6.2.3 for Fig. 6.4 were used to identify the range of pK_{aH1} values that a diamine would need in order to have a large change in percent protonation when CO_2 is added or removed from the system as a function of the total amount of amine in the system. The equations identify the minimum pK_{aH1} required to achieve a desired high fraction of protonation in the presence of CO_2 or the maximum pK_{aH1} required to achieve a desired low fraction of protonation in the absence of CO_2. Equations for three variables, $[BH_2^{2+}]$aq, pK_{aH1}, and $[H^+]_{aq}$, are defined. Combining these three equations, derived below, the minimum or maximum pK_{aH1} required for ideal switchability (defined by a low or high fraction of protonation) can be calculated. The concentration of di-protonated species in the aqueous phase, $[BH_2^{2+}]_{aq}$ is calculated first. The log K_{ow} value of the amine and its conjugate acids must be known. The values for monoamines were calculating by Eqn. A1.76 using $[H^+]_{aq}$ values calculated by Eqn. A1.93.

A1.9.1 Calculation of $[BH_2^{2+}]_{aq}$

$$[B]_{org} = K_{ow}[B]_{aq} \quad \text{Eqn. A1.33}$$

$$[BH^+]_{org} = K'_{ow}[BH^+]_{aq} \quad \text{Eqn. A1.35}$$

$$[BH_2^{2+}]_{org} = K''_{ow}[BH_2^{2+}]_{aq} \quad \text{Eqn. A1.95}$$

$$K_{aH1} = \frac{[H^+]_{aq}[B]_{aq}}{[BH^+]_{aq}} \quad \text{Eqn. A1.97}$$

$$K_{aH2} = \frac{[H^+]_{aq}[BH^+]_{aq}}{[BH_2^{2+}]_{aq}}$$ Eqn. A1.104

$$\Delta log K_{ow} = log K_{ow} - log K'_{ow} = \log\left(\frac{K_{ow}}{K'_{ow}}\right)$$ Eqn. A1.36

$$\log K''_{ow} = \log K'_{ow} - \Delta \log K_{ow} = \log K_{ow} - 2\Delta \log K_{ow}$$ Eqn. A1.105

$$R = \frac{K_{aH2}}{K_{aH1}}$$ Eqn. A1.106

$$[B]_0 = \frac{B_0}{V_{aq}}$$ Eqn. A1.81

$$K_w = [H^+]_{aq}\left[OH^-_{aq}\right]$$ Eqn. A1.1

$$K_H = \frac{\left[CO_{2,aq}\right]}{P_{CO2}}$$ Eqn. A1.5

$$K_1 = \frac{[H^+]_{aq}\left[HCO^-_{3,aq}\right]}{\left[CO_{2,aq}\right]}$$ Eqn. A1.7

$$P = \frac{BH^+_{aq} + 2BH^{2+}_{2,aq} + BH^+_{org} + 2BH^{2+}_{2,org}}{2B_0}$$ Eqn. A1.107

$$P = \frac{[BH^+]_{aq} + 2[BH_2^{2+}]_{aq} + \frac{BH^+_{org}}{V_{aq}} + \frac{2BH^{2+}_{org}}{V_{aq}}}{2[B]_0}$$ Eqn. A1.108

$$P = \frac{[BH^+]_{aq} + 2[BH_2^{2+}]_{aq} + \frac{[BH^+]_{org}V_{org}}{V_{aq}} + \frac{2[BH_2^{2+}]_{org}V_{org}}{V_{aq}}}{2[B]_0}$$ Eqn. A1.109

$$P = \frac{[BH^+]_{aq} + 2[BH_2^{2+}]_{aq} + [BH^+]_{org}V_{rat} + 2[BH_2^{2+}]_{org}V_{rat}}{2[B]_0}$$ Eqn. A1.110

$$P = \frac{[BH^+]_{aq} + 2[BH_2^{2+}]_{aq} + [BH^+]_{aq}K'_{ow}V_{rat} + 2[BH_2^{2+}]_{aq}K''_{ow}V_{rat}}{2[B]_0}$$ Eqn. A1.111

$$P$$ Eqn. A1.112

$$= \frac{\frac{[BH_2^{2+}]_{aq}K_{aH2}}{[H^+]_{aq}} + 2[BH_2^{2+}]_{aq} + \frac{[BH_2^{2+}]_{aq}K_{aH2}K'_{ow}V_{rat}}{[H^+]_{aq}} + 2[BH_2^{2+}]_{aq}K''_{ow}V_{r}}{2[B]_0}$$

$$P = \frac{[BH_2^{2+}]_{aq}\left(\frac{K_{aH2}}{[H^+]_{aq}} + 2 + \frac{K_{aH2}K'_{ow}V_{rat}}{[H^+]_{aq}} + 2K''_{ow}V_{rat}\right)}{2[B]_0}$$ Eqn. A1.113

$$2[B]_0P = [BH_2^{2+}]_{aq}\left(\frac{K_{aH2}}{[H^+]_{aq}} + 2 + \frac{K_{aH2}K'_{ow}V_{rat}}{[H^+]_{aq}} + 2K''_{ow}V_{rat}\right)$$ Eqn. A1.114

$$[BH_2^{2+}]_{aq} = \frac{2[B]_0P}{\frac{K_{aH2}}{[H^+]_{aq}} + 2 + \frac{K_{aH2}K'_{ow}V_{rat}}{[H^+]_{aq}} + 2K''_{ow}V_{rat}}$$ Eqn. A1.115

A1.9.2 Calculation of minimum/maximum pK_{aH1}

$$B_0 = B_{aq} + BH^+_{aq} + BH^{2+}_{2,aq} + B_{org} + BH^+_{org} + BH^{2+}_{2,org}$$ Eqn. A1.116

$$[B]_0 = [B]_{aq} + [BH^+]_{aq} + [BH_2^{2+}]_{aq} + \frac{B_{org}}{V_{aq}} + \frac{BH^+_{org}}{V_{aq}} + \frac{BH^{2+}_{2,org}}{V_{aq}}$$ Eqn. A1.117

$$[B]_0 = [B]_{aq} + [BH^+]_{aq} + [BH_2^{2+}]_{aq} + \frac{[B]_{org}V_{org}}{V_{aq}} + \frac{[BH^+]_{org}V_{org}}{V_{aq}}$$ Eqn. A1.118

$$+ \frac{[BH_2^{2+}]_{org}V_{org}}{V_{aq}}$$

$$[B]_0 = [B]_{aq} + [BH^+]_{aq} + [BH_2^{2+}]_{aq} + [B]_{org}V_{rat} + [BH^+]_{org}V_{rat}$$ Eqn. A1.119

$$+ [BH_2^{2+}]_{org}V_{rat}$$

$$[B]_0 = [B]_{aq} + [BH^+]_{aq} + [BH_2^{2+}]_{aq} + [B]_{aq}K_{ow}V_{rat} + [BH^+]_{aq}K'_{ow}V_{rat}$$ Eqn. A1.120

$$+ [BH_2^{2+}]_{org}K''_{ow}V_{rat}$$

$$[B]_0 = \frac{[BH^+_{aq}]K_{aH2}}{[H^+]_{aq}} + [BH^+]_{aq} + [BH_2^{2+}]_{aq} + \frac{[BH^+]_{aq}K_{aH2}}{[H^+_{aq}]}K_{ow}V_{rat}$$ Eqn. A1.121

$$+ [BH^+]_{aq}K'_{ow}V_{rat} + [BH_2^{2+}]_{aq}K''_{ow}V_{rat}$$

$$[B]_0 = \frac{[BH_2^{2+}]_{aq} K_{aH1} K_{aH2}}{[H^+]_{aq}{}^2} + \frac{[BH_2^{2+}]_{aq} K_{aH2}}{[H^+]_{aq}} + [BH_2^{2+}]_{aq} \quad \text{Eqn. A1.122}$$

$$+ \frac{[BH_2^{2+}]_{aq} K_{aH1} K_{aH2}}{[H^+]_{aq}{}^2} K_{ow} V_{rat} + \frac{[BH_2^{2+}]_{aq} K_{aH2}}{[H^+]_{aq}} K'_{ow} V_{rat}$$

$$+ [BH_2^{2+}]_{aq} K''_{ow} V_{rat}$$

$$[B]_0 = [BH_2^{2+}]_{aq} \left(\frac{K_{aH1} K_{aH2}}{[H^+]_{aq}{}^2} + \frac{K_{aH2}}{[H^+]_{aq}} + 1 + \frac{K_{aH1} K_{aH2}}{[H^+]_{aq}{}^2} K_{ow} V_{rat} \right. \quad \text{Eqn. A1.123}$$

$$\left. + \frac{K_{aH2}}{[H^+]_{aq}} K'_{ow} V_{rat} + K''_{ow} V_{rat} \right)$$

$$\frac{[B]_0}{\frac{K_{aH1} K_{aH2}}{[H^+]_{aq}{}^2} + \frac{K_{aH2}}{[H^+]_{aq}} + 1 + \frac{K_{aH1} K_{aH2}}{[H^+]_{aq}{}^2} K_{ow} V_{rat} + \frac{K_{aH2}}{[H^+]_{aq}} K'_{ow} V_{rat} + K''_{ow} V_{rat}} \quad \text{Eqn. A1.124}$$

$$= [BH_2^{2+}]_{aq}$$

$$\frac{[B]_0}{\frac{K_{aH1} K_{aH2}}{[H^+]_{aq}{}^2} + \frac{K_{aH2}}{[H^+]_{aq}} + 1 + \frac{K_{aH1} K_{aH2}}{[H^+]_{aq}{}^2} K_{ow} V_{rat} + \frac{K_{aH2}}{[H^+]_{aq}} K'_{ow} V_{rat} + K''_{ow} V_{rat}} \quad \text{Eqn. A1.125}$$

$$= \frac{2[B]_0 P}{\frac{K_{aH2}}{[H^+]_{aq}} + 2 + \frac{K_{aH2} K'_{ow} V_{rat}}{[H^+]_{aq}} + 2K''_{ow} V_{rat}}$$

$$\frac{K_{aH2}}{[H^+]_{aq}} + 2 + \frac{K_{aH2} K'_{ow} V_{rat}}{[H^+]_{aq}} + 2K''_{ow} V_{rat} \quad \text{Eqn. A1.126}$$

$$= \frac{2PK_{aH1} K_{aH2}}{[H^+]_{aq}{}^2} + \frac{2PK_{aH2}}{[H^+]_{aq}} + 2P + \frac{2PK_{aH1} K_{aH2}}{[H^+]_{aq}{}^2} K_{ow} V_{rat}$$

$$+ \frac{2PK_{aH2}}{[H^+]_{aq}} K'_{ow} V_{rat} + 2PK''_{ow} V_{rat}$$

$$\frac{RK_{aH1}}{[H^+]_{aq}} + 2 + \frac{RK_{aH1}K'_{ow}V_{rat}}{[H^+]_{aq}} + 2K''_{ow}V_{rat} \quad \text{Eqn. A1.127}$$

$$= \frac{2PRK_{aH1}{}^2}{[H^+]_{aq}{}^2} + \frac{2PRK_{aH1}}{[H^+]_{aq}} + 2P + \frac{2PRK_{aH1}{}^2}{[H^+]_{aq}{}^2}K_{ow}V_{rat}$$

$$+ \frac{2PRK_{aH1}}{[H^+]_{aq}}K'_{ow}V_{rat} + 2PK''_{ow}V_{rat}$$

$$\frac{(1 + K_{ow}V_{rat})2PR}{[H^+]_{aq}{}^2}K_{aH1}{}^2 + \frac{(2P + 2PK'_{ow}V_{rat} - 1 - K'_{ow}V_{rat})R}{[H^+]_{aq}}K_{aH1} \quad \text{Eqn. A1.128}$$

$$+ (2P + 2PK''_{ow}V_{rat} - 2 - 2K''_{ow}V_{rat}) = 0$$

$$a = \frac{(1 + K_{ow}V_{rat})2PR}{[H^+]_{aq}{}^2} \quad \text{Eqn. A1.129}$$

$$b = \frac{(2P + 2PK'_{ow}V_{rat} - 1 - K'_{ow}V_{rat})R}{[H^+]_{aq}} \quad \text{Eqn. A1.130}$$

$$c = (2P + 2PK''_{ow}V_{rat} - 2 - 2K''_{ow}V_{rat}) \quad \text{Eqn. A1.131}$$

$$K_{aH1} = \frac{-b \pm \sqrt{b^2 - 4ac}}{2a} \quad \text{Eqn. A1.132}$$

A1.9.3 Equation for $[H^+]_{aq}$

$$[H^+]_{aq} + [BH^+]_{aq} + 2[BH_2^{2+}]_{aq} = \left[OH^-_{aq}\right] + \left[HCO^-_{3,aq}\right] \quad \text{Eqn. A1.133}$$

$$[H^+]_{aq} + \frac{[BH_2^{2+}]_{aq}K_{aH2}}{[H^+]_{aq}} + 2[BH_2^{2+}]_{aq} = \left[OH^-_{aq}\right] + \left[HCO^-_{3,aq}\right] \quad \text{Eqn. A1.134}$$

$$[H^+]_{aq} + \frac{[BH_2^{2+}]_{aq}K_{aH2}}{[H^+]_{aq}} + 2[BH_2^{2+}]_{aq} = \frac{K_w}{[H^+]_{aq}} + \left[HCO^-_{3,aq}\right] \quad \text{Eqn. A1.135}$$

$$[H^+]_{aq} + \frac{[BH_2^{2+}]_{aq}K_{aH2}}{[H^+]_{aq}} + 2[BH_2^{2+}]_{aq} = \frac{K_w}{[H^+]_{aq}} + \frac{\left[CO_{2,aq}\right]K_1}{[H^+]_{aq}} \quad \text{Eqn. A1.136}$$

$$[H^+]_{aq} + \frac{[BH_2^{2+}]_{aq}K_{aH2}}{[H^+]_{aq}} + 2[BH_2^{2+}]_{aq} = \frac{K_w}{[H^+]_{aq}} + \frac{K_H P_{CO2}K_1}{[H^+]_{aq}} \quad \text{Eqn. A1.137}$$

$$[H^+]_{aq} + \frac{[BH_2^{2+}]_{aq} R K_{aH1}}{[H^+]_{aq}} + 2[BH_2^{2+}]_{aq} = \frac{K_w}{[H^+]_{aq}} + \frac{K_H P_{CO2} K_1}{[H^+]_{aq}} \quad \text{Eqn. A1.138}$$

$$[H^+]_{aq} + \frac{[BH_2^{2+}]_{aq} R K_{aH1}}{[H^+]_{aq}} + 2[BH_2^{2+}]_{aq} - \frac{K_w}{[H^+]_{aq}} - \frac{K_H P_{CO2} K_1}{[H^+]_{aq}} = 0 \quad \text{Eqn. A1.139}$$

A1.10 Calculating the percent protonation of a diamine in water

$$B_0 = B_{aq} + BH_{aq}^{+} + BH_{2,aq}^{2+} \quad \text{Eqn. A1.153}$$

$$[B]_0 = [B]_{aq} + [BH^+]_{aq} + [BH_2^{2+}]_{aq} \quad \text{Eqn. A1.154}$$

$$[B]_0 = [B]_{aq} + [BH^+]_{aq} + \frac{[BH^+]_{aq}[H^+]_{aq}}{K_{aH2}} \quad \text{Eqn. A1.155}$$

$$[B]_0 = [B]_{aq} + \frac{[B]_{aq}[H^+]_{aq}}{K_{aH1}} + \frac{[B]_{aq}[H^+]_{aq}^{\ 2}}{K_{aH1}K_{aH2}} \quad \text{Eqn. A1.156}$$

$$[B]_0 = [B]_{aq}\left(1 + \frac{[H^+]_{aq}}{K_{aH1}} + \frac{[H^+]_{aq}^{\ 2}}{K_{aH1}K_{aH2}}\right) \quad \text{Eqn. A1.157}$$

$$[B]_{aq} = \frac{[B]_0}{\left(1 + \frac{[H^+]_{aq}}{K_{aH1}} + \frac{[H^+]_{aq}^{\ 2}}{K_{aH1}K_{aH2}}\right)} \quad \text{Eqn. A1.158}$$

$$\%B = \frac{[B]_{aq}}{[B]_0} \times 100\% \quad \text{Eqn. A1.159}$$

$$\%BH^+ = \frac{\%B[H^+]_{aq}}{K_{aH1}} \quad \text{Eqn. A1.160}$$

$$\%BH_2^{2+} = \frac{\%BH^+[H^+]_{aq}}{K_{aH2}} \quad \text{Eqn. A1.161}$$

$$\%P = \frac{\%BH^+ + 2 \times \%BH_2^{2+}}{2} \quad \text{Eqn. A1.162}$$

Appendix 2
QSAR Software Prediction Accuracy and Acceptability Function Details

A2.1 Description of prediction software

A2.1.1 Toxicity Estimation Software Tool

The Toxicity Estimation Software Tool (TEST), developed by the United States Environmental Protection Agency (US EPA), is a program for calculating Quantitative Structure Activity Relationships (QSARs) that relate chemical structure to toxic endpoints and physical property endpoints.[1] Several different QSAR models are available within the software.[2] These models are described in the TEST user guide as follows:[3]

- **Hierarchical method:** The toxicity for a given query compound is estimated using the weighted average of the predictions from several different models. The different models are obtained by using Ward's method to divide the training set into a series of structurally similar clusters. A genetic algorithm-based technique is used to generate models for each cluster. The models are generated prior to runtime.
- **FDA method:** The prediction for each test chemical is made using a new model that is fit to the chemicals that are most similar to the test compound. Each model is generated at runtime.
- **Single model method:** Predictions are made using a multilinear regression model that is fit to the training set (using molecular descriptors as independent variables) using a genetic algorithm-based approach. The regression model is generated prior to runtime.

- **Group contribution method:** Predictions are made using a multilinear regression model that is fit to the training set (using molecular fragment counts as independent variables). The regression model is generated prior to runtime.
- **Nearest neighbor method:** The predicted toxicity is estimated by taking an average value for the desired endpoint of the three chemicals in the training set that are most similar to the test chemical.
- **Consensus method:** The predicted toxicity is estimated by taking an average of the predicted toxicities from the above QSAR methods (provided the predictions are within the respective applicability domains).
- **Random forest method:** The predicted toxicity is estimated using a decision tree which bins a chemical into a certain toxicity score (i.e. positive or negative developmental toxicity) using a set of molecular descriptors as decision variables. The random forest method is currently only available for the developmental toxicity endpoint. The random forest models for the developmental toxicity endpoint were developed by researchers at the Mario Negri Institute for Pharmacological Research as part of the CAESAR project.[4]
- **Mode of action method:** The predicted toxicity is estimated using a two-step process. In the first step, the mode of action is determined from the linear discriminant analysis model with the highest score. In the second step, the toxicity is estimated using the multilinear regression model corresponding to the predicted mode of action. The mode of action method is currently only available for the 96 hour fathead minnow LC_{50} endpoint.

Each of these methods was constructed using data sets that are packaged with the software. The total number of compounds in each data set varied depending on which endpoint is being

considered. For example, the daphnia magna LC_{50} data set contained 353 compounds, while the melting point data set contained 9385 compounds.

In addition to the methods listed, a consensus model is available that calculates endpoints using five of the methods described above: hierarchical clustering, FDA, single-model, group contribution, and nearest neighbor. The consensus method reports the average endpoint value from these predictions. The consensus method gave the most accurate predictions during the external validation of the software.[3]

Further information regarding TEST can be found in the TEST user manual.[1]

A2.1.2 ACD/Percepta

The Percepta platform, created by Advanced Chemistry Developments, can be used to predict a wide variety of physical chemistry and toxicological properties.[5] In this thesis, ACD/Percepta was used to calculate pK_{aH} values. The method employed involved the identification of the ionizable group (e.g. trialkylamine, phenol) followed by the application of a suitable empirical equation for that ionizable group to account for the effects of the other substituents on the ionizable group. The method was optimized using 15932 structures and more than 30000 experimental values. Further information can be found in the ACD/Percepta user manual.[5]

A2.1.3 KOWWIN

KOWWIN is a QSAR program developed at Syracuse Research Corporation for calculating the partition coefficient of compounds. The program uses a fragment contribution method described by Meylan and Howard.[6] The method is validated by comparison with a data set of over 13000 compounds. KOWWIN is available as part of the US EPA's EPISUITE software.[7]

A2.1.4 OpenChemLib (OsirisP)

The OpenChemLib log K_{ow} predictor is a replicate of the OsirisP predictor, an in-house method developed by Actelion and employed in their open-source DataWarrior software.[8,9] OsirisP uses a fragment contribution method distinguishing 368 different types of fragments. The method was optimized with a test set of over 5000 compounds.

A2.2 Characterizing the accuracy of QSAR software for predicting the properties of amines

The accuracy of QSAR software for predicting the properties of amines was determined by searching databases for amines with experimentally determined values for the properties in question and comparing these experimental values with the values predicted by the software. Only amines with structures similar to those being screened for (as described in Chapter 4) were considered. Therefore, many amine-containing compounds were *not* considered for this study, such as compounds containing elements other than C, H, O, and N, as well as compounds containing acidic functional groups (e.g. carboxylic acids, phenols). Because the software was only used for predicting values for amines, it was anticipated that limiting the accuracy analysis to only suitable amine-containing compounds would give a more representative characterization of the software's accuracy than a general accuracy analysis would. Graphs of the predicted vs. experimental values for different properties are shown below (Figs. A2.1-2.11). A summary of these analyses is shown in Table A2.1.

Table A2.1 Mean absolute errors (MAEs) for different properties reported for test and training sets and as found for amines in this research.

Property	Reported MAE	MAE for amines
-log(LC_{50}) (fathead minnow, 96 h)[a]	0.545	0.32
-log(LC_{50}) (daphnia magna, 48 h)[a]	0.727	n/a[d]
-log(LD_{50}) (oral, rat)[a]	0.431	0.30
log(BAF)[a]	0.513	n/a[d]
boiling point[a]	11.460	9.0
flash point[a]	16.908	12.0
-log(vapour pressure)[a]	0.466	0.45
melting point[a]	30.207	25.7
p$K_{a\mathrm{H}}$[b]	0.4	0.2
log K_{ow}[c]	OpenChemLib: n/a[e] KOWWIN: 0.356	OpenChemLib: 0.39 KOWWIN: 0.33

[a]Using TEST software.

[b]Using ACD/Percepta software.

[c]Using OpenChemLib or KOWWIN

[d]Not enough experimental data available to determine a reliable MAE

[e]MAE for the OpenChemLib log K_{ow} prediction is not reported in the software's documentation.

A2.2.1 Log K_{ow} accuracy

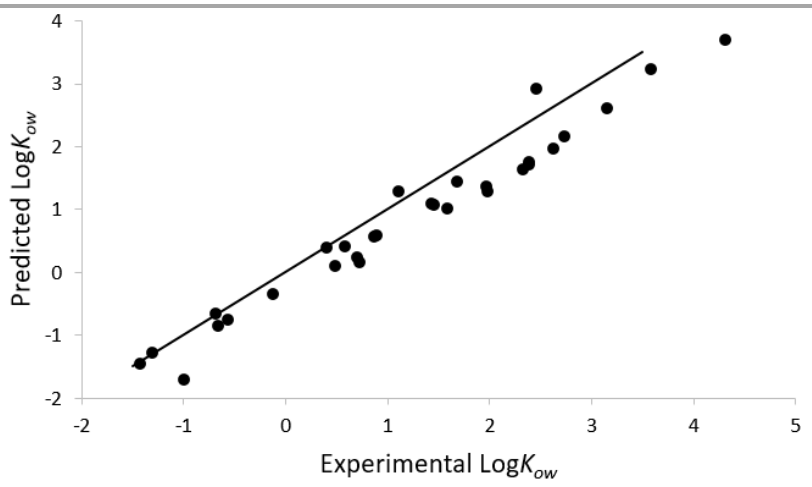

Fig. A2.1 A comparison of log K_{ow} values predicted by OpenChemLib with reported (experimental) Log K_{ow} values. The solid line represents a perfect prediction.

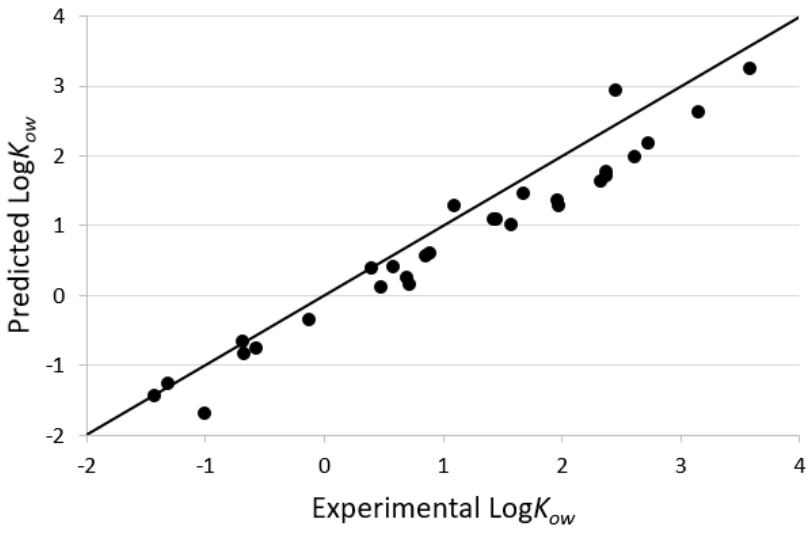

Fig. A2.2 A comparison of log K_{ow} values predicted by KOWWIN with reported (experimental) Log K_{ow} values. The solid line represents a perfect prediction.

A2.2.2 pK_{aH} accuracy

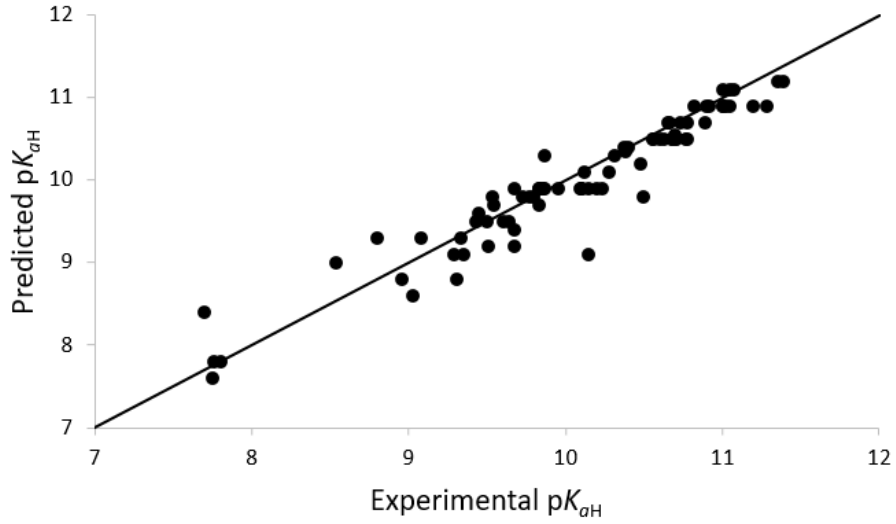

Fig. A2.3 A comparison of pK_{aH} values predicted by ACD/Percepta with reported (experimental) pK_{aH} values. The solid line represents a perfect prediction.

A2.2.3 Melting point accuracy

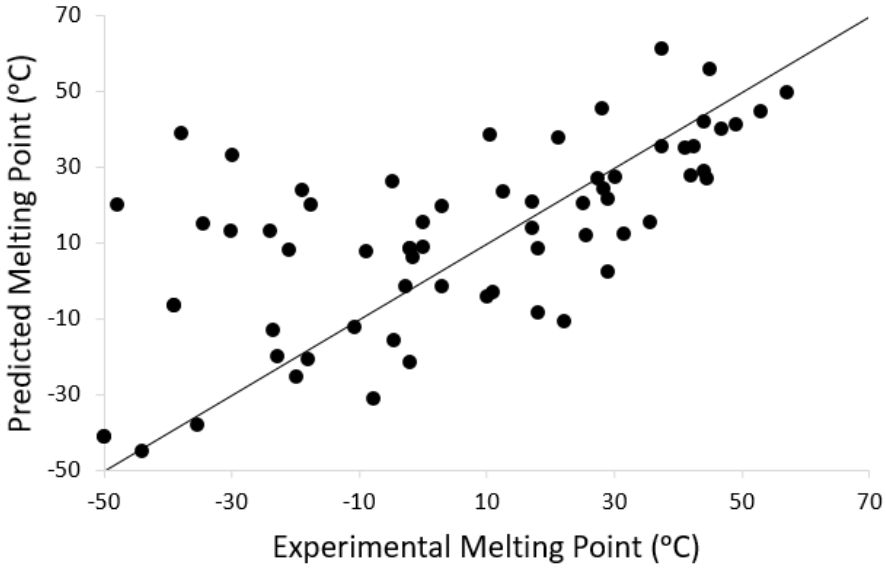

Fig A2.4 A comparison of melting points predicted by KOWWIN with reported (experimental) melting points. The solid line represents a perfect prediction.

A2.2.4 LD_{50} (oral, rat) accuracy

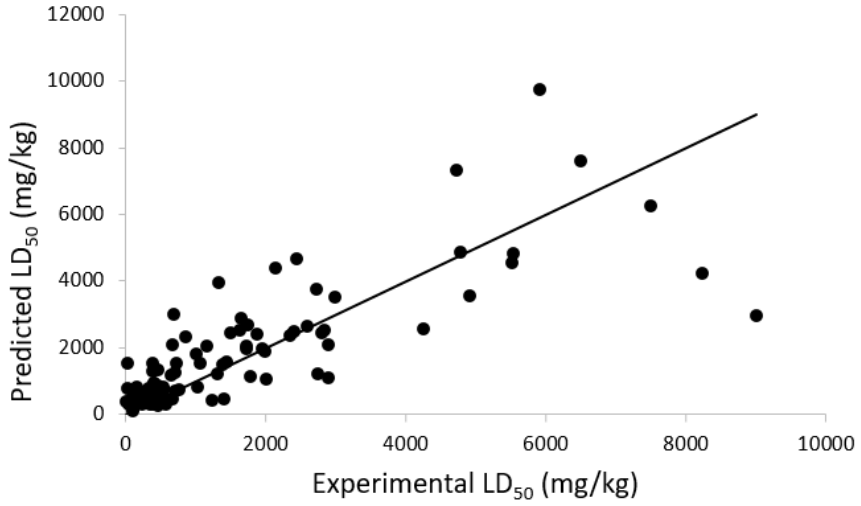

Fig. A2.5 A comparison of LD_{50} (oral, rat) values predicted by KOWWIN with reported (experimental) LD_{50} (oral, rat) values. The solid line represents a perfect prediction.

A2.2.5 LC_{50} (fathead minnow, 96 h) accuracy

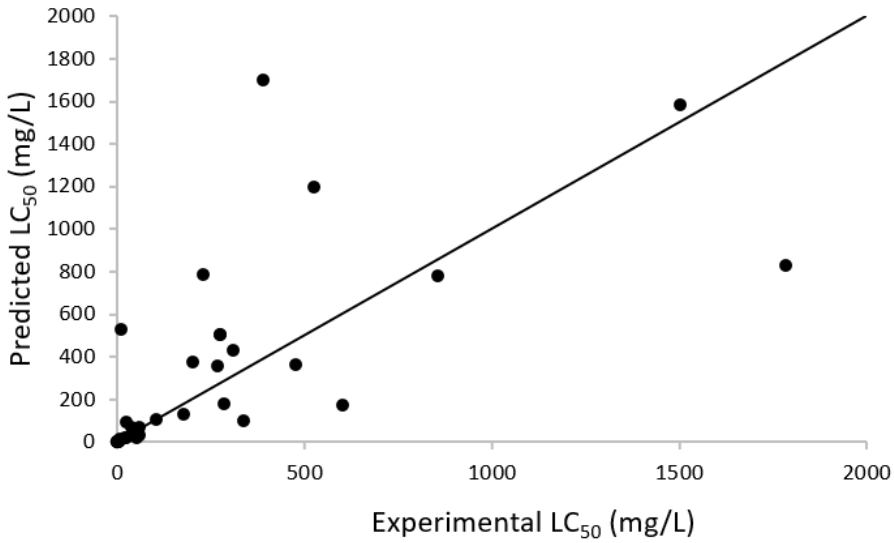

Fig. A2.6 A comparison of LC_{50} (fathead minnow, 96 h) values predicted by KOWWIN with reported (experimental) LD_{50} (fathead minnow, 96 h) values. The solid line represents a perfect prediction.

A2.2.6 LC_{50} (daphnia magna, 48 h) accuracy

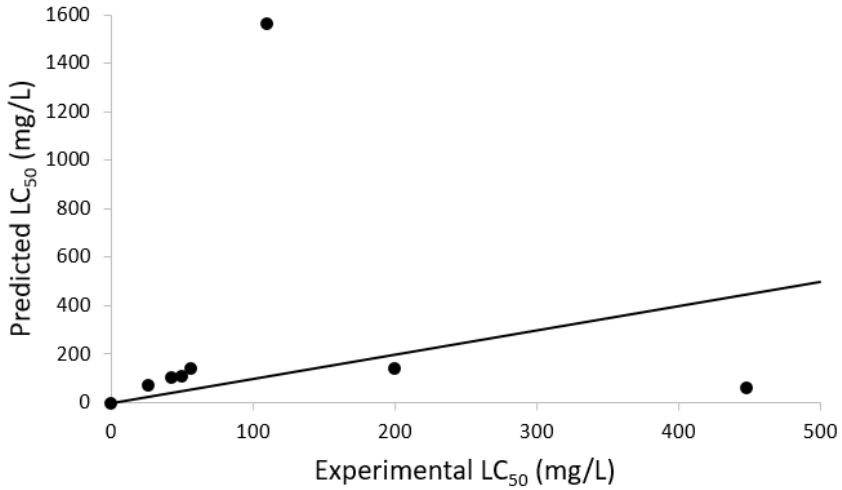

Fig. A2.7 A comparison of LC_{50} (daphnia magna, 48 h) values predicted by KOWWIN with reported (experimental) LD_{50} (daphnia magna, 48 h) values. The solid line represents a perfect prediction.

A2.2.7 Bioaccumulation factor accuracy

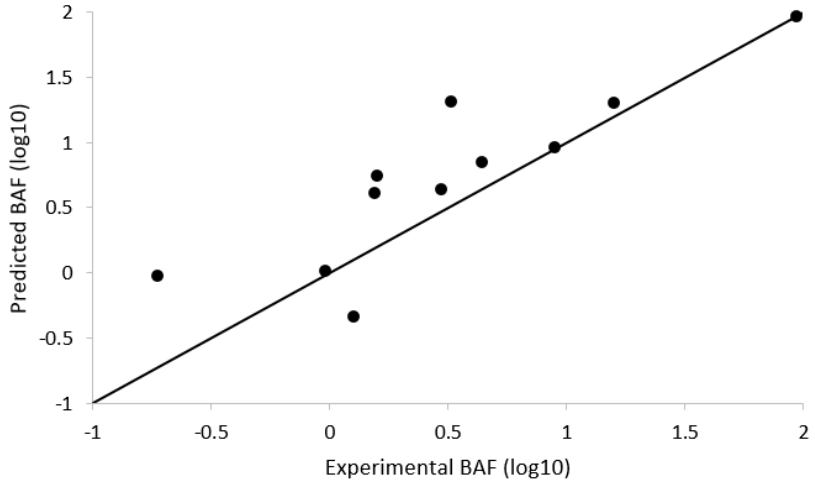

Fig. A2.8 A comparison of bioaccumulation factors predicted by KOWWIN with reported (experimental) bioaccumulation factors. The solid line represents a perfect prediction.

A2.2.8 Flash point accuracy

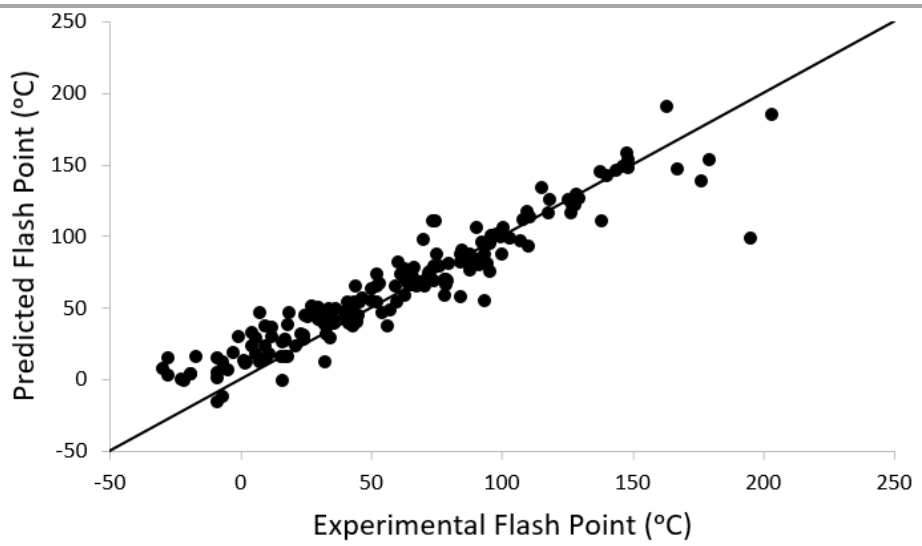

Fig. A2.9 A comparison of flash points predicted by KOWWIN with reported (experimental) flash points. The solid line represents a perfect prediction.

A2.2.9 Boiling point accuracy

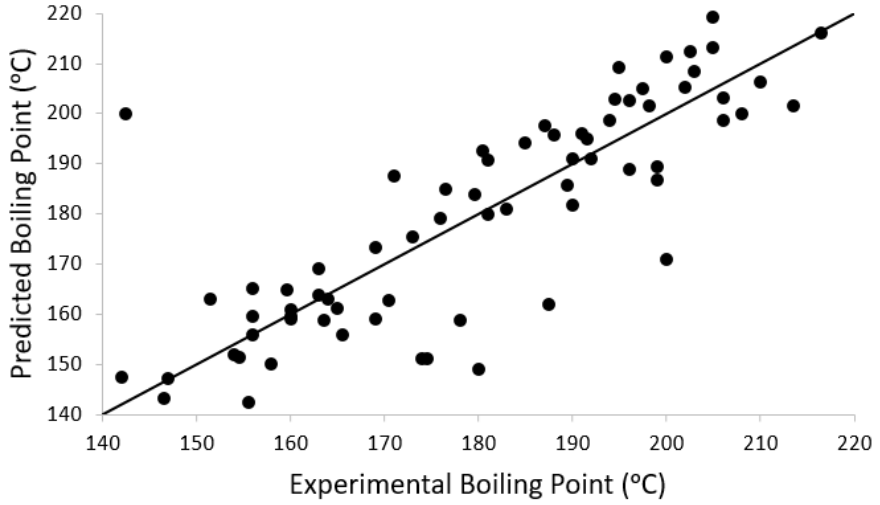

Fig. A2.10 A comparison of boiling points predicted by KOWWIN with reported (experimental) boiling points. The solid line represents a perfect prediction.

A2.2.10 Vapour pressure accuracy

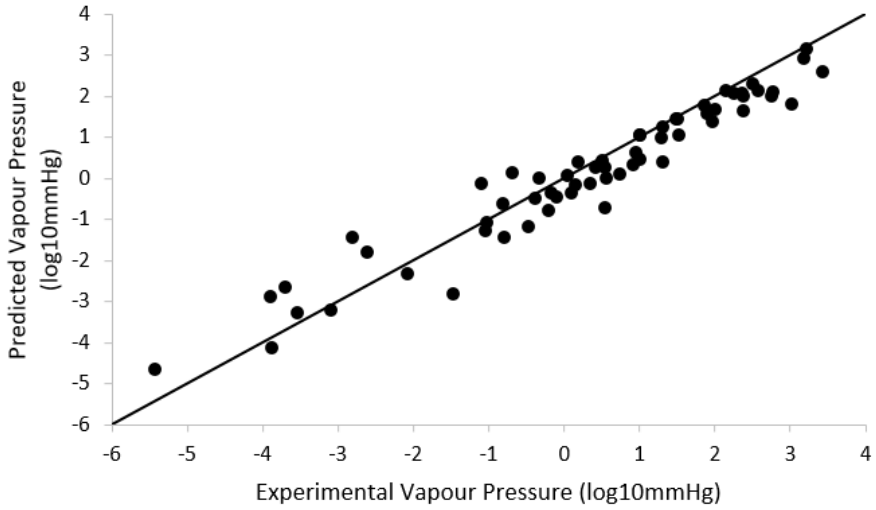

Fig. A2.11 A comparison of vapour pressures at 25 °C predicted by KOWWIN with reported (experimental) vapour pressures at 25 °C. The solid line represents a perfect prediction.

A2.2.11 Solubility accuracy

Solubility in water is a useful property to use in SHS screening because a compound cannot be a SHS if it is completely miscible with water, often reported as a solubility of 1000 g/L. The solubility predictions performed by TEST proved to be a poor predictor of miscibility with water as shown in Fig. A2.12. Compounds reported to be completely miscible with water have predicted values as low as 8 g/L. Other solubility predictors such as EPIWEB and ACD/Labs predictors had similarly poor performances. For this reason, solubility predictions were not used in this study.

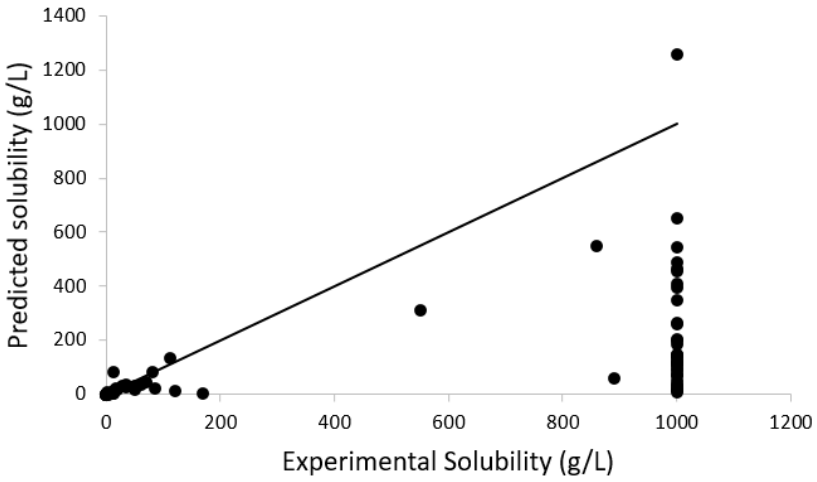

Fig. A2.12 A comparison of aqueous solubilities at 25 °C predicted by TEST with reported (experimental) solubilities at 25 °C. The solid line represents a perfect prediction.

A2.3 Acceptability functions used in virtual screening processes

Acceptability functions were created as described in Chapter 4 by accounting for the accuracy of the predictions when determining how acceptable a predicted value is. The acceptability functions are listed in the next subsection and graphs of the functions fit to target values are displayed as well.

A2.3.1 Log K_{ow}

Three different log K_{ow} functions were made: one for predictions made with the OpenChemLib predictor and two for predictions made with the KOWWIN predictor. Two acceptability functions are required for log K_{ow} because SHSs have both an upper and a lower limit. However, for the predictions made with OpenChemLib in Chapter 4, an upper cutoff value of log K_{ow} = 2.6 was used as an initial filter to decrease the computation time. Compounds with predicted log K_{ow} > 2.60 were rejected. This initial cutoff value was sufficient to eliminate all structures with low acceptability values from the upper log K_{ow} acceptability function. Therefore, only a lower log K_{ow} acceptability function was used in Chapter 4.

Lower log K_{ow} acceptability function for OpenChemLib predictions (target value: log $K_{ow} \geq 1.2$):

$$A_{logKow} = \frac{1}{1+\left(\frac{25.85}{logKow+24.29}\right)^{196.96}} \quad \text{Eqn. A2.1}$$

Lower log K_{ow} acceptability function for KOWWIN predictions (target value: log $K_{ow} \geq 2.0$):

$$A_{Kow} = \frac{1}{1+\left(\frac{25.17}{\log K_{ow}+23.02}\right)^{169.98}} \quad \text{Eqn. A2.2}$$

Upper log K_{ow} acceptability function for KOWWIN predictions (target value: log $K_{ow} \leq 5.0$):

$$A_{Kow} = \frac{1}{1+\left(\frac{11.19}{\log K_{ow}+6.53}\right)^{-75.11}} \quad \text{Eqn. A2.3}$$

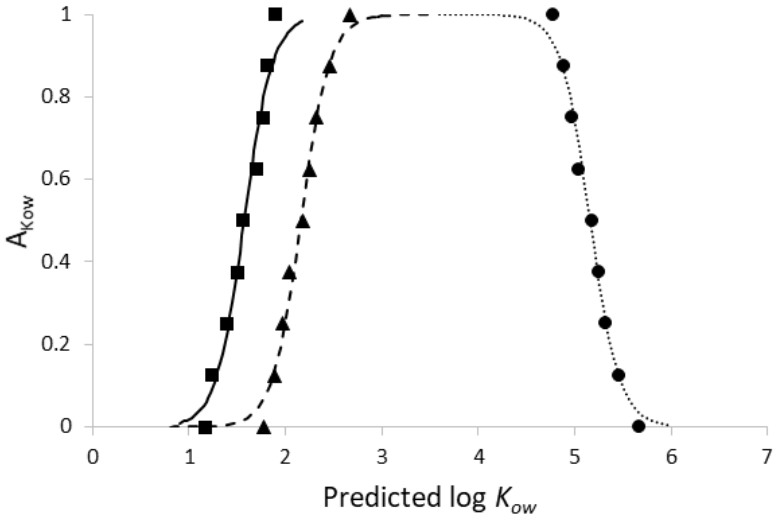

Fig A2.13 A graph showing the acceptability functions for A_{KOW}. The lines represent the A_{KOW} calculated by the equations for a given log K_{ow}. The dots represent the data that the acceptability functions were fit to, i.e. the 10th, 20th, 30th, …. 90th percentile deviations from the target value. Data are included for the lower log K_{ow} value for monoamines used in Chapter 4 (solid line and squares), the lower log K_{ow} value for diamines used in Chapter 6 (dashed line and triangles), and the upper log K_{ow} value for diamines used in Chapter 6 (dotted line and circles).

A2.3.2 pK_{aH}

Lower pK_{aH} acceptability function for ACD/Percepta predictions (target value: p$K_{aH} \geq 9.0$)

$$A_{pKa} = \frac{1}{1+\left(\frac{9.06}{pKa-0.0339}\right)^{107.28}} \qquad \text{Eqn. A2.4}$$

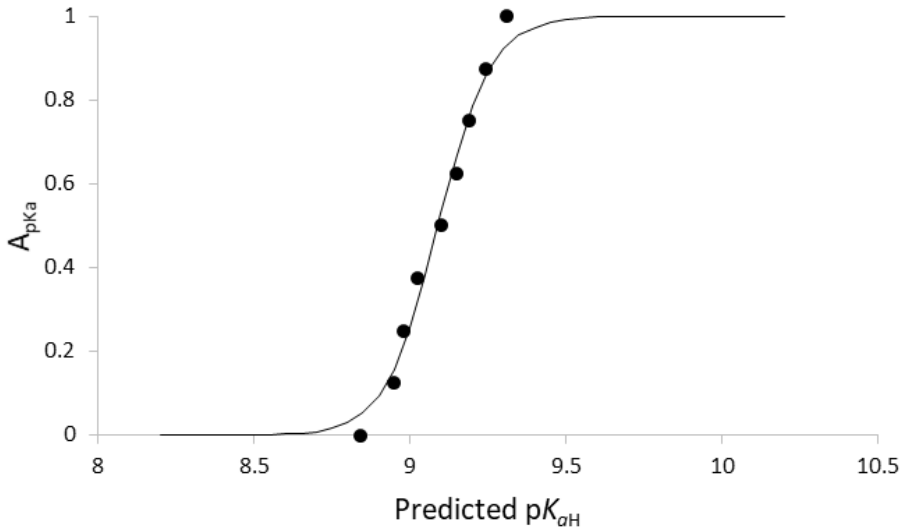

Fig A2.14 A graph showing the acceptability functions for A_{pKa}. The line represents the A_{pKa} calculated by the equation for a given pK_{aH}. The dots represent the data that the acceptability functions were fit to, i.e. 10th, 20th, 30th, …. 90th percentile deviations from the target value.

A2.3.3 Melting point

Upper melting point acceptability function for TEST predictions (target value: melting point ≤ 25 °C):

$$A_{MP} = \frac{1}{1+\left(\frac{59.53}{75-MP}\right)^5} \quad \text{Eqn. A2.5}$$

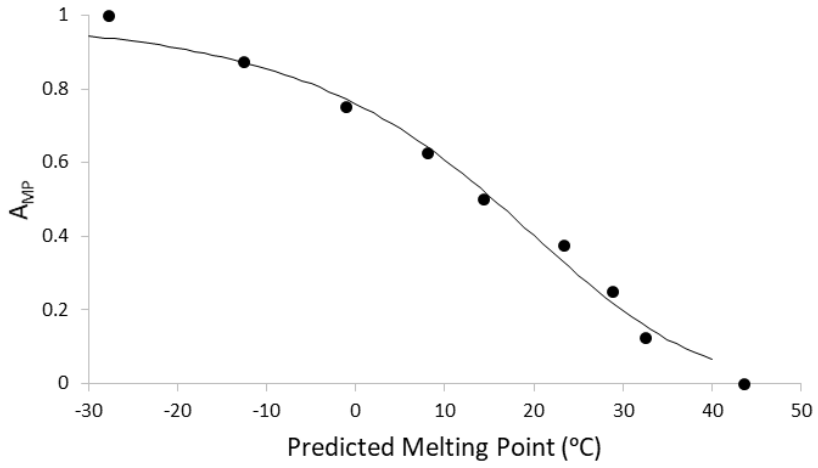

Fig A2.15 A graph showing the acceptability functions for A_{MP}. The line represents the A_{MP} calculated by the equation for a given melting point. The dots represent the data that the acceptability functions were fit to, i.e. the 10th, 20th, 30th, …. 90th percentile deviations from the target value.

A2.3.4 LD_{50} (oral, rat)

Lower LD_{50} acceptability function for TEST prediction (target value: $LD_{50} \geq 2000$ mg/kg):

$$A_{LD50} = \frac{1}{1+\left(\frac{1255.33}{LD_{50_{rat}}-121.86}\right)^{2.89}} \quad \text{Eqn. A2.6}$$

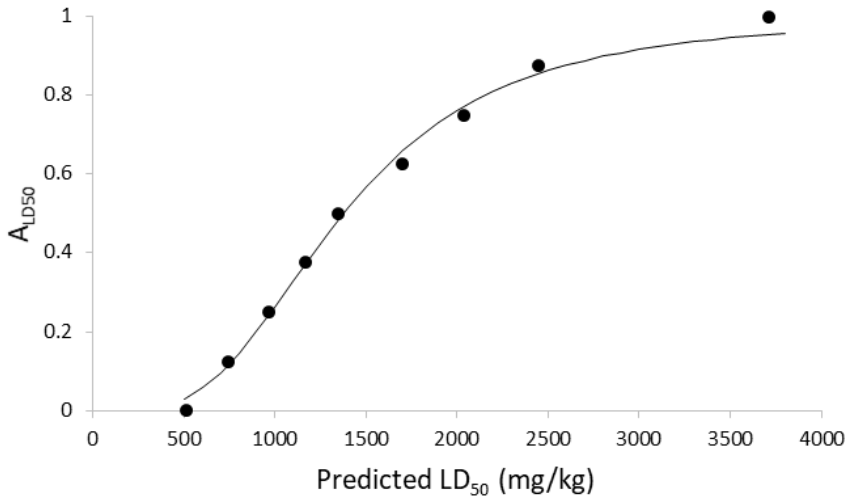

Fig A2.16 A graph showing the acceptability functions for A_{LD50}. The line represents the A_{LD50} calculated by the equation for a given LD_{50} value. The dots represent the data that the acceptability functions were fit to, i.e. the 10th, 20th, 30th, …. 90th percentile deviations from the target value.

A2.3.5 LC_{50} (fathead minnow, 96 h)

Lower LC_{50} acceptability function for TEST prediction (target value: $LC_{50} \geq 100$ mg/L):

$$A_{FMLC50} = \frac{1}{1+\left(\frac{73.92}{FMLC_{50}+3.24}\right)^{2.6}} \quad \text{Eqn. A2.7}$$

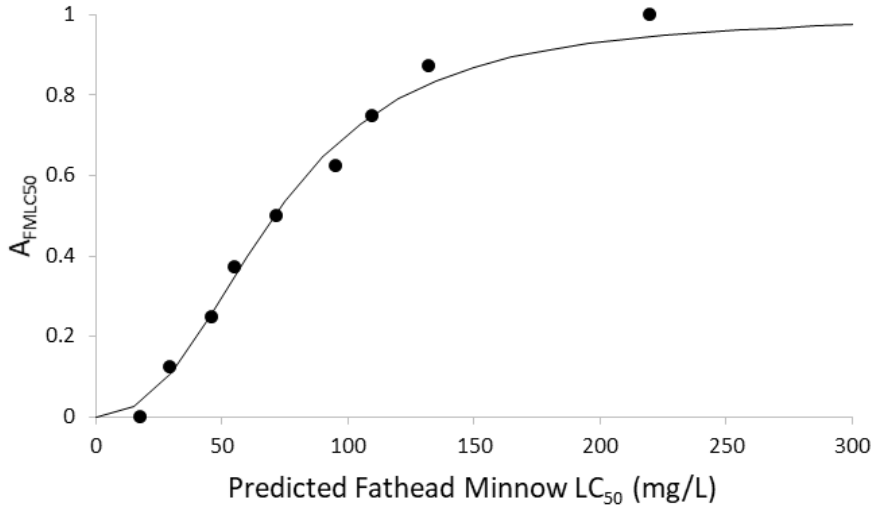

Fig A2.17 A graph showing the acceptability functions for A_{FMLC50}. The line represents the A_{FMLC50} calculated by the equation for a given LC_{50} (fathead minnow, 96 h) value. The dots represent the data that the acceptability functions were fit to, i.e. the 10^{th}, 20^{th}, 30^{th}, …. 90^{th} percentile deviations from the target value.

A2.3.6 LC_{50} (daphnia magna, 48 h)

Insufficient experimentally determined values were found to characterize the accuracy of the TEST predictions, therefore compounds were assigned acceptability values based on a linear acceptability function. LC_{50} values <10 mg/L were assigned an acceptability value of 0, LC_{50} values >200 mg/L were assigned an acceptability value of 1, and intermediate LC_{50} values were assigned an acceptability according to the following function:

$$A_{DMLC50} = 0.0053 \times DM_{LC50} - 0.06 \qquad \text{Eqn. A2.8}$$

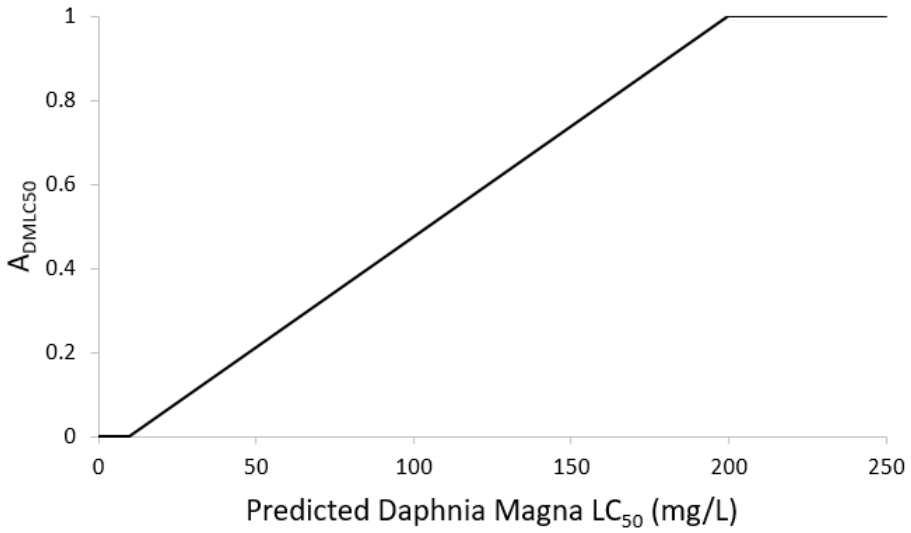

Fig A2.18 A graph showing the acceptability functions for A_{DMLC50}. The line represents the A_{DMLC50}, calculated as described above.

A2.3.7 Bioaccumulation factor

Insufficient experimentally determined values were found to characterize the accuracy of the TEST predictions, therefore any compound with a bioaccumulation factor less than 500 was assigned an acceptability (A_{BAF}) of 1 and any compound with a bioaccumulation factor 500 or greater was assigned an acceptability of 0.

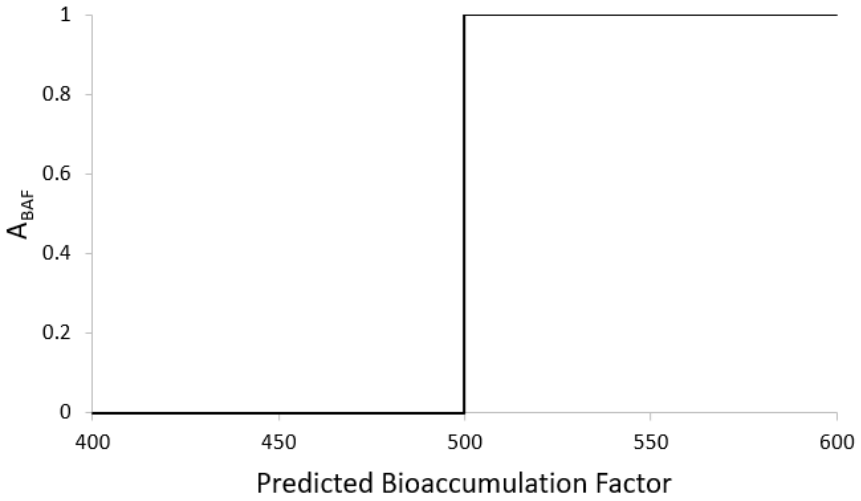

Fig A2.19 A graph showing the acceptability functions for A_{BAF}. The line represents the A_{BAF}, calculated as described above.

A2.3.8 Flash point

Lower flash point acceptability function for TEST prediction (target value: flash point ≥ 80 °C):

$$A_{FP} = \frac{1}{1+\left(\frac{74.01}{FP-2.87}\right)^{16.73}} \quad \text{Eqn A2.9}$$

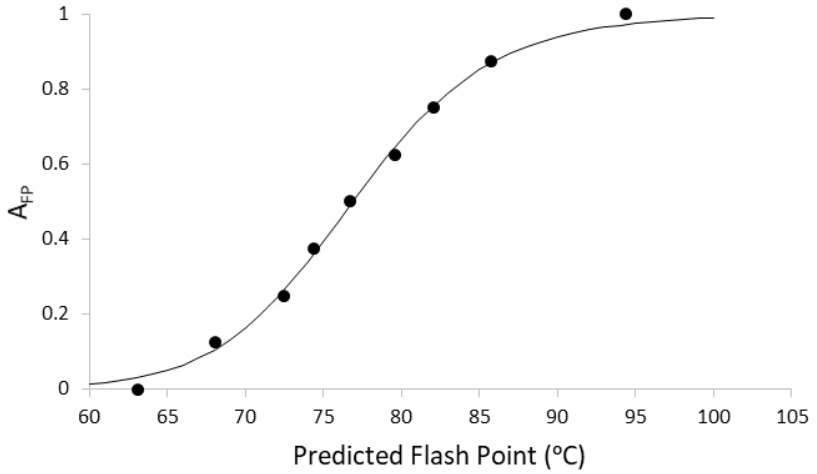

Fig A2.20 A graph showing the acceptability functions for A_{FP}. The line represents the A_{FP} calculated by the equation for a given flash point. The dots represent the data that the acceptability functions were fit to, i.e. the 10th, 20th, 30th, …. 90th percentile deviations from the target value.

A2.3.9 Boiling point

Lower boiling point acceptability function for TEST prediction (target value: boiling point ≥ 180 °C):

$$A_{BP} = \frac{1}{1+\left(\frac{138.8}{BP-38.22}\right)^{35.62}}$$ Eqn A2.10

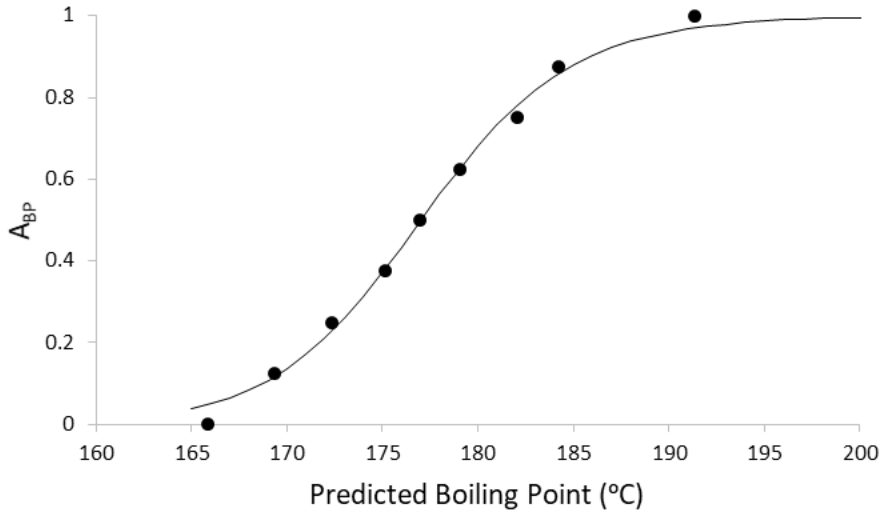

Fig A2.21 A graph showing the acceptability functions for A_{BP}. The line represents the A_{BP} calculated by the equation for a given boiling point. The dots represent the data that the acceptability functions were fit to i.e. the 10th, 20th, 30th, …. 90th percentile deviations from the target value.

A2.3.10 Vapour pressure

The vapour pressure acceptability of each compound was assigned a value based on the likely intensity of the odour of the compound. Vapour pressures less than 0.03 torr, or -1.5 on a logarithmic scale, were assumed to correspond to an odourless compound and were assigned an acceptability of 1. Vapour pressures more than 0.5 torr, or -0.3 on a logarithmic scale, were assigned an acceptability of 0. Compounds with intermediate vapour pressures predicted by TEST were assigned an acceptability according to the following function (based on the log of their vapour pressure):

$$A_{VP} = -1 - 0.6667 \times logVP \qquad \text{Eqn. A2.11}$$

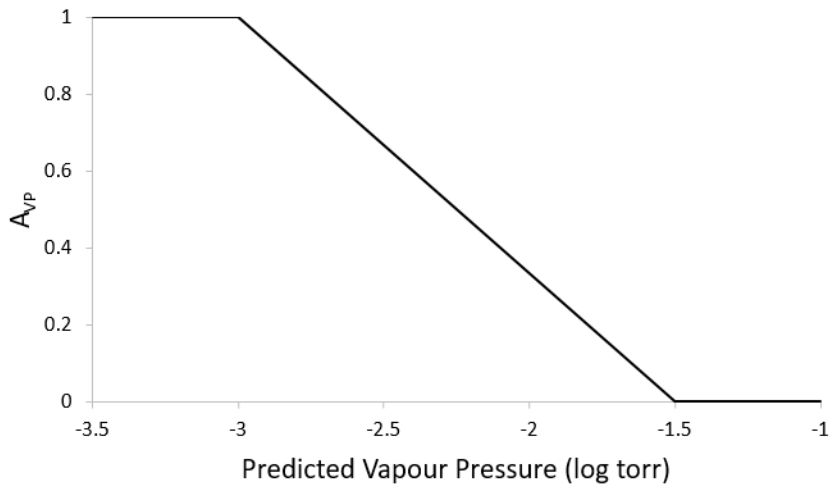

Fig A2.22 A graph showing the acceptability functions for A_{VP}. The line represents the A_{VP}, calculated as described above.

A2.4 References

1) Toxicity Estimation Software Tool (TEST) v4.1, US EPA. https://www.epa.gov/chemical-research/toxicity-estimation-software-tool-test (accessed Jan. 29, 2018).

2) T. M. Martin, P. Harten, R. Venkatapathy, S. Das and D. M. Young, *Toxicol. Mech. Methods*, 2008, **18**, 251–266.

3) US EPA, User's Guide for T.E.S.T. (version 4.2) (Toxicity Estimation Software Tool) A Program to Estimate Toxicity from Molecular Structure, https://www.epa.gov/chemical-research/users-guide-test-version-42-toxicity-estimation-software-tool-program-estimate (accessed October 26, 2017).

4) CAESAR, http://www.caesar-project.eu/index.php?page=results&section=endpoint&ne=5 (accessed October 26, 2017).

5) *ACD/Percepta, version 12.0,* Advanced Chemistry Development, Inc., Toronto, ON, Canada, www.acdlabs.com, 2014.

6) W. M. Meylan and P. H. Howard, *J. Pharm. Sci.*, 1995, **84**, 83–92.

7) *Estimation Programs Interface Suite for Microsoft Windows*, US EPA, Washington, DC, USA, 2012.

8) T. Sander, J. Freyss, M. von Korff and C. Rufener, *J. Chem. Inf. Model.*, 2015, **55**, 460–473.

9) www.openmolecules.org, http://www.openmolecules.org/datawarrior/index.html, (accessed 26 October 2017).

Appendix 3

^{1}H NMR and crystallography data

A3.1 ^{1}H NMR data

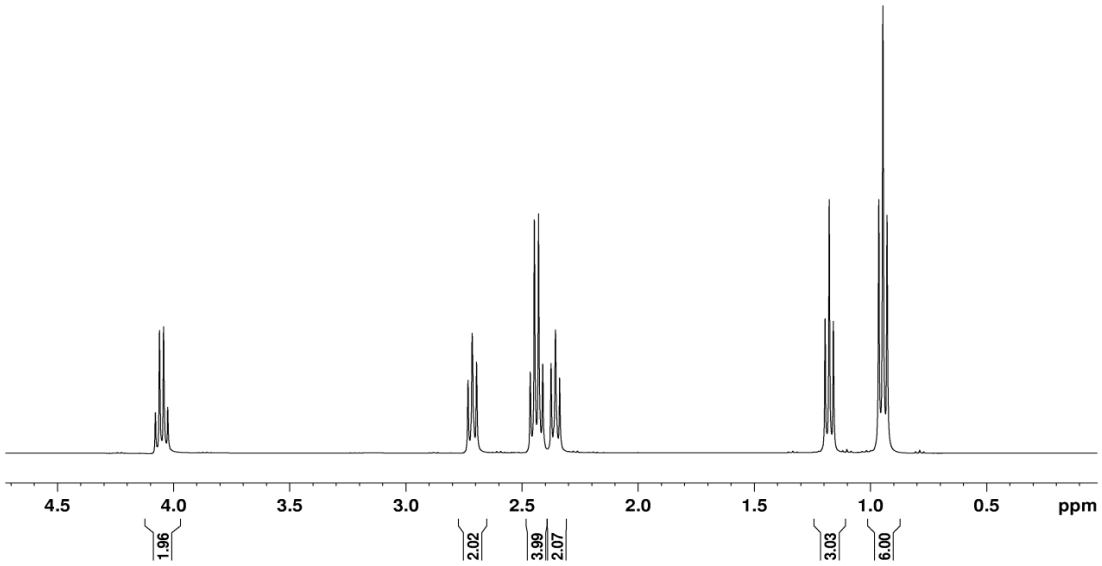

Fig A3.1 ^{1}H NMR spectrum of ethyl 3-(diethylamino)propanoate in chloroform-d.

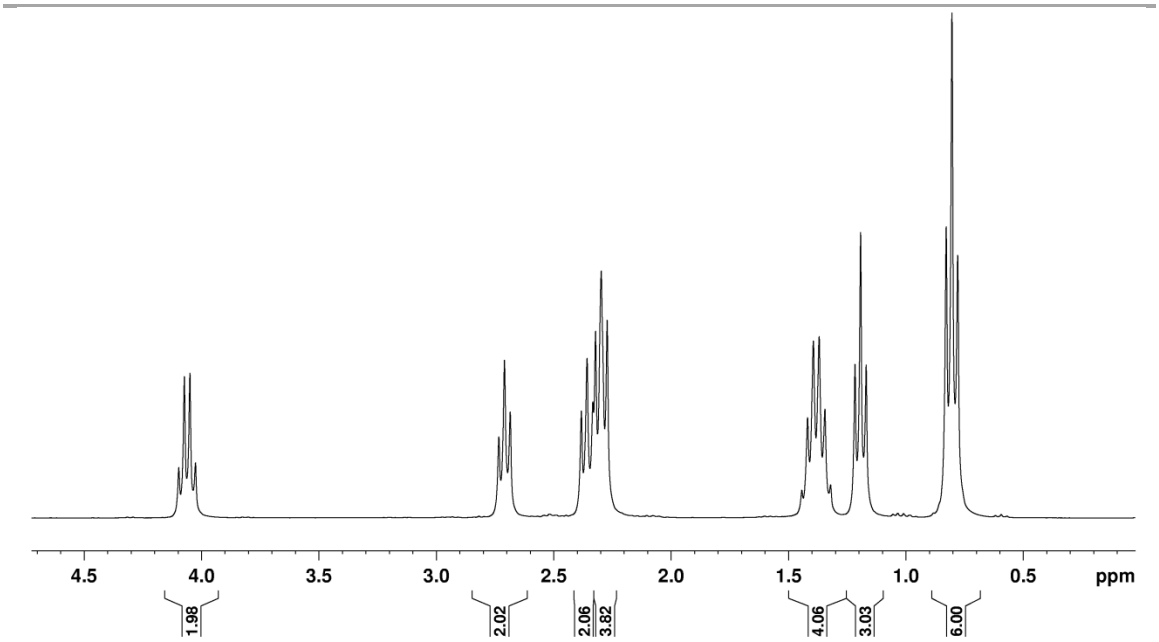

Fig A3.2 ^{1}H NMR spectrum of ethyl 3-(dipropylamino)propanoate in chloroform-d.

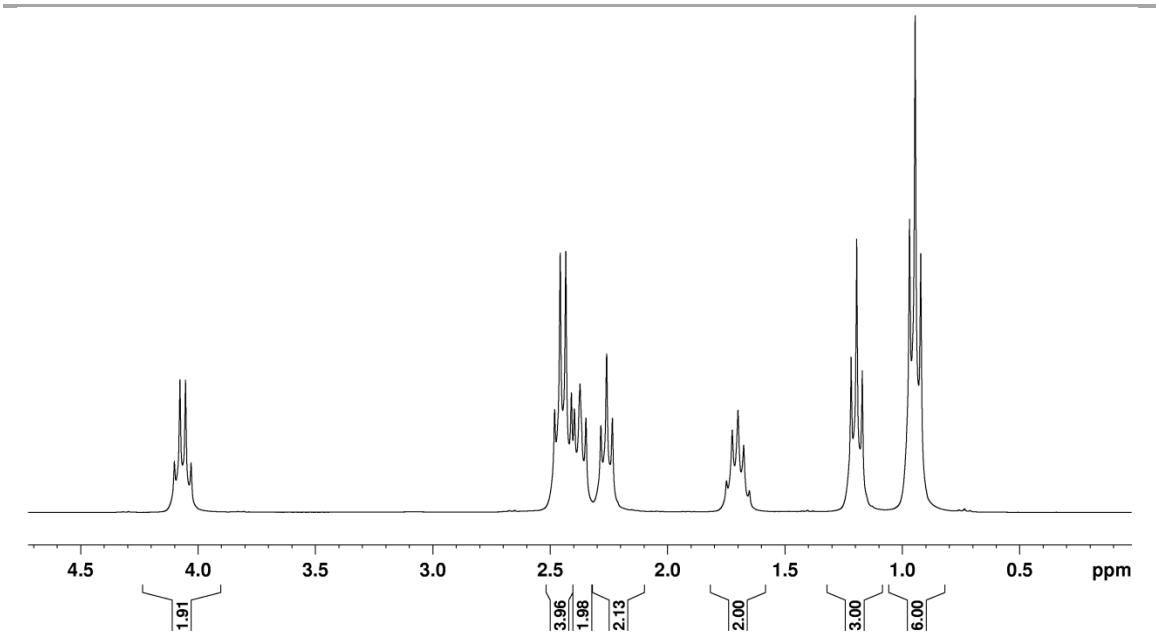

Fig A3.3 ^{1}H NMR spectrum of ethyl 4-(diethylamino)butanoate in chloroform-d.

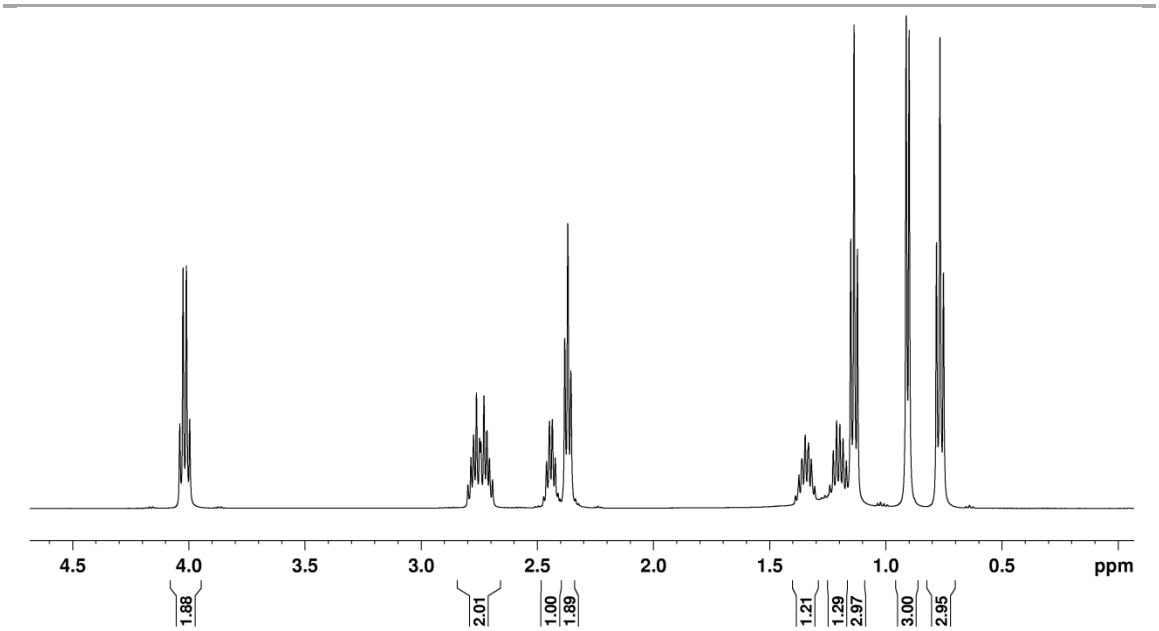

Fig A3.4 ^{1}H NMR spectrum of ethyl 3-(*sec*-butylamino)propanoate in chloroform-d.

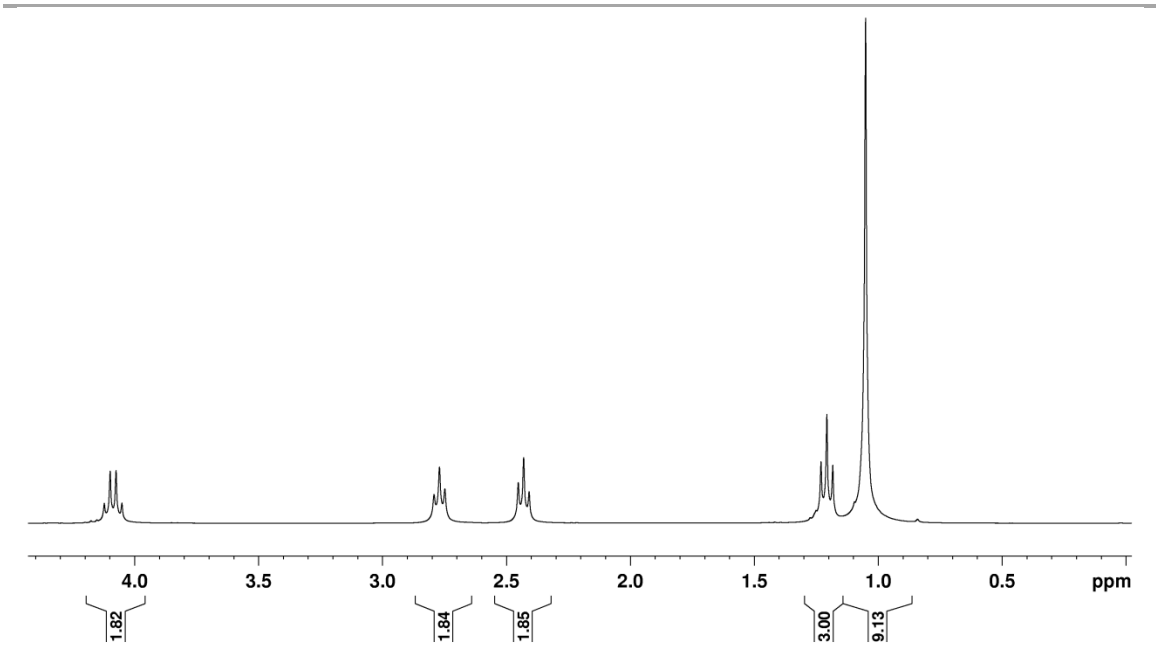

Fig A3.5 ^{1}H NMR spectrum of ethyl 3-(*tert*-butylamino)propanoate in chloroform-d.

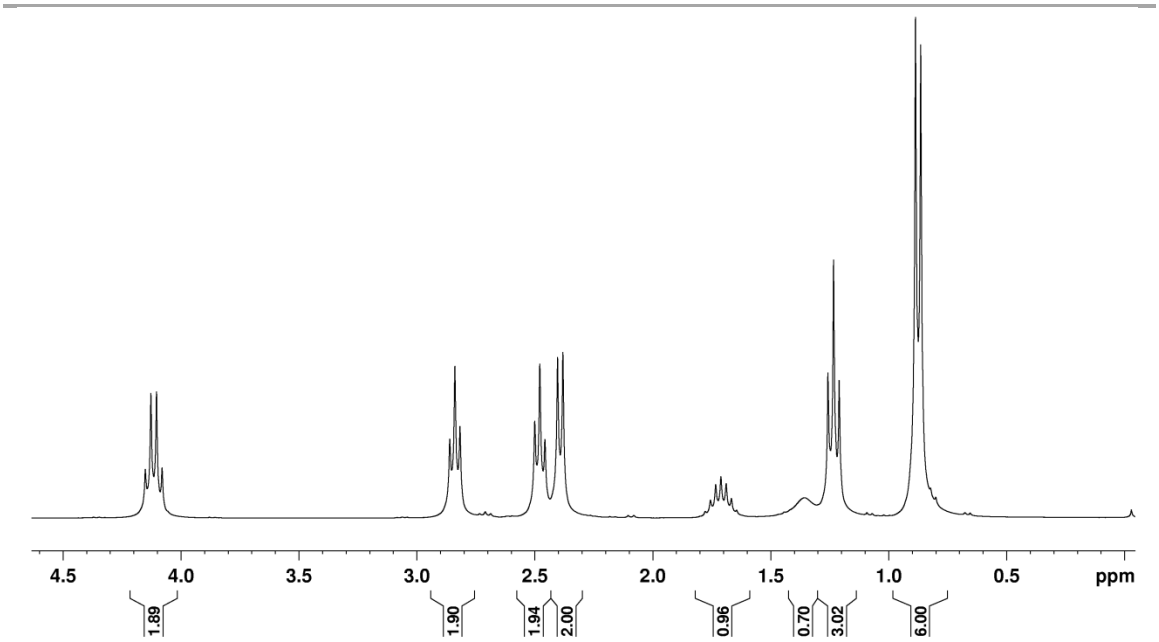

Fig A3.6 ^{1}H NMR spectrum of ethyl 3-(isobutylamino)propanoate in chloroform-d.

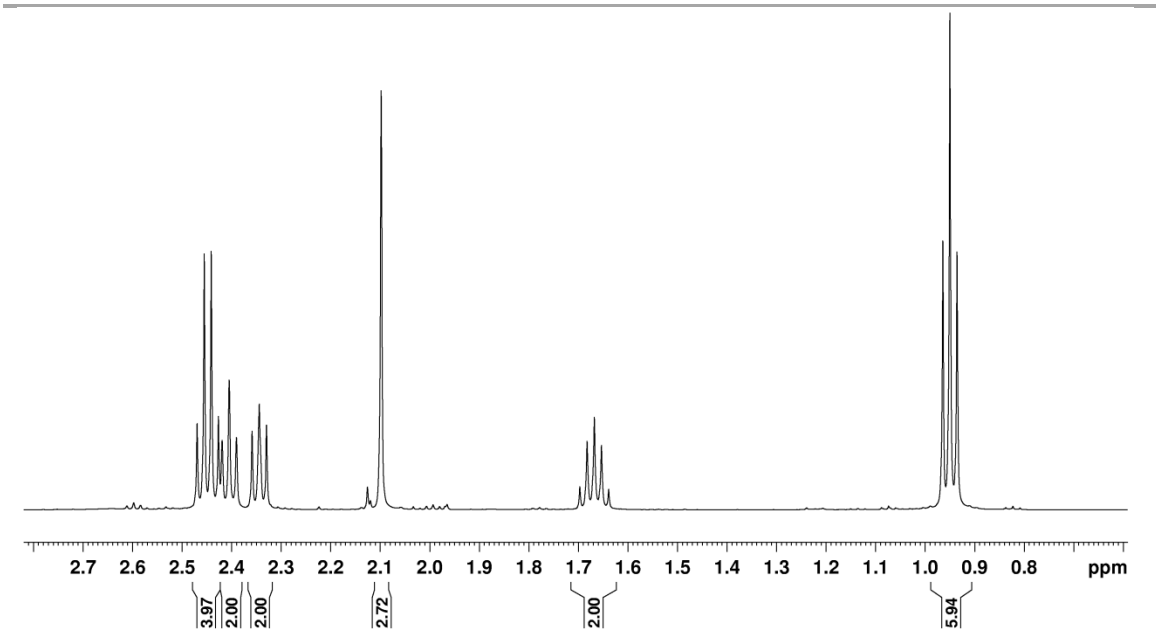

Fig A3.7 ^{1}H NMR spectrum of 5-(diethylamino)pentan-2-one in chloroform-d.

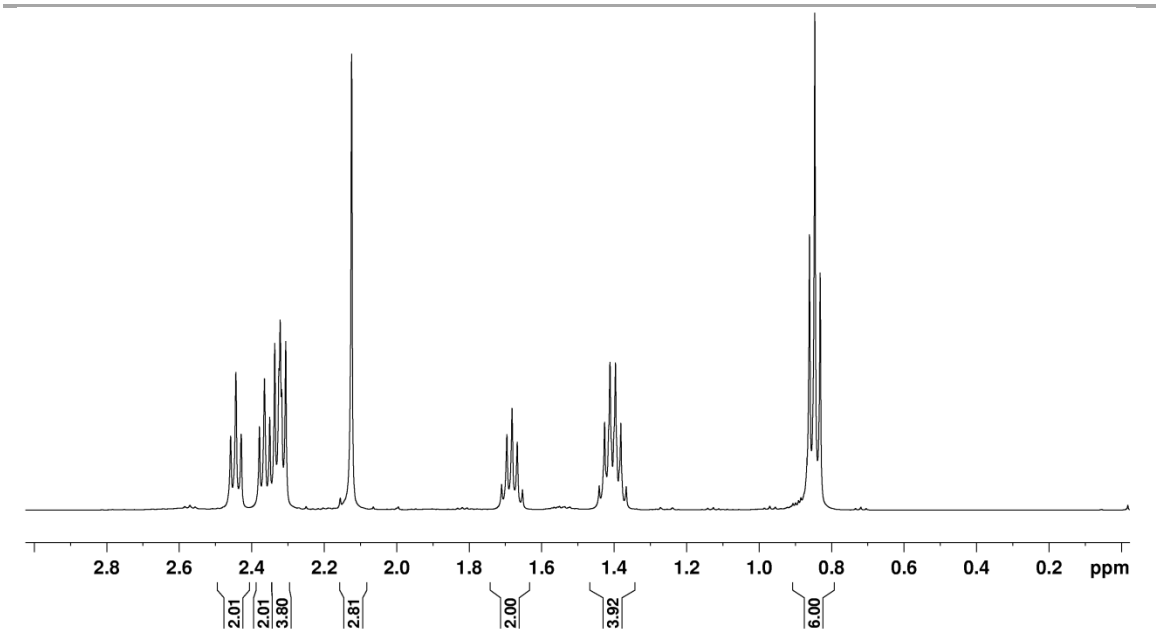

Fig A3.8 ^{1}H NMR spectrum of 5-(dipropylamino)pentan-2-one in chloroform-d.

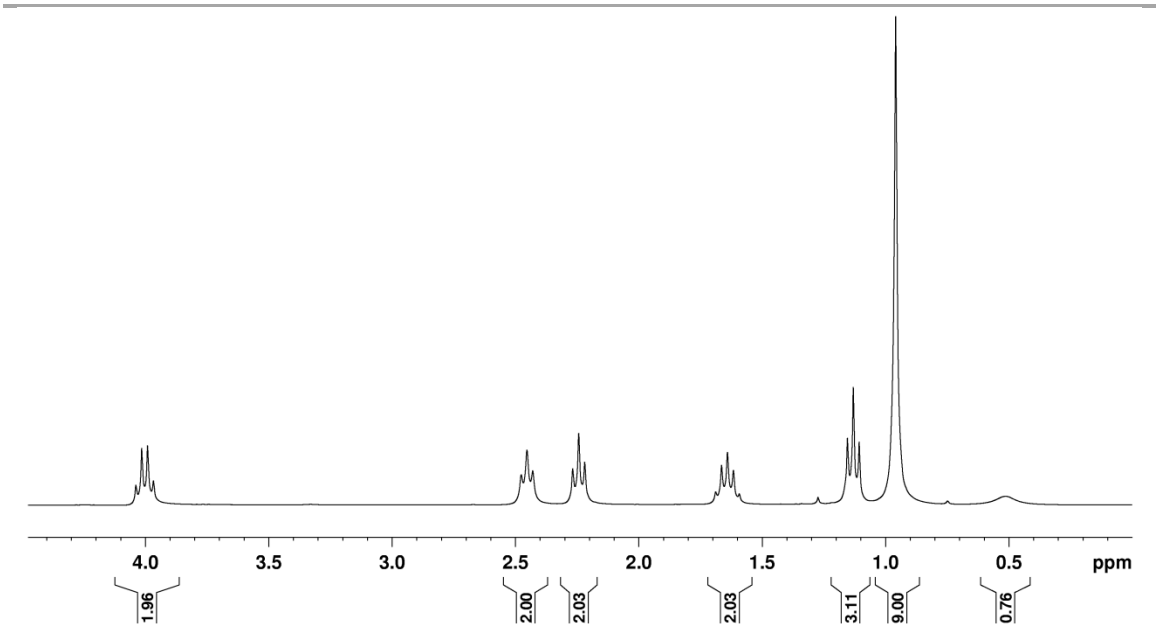

Fig A3.9 ^{1}H NMR spectrum of ethyl 4-(*tert*-butylamino)butanoate in chloroform-d.

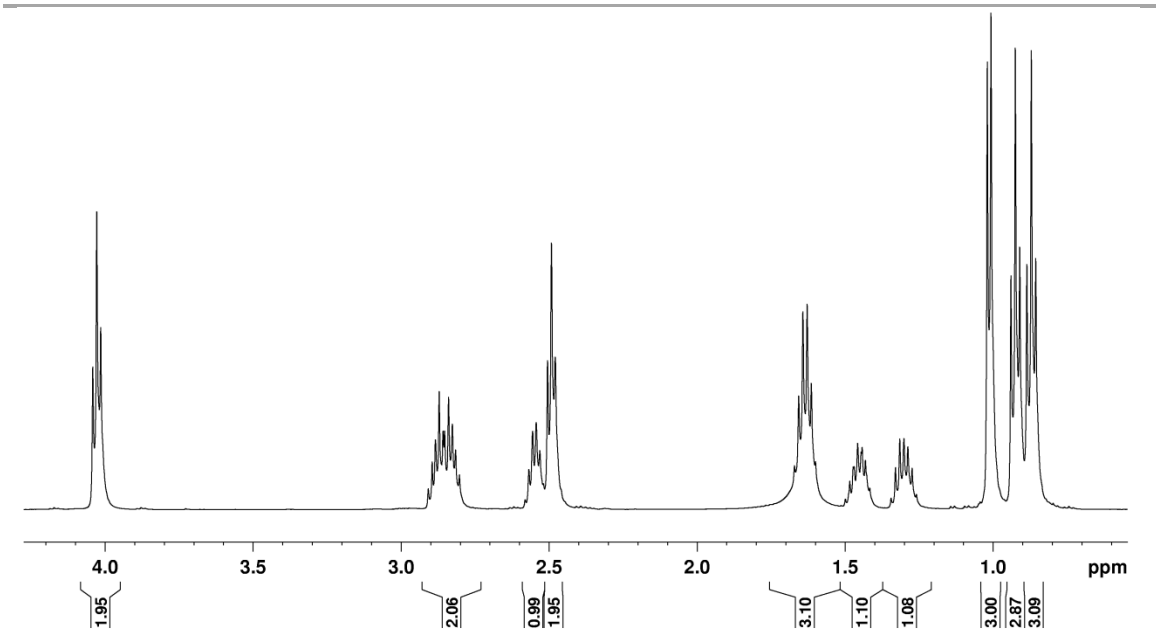

Fig A3.10 ^{1}H NMR spectrum of propyl 3-(*sec*-butylamino)propanoate in chloroform-d.

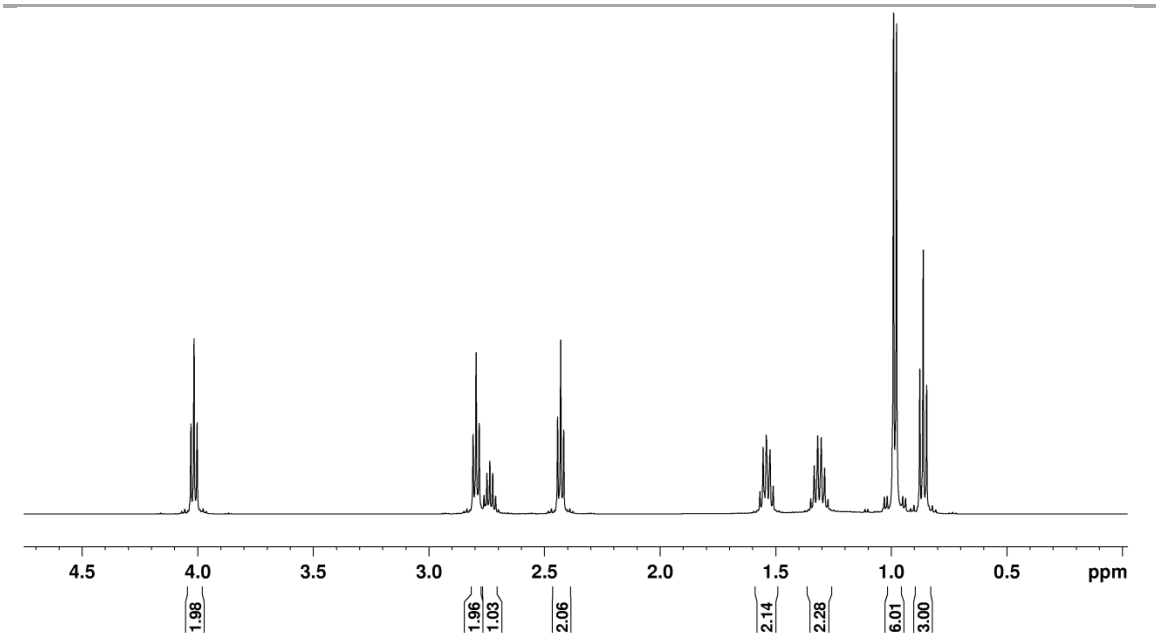

Fig A3.11 ^{1}H NMR spectrum of butyl 3-(isopropylamino)propanoate chloroform-d.

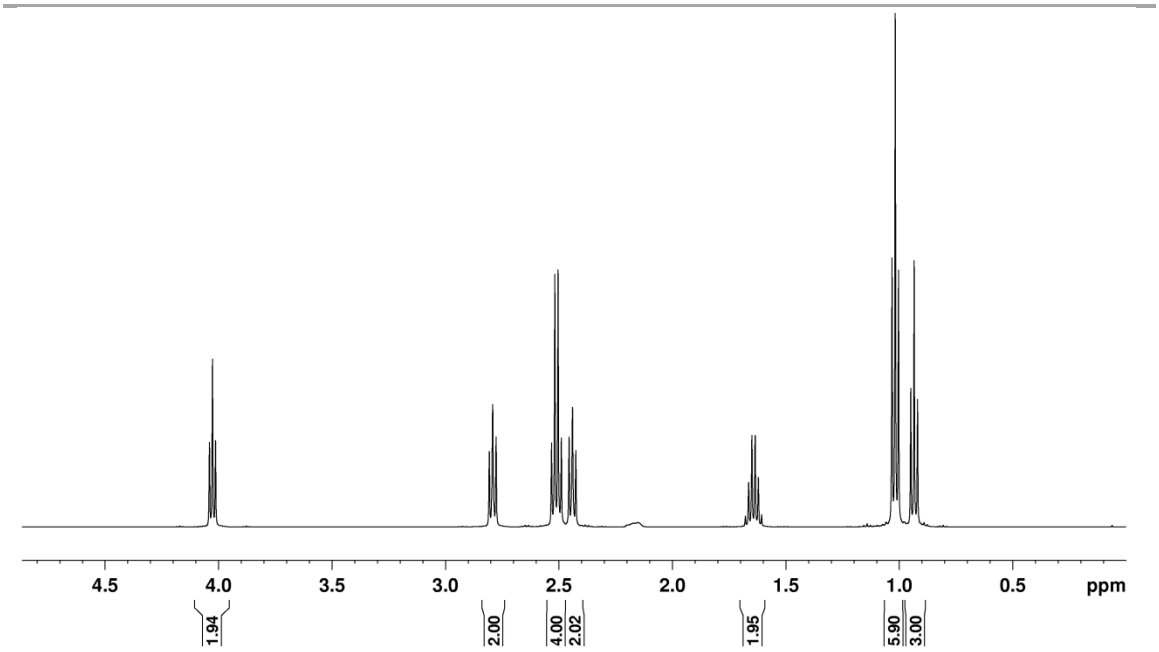

Fig A3.12 ^{1}H NMR spectrum of propyl 3-(diethylamino)propanoate in chloroform-d.

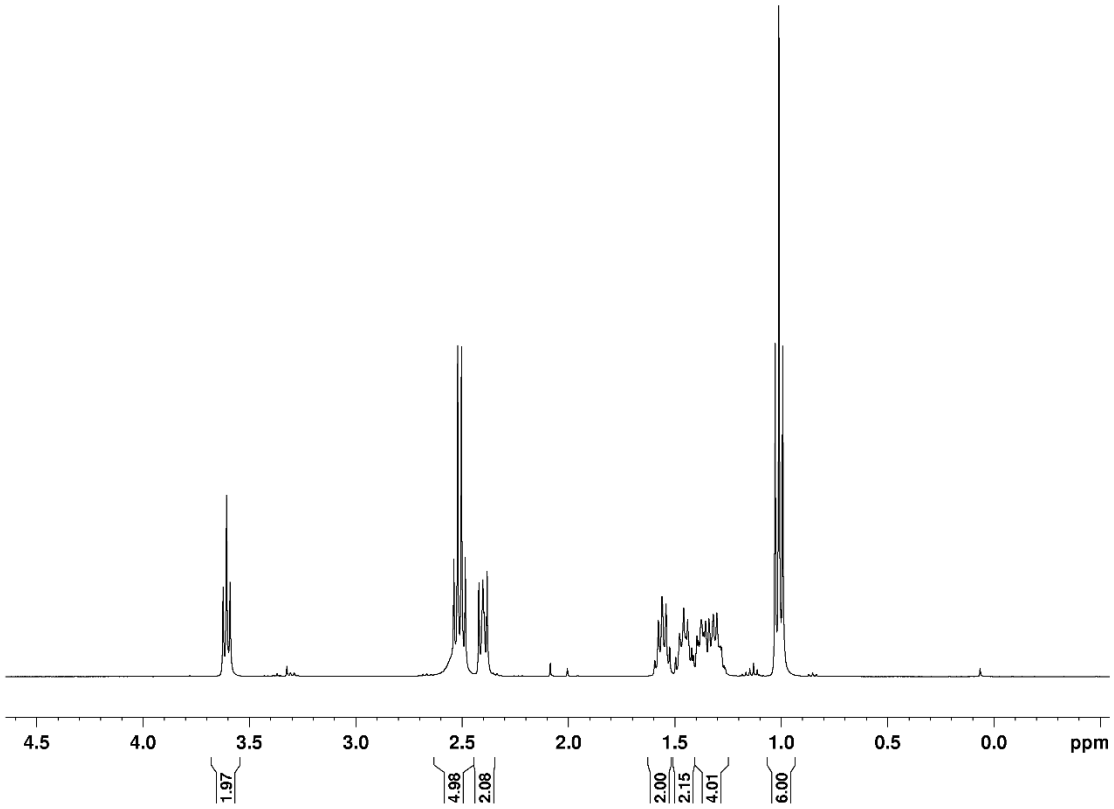

Fig A3.13 ^{1}H NMR spectrum of 6-diethylamino-1-hexanol in chloroform-d.

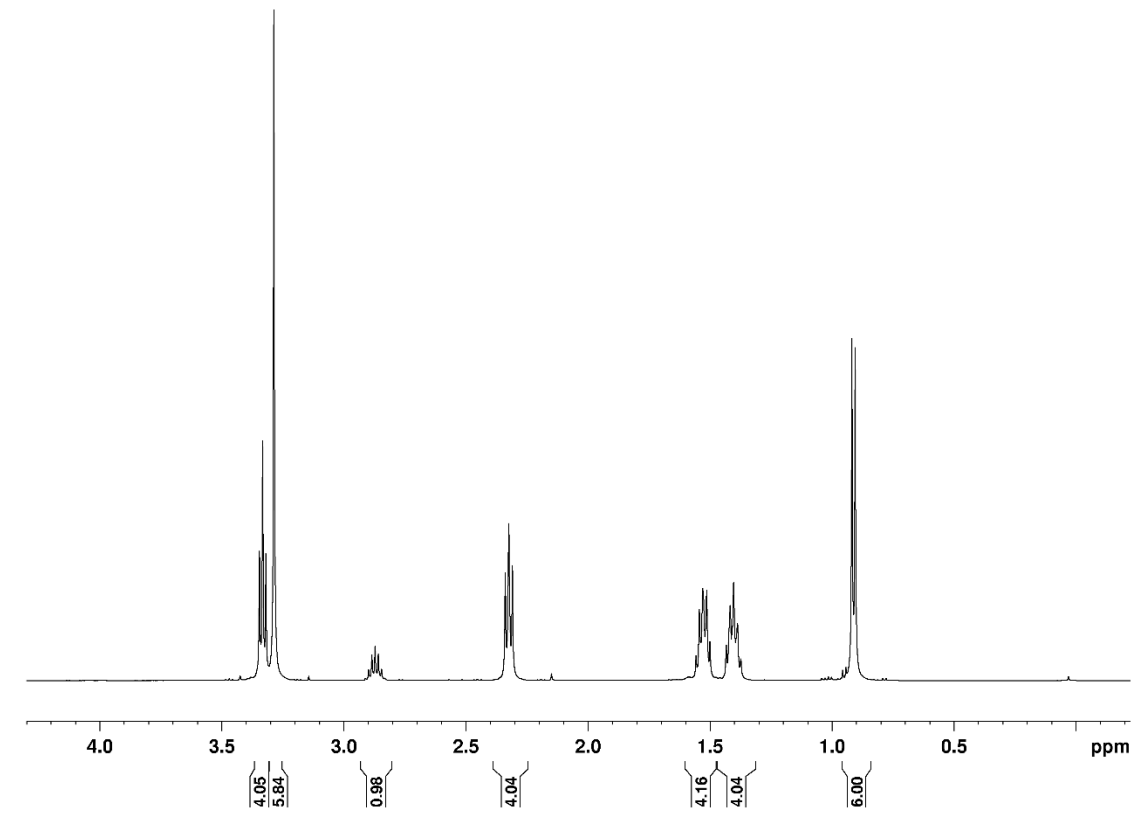

Fig A3.14 ^{1}H NMR spectrum of di-*N*,*N*-(4-methoxybutyl)isopropylamine in chloroform-d.

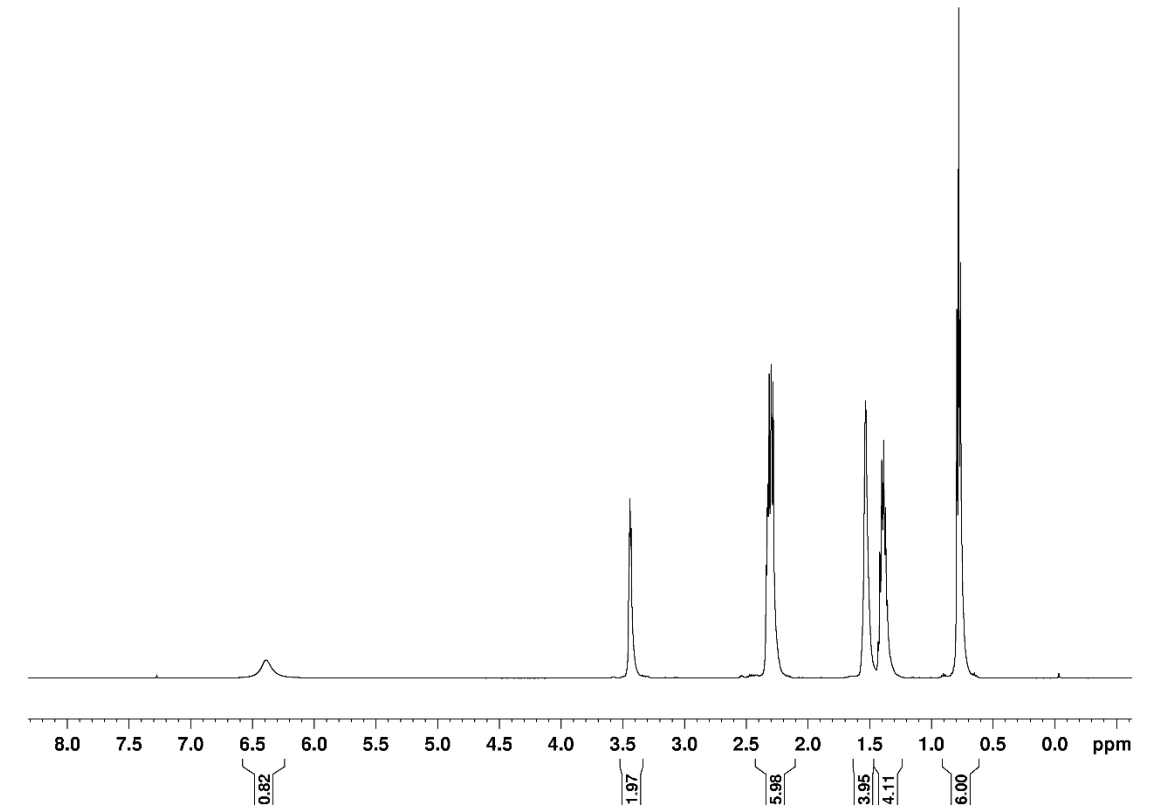

Fig A3.15 ^{1}H NMR spectrum of 4-dipropylamino-1-butanol in chloroform-d.

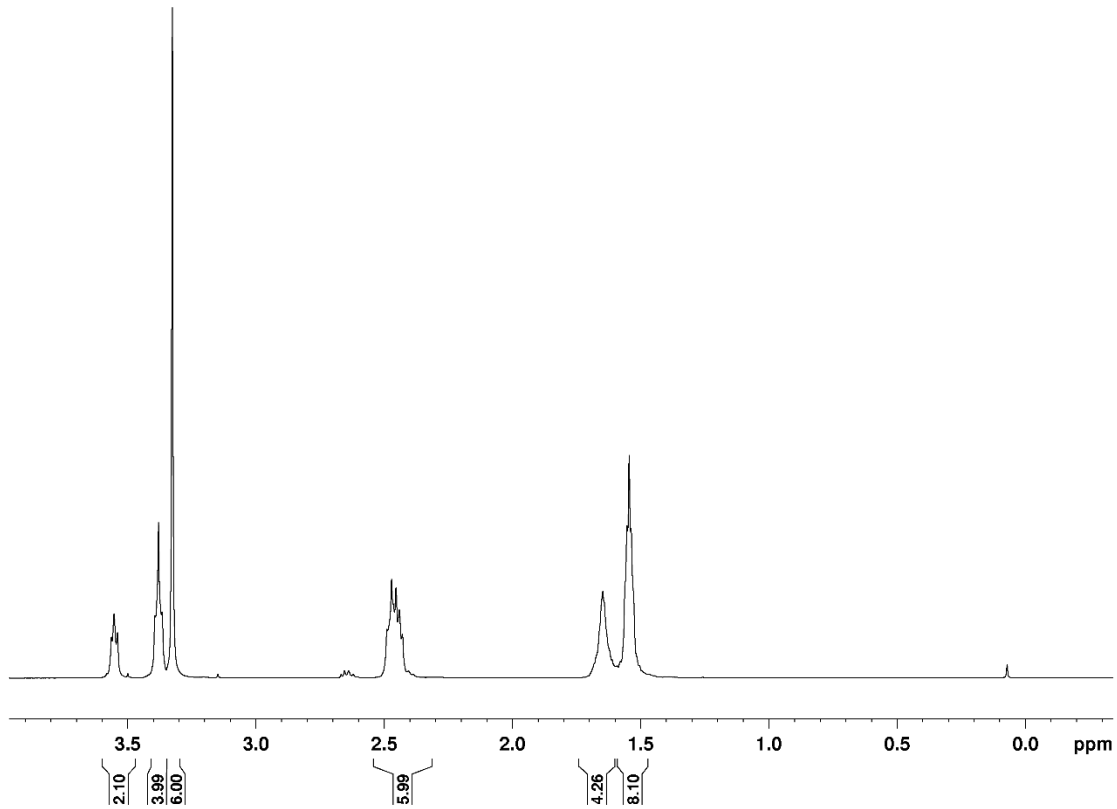

Fig A3.16 ^{1}H NMR spectrum of di-*N*,*N*-(4-methoxybutyl)-4-amino-1-butanol in chloroform-d.

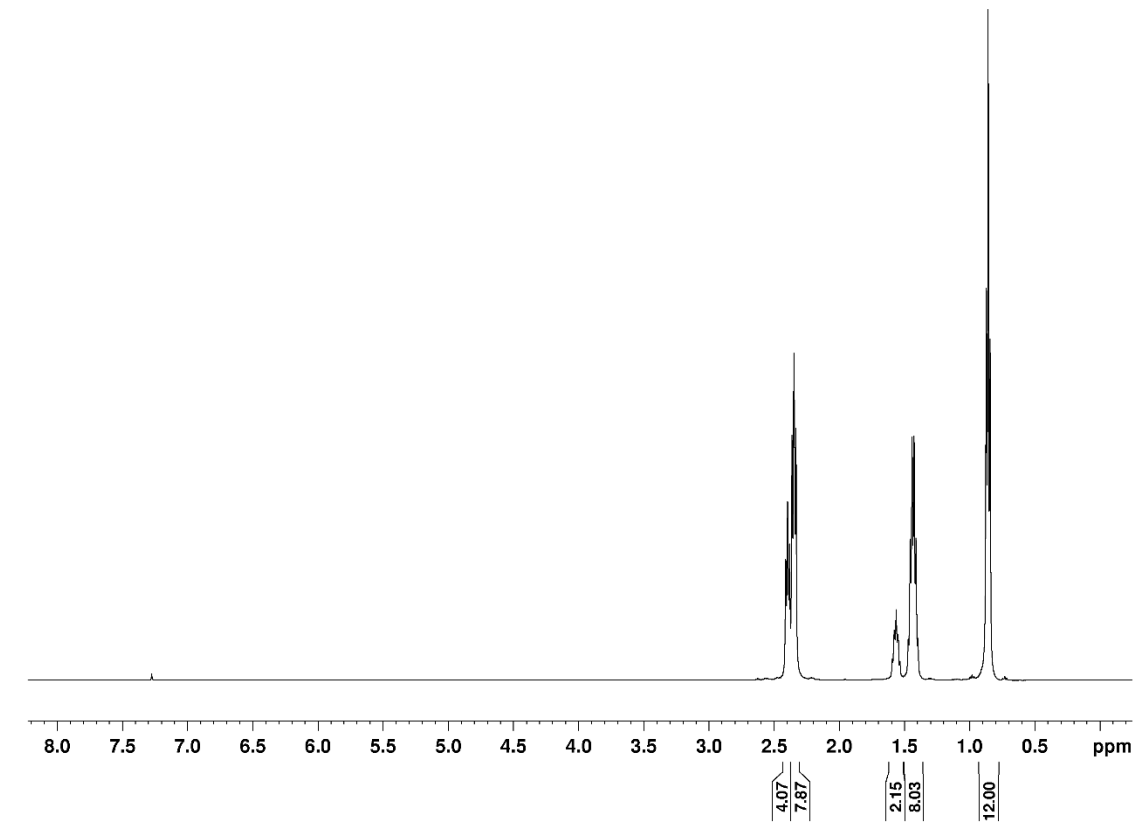

Fig A3.17 ^{1}H NMR spectrum of *N*,*N*,*N'*,*N'*-tetrapropyl-1,3-propanediamine in chloroform-d.

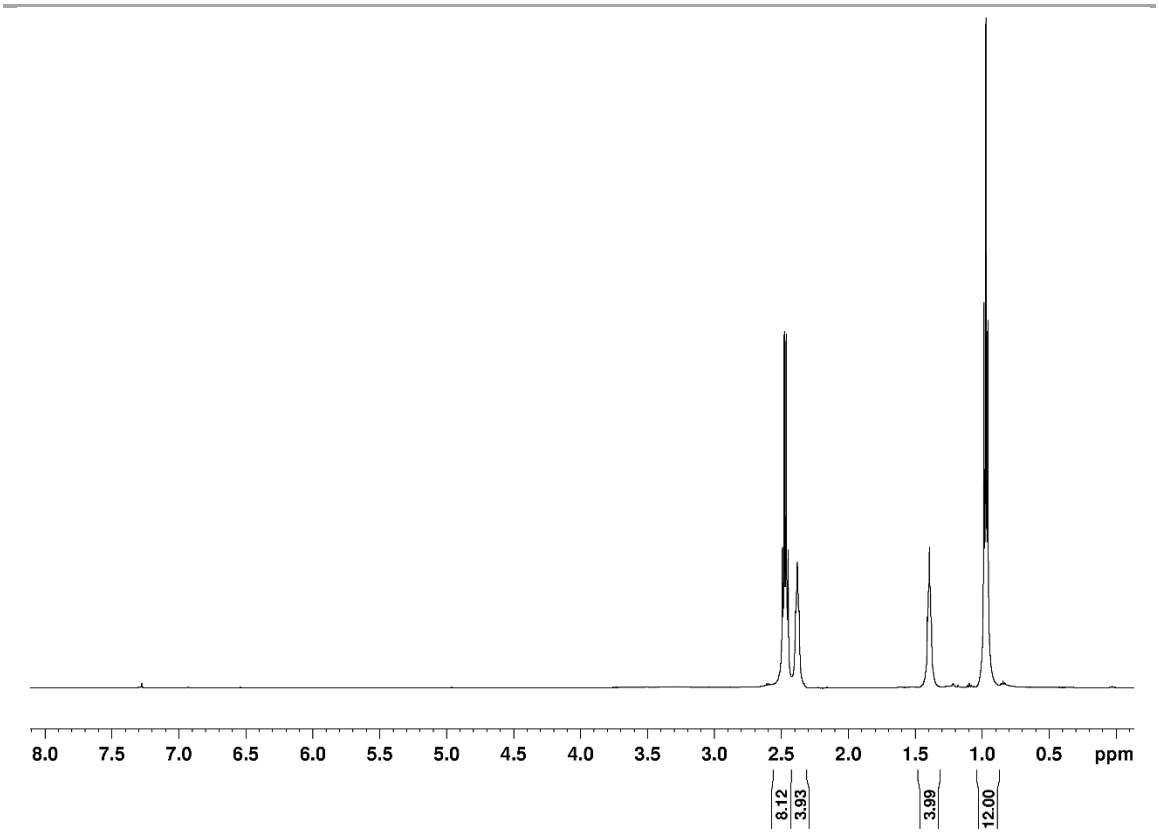

Fig A3.18 ^{1}H NMR spectrum of *N*,*N*,*N'*,*N'*-tetraethyl-1,4-butanediamine in chloroform-d.

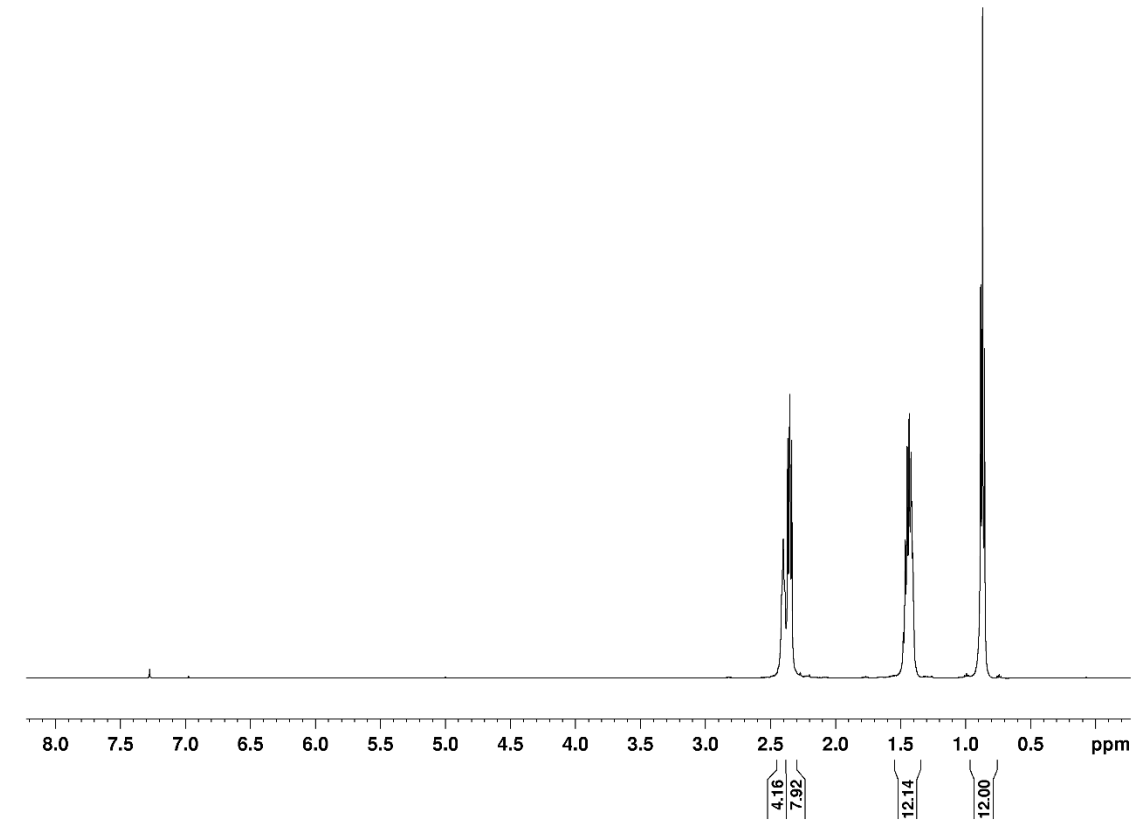

Fig A3.19 ^{1}H NMR spectrum of *N*,*N*,*N'*,*N'*-tetrapropyl-1,4-butanediamine in chloroform-d.

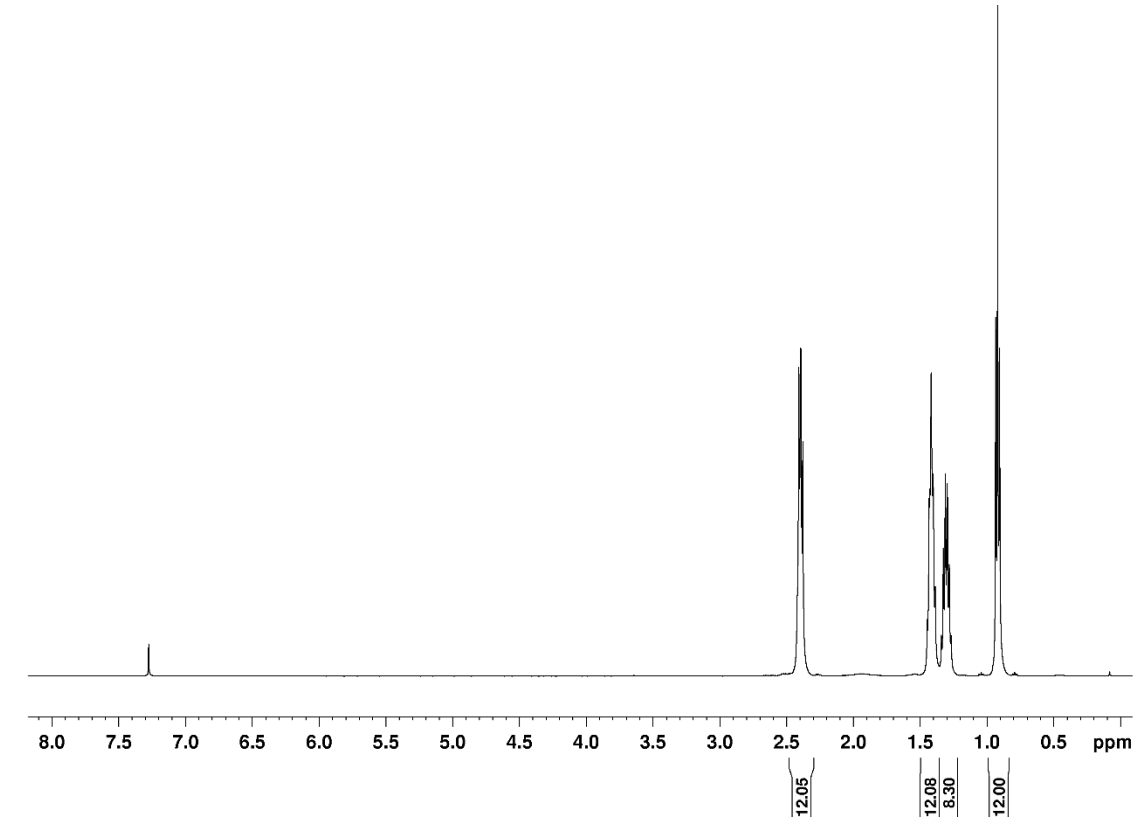

Fig A3.20 ^{1}H NMR spectrum of *N*,*N*,*N'*,*N'*-tetrabutyl-1,4-butanediamine in chloroform-d.

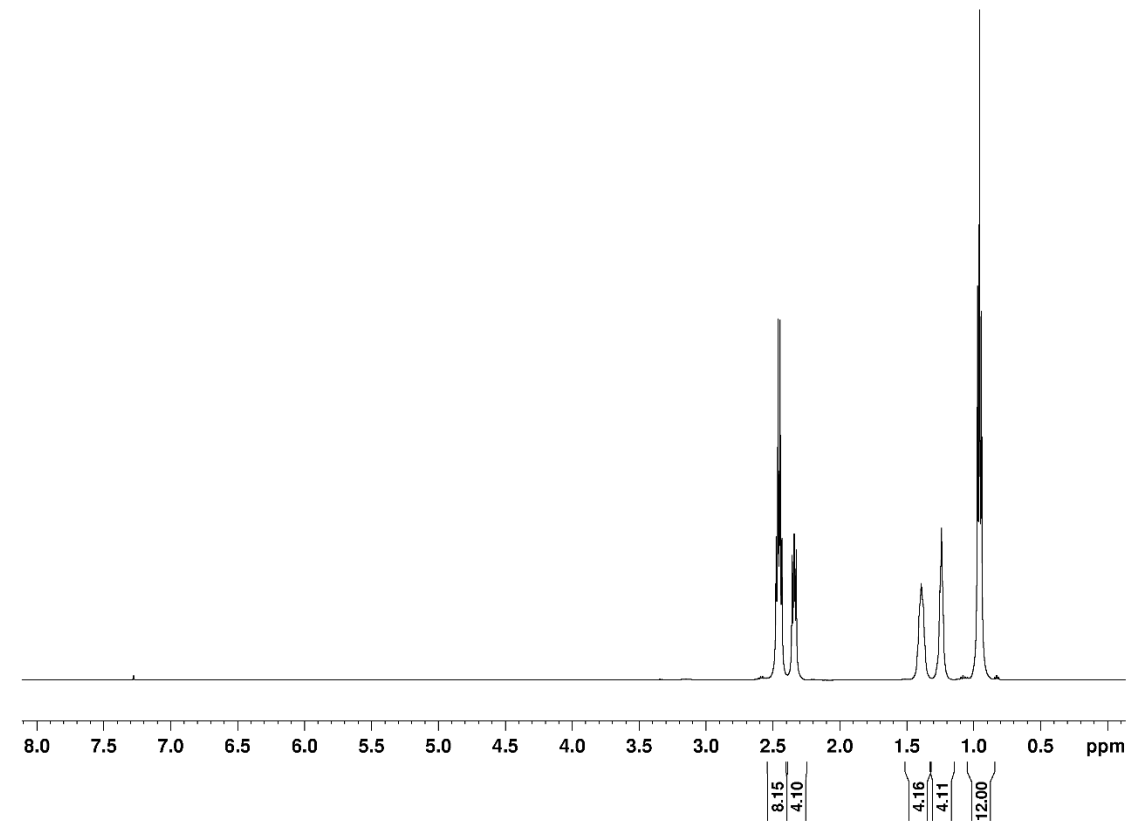

Fig A3.21 ^{1}H NMR spectrum of *N*,*N*,*N'*,*N'*-tetraethyl-1,6-hexanediamine in chloroform-d.

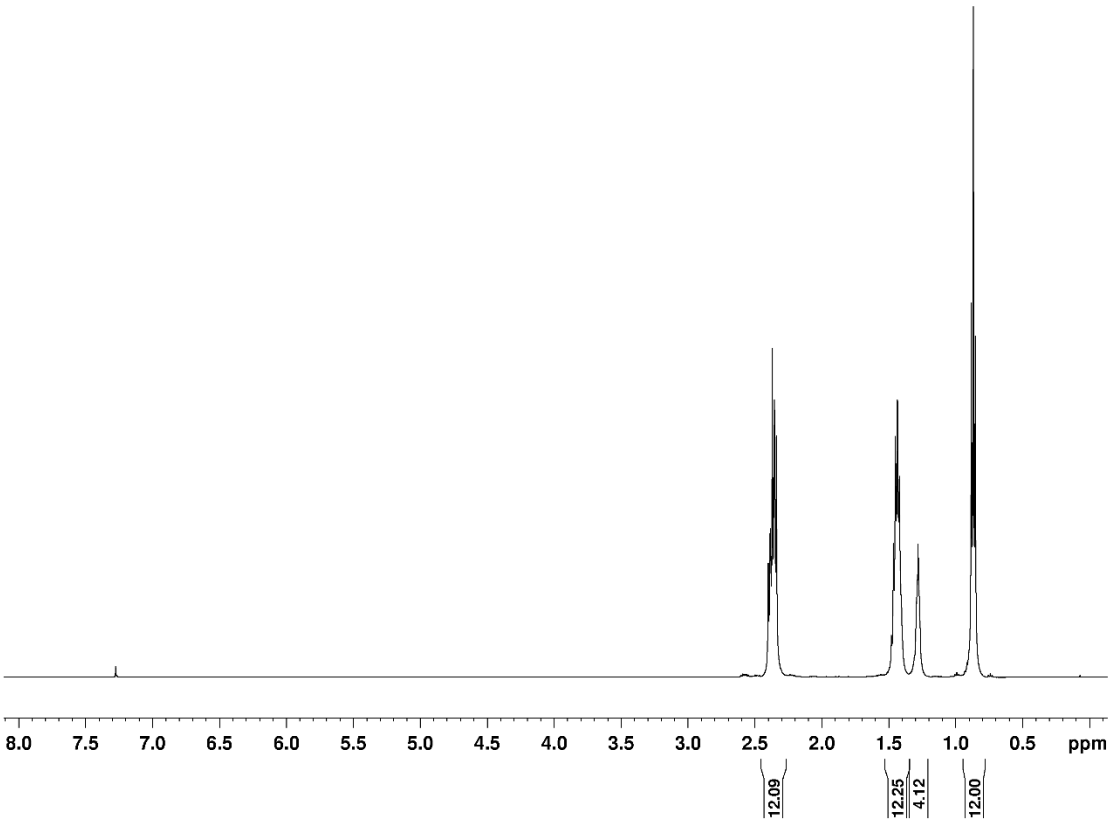

Fig A3.22 ^{1}H NMR spectrum of *N*,*N*,*N'*,*N'*-tetrapropyl-1,6-hexanediamine in chloroform-d.

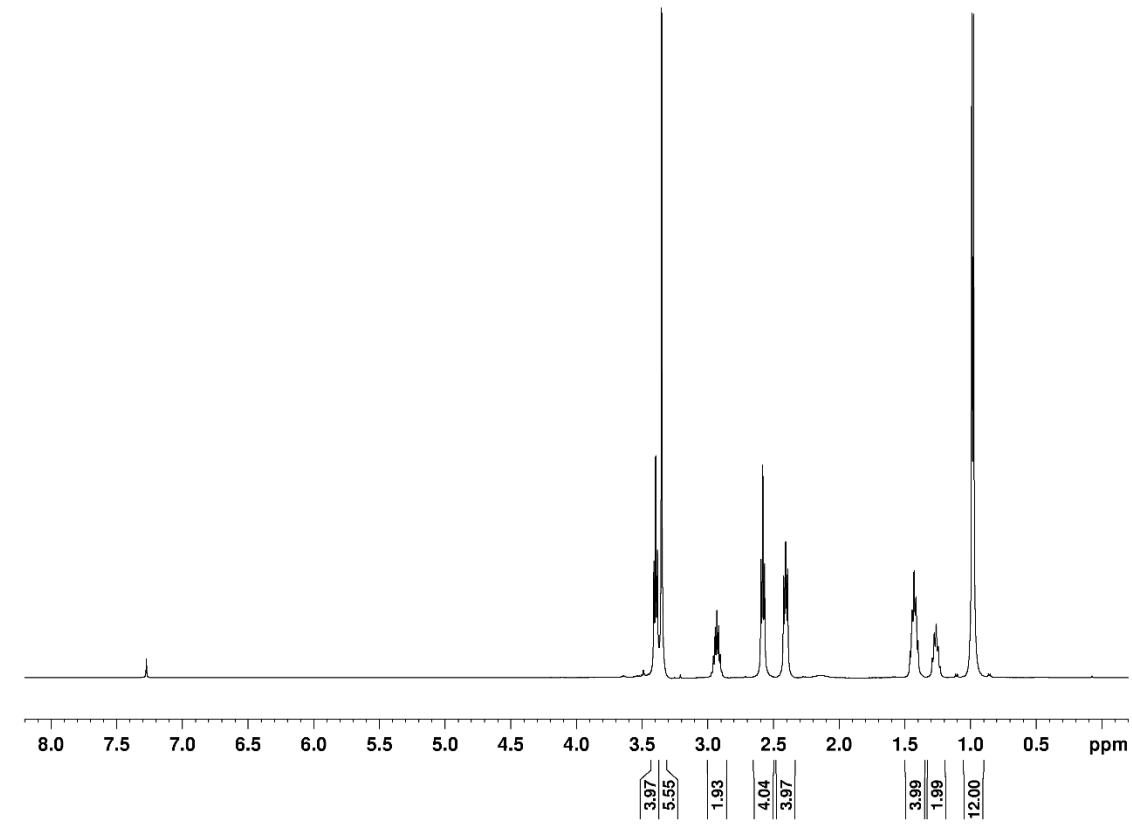

Fig A3.23 ^{1}H NMR spectrum of *N,N'*-dimethoxyethyl-*N',N'*-diisopropyl-1,5-pentanediamine in chloroform-d.

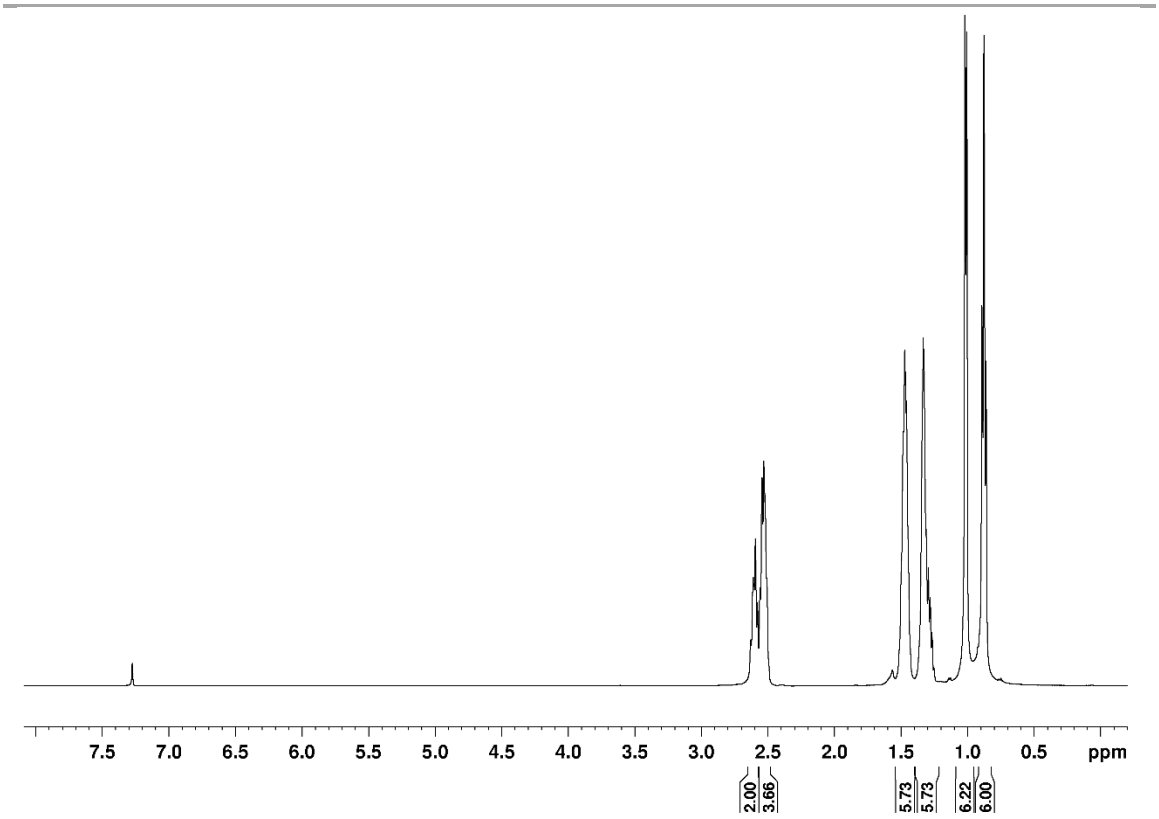

Fig A3.24 [1]H NMR spectrum of *N,N'*-di-*sec*-butyl-1,6-hexanediamine in chloroform-d.

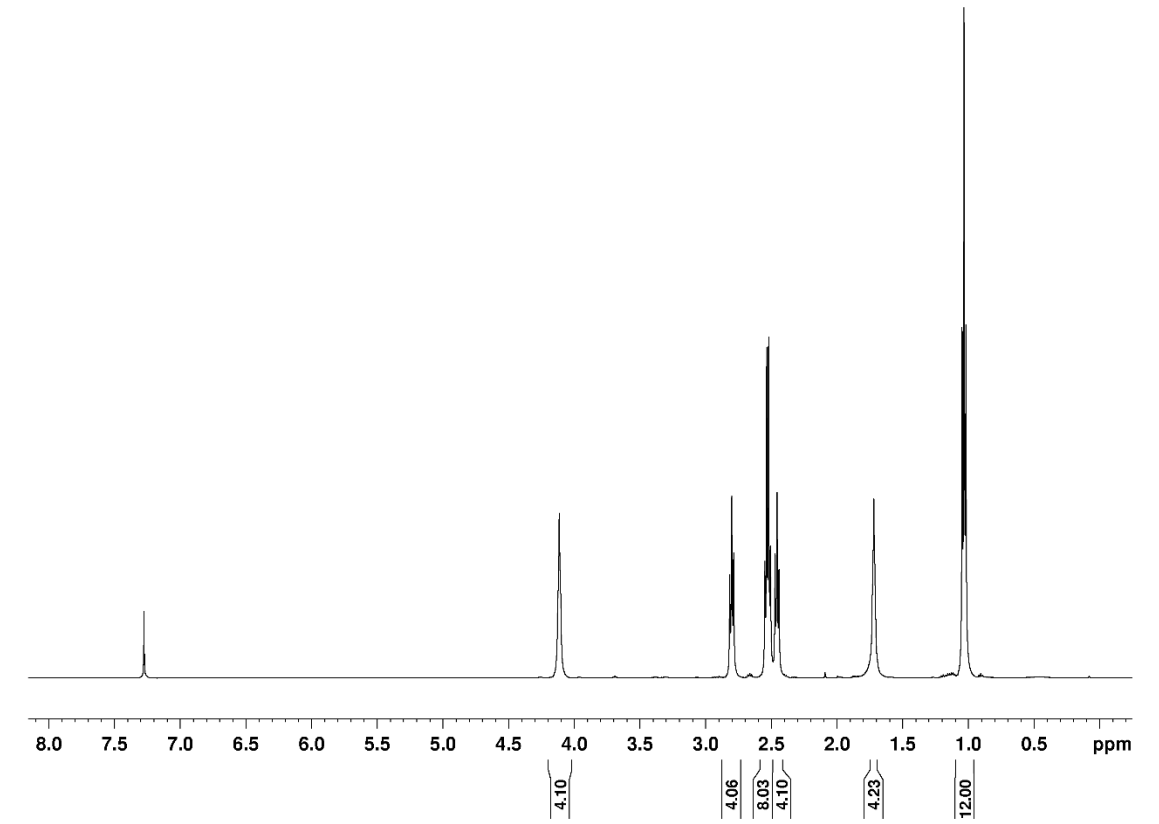

Fig A3.25 ^{1}H NMR spectrum 1,4-butanediol di-(3-diethylamino)propanoate in chloroform-d.

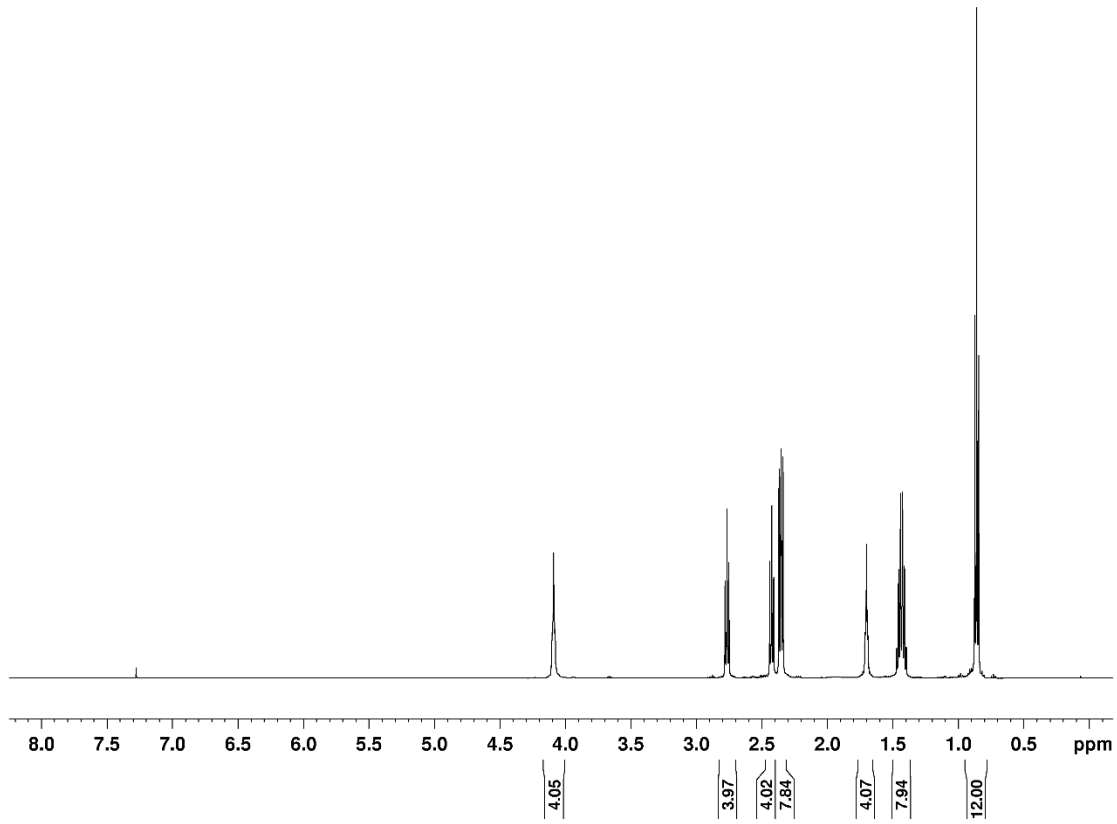

Fig A3.26 ^{1}H NMR spectrum 1,4-butanediol di-(3-dipropylamino)propanoate in chloroform-d.

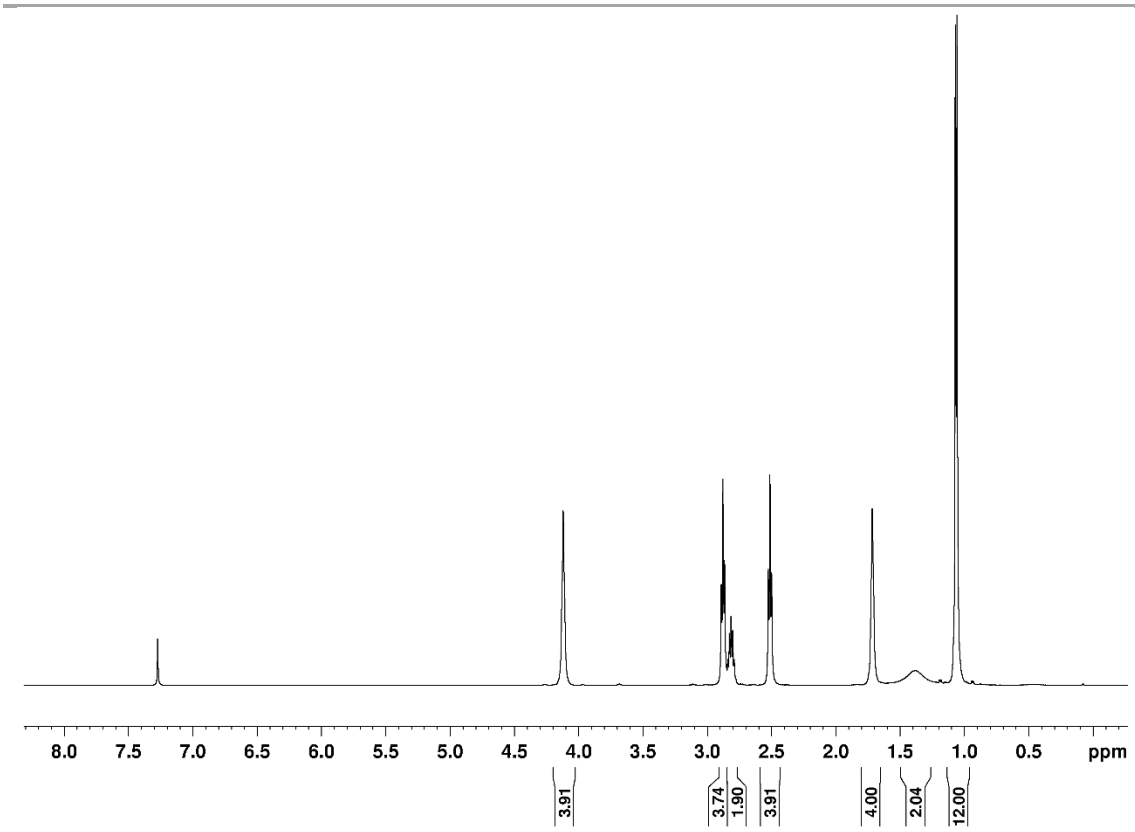

Fig A3.27 ^{1}H NMR spectrum 1,4-butanediol di-(3-isopropylamino)propanoate in chloroform-d.

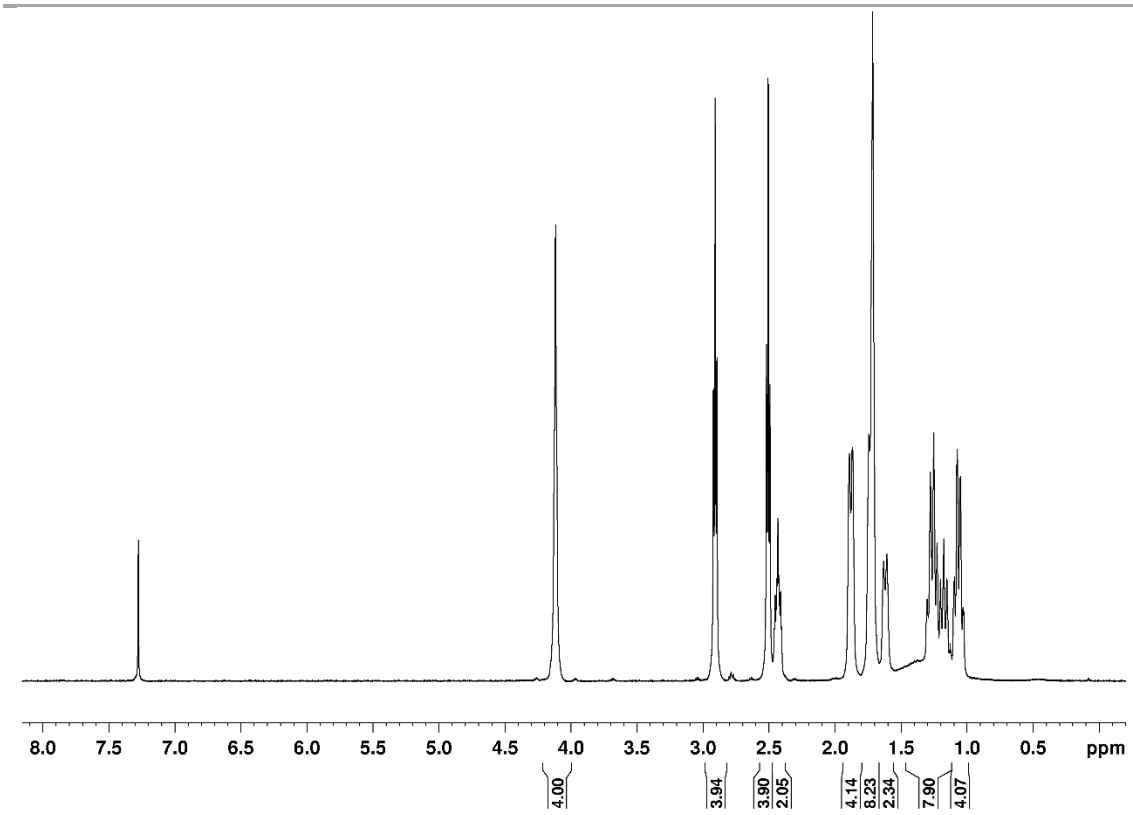

Fig A3.28 ^{1}H NMR spectrum 1,4-butanediol di-(3-cyclohexylamino)propanoate in chloroform-d.

A3.2 Crystallographic data for dibutylammonium bicarbonate

The crystallographic analysis of dibutylammonium bicarbonate was performed by Dr. Jia-sheng Lu.

A crystal of dibutylammonium bicarbonate (needle-shaped, size 0.10 x 0.03 x 0.03 mm) was mounted on a glass fiber with grease and cooled to -93 °C in a stream of nitrogen gas with the rate being controlled with a Cryostream Controller 700. Data collection was performed on a Bruker SMART APEX II X-ray diffractometer with graphite-monochromated Mo K_α radiation (λ = 0.71073 Å), operating at 50 kV and 30 mA over 2θ ranges of 4.30 ~ 52.00º. No significant decay was observed during data collection.

Data were processed on a PC using the Bruker AXS Crystal Structure Analysis Package:[1] Data collection: APEX2 (Bruker, 2010); cell refinement: SAINT (Bruker, 2009); data reduction: SAINT (Bruker, 2009); absorption correction: SADABS (Bruker, 2008); structure solution: XPREP (Bruker, 2008) and SHELXTL (Bruker, 2000); structure refinement: SHELXTL; molecular graphics: SHELXTL; publication materials: SHELXTL. Neutral atom scattering factors were taken from Cromer and Waber.[2] The crystal is orthorhombic space group *P*ccn, based on the systematic absences, *E* statistics and successful refinement of the structure. The structure was solved by direct methods. Full-matrix least-square refinements minimizing the function $\sum w (F_o^2 - F_c^2)^2$ were applied to the compound. All non-hydrogen atoms were refined anisotropically. All H atoms were placed in geometrically calculated positions and refined as riding atoms, with Uiso(H) = 1.2 UeqC.

Convergence to final R_1 = 0.0614 and wR_2 = 0.1413 for 1867 (I>2σ(I)) independent reflections, and R_1 = 0.0883 and wR_2 = 0.1531 for all 2564 (R(int) = 0.0651) independent reflections, with 128 parameters and 0 restraints, were achieved.[3] The largest residual peak and hole were determined to be 0.324 and – 0.285 e/Å^3, respectively. Crystallographic data, atomic

coordinates and equivalent isotropic displacement parameters, bond lengths and angles, anisotropic displacement parameters, hydrogen coordinates and isotropic displacement parameters are given in Tables A3.1 to A3.5. The molecular structure is shown in Fig. A3.29.

This structure has been deposited in the Cambridge Crystallographic Data Centre (deposition number: 967314 FISQOP).

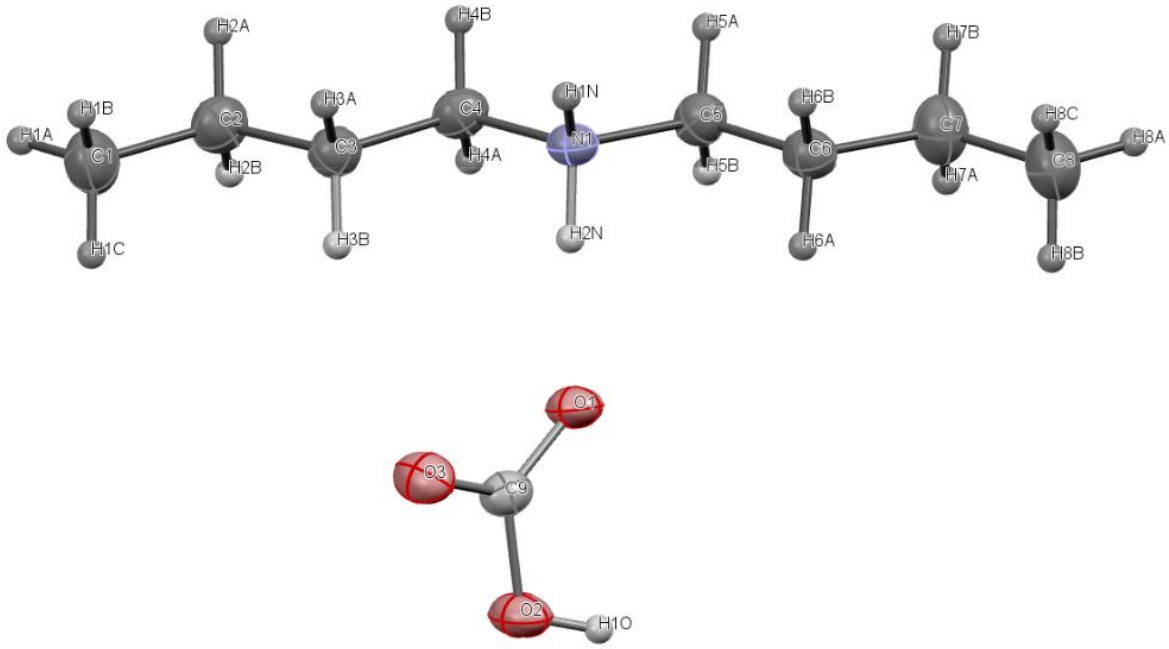

Fig. A3.29 The molecular structure of dibutylammonium bicarbonate (displacement ellipsoids for non-H atoms are shown at the 50% probability level and H atoms are omitted).

Table A3.1 Crystal data and structure refinement for dibutylammonium bicarbonate

Identification code	pj81	
Empirical formula	C6 H21 N O3	
Formula weight	191.27	
Temperature	180(2)K	
Wavelength	0.71073 Å	
Crystal system	Orthorhombic	
Space group	Pccn	
Unit cell dimensions	a = 14.5983(15) Å	α = 90°
	b = 20.935(2) Å	β = 90°
	c = 8.5228(9) Å	γ = 90°
Volume	2604.7(5) $Å^3$	
Z	8	
Density (calculated)	0.975 Mg/m^3	
Absorption coefficient	0.072 mm^{-1}	
F(000)	848	
Crystal size	0.10 x 0.03 x 0.03 mm^3	
Theta range for data collection	1.70 to 25.99°	
Index ranges	-18<=h<=18, -25<=k<=25, -10<=l<=10	
Reflections collected	23846	
Independent reflections	2563 [R(int) = 0.0651]	
Completeness to theta = 25.99°	100.0 %	
Absorption correction	multi-scan	
Max. and min. transmission	0.9978 and 0.9929	
Refinement method	Full-matrix least-squares on F^2	
Data / restraints / parameters	2563 / 0 / 128	
Goodness-of-fit on F^2	1.075	
Final R indices [I>2sigma(I)]	R1 = 0.0614, wR2 = 0.1413	
R indices (all data)	R1 = 0.0883, wR2 = 0.1531	
Largest diff. peak and hole	0.324 and -0.285 $e.Å^{-13}$	

Table A3.2 Atomic coordinates (x 10^4) and equivalent isotropic displacement parameters ($Å^2$ x 10^3) for dibutylammonium bicarbonate. U(eq) is defined as one third of the trace of the orthogonalized U^{ij} tensor.

	x	y	z	U(eq)
C(6)	4821(2)	3385(1)	3187(3)	32(1)
C(5)	5804(2)	3596(1)	3357(3)	32(1)
C(4)	6824(2)	4478(1)	4290(3)	31(1)
C(3)	6835(2)	5153(1)	4921(3)	31(1)
C(2)	7807(2)	5410(1)	5071(3)	38(1)
C(7)	4743(2)	2732(1)	2416(3)	45(1)
C(1)	7833(2)	6088(1)	5717(3)	46(1)
C(8)	3764(2)	2509(1)	2205(4)	53(1)
C(9)	4787(1)	5586(1)	1792(2)	26(1)
O(1)	5035(1)	5013(1)	1926(2)	31(1)
O(2)	4667(1)	5819(1)	338(2)	38(1)
O(3)	4642(1)	5970(1)	2890(2)	37(1)
N(1)	5863(1)	4239(1)	4110(2)	26(1)

Table A3.3 Bond lengths [Å] and angles [°] for dibutylammonium bicarbonate.

C(6)-C(5)	1.509(3)
C(6)-C(7)	1.520(3)
C(5)-N(1)	1.494(3)
C(4)-N(1)	1.497(3)
C(4)-C(3)	1.512(3)
C(3)-C(2)	1.523(3)
C(2)-C(1)	1.523(3)
C(7)-C(8)	1.514(4)
C(9)-O(3)	1.251(3)
C(9)-O(1)	1.260(3)
C(9)-O(2)	1.344(3)
C(5)-C(6)-C(7)	112.11(19)
N(1)-C(5)-C(6)	111.20(18)
N(1)-C(4)-C(3)	110.95(17)
C(4)-C(3)-C(2)	111.74(19)
C(1)-C(2)-C(3)	112.6(2)
C(8)-C(7)-C(6)	113.6(2)
O(3)-C(9)-O(1)	126.4(2)
O(3)-C(9)-O(2)	115.74(19)
O(1)-C(9)-O(2)	117.88(18)
C(5)-N(1)-C(4)	113.53(17)

Symmetry transformations used to generate equivalent atoms:

Table A3.4 Anisotropic displacement parameters ($Å^2 x\ 10^3$) for dibutylammonium bicarbonate. The anisotropic displacement factor exponent takes the form: $-2\pi^2[h^2a^{*2}U^{11} + \ldots + 2hka^*b^*U^{12}]$.

	U11	U22	U33	U23	U13	U12
C(6)	34(1)	29(1)	32(1)	0(1)	0(1)	4(1)
C(5)	35(1)	29(1)	32(1)	-6(1)	-3(1)	7(1)
C(4)	26(1)	36(1)	33(1)	0(1)	-2(1)	5(1)
C(3)	31(1)	32(1)	32(1)	0(1)	-2(1)	2(1)
C(2)	30(1)	40(1)	44(1)	1(1)	-3(1)	0(1)
C(7)	43(2)	39(1)	52(2)	-9(1)	1(1)	-2(1)
C(1)	45(2)	38(1)	56(2)	0(1)	-4(1)	-8(1)
C(8)	61(2)	40(1)	57(2)	-1(1)	-7(2)	-14(1)
C(9)	23(1)	32(1)	22(1)	1(1)	2(1)	2(1)
O(1)	39(1)	31(1)	22(1)	3(1)	-4(1)	7(1)
O(2)	57(1)	33(1)	23(1)	4(1)	-2(1)	9(1)
O(3)	56(1)	33(1)	23(1)	-2(1)	5(1)	7(1)
N(1)	28(1)	27(1)	22(1)	2(1)	0(1)	4(1)

Table A3.5 Hydrogen coordinates (x 10^4) and isotropic displacement parameters ($Å^2$ x 10^3) for dibutylammonium bicarbonate.

	x	y	z	U(eq)
H(6A)	4483	3702	2548	38
H(6B)	4531	3369	4237	38
H(5A)	6142	3282	4002	38
H(5B)	6095	3612	2309	38
H(4A)	7137	4467	3259	38
H(4B)	7164	4194	5015	38
H(3A)	6536	5160	5964	37
H(3B)	6479	5432	4211	37
H(2A)	8162	5127	5773	45
H(2B)	8103	5404	4026	45
H(7A)	5044	2748	1376	54
H(7B)	5077	2416	3065	54
H(1A)	8472	6228	5813	69
H(1B)	7541	6098	6752	69
H(1C)	7505	6375	5003	69
H(8A)	3763	2075	1772	79
H(8B)	3445	2797	1484	79
H(8C)	3452	2509	3223	79
H(1O)	4431	5537	-235	57
H(2N)	5530(20)	4539(14)	3400(40)	60(8)
H(1N)	5600(20)	4221(13)	5080(40)	60(9)

A3.3 References

1) Bruker AXS Crystal Structure Analysis Package:
-Bruker (2000). SHELXTL. Version 6.14. Bruker AXS Inc., Madison, Wisconsin, USA.
-Bruker (2008). SADABS. Version 2008/1. Bruker AXS Inc., Madison, Wisconsin, USA.
-Bruker (2008). XPREP. Version 2008/2. Bruker AXS Inc., Madison, Wisconsin, USA.
-Bruker (2009). SAINT. Version 7.68A. Bruker AXS Inc., Madison, Wisconsin, USA.
-Bruker (2010). APEX2. Version 2010.3-0. Bruker AXS Inc., Madison, Wisconsin, USA.

2) D. T. Cromer and J. T. Waber, *International Tables for X-ray Crystallography*, Kynoch Press: Birmingham, UK, 1974, vol. 4, Table 2.2 A.

3) $R_1 = \sum | |Fo| - |Fc| | / \sum |Fo|$
$wR_2 = \{\sum [w (Fo^2 - Fc^2)^2] / \sum [w(Fo^2)^2]\}^{1/2}$
($w = 1 / [\sigma^2(Fo^2) + (0.0381P)^2 + 1.1183P]$, where $P = [\text{Max} (Fo^2, 0) + 2Fc^2] / 3$)

Appendix 4

pK_{aH} Value Measurements

A4.1 Measuring aqueous pK_{aH} values from a potentiometric titration curve

The pK_{aH} value of an amine can be measured from a potentiometric titration curve using the procedure described here. A small amount of amine (~100 μL) was dissolved in 50 mL of water. The pH of the solution was measured using an Orion 4-Star pH meter (Thermo Scientific). Afterwards, small portions of a ~0.1 M aqueous HCl solution was added using a burette. The volume of added HCl solution was recorded after each addition as well as the pH of the amine solution. The additions continued until the pH of the solution decreased to ~3. A plot of pH vs. volume of titrant was prepared using these data. An example pH vs. volume plot is shown in Fig. A4.1. A derivative plot (δ(pH)/δ(V) vs. volume of titrant) was also prepared to identify the equivalence point of the titration, the point at which enough HCl has been added to fully protonate the amine. The equivalence point is the volume of titrant at which the largest negative derivative is obtained. An example derivative plot is shown in Fig. A4.2. From the equivalence point, the half-equivalence point, the volume of titrant at which half of the amine is protonated, can be calculated. The pH at the half equivalence point is taken to be the pK_{aH} of the amine.

A4.2 Measuring aqueous pK_{aH} values from data obtained in water:ethanol mixed solvents

In some cases, the aqueous pK_{aH} value must be determined for an amine that is poorly soluble in water. In these cases, the procedure described in the previous section does not allow for accurate pK_{aH} measurements. An alternative procedure to overcome this solubility issue has been reported by Gowland and Schmid.[1] In this procedure, a series of pK_{aH} measurements are made in water:ethanol mixtures with different ratios of each solvent for every measurement. The addition

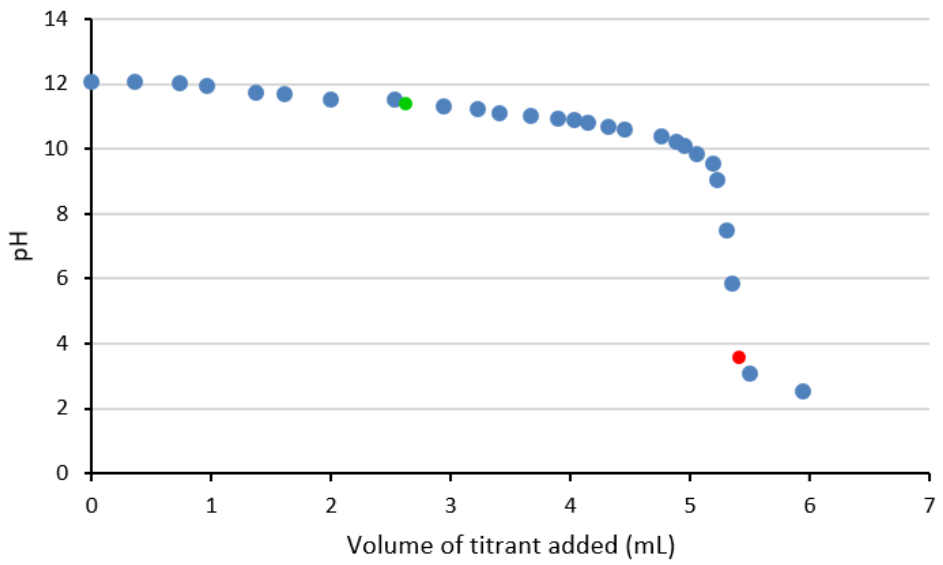

Fig. A4.1 A potentiometric titration curve for di-*sec*-butylamine. The equivalence point is represented by the red dot and the half-equivalence point is represented by the green dot.

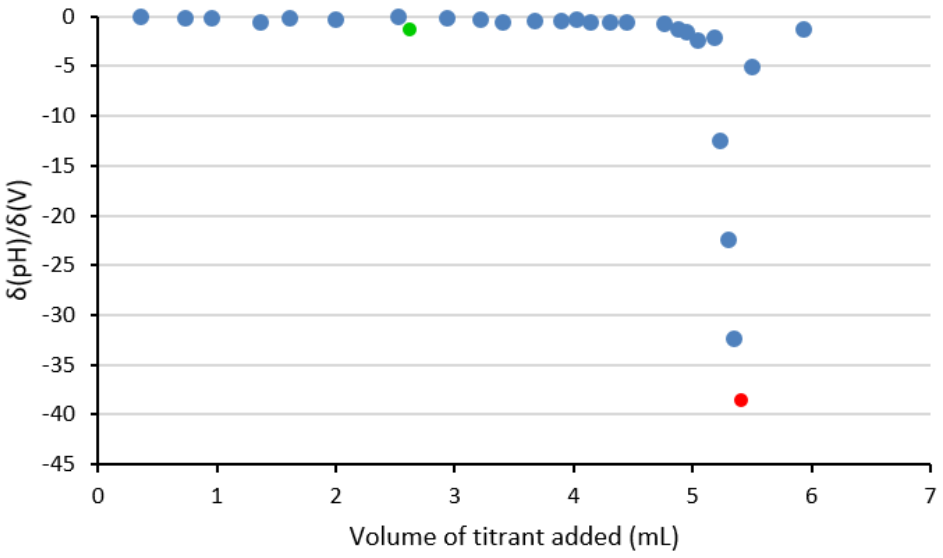

Fig A4.2 A derivative plot for the titration curve shown in Fig. A4.1. The equivalence point is represented by the red dot and the half equivalence point is represented by the green dot.

of the ethanol co-solvent allows the amine to completely dissolve in the solvent. The pK_{aH} measurements are performed using the same procedure described in section A4.1 except the amine is dissolved in water:ethanol mixtures rather than in pure water. From these data, a plot of pK_{aH} vs. wt% of ethanol is made. An example of such a graph is shown in Fig A4.3. The data are fit to a linear function and extrapolated to 0 wt% ethanol to identify the pK_{aH} of the amine in pure water.

A4.3 Measuring aqueous pK_{aH} values of diamines with overlapping ionization constants

When the two pK_{aH} values of a dibasic species are different by less than 3 units, the ionizations of the two basic sites overlap significantly and adds complications to titrations that prevent the accurate determination of either pK_{aH} value by simple titration analysis.[2] Because of the similarity of the two pK_{aH} values, it is possible for a significant portion of the sample to be

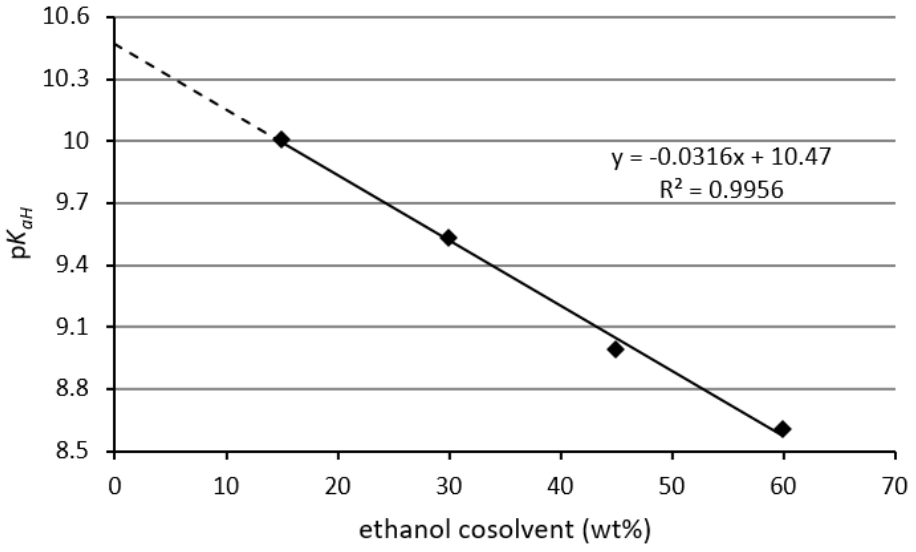

Fig. A4.3 A plot of the pK_{aH} values for *N*,*N*-dibutylamino-1-propanol in water:ethanol mixtures at different concentrations of ethanol. The pK_{aH} of the amine in pure water can be determined by extrapolating the linear fit to the x-axis.

doubly-protonated before the entire sample has been singly-protonated. In these cases, the pK_{aH1} and pK_{aH2} values do not occur at the quarter-equivalence and three-quarter-equivalence points, respectively, due to overlapping ionization. In order to accurately determine the pK_{aH} values of diprotic acids, a more complex analysis of titrimetric data is required.

Speakman developed a more rigorous procedure for determining the pK_a values of diprotic acids.[3] The analysis requires titration data obtained with the use of a standardized titrant (a titrant with a concentration measured to high precision). The initial concentration of the analyte and volume of water added must also be known. Apart from these requirements, the titration procedure described in section A4.1 can be used to obtain the necessary data for this analysis. Albert and Serjeant described a program written in Fortran to perform this analysis computationally.[2] This code was translated to operate in MATLAB and modified for the determination of the pK_{aH} values of bases rather than the pK_a values of acids. A copy of the MATLAB code is presented in section A4.3.1. The data obtained from the titration can be inputted into the software, which will return the pK_{aH1} and pK_{aH2} values of the analyte. An example of the input data and the output pK_{aH} values for a titration is shown in Table A4.1. This approach allows for the accurate determination of the two pK_{aH} values in dibasic compounds when the two values are different by less than 3 units.

Table A4.1 Input data for the analysis of the titration of 1,4-butanediol di-(3-(isopropylamino)propanoate), compound **7a** from Chapter 6, and the pK_{aH} values calculated using the MATLAB code shown in section A4.3.1.

Initial Volume: 50.00 mL

Titrant concentration: 0.10423 M

Initial analyte concentration: 0.004283 M

Volume of titrant added (mL)	pH
0.17	10.22
0.29	10.13
0.43	10.05
0.59	9.94
0.78	9.84
0.85	9.78
0.91	9.72
1.00	9.65
1.10	9.58
1.18	9.53
1.27	9.46
1.36	9.39
1.46	9.31
1.56	9.23
1.67	9.14
1.77	9.04
1.86	8.95
1.99	8.8
2.08	8.67
2.18	8.51
2.26	8.23
2.36	7.79

Calculated pK_{aH1}: 9.45

Calculated pK_{aH2}: 8.47

A4.3.1 MATLAB code

```
%Initial data
pH = [ ]; %put pH data here
Vinit = 50; %mL
Vadded = [ ]; %put volume of titrant added here (mL)
Ntitrant = 0.10423; %concentration of the titrant (mol/L)
Ctitrant = Vadded./1000.*Ntitrant./((Vinit + Vadded)./1000); %concentration of the
titrant in the analyte solution after addition (mol/L)
Canalyte = 0.06776./(316.4363.*((Vinit + Vadded)./1000)); %concentration of analyte
(mol/L)
actH = 10.^(-pH);
actOH = 10.^(-14+pH);

%Solve F initially
F = (Ctitrant + actOH - actH)./Canalyte;
K1 = 10;
K2 = 9;
OLDK1t = 10^-10;
OLDK2t = 10^-9;
NEWK1t = 10^-8;
NEWK2t = 10^-7;
n=1;
while(n < 100)
%solve eqn1 for Km 1 and 2
eqn1x = actOH.^2.*F./(2-F);
eqn1y = actOH.*(1-F)./(2-F);
fit1 = polyfit(eqn1x, eqn1y, 1);
K1 = 1./fit1(1);
K2 = -fit1(2);

%find concs of species
G = actOH.^2 + K1.*actOH + K1.*K2;
concBH = actOH.*K1.*Canalyte./G;
concBH2 = K1.*K2.*Canalyte./G;
%use concs to find ionic strength, use that to find concs
I = 0.5.*(Ctitrant + concBH + 4.*concBH2 + actH + actOH);
FS = sqrt(I)./(1+1.5.*sqrt(I));
concOH = actOH./10.^(0.5115.*FS);
concH = 10.^(-14)./concOH;

%solve for Kt 1 and 2
F = (Ctitrant + concOH - concH)./Canalyte;
X = actOH.^2.*F./(2-F);
Y = actOH.*(1-F)./(2-F);
```

```
eqn2y = Y./(10.^(1.5345.*FS));
eqn2x = X./(10.^(2.046.*FS));
fit2 = polyfit(eqn2x, eqn2y, 1);
OLDK1t = NEWK1t;
OLDK2t = NEWK2t;
NEWK1t = 1./fit2(1);
NEWK2t = -fit2(2);
n = n+1;
end
pK1 = 14+log10(NEWK1t) %outputs the pKaH1 value
pK2 = 14+log10(NEWK2t) %outputs the pKaH2 value
```

A4.4 References

1) J. A. Gowland and G. H. Schmid, *Can. J. Chem.*, 1969, **47**, 2953–2958.

2) A. Albert and E. P. Serjeant, *The determination of ionization constants: a laboratory manual*, Chapman and Hall, London ; New York, 3rd ed., 1984.

3) J. C. Speakman, *J. Chem. Soc.*, 1940, 855–859.